Unravelling the effects of environmental variation on the population dynamics of structured populations

Bethan Jane Hindle

Department of Animal and Plant Sciences

University of Sheffield

Submitted for degree of Doctorate of Philosophy

October 2017

Abstract

Complex environmental effects, combined with little temporal replication in most data sets, make investigating the ecological consequences of rapid climate change difficult with current tools. Structured population models are widely used to explore population responses to environmental variation. I develop and apply new statistical methods to parameterise such models.

First I describe a structural equation model (SEM) approach for capturing temporal covariation among demographic rates via latent variable(s). When rates are positively correlated the latent variable(s) act as axes of 'environmental quality'. This provides a simpler target for identifying the drivers of variation, than treating each process independently. Where drivers cannot be identified perturbing the latent variable(s) may represent the best alternative for exploring population-level responses to environmental change.

Quantifying the effects of underlying drivers allows population viability under different management strategies to be predicted. Such studies frequently assume a stationary environment, despite rapid climate change. Where climatic drivers are included, single temporal windows of influence are typically chosen *a priori*. I show forecasted climate change alters predicted population viability under different management regimes in a rare fire-adapted herb. I illustrate that the effect of a single climatic variable may differ over time, suggesting *a priori* selection of single temporal windows can decrease predictive performance.

I use the SEM approach to show that most (co)variation in survival and fecundity across different age-sex classes in a Soay sheep population is driven by a single environmental axis. I show climatic conditions during the energetically expensive autumn rut are nearly as important for overwinter mortality as the winter periods focused on in previous studies. I explore how density dependence, a temporal trend, population structure, and environmental variation interact to drive dynamics in this population.

Throughout this thesis I apply novel methods that increase our ability to accurately forecast population dynamics under environmental change.

Statement of Contributions

The personal pronoun 'we' is used throughout the thesis as this work was developed, supported, or improved by input and advice from collaborators. Nevertheless the vast majority of the ideas, modelling, analysis, and writing in this thesis are the candidate's work. Major contributions are listed here and any additional contributions are noted in the acknowledgements at the end of each chapter.

Chapters 1 (general introduction) and 6 (general discussion) were written by the candidate with editorial advice from Dylan Childs.

Chapter 2 has been submitted as a manuscript for publication and has been made publically available on BioRxiv. The initial idea was developed by the candidate and Dylan Childs. Data were provided by Andy Shepphard, Eric Menges, and Pedro Quintana-Asecencio. The modelling, analysis, and writing was carried out by the candidate. General editorial advice was provided by Dylan Childs, Mark Rees, Eric Menges, and Pedro Quintana-Asecencio.

Chapter 3 is in preparation as a manuscript. The development of the initial idea, modelling, analysis, and writing were carried out by the candidate. Data were provided by Eric Menges and Pedro Quintana-Asecencio. General editorial advice was provided by Dylan Childs, Eric Menges, and Pedro Quintana-Asecencio.

Chapter 4 has been submitted as a manuscript for publication. The candidate and Dylan Childs developed the initial idea. Data were provided by Josephine Pemberton and Jill Pilkington. The modelling, analysis, and writing was carried out by the candidate. General editorial advice was provided by Dylan Childs and Josephine Pemberton.

Chapter 5 is in preparation as a manuscript. The candidate and Dylan Childs developed the initial idea. Data were provided by Josephine Pemberton and Jill Pilkington. The modelling, analysis, and writing was carried out by the candidate. General editorial advice was provided by Dylan Childs.

Declaration by the author

This thesis contains original work, and does not contain material previously published or written by other persons, except where due reference has been made in the text. The contribution of collaborators to the conceptualisation, data collection, statistical analysis, authorship, and editing of this thesis has been clearly stated. This thesis content results from work I have undertaken since starting my research higher degree and includes no work submitted to qualify for any other degree or diploma in any university or other institution. I have clearly stated which parts of the thesis have been submitted for scientific publication and have obtained the required permissions to include this work. I acknowledge that copyright of the thesis content resides with the copyright holder(s) of that material.

Acknowledgements

First, I am extremely grateful to Dylan Childs who has provided a huge amount of guidance and support throughout my PhD.

This thesis would not have been possible without the work of numerous people who have had the foresight and dedication to collect long-term individual level data and the generosity to share such data. Countless volunteers have carried out much of the data collection. I am extremely grateful to everyone at the Soay sheep project, especially Josephine Pemberton and Jill Pilkington. I am also indebted to Jill for persuading Dylan to let me out of the office for a month to catch lambs on St Kilda. I have had useful conversations and feedback from many other members of the project during my PhD. Eric Menges and Pedro Quintana-Ascencio very kindly let me use their data on *Eryngium cuneifolium* and have provided extremely invaluable advice along the way. I am also grateful to Andy Sheppard who provided demographic data on *Carduus nutans* and Mark Rees for his useful advice.

I would like to thank the Child's lab group who have provided advice, encouragement, and a large amount of cheese at every step of my PhD. Particular thanks must go to Jason Griffiths, Shaun Coutts, and Tamora James who have provided frequent support and advice, whilst I've been venting my frustrations at JAGS. The rest of the office (past and present) are too many to name, but have always been supportive, keen to go for a pint, and have provided many cakes over the past four years (fortunately most of which have been considerably more edible than mine and Jason's joint attempts).

Finally, I would like to thank my friends and family for their support. They have bought me more sheep related gifts for Christmas than I knew was possible and have tried not to ask if I've finished yet too many times (with the exception of Tom, who's asked at regular intervals for the past two years at least). I'm grateful to Christine, Tara, and Anna who sent delicious packages that kept me going through the last weeks of writing. Finally, particular thanks must go to my parents, who have always been supportive, and Andy, who has put up with more of my stress during writing up than anyone else.

This research was funded by a National Environment Research Council and University of Sheffield PhD studentship.

Chapter 1: General Introduction

Introduction

The environments that populations inhabit are inherently variable in time, with variation in inter- and intra-specific densities, as well as abiotic factors, such as the weather. Temporal variation in the environment causes variability in individuals' vital rates, such as survival, growth, and fecundity. This has widespread consequences for population dynamics (Boyce *et al.* 2006), species' distributions (Gauzere, Prince & Devictor 2017), life history evolution (Metcalf & Pavard 2007; Pelletier *et al.* 2007), species interactions (Alarcon, Waser & Ollerton 2008), and community composition (Boersma *et al.* 2016; Stuble *et al.* 2017). Recent rapid global climate change has increased interest in predicting the ecological consequences of environmental variation (Stenseth *et al.* 2002; Evans 2012; Jenouvrier 2013; Wolkovich *et al.* 2014). This has broad applications, including in the management of endangered (Oppel *et al.* 2014) and economically important species (Shelton & Mangel 2011), the control of invasive species (Ruffell *et al.* 2015), and the spread of disease (Ewing *et al.* 2016). As experimental approaches to such problems are generally impractical in natural populations, structured demographic models parameterised with individual-level, longitudinal data sets are often used to assess the impact of environmental variation (Clutton-Brock & Sheldon 2010a; Clutton-Brock & Sheldon 2010b; Coulson 2012). However, parameterisation can be challenging, due to the complexity of environmental effects on the vital rates (Grosbois *et al.* 2008; Ehrlen *et al.* 2016) and the short extent of temporal and spatial replication in most demographic data sets (Salguero-Gomez *et al.* 2015; Salguero-Gomez *et al.* 2016).

In this chapter I start by considering the ecological impacts of climate change. I then provide an overview on stochastic structured population models. Next, I discuss how structured population models can be used to predict population responses to environmental change and the challenges with parameterising environmentally explicit models. I move on to review the statistical methods available to deal with such challenges. I conclude this chapter with a summary and an outline of the aims of the remaining thesis chapters.

Climate as a driver of ecological change

Climate change is expected to be one of the primary drivers of changes in biodiversity this century, with widespread extinctions predicted (Thomas *et al.* 2004; Maclean & Wilson 2011). Recent rates of climate change are unprecedented; average global temperatures increased by approximately 0.72°C between 1951 and 2012 (IPCC 2013) and are predicted to be 0.3-4.8°C higher by the end of the 21st century than in 1986-2005 (IPCC 2014). Recent emissions indicate that the higher end of this range is more likely (Peters *et al.* 2013). Furthermore, temperature increases are not uniform across the globe; in some areas warming is expected to be much more rapid (IPCC 2014). Temperature is not the only climatic variable that is changing, with for

example higher precipitation levels in the Northern Hemisphere (IPCC 2014). The wider impacts of temperature increases include decreasing snow cover and increasing sea levels (IPCC 2014). An increase in the variability of many climatic variables is also predicted, with higher frequencies of extreme weather events, such as heat waves and droughts, expected (Easterling *et al.* 2000; Jentsch, Kreyling & Beierkuhnlein 2007).

Ecological responses to climate change are widely recorded, and include poleward shifts in distribution, phenological change such as the advancing of spring events, changes in abundance, (local) extinctions, and adaptive evolution (Sparks & Yates 1997; Parmesan *et al.* 1999; Hickling *et al.* 2006; Cahill *et al.* 2013). Such changes do not occur in isolation from each other; for example, the ability of species to track suitable climatic conditions is expected to be a key determinant of future extinction risk (Thomas *et al.* 2004). The response of a species to climate change may be constrained by many factors, including habitat availability, dispersal ability, and interactions among species. For example, increasing temperatures have increased the area of climatically suitable land in Britain for many butterfly species, however they have generally decreased in abundance and distribution due to habitat loss and degradation (Warren *et al.* 2001). Species in isolated habitats, such as mountain tops, are at high risk as their immediate ranges contract (Thomas 2011). Disparate shifts in distribution and changes in abundance across different species will result in changes in community composition (Warren *et al.* 2001) and species interactions (Olsen *et al.* 2016). Where species are reliant on interactions with specific other species, this may constrain their ability to track climate change, unless they are able to adapt to interact with other species (e.g. Pateman *et al.* 2012). Local extinctions attributed to climate change have generally been mediated through the indirect effects of changes to species interactions, rather than direct physiological tolerances to new climatic conditions (Cahill *et al.* 2013). Interactions among species may be disturbed by shifts in temporal as well as spatial distributions (Parmesan 2007), if changes in phenology result in a lack of temporal synchronisation (Kellermann & van Riper 2015).

At the local scale, a population's response to environmental change is ultimately driven by variation in individuals' vital rates. This may be driven by fluctuations around the average environment, temporal trends in the average environment, or a combination of both (Stenseth *et al.* 2002; Lawson *et al.* 2015). The expected increase in climatic variability under climate change may be as biologically significant as changes to the average climatic conditions (Benton & Grant 1996; Benton & Grant 1999; Boyce *et al.* 2006; Garcia-Carreras & Reuman 2013). For example, extreme weather events may increase the rate of local population extinctions (Tinsley *et al.* 2015). Organisms are adapted in various ways to cope with temporal variation in the environment, for example through demographic buffering, where the vital rates to which the population growth rate is most sensitive are the least variable over time (Pfister 1998; though see Jongejans *et al.* 2010). Bet hedging strategies, whereby a decrease in average fitness is compensated for by a decrease in the temporal variation of fitness provide another mechanism

for coping with unpredictable environments (Slatkin 1974; Philippi & Seger 1989; Childs, Metcalf & Rees 2010; Simons 2011). For example, seed banks in annual plants allow seeds from the same plant to germinate in different years, reducing the risk of all of that individual's offspring emerging in a year with harsh environmental conditions and high mortality risk (Childs, Metcalf & Rees 2010). As demographic buffering and bet hedging strategies evolve as a result of environmental unpredictability, selection for such strategies may be expected to increase as levels of environmental variation increase (Simons 2011).

Overall the ecological effects of climate change are thus expected to be widespread, but will differ among taxonomic groups and locations, depending on a range of factors including habitat, species interactions, and species' life history strategies (Walther *et al.* 2002; Parmesan 2006). The risk of extinction for many species will be high without appropriate conservation measures (Thomas *et al.* 2004; Maclean & Wilson 2011). Effective species management requires the underlying drivers of variation in population performance to be identified (Thomas, Simcox & Hovestadt 2011; Froidevaux *et al.* 2017). Quantifying the effects of climatic drivers on the vital rates allows population responses to anticipated environmental change to be predicted (Hunter *et al.* 2010; Jenouvrier *et al.* 2014). Such projections are necessary to identify which species are most at risk under changing climates and design appropriate conservation measures to ameliorate the effects of drivers causing a decrease in population performance (Jenouvrier 2013).

Structured population models

In stochastic environments population dynamics are dependent on the mean and temporal (co)variance of vital rates across the life cycle (Levy *et al.* 2015). Both the mean and the variance of such rates may differ according to individual state variables, such as age (Descamps *et al.* 2008; Sharp & Clutton-Brock 2010), stage (Menges & Quintana-Ascencio 2004), sex (e.g. Owen-Smith 1993; Tavecchia *et al.* 2001), and size (Walters & Reich 2000). For example, in large herbivores prime adult survival is generally high and relatively constant across years, whilst juvenile and senescent individuals exhibit low and temporally variable survival (Gaillard, Festa-Bianchet & Yoccoz 1998; Gaillard *et al.* 2000; Gaillard & Yoccoz 2003). Such differences among individuals across the life cycle mean the structure of the population can have important consequences for population dynamics (Coulson *et al.* 2001); populations of the same size undergoing the same environmental conditions will exhibit different dynamics, if they differ in population structure (Coulson *et al.* 2001; Benton & Beckerman 2005).

Structured population models are necessary to explore population level responses to environmental variation in the presence of such state-dependent variation in performance (Coulson 2012). Structured models estimate state-fate relationships using either discrete states, such as stage (leading to a matrix population model (MPM); Caswell 2001), or continuous states, such as size or individual quality (resulting in an integral projection model (IPM);

Easterling, Ellner & Dixon 2000; Ellner, Childs & Rees 2016). Such models have been extended to include species with complex traits (e.g. Ellner & Rees 2006; Rees *et al.* 2006), spatial structure (e.g. Adler, Ellner & Levine 2010; Jongejans *et al.* 2011), interspecific interactions (e.g. Rose, Louda & Rees 2005; Hegland, Jongejans & Rydgren 2010), and demographic stochasticity (e.g. Vindenes, Engen & Saether 2011; Vindenes, Saether & Engen 2012). A range of tools have been developed to explore population responses to changing conditions using a structured population modelling framework (Caswell 2001; Ellner, Childs & Rees 2016). For example, prospective sensitivity analyses allow predictions of how metrics such as the population growth rate will be affected by changes to the different vital rates and thus have been widely used to determine which demographic processes management strategies should target (Morris, Shertzer & Rice 2011; Bentzen & Powell 2012; Chiquet *et al.* 2013; Rand, Richmond & Dougherty 2017).

Environmental stochasticity can be introduced into structured population models by allowing the vital rates to vary temporally. Stochastic demographic models have been widely used to explore population dynamics and life history evolution in stationary stochastic environments (e.g. Childs *et al.* 2004; Jaffre & Le Galliard 2016). Stochastic structured population models typically use one of two main approaches for incorporating temporal variation (Rees & Ellner 2009; Metcalf *et al.* 2015). In a matrix (MPM) or kernel (IPM) selection approach, a matrix or kernel is estimated for each year and these are randomly sampled from at each time step in the simulation (e.g. Childs *et al.* 2004). Alternatively, using a parameter selection approach, the temporally varying parameters are sampled from their joint probability distribution at each iteration (e.g. Vindenes *et al.* 2014). The predictive accuracy of kernel selection and parameter selection approaches are similar, providing that covariances among the temporally variable parameters are appropriately accounted for (Metcalf *et al.* 2015). Using a kernel selection approach the covariances are automatically preserved, whilst under a parameter selection approach a covariance matrix is estimated.

Accounting for temporal covariances is important as they can have substantial effects on population dynamics (Doak *et al.* 2005; Tuljapurkar, Gaillard & Coulson 2009; Tomimatsu & Ohara 2010). For example, covariance terms explained between one third and one half of the variation in population growth rate in three ungulate populations (Coulson, Gaillard & Festa-Bianchet 2005). Positive covariances increase variation in the population growth rate, while negative associations among vital rates reduce this variation. Temporal covariances may be driven by a number of different processes. Positive covariances may occur if different vital rates or age classes are affected by the same environmental variables (Jongejans *et al.* 2010). On the other hand, negative covariances may arise from tradeoffs between the rates or if a single environmental variable has opposing effects on different rates (Jongejans & De Kroon 2005). For example, in California oaks increased rainfall is associated with an increase in growth but a decrease in fecundity (Knops, Koenig & Carmen 2007).

Challenges of parameterising environmentally explicit demographic models

To predict the effects of environmental change on species' population dynamics their vital rates are typically estimated as functions of environmental drivers (Gotelli & Ellison 2006; Ehrlen *et al.* 2016), such as climatic variables (e.g. Hunter *et al.* 2010), disturbance regimes (e.g. Menges & Quintana-Ascencio 2004), and biotic factors (e.g. Hegland, Jongejans & Rydgren 2010; Adler, Dalgleish & Ellner 2012). Perturbation analyses then allow predictions of population responses to altered environmental conditions to be made. This approach is widely used to understand the potential impacts of different management strategies (e.g. Menges & Quintana-Ascencio 2004; Sletvold *et al.* 2013) or anticipated climate change (e.g. Gotelli & Ellison 2006; Hunter *et al.* 2010; Salguero-Gomez *et al.* 2012). Environmentally explicit demographic models may be parameterised using experimental data (e.g. Sletvold *et al.* 2013) or by correlating observed demographic and environmental data (e.g. Dahlgren & Ehrlen 2009). Parameterising such models is challenging, as there may be a large number of putative environmental drivers (Grosbois *et al.* 2008) and the effects of such drivers are often complex. Drivers are unlikely to act in isolation on the vital rates. For example, the magnitude of temperature effects on the alpine plant, *Dracocephalum austriacum,* is dependent on the steepness of the slope on which it is located (Nicole *et al.* 2011). Environmental variables are also often correlated with each other; such that it can be difficult to determine which are causally related to the vital rates and which are simply correlated with causal drivers (Grosbois *et al.* 2008). Moreover, the low spatial and temporal replication present in most demographic data sets (Salguero-Gomez *et al.* 2015; Salguero-Gomez *et al.* 2016) restricts the number of possible effects that can be estimated, whilst funding and time constraints may limit the amount of data available on possible environmental drivers (Ehrlen *et al.* 2016).

In addition to identifying the drivers of vital rate variation, the temporal windows over which the vital rates are sensitive to each driver must be determined. Demographic data are typically collected annually, but the effects of many environmental variables, such as climatic variables, may vary over much finer timescales (Altwegg & Anderson 2009; Foster, Schmalzer & Fox 2014; Kruuk, Osmond & Cockburn 2015; Pearce-Higgins *et al.* 2015). For example, in the blue crane, *Anthropoides paradiseus*, population growth rate can be positively or negatively affected by increased variation in rainfall during the breeding season, depending on the timing (Altwegg & Anderson 2009). Moreover, time lags may exist between an environmental event occurring and the response in demographic performance to that event. Carry over effects, where the past environment affected the condition of an individual, with knock-on effects for its current vital rates are one cause of such lags (Harrison *et al.* 2011; Gardner *et al.* 2017). Alternatively lagged effects may be due to indirect effects, where an environmental driver affects interacting species, such as prey, predators, or competitors (Hedd *et al.* 2006; Cahill *et al.* 2013; Lord, Barry & Graves 2017). The indirect effects of climatic variables are sometimes more biologically significant than direct effects (Brown 2011; Cahill *et al.* 2013; Davis,

Stephens & Kjellander 2016). Effects that occur over different temporal windows must thus be considered, otherwise predictions of future population dynamics under climate change may be biased (van de Pol & Cockburn 2011).

The spatial scale of environmental drivers must also be considered. Large-scale climatic indices, such as North Atlantic Oscillation (NAO), have often outperformed local variables as predictors of vital rates (Post & Stenseth 1999; Hallett *et al.* 2004; Sandvik, Coulson & Saether 2008). However, mechanistically, it is changes to the local weather conditions that the vital rates will be sensitive to (Sandvik, Coulson & Saether 2008). The difference in predictive performance is likely to be due to a lack of understanding of which local covariates are important, the critical windows over which they act, and how these variables interact with each other and with other variables such as intraspecific density (Stenseth *et al.* 2003; Hallett *et al.* 2004; Stenseth & Mysterud 2005). The degree to which vital rates are driven by different environmental drivers may differ over a species' range (Saether *et al.* 2003; Anders & Post 2006). However, where studies attempting to determine how climatic sensitivity varies spatially use large-scale climatic indices, reported differences in sensitivities may be explained by spatial variation in the relationship between the large-scale index and the local climatic variables that actually drive variation in the vital rates (Anders & Post 2006). The relationship between large-scale indices and local conditions may vary even on relatively small scales, with for example correlations between NAO and snow depth found to be positive at high altitudes and negative at low altitudes at a study area in Norway (Mysterud *et al.* 2000). Such relationships may also vary temporally (Ottersen *et al.* 2001; Stenseth *et al.* 2003). Thus, despite the apparently high predictive performance of such large-scale climatic indices they may provide misleading results if extrapolated to wider temporal or spatial scales (Stenseth *et al.* 2003).

In most species the vital rates are affected by a combination of biotic and abiotic variables (Coulson *et al.* 2001; Sletvold *et al.* 2013; Dahlgren, Ostergard & Ehrlen 2014). Thus to accurately predict long term population dynamics under changing abiotic conditions the effects of biotic drivers such as intraspecific density must also be quantified (Barbraud & Weimerskirch 2003; Coulson *et al.* 2004). Where data are spatially replicated, correlations between abiotic environmental variables and carrying capacities may make it impossible to accurately quantify abiotic effects without simultaneously estimating the effects of intraspecific density (Ehrlen *et al.* 2016). Where the vital rates are influenced by conspecific density, individuals may be sensitive to different components of the population (Mysterud, Coulson & Stenseth 2002). For example, in red deer, *Cervus elaphus*, there is little habitat overlap between the males and females except during the rut, suggesting survival is more likely to be a function of the number of individuals of the focal sex than total population size (Coulson *et al.* 1997; Conradt, Clutton-Brock & Thomson 1999).

Moreover, it may be necessary to incorporate interactions between population density and abiotic drivers, as the strength of negative density dependence is likely to vary according to

6

the abiotic environment (Jacquemyn, Brys & Honnay 2009; Wang *et al.* 2009). During years with favourable environments (e.g. high resource availability) the effect of a high intraspecific density is likely to be relatively low. Conversely in years with a harsh abiotic environment the impact of a high population density would be expected to be higher as individuals compete over more limited resources. For example, winter survival in the blue petrel, *Halobaena caerulea*, shows dramatic decreases under harsh weather conditions and high densities (Barbraud & Weimerskirch 2003), whilst improving climatic conditions led to outbreaks of the cotton bollworm, *Helicoverpa armigera*, through the weakening of density dependence effects (Ouyang *et al.* 2014).

Statistical tools for identifying and quantifying the effects of environmental drivers

The challenges associated with identifying causal drivers and accurately quantifying their effects mean that a small number of candidate drivers are often chosen (Ehrlen *et al.* 2016; Van der Pol *et al.* 2016). Each putative driver is typically assumed to act over a single temporal window, which is chosen *a priori* (Van der Pol *et al.* 2016). These decisions are usually made based on expert knowledge of the focal species or closely related taxa (Frederiksen *et al.* 2014). Such studies have typically focused on the most obvious drivers (Ehrlen *et al.* 2016), such as time since fire in fire-adapted populations (Menges & Quintana-Ascencio 2004) and water availability in arid areas (Martorell 2007). There is likely to be a focus on direct effects that occur with little time lag between the driver and the vital rate response, as these responses will be most obvious in the field. This limits our ability to learn about novel ways in which species might respond to their environment. Additionally, as environmental effects are often complex, studies focusing on single drivers are likely to retain a lot of unexplained temporal variation (Altwegg & Anderson 2009; Trauernicht *et al.* 2016). The predictive performance of such models may therefore be low if unidentified drivers are important determinants of the vital rates (Ehrlen *et al.* 2016).

Including many putative drivers, each with multiple possible temporal windows, leads to a rapid increase in the number of parameters to estimate. This can increase the risk of spurious relationships being detected, particularly if the number of independent observations is limited (Frederiksen *et al.* 2014). Thus, effective statistical methods are needed to select causal drivers from a potentially large number of possibilities. Sliding window approaches have frequently been used to determine the temporal windows over which environmental variables drive variation in the vital rates (Husby *et al.* 2010; Stopher *et al.* 2014; Kruuk, Osmond & Cockburn 2015; Van der Pol *et al.* 2016). For each putative driver, the fit of models using a range of start and end dates for the temporal window are compared. A single temporal window is typically chosen for each driver (Husby *et al.* 2010; Stopher *et al.* 2014; though see Kruuk, Osmond & Cockburn 2015), thus ignoring the possibility of temporal lags of different lengths. Once the window of influence has been identified for each driver, models containing different

combinations of the possible drivers can be compared to select the final model. Different methods have been used to compare the model fit, including Akaike Information Criteria (AIC; Stopher *et al.* 2014; Kruuk, Osmond & Cockburn 2015) or R^2 (Husby *et al.* 2010; Phillimore *et al.* 2012). Information theoretic (IT) approaches, such as AIC, have been widely advocated as an alternative to null hypothesis testing (Johnson & Omland 2004; Rushton, Ormerod & Kerby 2004). AIC penalises more complex models, using the number of parameters to be estimated (K) as a measure of complexity, as follows: $\text{AIC} = -2LL + 2K$, where LL is the log-likelihood. However, several studies have suggested that problems such as overfitting may be common to both null hypothesis testing and IT approaches (Raffalovich *et al.* 2008; Murtaugh 2009; Dahlgren 2010). The large number of models typically compared using a sliding window approach may result in overfitting, especially at low sample sizes (Van der Pol *et al.* 2016).

Overfitting can be reduced by using shrinkage methods such as ridge regression (Hoerl & Kennard 1970), where a penalty is applied to the magnitude of the parameter coefficients via penalized likelihood. In ridge regression the penalty term is given by $\lambda \sum_{k=1}^{K} \beta_k^{2}$, where β_k are the parameter estimates and λ controls the degree of shrinkage (where λ is equal to zero no shrinkage is applied). λ can be estimated as part of the model fitting process, for example using cross validation. Alternatively, in least absolute shrinkage and selection operator (LASSO) regression the penalty is applied to the sum of the absolute parameter estimates, as follows: $\lambda \sum_{k=1}^{K} |\beta_k|$. Under this approach the coefficients for some covariates may be shrunk to exactly zero (Tibshirani 1996; Tibshirani 2011), allowing for shrinkage and variable selection simultaneously. The elastic net combines a penalty on the absolute coefficients and the square of the coefficients, as follows: $\lambda(\sum_{k=1}^{K} \alpha\beta_k^{2} + (1 - \alpha)|\beta_k|)$ (Zou & Hastie 2005), where $0 \leq \alpha \leq 1$. Ridge regression and LASSO are thus special cases of the elastic net, where α=1 and α=0 respectively. The elastic net tends to perform better than LASSO when the number of predictors per observation is high or where the predictors are correlated (Zou & Hastie 2005). In a Bayesian framework shrinkage and model selection can be applied through the coefficient priors (O'Hara & Sillanpaa 2009; Li & Lin 2010). For example, estimating coefficients using a double exponential prior is equivalent to a LASSO regression (Park & Casella 2008). These shrinkage methods have a higher predictive accuracy than traditional variable selection methods when the number of observations per predictor is low (Reineking & Schroder 2006; Dahlgren 2010), which is often the case when parameterising environmentally explicit structured population models. Thus shrinkage approaches are increasingly being used to estimate environmental effects on vital rates (Gerber *et al.* 2015; Butler, Metzger & Harris 2017; Tredennick, Hooten & Adler 2017).

These shrinkage methods however do not account for the fact that the effects of a climatic variable over a small interval in time are likely to be similar (Sims *et al.* 2007). A difference penalty regression offers one solution to this problem. This approach introduces a penalty on the difference between neighbouring coefficients over the time series of the putative

environmental driver (Sims *et al.* 2007). For example, where the penalty is on the difference between adjacent parameter estimates, the penalty term is given by $\lambda \sum_{k=2}^{K} (\Delta\beta_k)^2$, where $\Delta\beta_k = \beta_k - \beta_{k-1}$. Alternatively, a functional linear model (FLM) may be used to estimate the demographic response to drivers that vary over fine scales as a smooth function over time (or space; Roberts 2008; Teller *et al.* 2016). Such models assume that the effect of an environmental variable is likely to be similar at adjacent time intervals; the direction and magnitude of the coefficients are allowed to differ smoothly over time using a penalized spline. For example, a climatic variable (x) may be included at regular time intervals $w = 1, 2, ... W$ (e.g. using weekly or monthly means) over year t. The probability of individual i in state s surviving (y) from year t to t+1 may then be given by

$$logit(y_{it}) = \alpha + \beta^s s_{it} + \sum_{w=1}^{W} f_x(w) x_{tw} + \varepsilon_t, \qquad \text{(eqn 1)}$$

where α is an intercept, β^s is a slope term for state variable s (e.g. size), x_{tw} is the value of climatic variable x in time interval (e.g. week) w of year t, $f_x(w)$ is a smooth function over time, and ε_t is a random year effect. The smooth function, $f_x(w)$, is parameterised by spline basis expansion. A quadratic smoothing penalty, that controls the degree of smoothing, is estimated as part of the model fitting procedure (Wood 2016; Wood 2017).

When identifying environmental drivers, different vital rates across the lifecycle are typically treated as independent processes, with for example separate models constructed for juvenile and adult survival and reproduction (e.g. Coulson *et al.* 2001; Pokallus & Pauli 2015). However, such processes rarely respond independently to environmental variation. Where positive correlations exist among different demographic processes the variation in these rates is likely to be driven by common environmental drivers (Nur & Sydeman 1999; Altwegg *et al.* 2006; Jongejans *et al.* 2010; Rotella *et al.* 2012). For example, in a barn owl population, *Tyto alba*, harsh winter weather was associated with a decrease in both juvenile and adult survival (Altwegg *et al.* 2006). Demographic structured equation models (SEMs) offer an alternative parameterisation. SEMs are widely used in ecological studies, for example to predict the joint responses of multiple species to environmental change (Warton *et al.* 2015). However, they are rarely used to parameterise single species demographic models, despite demographic rates often being temporally correlated (Jongejans *et al.* 2010) and such correlations having important effects on population dynamics (Coulson, Gaillard & Festa-Bianchet 2005). Here, latent variable(s) are introduced to capture the covariances among the disparate demographic processes (Evans, Holsinger & Menges 2010; Elderd & Miller 2016). This allows the joint responses to environmental variation across different rates and age-sex classes to be explored. Where the data are sufficiently replicated a higher-level model can be introduced, decomposing the variation in the latent variable(s) into the effects of environmental drivers and residual variation.

Conclusions and thesis outline

Rapid levels of environmental change have necessitated the development of suitable methods for investigating its ecological consequences. Structured population models, underpinned by empirically derived estimates of environment-demography relationships, may be used to explore population responses to such change (Coulson 2012). However, the complexity of environmental effects coupled with the small degree of temporal replication in most demographic data sets (Salguero-Gomez *et al.* 2015; Salguero-Gomez *et al.* 2016), makes the parameterisation of such models challenging. Here, I develop and apply novel statistical methods to allow the efficient use of the relatively limited data available to increase our understanding of how populations respond to environmental variation.

First, I describe a method that allows population responses to environmental change to be explored, while accounting for the fact that multiple demographic processes respond in concert to changing conditions (Chapter 2). Under this demographic structural equation (SEM) approach one or more latent variable(s) are introduced to capture the temporal covariation among the demographic rates. Where the rates are positively correlated the latent variable(s) may be conceived as axes of environmental quality. I use simulation studies to compare the accuracy of population growth rate estimates under this approach to the traditional parameter selection method of estimating an unstructured covariance matrix. I use two case studies to illustrate that, by perturbing the latent variable introduced by our model, I can make predictions about likely population level responses to environmental change. First, I predict the effects of different environmental conditions on bet hedging reproductive strategies in the monocarp *Carduus nutans*. Then I demonstrate how, with the addition of a single parameter, the effects of an environmental driver can be estimated, using a demographic model of the fire-adapted herb *Eryngium cuneifolium*. I use perturbation analyses to explore population level responses to different management strategies in this rare endemic.

Identifying the climatic drivers of vital rates allows population responses to anticipated environmental change to be predicted (Hunter *et al.* 2010; Salguero-Gomez *et al.* 2012). However, when population viability analyses are used to determine optimal management strategies the environment is often assumed to be stationary (though see e.g. Bernardo, Albrecht & Knight 2016). Moreover, where climatic drivers have been incorporated these have typically been assumed to act over single temporal windows, which are selected *a priori* (Van der Pol *et al.* 2016). I explore the effects of forecasted climate change on population viability in *E. cuneifolium*, under a range of management regimes (Chapter 3). I use functional linear models (FLMs) to determine the critical windows over which *E. cuneifolium's* vital rates are sensitive to climatic variation*,* whilst allowing the effect of a single climatic variable to vary in both magnitude and direction over the year (Chapter 3; Teller *et al.* 2016).

Despite strong positive correlations among demographic processes in a population of Soay sheep, *Ovis aries,* previous studies have treated each process (i.e. survival and fecundity of

each age-sex class) independently when identifying the underlying drivers (Coulson *et al.* 2001). Additionally, whilst many previous studies have quantified the effects of climatic drivers of dynamics in this population (e.g. Milner, Elston & Albon 1999; Catchpole *et al.* 2000; Coulson *et al.* 2001; Stenseth *et al.* 2004) they have tended to focus on the winter period, when most of the mortality occurs. The demographic SEM approach described above (Chapter 2) can provide a simpler target for the challenging task of identifying the underlying drivers of demographic rates. I use this approach to explore how many axes of environmental variation drive the temporal variation in survival, reproduction, and twinning across six age-sex classes in this population (Chapter 4). I then decompose the variation in the primary environmental axis into the effects of instraspecific density and abiotic drivers. I use the FLM approach to explore whether there is evidence of lagged climatic effects in this population, for example due to carry over or indirect vegetation effects. I compare the predictive performance of the FLM approach to using the large-scale NAO climatic index and to choosing the temporal window of influence *a priori* for a local climatic variable (Chapter 4).

Finally, I use the SEM framework to construct a demographic projection model to explore how density dependence, population structure, and environmental variation interact to drive population dynamics in the Soay sheep population (Chapter 5). The dynamics in the Soay sheep population appear to have changed over the course of the study period, from unstable overcompensatory density dependence to more stable population dynamics towards the end of the study period. I use a variant of the demographic SEM from Chapter 4 to parameterise an age and sex structured MPM and use this to explore possible causes of the temporal shift in the dynamics of this population (Chapter 5).

References

Adler, P.B., Dalgleish, H.J. & Ellner, S.P. (2012) Forecasting plant community impacts of climate variability and change: when do competitive interactions matter? *Journal of Ecology,* **100,** 478-487.

Adler, P.B., Ellner, S.P. & Levine, J.M. (2010) Coexistence of perennial plants: an embarrassment of niches. *Ecology Letters,* **13,** 1019-1029.

Alarcon, R., Waser, N.M. & Ollerton, J. (2008) Year-to-year variation in the topology of a plant-pollinator interaction network. *Oikos,* **117,** 1796-1807.

Altwegg, R. & Anderson, M.D. (2009) Rainfall in arid zones: possible effects of climate change on the population ecology of blue cranes. *Functional Ecology,* **23,** 1014-1021.

Altwegg, R., Roulin, A., Kestenholz, M. & Jenni, L. (2006) Demographic effects of extreme winter weather in the barn owl. *Oecologia,* **149,** 44-51.

Anders, A.D. & Post, E. (2006) Distribution-wide effects of climate on population densities of a declining migratory landbird. *Journal of Animal Ecology,* **75,** 221-227.

Barbraud, C. & Weimerskirch, H. (2003) Climate and density shape population dynamics of a marine top predator. *Proceedings of the Royal Society B-Biological Sciences,* **270,** 2111-2116.

Benton, T.G. & Beckerman, A.P. (2005) Population dynamics in a noisy world: Lessons from a mite experimental system. *Advances in Ecological Research, Vol. 37: Population Dynamics and Laboratory Ecology,* **37,** 143-181.

Benton, T.G. & Grant, A. (1996) How to keep fit in the real world: Elasticity analyses and selection pressures on life histories ln a variable environment. *American Naturalist,* **147,** 115-139.

Benton, T.G. & Grant, A. (1999) Elasticity analysis as an important tool in evolutionary and population ecology. *Trends in Ecology & Evolution,* **14,** 467-471.

Bentzen, R.L. & Powell, A.N. (2012) Population Dynamics of King Eiders Breeding in Northern Alaska. *Journal of Wildlife Management,* **76,** 1011-1020.

Bernardo, H.L., Albrecht, M.A. & Knight, T.M. (2016) Increased drought frequency alters the optimal management strategy of an endangered plant. *Biological Conservation,* **203,** 243-251.

Boersma, K.S., Nickerson, A., Francis, C.D. & Siepielski, A.M. (2016) Climate extremes are associated with invertebrate taxonomic and functional composition in mountain lakes. *Ecology and Evolution,* **6,** 8094-8106.

Boyce, M.S., Haridas, C.V., Lee, C.T. & Demography, N.S. (2006) Demography in an increasingly variable world. *Trends in Ecology & Evolution,* **21,** 141-148.

Brown, G.S. (2011) Patterns and causes of demographic variation in a harvested moose population: evidence for the effects of climate and density-dependent drivers. *Journal of Animal Ecology,* **80,** 1288-1298.

Butler, M.J., Metzger, K.L. & Harris, G.M. (2017) Are whooping cranes destined for extinction? Climate change imperils recruitment and population growth. *Ecology and Evolution,* **7,** 2821-2834.

Cahill, A.E., Aiello-Lammens, M.E., Fisher-Reid, M.C., Hua, X., Karanewsky, C.J., Ryu, H.Y., Sbeglia, G.C., Spagnolo, F., Waldron, J.B., Warsi, O. & Wiens, J.J. (2013) How does climate change cause extinction? *Proceedings of the Royal Society B-Biological Sciences,* **280.**

Caswell, H. (2001) Matrix population models: Construction, analysis, and interpretation. *Matrix population models: Construction, analysis, and interpretation*, i-xxii, 1-722.

Catchpole, E.A., Morgan, B.J.T., Coulson, T.N., Freeman, S.N. & Albon, S.D. (2000) Factors influencing Soay sheep survival. *Journal of the Royal Statistical Society Series C-Applied Statistics,* **49,** 453-472.

Childs, D.Z., Metcalf, C.J.E. & Rees, M. (2010) Evolutionary bet-hedging in the real world: empirical evidence and challenges revealed by plants. *Proceedings of the Royal Society B-Biological Sciences,* **277,** 3055-3064.

Childs, D.Z., Rees, M., Rose, K.E., Grubb, P.J. & Ellner, S.P. (2004) Evolution of size-dependent flowering in a variable environment: construction and analysis of a stochastic integral projection model. *Proceedings of the Royal Society B-Biological Sciences,* **271,** 425-434.

Chiquet, R.A., Ma, B.L., Ackleh, A.S., Pal, N. & Sidorovskaia, N. (2013) Demographic analysis of sperm whales using matrix population models. *Ecological Modelling,* **248,** 71-79.

Clutton-Brock, T. & Sheldon, B.C. (2010a) Individuals and populations: the role of long-term, individual-based studies of animals in ecology and evolutionary biology. *Trends in Ecology & Evolution,* **25,** 562-573.

Clutton-Brock, T. & Sheldon, B.C. (2010b) The Seven Ages of Pan. *Science,* **327,** 1207-1208.

Conradt, L., Clutton-Brock, T.H. & Thomson, D. (1999) Habitat segregation in ungulates: are males forced into suboptimal foraging habitats through indirect competition by females? *Oecologia,* **119,** 367-377.

Coulson, T. (2012) Integral projections models, their construction and use in posing hypotheses in ecology. *Oikos,* **121,** 1337-1350.

Coulson, T., Albon, S., Guinness, F., Pemberton, J. & CluttonBrock, T. (1997) Population substructure, local density, and calf winter survival in red deer (Cervus elaphus). *Ecology,* **78,** 852-863.

Coulson, T., Catchpole, E.A., Albon, S.D., Morgan, B.J.T., Pemberton, J.M., Clutton-Brock, T.H., Crawley, M.J. & Grenfell, B.T. (2001) Age, sex, density, winter weather, and population crashes in Soay sheep. *Science,* **292,** 1528-1531.

Coulson, T., Gaillard, J.M. & Festa-Bianchet, M. (2005) Decomposing the variation in population growth into contributions from multiple demographic rates. *Journal of Animal Ecology,* **74,** 789-801.

Coulson, T., Guinness, F., Pemberton, J. & Clutton-Brock, T. (2004) The demographic consequences of releasing a population of red deer from culling. *Ecology,* **85,** 411-422.

Dahlgren, J.P. (2010) Alternative regression methods are not considered in Murtaugh (2009) or by ecologists in general. *Ecology Letters,* **13,** E7-E9.

Dahlgren, J.P. & Ehrlen, J. (2009) Linking environmental variation to population dynamics of a forest herb. *Journal of Ecology,* **97,** 666-674.

Dahlgren, J.P., Ostergard, H. & Ehrlen, J. (2014) Local environment and density-dependent feedbacks determine population growth in a forest herb. *Oecologia,* **176,** 1023-1032.

Davis, M.L., Stephens, P.A. & Kjellander, P. (2016) Beyond Climate Envelope Projections: Roe Deer Survival and Environmental Change. *Journal of Wildlife Management,* **80,** 452-464.

Descamps, S., Boutin, S., Berteaux, D. & Gaillard, J.-M. (2008) Age-specific variation in survival, reproductive success and offspring quality in red squirrels: evidence of senescence. *Oikos,* **117,** 1406-1416.

Doak, D.F., Morris, W.F., Pfister, C., Kendall, B.E. & Bruna, E.M. (2005) Correctly estimating how environmental stochasticity influences fitness and population growth. *American Naturalist,* **166,** E14-E21.

Easterling, D.R., Meehl, G.A., Parmesan, C., Changnon, S.A., Karl, T.R. & Mearns, L.O. (2000) Climate extremes: Observations, modeling, and impacts. *Science,* **289,** 2068-2074.

Easterling, M.R., Ellner, S.P. & Dixon, P.M. (2000) Size-specific sensitivity: Applying a new structured population model. *Ecology,* **81,** 694-708.

Ehrlen, J., Morris, W.F., von Euler, T. & Dahlgren, J.P. (2016) Advancing environmentally explicit structured population models of plants. *Journal of Ecology,* **104,** 292-305.

Elderd, B.D. & Miller, T.E.X. (2016) Quantifying demographic uncertainty: Bayesian methods for integral projection models. *Ecological Monographs,* **86,** 125-144.

Ellner, S.P., Childs, D.Z. & Rees, M. (2016) *Data-driven modelling of structured populations: A practical guide to the Integral Projection Model*. Springer, Switzerland.

Ellner, S.P. & Rees, M. (2006) Integral projection models for species with complex demography. *American Naturalist,* **167,** 410-428.

Evans, M.E.K., Holsinger, K.E. & Menges, E.S. (2010) Fire, vital rates, and population viability: a hierarchical Bayesian analysis of the endangered Florida scrub mint. *Ecological Monographs,* **80,** 627-649.

Evans, M.R. (2012) Modelling ecological systems in a changing world. *Philosophical Transactions of the Royal Society B-Biological Sciences,* **367,** 181-190.

Ewing, D.A., Cobbold, C.A., Purse, B.V., Nunn, M.A. & White, S.M. (2016) Modelling the effect of temperature on the seasonal population dynamics of temperate mosquitoes. *Journal of Theoretical Biology,* **400,** 65-79.

Foster, T.E., Schmalzer, P.A. & Fox, G.A. (2014) Timing matters: the seasonal effect of drought on tree growth. *Journal of the Torrey Botanical Society,* **141,** 225-241.

Frederiksen, M., Lebreton, J.D., Pradel, R., Choquet, R. & Gimenez, O. (2014) Identifying links between vital rates and environment: a toolbox for the applied ecologist. *Journal of Applied Ecology,* **51,** 71-81.

Froidevaux, J.S.P., Boughey, K.L., Barlow, K.E. & Jones, G. (2017) Factors driving population recovery of the greater horseshoe bat (Rhinolophus ferrumequinum) in the UK: implications for conservation. *Biodiversity and Conservation,* **26,** 1601-1621.

Gaillard, J.M., Festa-Bianchet, M. & Yoccoz, N.G. (1998) Population dynamics of large herbivores: variable recruitment with constant adult survival. *Trends in Ecology & Evolution,* **13,** 58-63.

Gaillard, J.M., Festa-Bianchet, M., Yoccoz, N.G., Loison, A. & Toigo, C. (2000) Temporal variation in fitness components and population dynamics of large herbivores. *Annual Review of Ecology and Systematics,* **31,** 367-393.

Gaillard, J.M. & Yoccoz, N.G. (2003) Temporal variation in survival of mammals: A case of environmental canalization? *Ecology,* **84,** 3294-3306.

Garcia-Carreras, B. & Reuman, D.C. (2013) Are Changes in the Mean or Variability of Climate Signals More Important for Long-Term Stochastic Growth Rate? *Plos One,* **8,** 9.

Gardner, J.L., Rowley, E., de Rebeira, P., de Rebeira, A. & Brouwer, L. (2017) Effects of extreme weather on two sympatric Australian passerine bird species. *Philosophical Transactions of the Royal Society B-Biological Sciences,* **372,** 11.

Gauzere, P., Prince, K. & Devictor, V. (2017) Where do they go? The effects of topography and habitat diversity on reducing climatic debt in birds. *Global Change Biology,* **23,** 2218-2229.

Gerber, B.D., Kendall, W.L., Hooten, M.B., Dubovsky, J.A. & Drewien, R.C. (2015) Optimal population prediction of sandhill crane recruitment based on climate-mediated habitat limitations. *Journal of Animal Ecology,* **84,** 1299-1310.

Gotelli, N.J. & Ellison, A.M. (2006) Forecasting extinction risk with nonstationary matrix models. *Ecological Applications,* **16,** 51-61.

Grosbois, V., Gimenez, O., Gaillard, J.M., Pradel, R., Barbraud, C., Clobert, J., Moller, A.P. & Weimerskirch, H. (2008) Assessing the impact of climate variation on survival in vertebrate populations. *Biological Reviews,* **83,** 357-399.

Hallett, T.B., Coulson, T., Pilkington, J.G., Clutton-Brock, T.H., Pemberton, J.M. & Grenfell, B.T. (2004) Why large-scale climate indices seem to predict ecological processes better than local weather. *Nature,* **430,** 71-75.

Harrison, X.A., Blount, J.D., Inger, R., Norris, D.R. & Bearhop, S. (2011) Carry-over effects as drivers of fitness differences in animals. *Journal of Animal Ecology,* **80,** 4-18.

Hedd, A., Bertram, D.F., Ryder, J.L. & Jones, I.L. (2006) Effects of interdecadal climate variability on marine trophic interactions: rhinoceros auklets and their fish prey. *Marine Ecology Progress Series,* **309,** 263-278.

Hegland, S.J., Jongejans, E. & Rydgren, K. (2010) Investigating the interaction between ungulate grazing and resource effects on Vaccinium myrtillus populations with integral projection models. *Oecologia,* **163,** 695-706.

Hickling, R., Roy, D.B., Hill, J.K., Fox, R. & Thomas, C.D. (2006) The distributions of a wide range of taxonomic groups are expanding polewards. *Global Change Biology,* **12,** 450-455.

Hoerl, A.E. & Kennard, R.W. (1970) Ridge regression - biased estimation for nonorthogonal problems. *Technometrics,* **12,** 55-&.

Hunter, C.M., Caswell, H., Runge, M.C., Regehr, E.V., Amstrup, S.C. & Stirling, I. (2010) Climate change threatens polar bear populations: a stochastic demographic analysis. *Ecology,* **91,** 2883-2897.

Husby, A., Nussey, D.H., Visser, M.E., Wilson, A.J., Sheldon, B.C. & Kruuk, L.E.B. (2010) Contrasting patterns of phenotypic plasticity in reproductive traits in two great tit (Parus major) populations. *Evolution,* **64,** 2221-2237.

IPCC (2013) Climate Change 2013: The Physical Science Basis. Contribution of Working Group I to the Fifth Assessment Report of the Intergovernmental

Panel on Climate Change [Stocker, T.F., D. Qin, G.-K. Plattner, M. Tignor, S.K. Allen, J. Boschung, A. Nauels, Y. Xia, V. Bex and P.M. Midgley

(eds.)]. Cambridge University Press, Cambridge, United Kingdom and New York, NY, USA, 1535 pp.

IPCC (2014) Climate change 2014: Synthesis report. Contribution of working groups I, II, III to the Fifth Assessment Report of the Intergovernmental Panel on Climate Change [Core writing team, R.K. Pachauri and L.A. Meyers (eds.)]. IPCC Geneva, Switzerland, 151pp.

Jacquemyn, H., Brys, R. & Honnay, O. (2009) Large population sizes mitigate negative effects of variable weather conditions on fruit set in two spring woodland orchids. *Biology Letters,* **5,** 495-498.

Jaffre, M. & Le Galliard, J.F. (2016) Population viability analysis of plant and animal populations with stochastic integral projection models. *Oecologia,* **182,** 1031-1043.

Jenouvrier, S. (2013) Impacts of climate change on avian populations. *Global Change Biology,* **19,** 2036-2057.

Jenouvrier, S., Holland, M., Stroeve, J., Serreze, M., Barbraud, C., Weimerskirch, H. & Caswell, H. (2014) Projected continent-wide declines of the emperor penguin under climate change. *Nature Climate Change,* **4,** 715-718.

Jentsch, A., Kreyling, J. & Beierkuhnlein, C. (2007) A new generation of climate-change experiments: events, not trends. *Frontiers in Ecology and the Environment,* **5,** 365-374.

Johnson, J.B. & Omland, K.S. (2004) Model selection in ecology and evolution. *Trends in Ecology & Evolution,* **19,** 101-108.

Jongejans, E. & De Kroon, H. (2005) Space versus time variation in the population dynamics of three co-occurring perennial herbs. *Journal of Ecology,* **93,** 681-692.

Jongejans, E., de Kroon, H., Tuljapurkar, S. & Shea, K. (2010) Plant populations track rather than buffer climate fluctuations. *Ecology Letters,* **13,** 736-743.

Jongejans, E., Shea, K., Skarpaas, O., Kelly, D. & Ellner, S.P. (2011) Importance of individual and environmental variation for invasive species spread: a spatial integral projection model. *Ecology,* **92,** 86-97.

Kellermann, J.L. & van Riper, C. (2015) Detecting mismatches of bird migration stopover and tree phenology in response to changing climate. *Oecologia,* **178,** 1227-1238.

Knops, J.M.H., Koenig, W.D. & Carmen, W.J. (2007) Negative correlation does not imply a tradeoff between growth and reproduction in California oaks. *Proceedings of the National Academy of Sciences of the United States of America,* **104,** 16982-16985.

Kruuk, L.E.B., Osmond, H.L. & Cockburn, A. (2015) Contrasting effects of climate on juvenile body size in a Southern Hemisphere passerine bird. *Global Change Biology,* **21,** 2929-2941.

Lawson, C.R., Vindenes, Y., Bailey, L. & van de Pol, M. (2015) Environmental variation and population responses to global change. *Ecology Letters,* **18,** 724-736.

Levy, O., Buckley, L.B., Keitt, T.H., Smith, C.D., Boateng, K.O., Kumar, D.S. & Angilletta, M.J. (2015) Resolving the life cycle alters expected impacts of climate change. *Proceedings of the Royal Society B-Biological Sciences,* **282,** 9.

Li, Q. & Lin, N. (2010) The Bayesian Elastic Net. *Bayesian Analysis,* **5,** 151-170.

Lord, J.P., Barry, J.P. & Graves, D. (2017) Impact of climate change on direct and indirect species interactions. *Marine Ecology Progress Series,* **571,** 1-11.

Maclean, I.M.D. & Wilson, R.J. (2011) Recent ecological responses to climate change support predictions of high extinction risk. *Proceedings of the National Academy of Sciences of the United States of America,* **108,** 12337-12342.

Martorell, C. (2007) Detecting and managing an overgrazing-drought synergism in the threatened Echeveria longissima (Crassulaceae): the role of retrospective demographic analysis. *Population Ecology,* **49,** 115-125.

Menges, E.S. & Quintana-Ascencio, P.F. (2004) Population viability with fire in Eryngium cuneifolium: Deciphering a decade of demographic data. *Ecological Monographs,* **74,** 79-99.

Metcalf, C.J.E., Ellner, S.P., Childs, D.Z., Roberto, S.-G., Merow, C., McMahon, S.M., Jongejans, E. & Rees, M. (2015) Statistical modelling of annual variation for inference on stochastic population dynamics using Integral Projection Models. *Methods in Ecology and Evolution,* **6,** 1007-1017.

Metcalf, C.J.E. & Pavard, S. (2007) Why evolutionary biologists should be demographers. *Trends in Ecology & Evolution,* **22,** 205-212.

Milner, J.M., Elston, D.A. & Albon, S.D. (1999) Estimating the contributions of population density and climatic fluctuations to interannual variation in survival of Soay sheep. *Journal of Animal Ecology,* **68,** 1235-1247.

Morris, J.A., Shertzer, K.W. & Rice, J.A. (2011) A stage-based matrix population model of invasive lionfish with implications for control. *Biological Invasions,* **13,** 7-12.

Murtaugh, P.A. (2009) Performance of several variable-selection methods applied to real ecological data. *Ecology Letters,* **12,** 1061-1068.

Mysterud, A., Coulson, T. & Stenseth, N.C. (2002) The role of males in the dynamics of ungulate populations. *Journal of Animal Ecology,* **71,** 907-915.

Mysterud, A., Yoccoz, N.G., Stenseth, N.C. & Langvatn, R. (2000) Relationships between sex ratio, climate and density in red deer: the importance of spatial scale. *Journal of Animal Ecology,* **69,** 959-974.

Nicole, F., Dahlgren, J.P., Vivat, A., Till-Bottraud, I. & Ehrlen, J. (2011) Interdependent effects of habitat quality and climate on population growth of an endangered plant. *Journal of Ecology,* **99,** 1211-1218.

Nur, N. & Sydeman, W.J. (1999) Survival, breeding probability and reproductive success in relation to population dynamics of Brandt's cormorants Phalacrocorax penicillatus. *Bird Study,* **46,** 92-103.

O'Hara, R.B. & Sillanpaa, M.J. (2009) A Review of Bayesian Variable Selection Methods: What, How and Which. *Bayesian Analysis,* **4,** 85-117.

Olsen, S.L., Topper, J.P., Skarpaas, O., Vandvik, V. & Klanderud, K. (2016) From facilitation to competition: temperature-driven shift in dominant plant interactions affects population dynamics in seminatural grasslands. *Global Change Biology,* **22,** 1915-1926.

Oppel, S., Hilton, G., Ratcliffe, N., Fenton, C., Daley, J., Gray, G., Vickery, J. & Gibbons, D. (2014) Assessing population viability while accounting for demographic and environmental uncertainty. *Ecology,* **95,** 1809-1818.

Ottersen, G., Planque, B., Belgrano, A., Post, E., Reid, P.C. & Stenseth, N.C. (2001) Ecological effects of the North Atlantic Oscillation. *Oecologia,* **128,** 1-14.

Ouyang, F., Hui, C., Ge, S., Men, X.-Y., Zhao, Z.-H., Shi, P.-J., Zhang, Y.-S. & Li, B.-L. (2014) Weakening density dependence from climate change and agricultural intensification triggers pest outbreaks: a 37-year observation of cotton bollworms. *Ecology and Evolution,* **4,** 3362-3374.

Owen-Smith, N. (1993) Comparative mortality rates of male and female kudus - the costs of sexual size dimorphism. *Journal of Animal Ecology,* **62,** 428-440.

Park, T. & Casella, G. (2008) The Bayesian Lasso. *Journal of the American Statistical Association,* **103,** 681-686.

Parmesan, C. (2006) Ecological and evolutionary responses to recent climate change. *Annual Review of Ecology Evolution and Systematics*, pp. 637-669.

Parmesan, C. (2007) Influences of species, latitudes and methodologies on estimates of phenological response to global warming. *Global Change Biology,* **13,** 1860-1872.

Parmesan, C., Ryrholm, N., Stefanescu, C., Hill, J.K., Thomas, C.D., Descimon, H., Huntley, B., Kaila, L., Kullberg, J., Tammaru, T., Tennent, W.J., Thomas, J.A. & Warren, M. (1999) Poleward shifts in geographical ranges of butterfly species associated with regional warming. *Nature,* **399,** 579-583.

Pateman, R.M., Hill, J.K., Roy, D.B., Fox, R. & Thomas, C.D. (2012) Temperature-Dependent Alterations in Host Use Drive Rapid Range Expansion in a Butterfly. *Science,* **336,** 1028-1030.

Pearce-Higgins, J.W., Eglington, S.M., Martay, B. & Chamberlain, D.E. (2015) Drivers of climate change impacts on bird communities. *Journal of Animal Ecology,* **84,** 943-954.

Pelletier, F., Clutton-Brock, T., Pemberton, J., Tuljapurkar, S. & Coulson, T. (2007) The evolutionary demography of ecological change: Linking trait variation and population growth. *Science,* **315,** 1571-1574.

Peters, G.P., Andrew, R.M., Boden, T., Canadell, J.G., Ciais, P., Le Quere, C., Marland, G., Raupach, M.R. & Wilson, C. (2013) Commentary: The challenge to keep global warming below 2 degrees C. *Nature Climate Change,* **3,** 4-6.

Pfister, C.A. (1998) Patterns of variance in stage-structured populations: Evolutionary predictions and ecological implications. *Proceedings of the National Academy of Sciences of the United States of America,* **95,** 213-218.

Philippi, T. & Seger, J. (1989) Hedging ones evolutionary bets, revisited. *Trends in Ecology & Evolution,* **4,** 41-44.

Phillimore, A.B., Stalhandske, S., Smithers, R.J. & Bernard, R. (2012) Dissecting the Contributions of Plasticity and Local Adaptation to the Phenology of a Butterfly and Its Host Plants. *American Naturalist,* **180,** 655-670.

Pokallus, J.W. & Pauli, J.N. (2015) Population dynamics of a northern-adapted mammal: disentangling the influence of predation and climate change. *Ecological Applications,* **25,** 1546-1556.

Post, E. & Stenseth, N.C. (1999) Climatic variability, plant phenology, and northern ungulates. *Ecology,* **80,** 1322-1339.

Raffalovich, L.E., Deane, G.D., Armstrong, D. & Tsao, H.S. (2008) Model selection procedures in social research: Monte-Carlo simulation results. *Journal of Applied Statistics,* **35,** 1093-1114.

Rand, T.A., Richmond, C.E. & Dougherty, E.T. (2017) Using matrix population models to inform biological control management of the wheat stem sawfly, Cephus cinctus. *Biological Control,* **109,** 27-36.

Rees, M., Childs, D.Z., Metcalf, J.C., Rose, K.E., Sheppard, A.W. & Grubb, P.J. (2006) Seed dormancy and delayed flowering in monocarpic plants: Selective interactions in a stochastic environment. *American Naturalist,* **168,** E53-E71.

Rees, M. & Ellner, S.P. (2009) Integral projection models for populations in temporally varying environments. *Ecological Monographs,* **79,** 575-594.

Reineking, B. & Schroder, B. (2006) Constrain to perform: Regularization of habitat models. *Ecological Modelling,* **193,** 675-690.

Roberts, A.M.I. (2008) Exploring relationships between phenological and weather data using smoothing. *International Journal of Biometeorology,* **52,** 463-470.

Rose, K.E., Louda, S.M. & Rees, M. (2005) Demographic and evolutionary impacts of native and invasive insect herbivores on Cirsium canescens. *Ecology,* **86,** 453-465.

Rotella, J.J., Link, W.A., Chambert, T., Stauffer, G.E. & Garrott, R.A. (2012) Evaluating the demographic buffering hypothesis with vital rates estimated for Weddell seals from 30 years of mark-recapture data. *Journal of Animal Ecology,* **81,** 162-173.

Ruffell, J., Innes, J., Bishop, C., Landers, T., Khin, J. & Didham, R.K. (2015) Using pest monitoring data to inform the location and intensity of invasive-species control in New Zealand. *Biological Conservation,* **191,** 640-649.

Rushton, S.P., Ormerod, S.J. & Kerby, G. (2004) New paradigms for modelling species distributions? *Journal of Applied Ecology,* **41,** 193-200.

Saether, B.E., Engen, S., Moller, A.P., Matthysen, E., Adriaensen, F., Fiedler, W., Leivits, A., Lambrechts, M.M., Visser, M.E., Anker-Nilssen, T., Both, C., Dhondt, A.A., McCleery, R.H., McMeeking, J., Potti, J., Rostad, O.W. & Thomson, D. (2003) Climate variation and regional gradients in population dynamics of two hole-nesting passerines. *Proceedings of the Royal Society B-Biological Sciences,* **270,** 2397-2404.

Salguero-Gomez, R., Jones, O.R., Archer, C.R., Bein, C., de Buhr, H., Farack, C., ... & Vaupel, J.W. (2016) COMADRE: a global data base of animal demography. *Journal of Animal Ecology,* **85,** 371-384.

Salguero-Gomez, R., Jones, O.R., Archer, C.R., Buckley, Y.M., Che-Castaldo, J., Caswell, H., ... & Vaupel, J.W. (2015) The COMPADRE Plant Matrix Database: an open online repository for plant demography. *Journal of Ecology,* **103,** 202-218.

Salguero-Gomez, R., Siewert, W., Casper, B.B. & Tielborger, K. (2012) A demographic approach to study effects of climate change in desert plants. *Philosophical Transactions of the Royal Society B-Biological Sciences,* **367,** 3100-3114.

Sandvik, H., Coulson, T. & Saether, B.E. (2008) A latitudinal gradient in climate effects on seabird demography: results from interspecific analyses. *Global Change Biology,* **14,** 703-713.

Sharp, S.P. & Clutton-Brock, T.H. (2010) Reproductive senescence in a cooperatively breeding mammal. *Journal of Animal Ecology,* **79,** 176-183.

Shelton, A.O. & Mangel, M. (2011) Fluctuations of fish populations and the magnifying effects of fishing. *Proceedings of the National Academy of Sciences of the United States of America,* **108,** 7075-7080.

Simons, A.M. (2011) Modes of response to environmental change and the elusive empirical evidence for bet hedging. *Proceedings of the Royal Society B-Biological Sciences,* **278,** 1601-1609.

Sims, M., Elston, D.A., Larkham, A., Nussey, D.H. & Albon, S.D. (2007) Identifying when weather influences life-history traits of grazing herbivores. *Journal of Animal Ecology,* **76,** 761-770.

Slatkin, M. (1974) Hedging ones evolutionary bets. *Nature,* **250,** 704-705.

Sletvold, N., Dahlgren, J.P., Oien, D.-I., Moen, A. & Ehrlen, J. (2013) Climate warming alters effects of management on population viability of threatened species: results from a 30-year experimental study on a rare orchid. *Global Change Biology,* **19,** 2729-2738.

Sparks, T.H. & Yates, T.J. (1997) The effect of spring temperature on the appearance dates of British butterflies 1883-1993. *Ecography,* **20,** 368-374.

Stenseth, N.C., Chan, K.S., Tavecchia, G., Coulson, T., Mysterud, A., Clutton-Brock, T. & Grenfell, B. (2004) Modelling non-additive and nonlinear signals from climatic noise in ecological time series: Soay sheep as an example. *Proceedings of the Royal Society B-Biological Sciences,* **271,** 1985-1993.

Stenseth, N.C. & Mysterud, A. (2005) Weather packages: finding the right scale and composition of climate in ecology. *Journal of Animal Ecology,* **74,** 1195-1198.

Stenseth, N.C., Mysterud, A., Ottersen, G., Hurrell, J.W., Chan, K.S. & Lima, M. (2002) Ecological effects of climate fluctuations. *Science,* **297,** 1292-1296.

Stenseth, N.C., Ottersen, G., Hurrell, J.W., Mysterud, A., Lima, M., Chan, K.S., Yoccoz, N.G. & Adlandsvik, B. (2003) Studying climate effects on ecology through the use of climate indices: the North Atlantic Oscillation, El Nino Southern Oscillation and beyond. *Proceedings of the Royal Society B-Biological Sciences,* **270,** 2087-2096.

Stopher, K.V., Bento, A.I., Clutton-Brock, T.H., Pemberton, J.M. & Kruuk, L.E.B. (2014) Multiple pathways mediate the effects of climate change on maternal reproductive traits in a red deer population. *Ecology,* **95,** 3124-3138.

Stuble, K.L., Zefferman, E.P., Wolf, K.M., Vaughn, K.J. & Young, T.P. (2017) Outside the envelope: rare events disrupt the relationship between climate factors and species interactions. *Ecology,* **98,** 1623-1630.

Tavecchia, G., Pradel, R., Boy, V., Johnson, A.R. & Cezilly, F. (2001) Sex- and age-related variation in survival and cost of first reproduction in greater flamingos. *Ecology,* **82,** 165-174.

Teller, B.J., Adler, P.B., Edwards, C.B., Hooker, G. & Ellner, S.P. (2016) Linking demography with drivers: climate and competition. *Methods in Ecology and Evolution,* **7,** 171-183.

Thomas, C.D. (2011) Translocation of species, climate change, and the end of trying to recreate past ecological communities. *Trends in Ecology & Evolution,* **26,** 216-221.

Thomas, C.D., Cameron, A., Green, R.E., Bakkenes, M., Beaumont, L.J., Collingham, Y.C., Erasmus, B.F.N., de Siqueira, M.F., Grainger, A., Hannah, L., Hughes, L., Huntley, B., van Jaarsveld, A.S., Midgley, G.F., Miles, L., Ortega-Huerta, M.A., Peterson, A.T., Phillips, O.L. & Williams, S.E. (2004) Extinction risk from climate change. *Nature,* **427,** 145-148.

Thomas, J.A., Simcox, D.J. & Hovestadt, T. (2011) Evidence based conservation of butterflies. *Journal of Insect Conservation,* **15,** 241-258.

Tibshirani, R. (1996) Regression shrinkage and selection via the Lasso. *Journal of the Royal Statistical Society Series B-Methodological,* **58,** 267-288.

Tibshirani, R. (2011) Regression shrinkage and selection via the lasso: a retrospective. *Journal of the Royal Statistical Society Series B-Statistical Methodology,* **73,** 273-282.

Tinsley, R.C., Stott, L.C., Viney, M.E., Mable, B.K. & Tinsley, M.C. (2015) Extinction of an introduced warm-climate alien species, Xenopus laevis, by extreme weather events. *Biological Invasions,* **17,** 3183-3195.

Tomimatsu, H. & Ohara, M. (2010) Demographic response of plant populations to habitat fragmentation and temporal environmental variability. *Oecologia,* **162,** 903-911.

Trauernicht, C., Murphy, B.P., Prior, L.D., Lawes, M.J. & Bowman, D. (2016) Human-Imposed, Fine-Grained Patch Burning Explains the Population Stability of a Fire-Sensitive Conifer in a Frequently Burnt Northern Australia Savanna. *Ecosystems,* **19,** 896-909.

Tredennick, A.T., Hooten, M.B. & Adler, P.B. (2017) Do we need demographic data to forecast plant population dynamics? *Methods in Ecology and Evolution,* **8,** 541-551.

Tuljapurkar, S., Gaillard, J.-M. & Coulson, T. (2009) From stochastic environments to life histories and back. *Philosophical Transactions of the Royal Society B-Biological Sciences,* **364,** 1499-1509.

van de Pol, M. & Cockburn, A. (2011) Identifying the Critical Climatic Time Window That Affects Trait Expression. *American Naturalist,* **177,** 698-707.

Van der Pol, M., Bailey, L.D., McLean, N., Rijsdijk, L., Lawson, C.R. & Brouwer, L. (2016) Identifying the best climatic predictors in ecology and evolution. *Methods in Ecology and Evolution,* **7,** 1246-1257.

Vindenes, Y., Edeline, E., Ohlberger, J., Langangen, O., Winfield, I.J., Stenseth, N.C. & Vollestad, L.A. (2014) Effects of Climate Change on Trait-Based Dynamics of a Top Predator in Freshwater Ecosystems. *American Naturalist,* **183,** 243-256.

Vindenes, Y., Engen, S. & Saether, B.E. (2011) Integral projection models for finite populations in a stochastic environment. *Ecology,* **92,** 1146-1156.

Vindenes, Y., Saether, B.E. & Engen, S. (2012) Effects of demographic structure on key properties of stochastic density-independent population dynamics. *Theoretical Population Biology,* **82,** 253-263.

Walters, M.B. & Reich, P.B. (2000) Seed size, nitrogen supply, and growth rate affect tree seedling survival in deep shade. *Ecology,* **81,** 1887-1901.

Walther, G.R., Post, E., Convey, P., Menzel, A., Parmesan, C., Beebee, T.J.C., Fromentin, J.M., Hoegh-Guldberg, O. & Bairlein, F. (2002) Ecological responses to recent climate change. *Nature,* **416,** 389-395.

Wang, G.M., Hobbs, N., Twombly, S., Boone, R., Illius, A., Gordon, I. & Gross, J. (2009) Density dependence in northern ungulates: interactions with predation and resources. *Population Ecology,* **51,** 123-132.

Warren, M.S., Hill, J.K., Thomas, J.A., Asher, J., Fox, R., Huntley, B., Roy, D.B., Telfer, M.G., Jeffcoate, S., Harding, P., Jeffcoate, G., Willis, S.G., Greatorex-Davies, J.N., Moss, D. & Thomas, C.D. (2001) Rapid responses of British butterflies to opposing forces of climate and habitat change. *Nature,* **414,** 65-69.

Warton, D.I., Blanchet, F.G., O'Hara, R.B., Ovaskainen, O., Taskinen, S., Walker, S.C. & Hui, F.K.C. (2015) So Many Variables: Joint Modeling in Community Ecology. *Trends in Ecology & Evolution,* **30,** 766-779.

Wolkovich, E.M., Cook, B.I., McLauchlan, K.K. & Davies, T.J. (2014) Temporal ecology in the Anthropocene. *Ecology Letters,* **17,** 1365-1379.

Wood, S.N. (2016) Just Another Gibbs Additive Modeller: Interfacing

JAGS and mgcv. arXiv:1602.02539

Wood, S.N. (2017) Generalized Additive Models: An Introduction with R. Chapman and Hall/CRC.

Zou, H. & Hastie, T. (2005) Regularization and variable selection via the elastic net. *Journal of the Royal Statistical Society Series B-Statistical Methodology,* **67,** 301-320.

Chapter 2: Exploring population responses to environmental change when there is never enough data: a structural equation modelling approach

Bethan J. Hindle[1*], Mark Rees[1], Andy W. Sheppard[2], Pedro F. Quintana-Ascencio[3], Eric S. Menges[4] & Dylan Z. Childs[1]

[1] Department of Animal and Plant Sciences, Alfred Denny Building, University of Sheffield, Western Bank, Sheffield, S10 2TN, UK

[2] Commonwealth Scientific and Industrial Research Organisation (CSIRO), Australia

[3] Department of Biology, University of Central Florida, 4000 Central Boulevard, Orlando, FL 32816, USA

[4] Archbold Biological Station, Venus, FL, USA

Abstract

1. Temporal variability in the environment drives variation in individuals' vital rates, with consequences for population dynamics and life history evolution. Integral projection models (IPMs) are data-driven models widely used to study population dynamics and life history evolution of structured populations in temporally variable environments. However, many data sets have insufficient temporal replication for the environmental drivers of vital rates to be identified with confidence, limiting their use for evaluating population level responses to environmental change.

2. Parameter selection, where the kernel is constructed at each time step by randomly selecting the time-varying parameters from their joint probability distribution, is one approach to including stochasticity in IPMs. We consider a structural equation modeling (SEM) approach for modelling the covariance matrix of time-varying parameters, whereby latent variable(s) describe the covariance among vital rate parameters. This decreases the number of parameters to estimate and, where the covariance is positive, the latent variable can be interpreted as a measure of environmental quality. We demonstrate this using simulation studies and two case studies.

3. The simulation studies suggest the SEM approach provides similarly accurate estimates of stochastic population growth rate to estimating an unstructured covariance matrix. We demonstrate how the latent parameter can be perturbed to show how selection on reproductive delays in the monocarp *Carduus nutans* changes under different environmental conditions. We develop a demographic model of the fire dependent herb *Eryngium cuneifolium* to show how a causal indicator (i.e. a driver of the changes in the environmental quality) can be incorporated with the addition of a single parameter. Using perturbation analyses we determine optimal management strategies for this species.

4. This approach estimates fewer parameters than previous approaches and allows novel eco-evolutionary insights. Predictions on population dynamics and life history evolution under different environmental conditions can be made without necessarily identifying causal factors. Environmental drivers can be incorporated with relatively few parameters, allowing for predictions on how populations will be affected by changes to these drivers.

Keywords

Carduus nutans; covariation; environmental variation; *Eryngium cuneifolium*; integral projection model; life history; population dynamics; structural equation model

Introduction

Environmental variation causes individuals' vital rates to vary, affecting population dynamics and life history evolution (Benton & Grant 1996; Boyce *et al.* 2006). Interest in understanding the ecological consequences of environmental variation has increased rapidly as a consequence of global climate change (Stenseth *et al.* 2002; Evans 2012). As experimental approaches to determining how natural populations are affected by environmental variation are frequently impractical, structured demographic models are often used to understand the population level effects of environmental change (Coulson 2012). Environmental effects on vital rates can be complex, with nonlinear effects, multiple interacting drivers, indirect effects, and correlations between the drivers (Darling & Cote 2008; Parmesan *et al.* 2013; Ehrlen *et al.* 2016). These challenges, and the relatively short length of many demographic data sets (Salguero-Gomez *et al.* 2015; Salguero-Gomez *et al.* 2016), mean it is often difficult to identify explicit environmental drivers of vital rates. This restricts the ability of models to predict how populations will respond environmental change (Crone *et al.* 2013).

Environmental variation can drive covariation amongst vital rates (Doak *et al.* 2005; Tomimatsu & Ohara 2010). All else equal, failing to account for this covariation will bias model outputs (Fieberg & Ellner 2001; Metcalf *et al.* 2015). Positive covariance among vital rates, occurring when multiple vital rates are affected by the same environmental drivers (Jongejans *et al.* 2010), increases the variance of the stochastic population growth rate. Negative covariance can also occur as a result of tradeoffs between rates or from opposing effects of environmental variables on different rates (Jongejans & De Kroon 2005; Knops, Koenig & Carmen 2007). However, in plants covariation is predominantly positive (Jongejans *et al.* 2010), and positive covariance appears widespread among other taxa including mammals (e.g. Rotella *et al.* 2012) and birds (e.g. Jenkins, Watson & Miller 1963; Nur & Sydeman 1999).

Stochastic demographic models, such as matrix population models (MPMs; see Caswell 2001) and integral projection models (IPMs; see Ellner, Childs & Rees 2016), are widely used to study population dynamics under temporally variable environments (e.g. Inchausti & Weimerskirch 2001; Vindenes *et al.* 2014). IPMs are usually parameterised by estimating state-fate relationships. Stochastic models allow these relationships to vary temporally using one of two main methods (Metcalf *et al.* 2015). Under a kernel selection approach, a projection kernel is estimated for each year and these are resampled (Rees *et al.* 2006; Williams *et al.* 2015) to preserve the covariance amongst the vital rates. Using a parameter selection approach, a unique kernel is constructed at each time step by randomly selecting the time-varying parameters from their joint probability distribution (Morris & Doak 2002; Vindenes *et al.* 2014). A potential limitation of the parameter selection approach is that an unstructured covariance matrix must be estimated for the set of time varying parameters, often from relatively few temporal replicates.

An alternative to estimating an unstructured covariance matrix is to use a structured model for the temporal parameters (co)variances. Hierarchical structural equation models

(SEMs), whereby one or more latent variables are introduced to capture the covariance among vital rate parameters, are a promising candidate. The latent variable(s) represent the underlying causes of covariation among observed variables, allowing complex multivariate relationships to be described in a simple way. Moreover, these models effectively capture hypotheses about causal variables that cannot be directly measured (Grace & Bollen 2008; Grace *et al.* 2010). The underlying drivers of variation in the latent variables can be included as causal indicators, which allows covariances to be partitioned into explained and unexplained sources of variation. However, despite the broad use of SEM approaches in ecological research (e.g. Zuur *et al.* 2003; Thorson *et al.* 2015; Ohlberger, Scheuerell & Schindler 2016) they are rarely used to parameterise demographic models.

This approach has two potential advantages. First, fewer parameters need to be estimated relative to an unstructured covariance matrix. Second, a small number of latent variables (often just one) may account for the covariation among the vital rates. When this covariance is positive, the latent variable(s) can be interpreted as axes of environmental quality or suitability, where positive values of a single latent variable correspond to environments in which survival, growth and reproduction are all higher than average. The latent term(s) then represent a target for further analysis. For example, perturbing the latent parameter allows predictions to be made on the effects of environmental change on population dynamics or life history selection. Where the degree of temporal replication in the data is insufficient for causal environmental drivers to be identified this may represent the best alternative for exploring how changes in the stochastic part of the environment affect such processes. This method is not dissimilar to the use of broad scale climate indices, such as the North Atlantic Oscillation, as proxies for local environmental conditions (Ottersen *et al.* 2001). Such indices do not directly influence the vital rates, but as they provide an index of the overall climate conditions, incorporating multiple local climate variables, they are often better predictors of the vital rates than local climate variables (Post & Stenseth 1999; Stenseth & Mysterud 2005).

We conduct simulation studies to compare the accuracy of the SEM approach to a standard parameter selection approach, with different numbers of temporally varying parameters. We then apply the approach in two case studies. We construct a demographic model of the monocarpic perennial *Carduus nutans*, and show how the latent parameter can be perturbed to make predictions about optimal life history strategies under changing environments. We explore how selection for strategies to delay reproduction differs as the mean and variance of environmental quality changes. Finally, we develop a demographic model of the rare herb *Eryngium cuneifolium* to show how a known environmental driver (time since fire) can be included as a causal indicator, i.e. an observed variable that influences the latent variable. We use perturbation analyses to determine the optimal fire return interval (FRI) for managing this species.

Simulation study: comparing structural equation modelling and unstructured approaches

We compared the accuracy of population growth estimates from the SEM approach to those derived using an unstructured covariance matrix. We considered two scenarios: a relatively simple life history with four temporally variable vital rates (the 'simple model'), typical of many published IPMs, and a two-stage (juvenile and adult) life history with a total of seven temporally variable vital rates (the 'complex model'). Demographic rate functions in both settings were parameterised using data from a long-term study of the St Kilda Soay sheep (Clutton-Brock & Pemberton 2004). These were used to construct a pair of density independent individual-based models (IBMs; Appendix A1), from which simulated data sets could be generated. Only the correlation coefficients for the temporally varying parameters were allowed to vary in each simulation, such that on each occasion, a correlation matrix was drawn at random from a uniform distribution over the space of positive definite matrices (using rcorrmatrix from the clusterGeneration package in R; Qiu & Joe 2015).

One hundred simulated data sets of 8,000 years were generated from each of the two IBMs. A range of realistic data set lengths were sampled: 12, 25, and 50 years (see Appendix A1 for details). To account for the covariance among vital rates, multivariate demographic models were then parameterised using an unstructured covariance matrix (UCM approach) and a latent variable (SEM approach) parameterisation (Fig. 1). In the simple model, 10 parameters (4 variance and 6 covariances) account for the temporal variation using the UCM approach, whilst the SEM approach estimates 8 parameters. In the complex model 28 parameters are required for the UCM approach and 14 for the SEM approach. The demographic models were fitted using Bayesian methods, implemented in JAGS (Plummer 2003) and run using the runjags package (Denwood in review) in R (R Core Team 2016).

IPMs were constructed from each set of posterior samples (Fig. 1; Appendix A1). The stochastic population growth rate was estimated after excluding the first 2,000 years of a 10,000 year simulation. This was repeated with 1,000 samples from the posterior. The true stochastic population growth rate was estimated using an IPM parameterised with the true parameter values used in the IBM.

The results of the simulation study are summarised in Fig. 2. The UCM approach led to marginally less diffuse estimates of stochastic population growth rate than the SEM approach. This was true for both the simple (Fig. 2a) and complex (Fig. 2b) models. However, even with 12 years of temporal replication the differences between the performance of the two methods was small, and with 25 years of replication both methods performed well.

ai)

Structural equation modelling approach

Growth
$g^t(z',z) \sim N(\mu^g_{[z,t]}, \sigma^g)$
$\mu^g_{[z,t]} = \beta^g_0 + \beta^g_z z + \beta^g_Q Q_{[t]} + \varepsilon^g_{[t]}$ → $\varepsilon^g_{[t]} \sim N(0, \sigma^g_{Yr})$

Survival
$\text{logit}(s^t(z)) = \beta^s_0 + \beta^s_z z + \beta^s_Q Q_{[t]} + \varepsilon^s_{[t]}$ → $\varepsilon^s_{[t]} \sim N(0, \sigma^s_{Yr})$

Reproduction
$\text{logit}(r^t(z)) = \beta^r_0 + \beta^r_z z + \beta^r_Q Q_{[t]} + \varepsilon^r_{[t]}$ → $\varepsilon^r_{[t]} \sim N(0, \sigma^r_{Yr})$

Recruit size
$rs^t(z') \sim N(\mu^{rs}_{[t+1]}, \sigma^{rs})$
$\mu^{rs}_{[t+1]} = \beta^{rs}_0 + \beta^{rs}_z z + \beta^{rs}_Q Q_{[t]} + \varepsilon^{rs}_{[t]}$ → $\varepsilon^{rs}_{[t]} \sim N(0, \sigma^{rs}_{Yr})$

$Q_{[t]} \sim N(0,1)$

Unstructured covariance matrix approach

Growth
$g^t(z',z) \sim N(\mu^g_{[z,t]}, \sigma^g)$
$\mu^g_{[z,t]} = \beta^g_0 + \beta^g_z z + \varepsilon^g_{[t]}$

Survival
$\text{logit}(s^t(z)) = \beta^s_0 + \beta^s_z z + \varepsilon^s_{[t]}$

Reproduction
$\text{logit}(r^t(z)) = \beta^r_0 + \beta^r_z z + \varepsilon^r_{[t]}$

Recruit size
$rs^t(z') \sim N(\mu^{rs}_{[t+1]}, \sigma^{rs})$
$\mu^{rs}_{[t+1]} = \beta^{rs}_0 + \beta^{rs}_z z + \varepsilon^{rs}_{[t]}$

$\varepsilon_{[t]} \sim MVN(0, \Sigma)$

ii)
$$n(z',t+1) = \int_\Omega [s^t(z)g^t(z',z) + 0.5 s^t(z)r^t(z)r_e rs^t(z',z)] n(z,t)dz$$

bi)

Structural equation modelling approach

Adult survival
$\text{logit}(a^t(z)) = \beta^a_0 + \beta^a_z z + \beta^a_Q Q_{[t]} + \varepsilon^a_{[t]}$ → $\varepsilon^a_{[t]} \sim N(0, \sigma^a_{Yr})$

Adult growth
$b^t(z',z) \sim N(\mu^b_{[z,t]}, \sigma^b)$
$\mu^b_{[z,t]} = \beta^b_0 + \beta^b_z z + \beta^b_Q Q_{[t]} + \varepsilon^b_{[t]}$ → $\varepsilon^b_{[t]} \sim N(0, \sigma^b_{Yr})$

Juvenile survival
$\text{logit}(s^t(z)) = \beta^s_0 + \beta^s_z z + \beta^s_Q Q_{[t]} + \varepsilon^s_{[t]}$ → $\varepsilon^s_{[t]} \sim N(0, \sigma^s_{Yr})$

Juvenile growth
$g^t(z',z) \sim N(\mu^g_{[z,t]}, \sigma^g)$
$\mu^g_{[z,t]} = \beta^g_0 + \beta^g_z z + \beta^g_Q Q_{[t]} + \varepsilon^g_{[t]}$ → $\varepsilon^g_{[t]} \sim N(0, \sigma^g_{Yr})$

Maturation
$\text{logit}(m^t(z)) = \beta^m_0 + \beta^m_z z + \beta^m_Q Q_{[t]} + \varepsilon^m_{[t]}$ → $\varepsilon^m_{[t]} \sim N(0, \sigma^m_{Yr})$

Reproduction
$\text{logit}(r^t(z)) = \beta^r_0 + \beta^r_z z + \beta^r_Q Q_{[t]} + \varepsilon^r_{[t]}$ → $\varepsilon^r_{[t]} \sim N(0, \sigma^r_{Yr})$

Recruit size
$rs^t(z') \sim N(\mu^{rs}_{[t+1]}, \sigma^{rs})$
$\mu^{rs}_{[t+1]} = \beta^{rs}_0 + \beta^{rs}_z z + \beta^{rs}_Q Q_{[t]} + \varepsilon^{rs}_{[t]}$ → $\varepsilon^{rs}_{[t]} \sim N(0, \sigma^{rs}_{Yr})$

$Q_{[t]} \sim N(0,1)$

Unstructured covariance matrix approach

Adult survival
$\text{logit}(a^t(z)) = \beta^a_0 + \beta^a_z z + \varepsilon^a_{[t]}$

Adult growth
$b^t(z',z) \sim N(\mu^b_{[z,t]}, \sigma^b)$
$\mu^b_{[z,t]} = \beta^b_0 + \beta^b_z z + \varepsilon^b_{[t]}$

Juvenile survival
$\text{logit}(s^t(z)) = \beta^s_0 + \beta^s_z z + \varepsilon^s_{[t]}$

Juvenile growth
$g^t(z',z) \sim N(\mu^g_{[z,t]}, \sigma^g)$
$\mu^g_{[z,t]} = \beta^g_0 + \beta^g_z z + \varepsilon^g_{[t]}$

Maturation
$\text{logit}(m^t(z)) = \beta^m_0 + \beta^m_z z + \varepsilon^m_{[t]}$

Reproduction
$\text{logit}(r^t(z)) = \beta^r_0 + \beta^r_z z + \varepsilon^r_{[t]}$

Recruit size
$rs^t(z') \sim N(\mu^{rs}_{[t+1]}, \sigma^{rs})$
$\mu^{rs}_{[t+1]} = \beta^{rs}_0 + \beta^{rs}_z z + \varepsilon^{rs}_{[t]}$

$\varepsilon_{[t]} \sim MVN(0, \Sigma)$

ii)
$$n_j(z',t+1) = \int_\Omega [s^t(z)g^t(z',z)(1-m^t(z)) + 0.5 s^t(z)m^t(z)r^t(z)r_e rs^t(z',z)]n_j(z,t)dz + \int_\Omega [0.5 a^t(z)r^t(z)r_e rs^t(z'z)]n_a$$

$$n_a(z',t+1) = \int_\Omega [s^t(z)g^t(z',z)m^t(z)]n_j(z,t)dz + \int_\Omega [a^t(z)b^t(z',z)]n_a(z,t)]dz$$

Figure 1: Structure of the i) vital rate models and ii) IPMs for the a) simple and b) complex life history simulation models. In the SEM approach factor-loading terms (β_Q) allowed the direction and magnitude of the latent parameter (Q) to differ among the vital rates. Submodel specific year effects (ε) accounted for any additional variation among years. In the UCM approach a fully unstructured covariance matrix (Σ) was estimated by sampling the year effects (ε) from a multivariate normal distribution. β_0 parameters are the intercepts and β_z are slopes with respect to size. aii) is the structure of the IPM for the simple life history model, where $n(z,t)$ is the size distribution of individuals at time t, $s^t(z)g^t(z',z)$ is a survival growth kernel and $0.5 s^t(z)r^t(z)r_e rs^t(z',z)$ gives the size distribution of new recruits. The superscript t denotes stochastic terms. bii) is the structure of the IPM for the complex model. The size distribution of juveniles at time t, $n_j(z,t)$, is given by the survival and growth of juveniles at $t-1$ that do not mature that year, $s^t(z)g^t(z',z)(1-m^t(z)$, and the reproduction of adults, $0.5 a^t(z)r^t(z)r_e rs^t(z',z)$, and juveniles that have matured that year, $0.5 s^t(z)m^t(z)r^t(z)r_e c^t(z',z)$. The size distribution of adults at time t, $n_a(z,t)$, is given by the survival-growth function of maturing juveniles, $s^t(z)g^t(z',z)m^t(z)$, and the survival growth function of adults, $a^t(z)b^t(z',z)$. In both a) and b) the functions in the IPMs correspond to the functions in i), with the exception of lamb recruitment (r_e), which is assumed not to vary with time (Appendix A1).
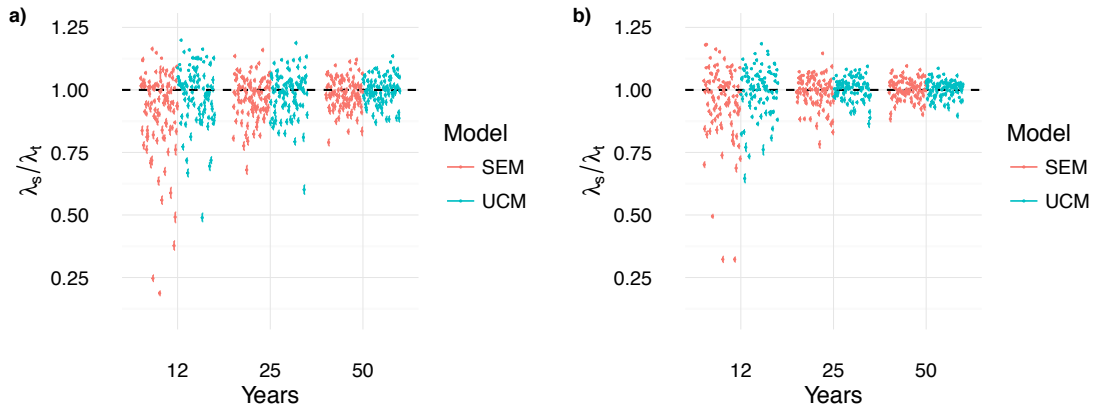
Figure 2: Ratio between the true (λ_t) and estimated (λ_s) stochastic population growth rates for the structural equation modelling (SEM) and unstructured covariance matrix (UCM) approaches for the a) simple and b) complex models. Points are the median and lines show the 0.025 and 0.975 quantiles across 1000 samples from the posteriors for each simulation. The dashed line is at one, where the estimated growth rate equals the true growth rate.

Case study 1: The effect of environmental quality on reproductive delays in *Carduus nutans*

Background and methods

Carduus nutans is a monocarpic thistle with a persistent seedbank and short-lived rosettes (Popay & Medd 1990; Wardle, Nicholson & Rahman 1992). We use a SEM model to explore how environmental change may affect selection for reproductive delays in this species. Reproductive delays can act as a form of diversified bet hedging, spreading a cohort across multiple years and therefore decreasing the effect of a bad year on the cohort as a whole (Cohen 1966; Tuljapurkar 1990; Rees *et al.* 2006; Childs, Metcalf & Rees 2010). In monocarpic perennial plants, reproduction may be deferred pre-establishment, through a seedbank, or post-establishment, through a delay in flowering (Childs *et al.* 2004; Rees *et al.* 2006). Post-establishment delays have the additional benefit of higher fecundity as individuals may grow larger, producing more seeds (Rees *et al.* 2006).

We define the fittest strategy to be the evolutionary stable strategy (ESS). The predicted ESS for the study population is substantial seed dormancy and the majority of plants to flower in their first year, with a flowering probability of ~0.75 for an average sized individual (Rees *et al.* 2006). Using our framework we predict how changes to the average or variability of the environment affect the ESS germination and flowering strategy. We re-parameterised the IPM of Rees et al (2006; Fig. 3a, Appendix A2). The model is structured by the natural logarithm of rosette area (z), a measure of plant size that predicts individual performance. Four stochastic vital rate functions, with temporally variable intercepts, were estimated; survival, growth, recruitment, and recruit size (Fig. 3).

The vital rate parameters (Fig. 3b) were estimated using MCMC sampling in JAGS through runjags (Denwood in review). The prior distributions were weakly informative (i.e. within biologically reasonable ranges) to improve mixing (Appendix A2; see Appendix A3 for

comparison with more informative priors). The vital rates were integrated into the IPM (Fig. 3) using the posterior means as parameter estimates. At each year in the simulation the latent parameter (Q) was sampled from a normal distribution with a mean of zero and a standard deviation of one. The submodel specific year effects (ε) were drawn from normal distributions with means of zero and the standard deviations (σ_{Yr}) estimated in the vital rates model.

Posterior checks suggested the latent parameter (Q) accounted for the covariation among the vital rates (Fig. S1). The 95% credible intervals of many parameters were relatively wide (Fig. 3c), as a result of the short temporal extent (eight years) of this data set. The positive covariance among the vital rates (Fig. 3 & S2) means the latent parameter (Q) can be assumed to be a measure of environmental quality. The highest levels of temporal variation were in survival and recruitment (Fig. S2). The joint flowering intercept and germination probability ESS were predicted using numerical invasion analysis (Childs *et al.* 2004) and were similar to those produced using a fixed effects, kernel selection approach (Appendix A4; Rees *et al.* 2006).

a) $S(t+1)=(1-d)(1-g)S(t)+(1-g)\int_{\Omega} f^{t}(z)n(z,t)dz,$

$n(z',t+1)=s_{g}^{t}(z')S(t)+\int_{\Omega}[p^{t}(z',z)+f^{t}(z',z)]n(z,t)dz$
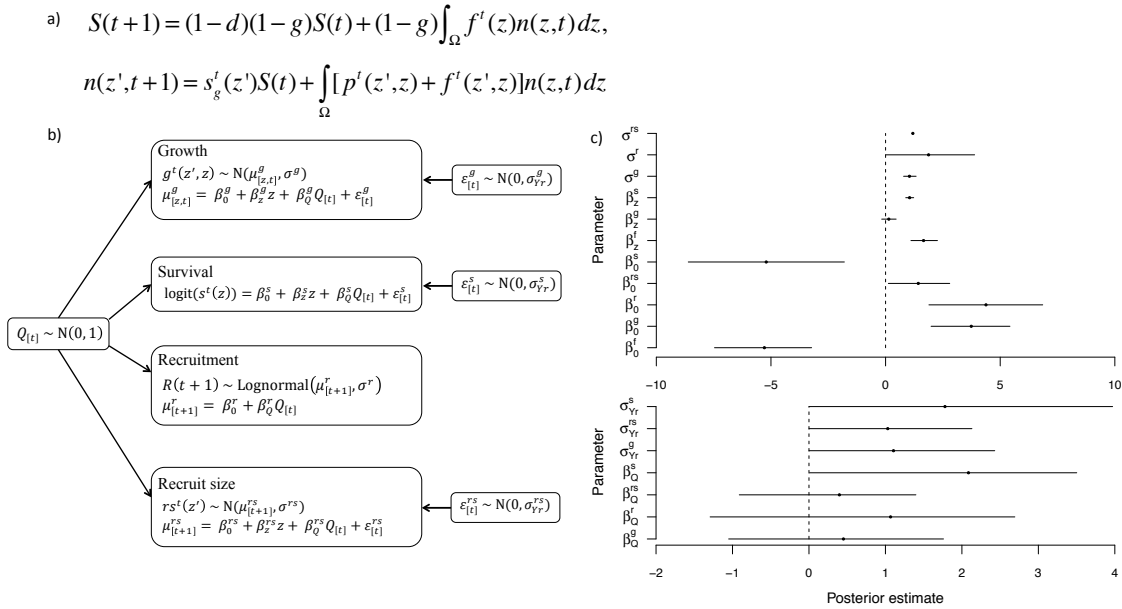
Figure 3: a) *Carduus* IPM kernel (see Appendix A2), where $S(t)$ is the number of seeds in the seedbank and $n(z',t)dz$ is the size distribution of rosettes in year t. The first term in the seedbank equation equates to seeds present in the seedbank at time t that have not died (with probability of seed mortality d) or germinated (with probability of germination g). The second term is seeds produced by rosettes, where $f^{t}(z)$ is a seed production function. The rosette equation can be split into three terms, describing seeds germinating from the seedbank ($s_{g}^{t}(z')$), rosette survival and growth ($p^{t}(z',z)$) and seeds produced that year that germinate immediately ($f^{t}(z',z)$). The superscript t denotes stochastic terms. b) Structure of the stochastic vital rates model, including equations for each submodel, and c) posterior distributions for (i) fixed parameters and (ii) parameters for incorporating temporal variation. The [t] subscripts indicate stochastic terms. β_0 parameters are the intercepts, β_z and β_Q parameters are slopes with respect to size (z) and the latent parameter (Q) respectively and ε are submodel specific year effects. $\sigma_{Yr}^{s}, \sigma_{Yr}^{rs}$ and σ_{Yr}^{g} are the standard deviations of the submodel specific year effects for survival, recruit size and growth respectively. Recruitment refers to the number of seedlings at the annual census; as this is a single number each year an additional year effect is not included here. c) shows the mean (points) and 95% credible interval (horizontal lines) for each parameter. Vertical dashed lines are at 0.
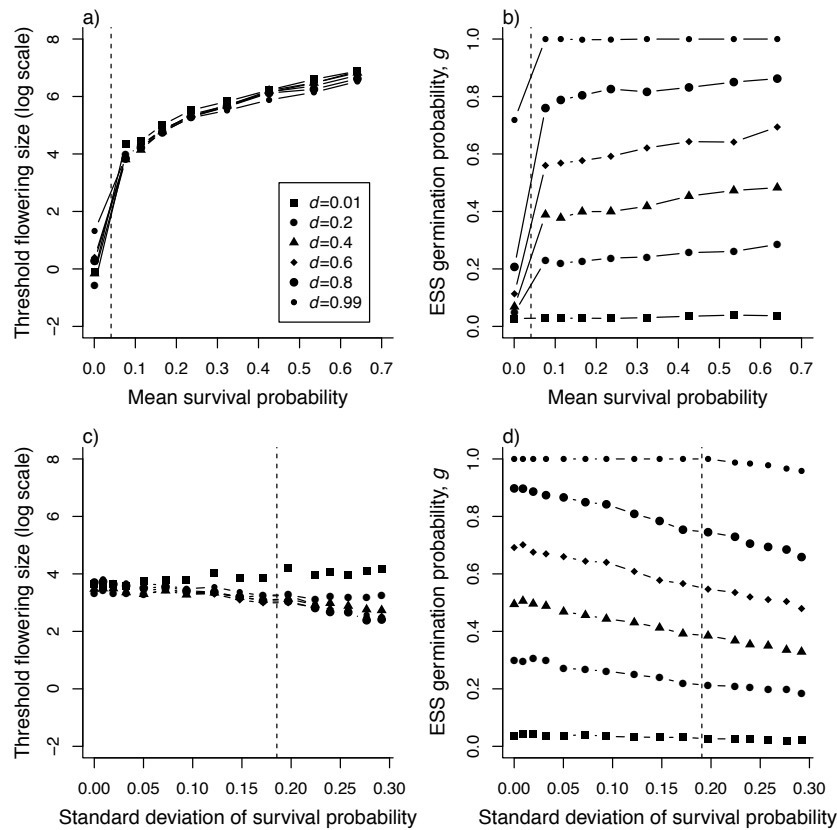
Figure 4: Effect of changing the mean (a & b) and variability (c & d) of the environmental quality (Q) on the joint ESS flowering intercept and germination strategies at different levels of seed mortality (d) in *Carduus*. Changes to the environmental quality here are shown through the impact on survival of an averaged sized individual (log size 1.95, which is the mode of the study population). Threshold flowering size is calculated as $-\beta_0^f / \beta_z^f$ (Childs *et al.* 2003). Dashed lines show the mean survival probability (a and b) and standard deviation of the survival probability (c and d) for the average sized individual in the environment experienced by the study population.

Perturbation analyses

A prospective sensitivity analysis was used to determine how selection on delayed flowering and germination may change as the mean and variance of environmental quality (Q) changes. The mean and standard deviations of Q were varied on a fixed grid and the ESS were predicted at each value. This was repeated for a range of seed mortalities (d=0.01, 0.1, 0.2…0.9, 0.99; Rees *et al.* 2006).

As the quality of the environment deteriorates there is selection for earlier flowering and reduced germination, whilst improving the quality of the environment leads to the opposite response, i.e. selection for a perennial life history dominates in higher quality environments (Figs 4 & S3). In lower quality environments selection acts on the germination probability, delaying reproduction pre-establishment by increasing the chance of seeds entering the seedbank. The estimated survival probability increases from 0.04 to 0.73 with an increase in Q from 0 to 2 for a rosette of log size 1.95 (mode of the study population). With a mean Q of 2 there is an advantage in delaying reproduction, as the risk of mortality is relatively small and larger plants can produce more seeds; here, selection acts on the flowering size, increasing the

size at which plants reproduce. The ESS threshold flowering size, on a log scale, doubles from 3.36 to 7.10 with an increase in mean Q from 0 to 2, resulting in a 9-fold increase in the estimated number of seeds produced. Increasing levels of environmental variability generally caused selection for earlier flowering and a lower germination probability (Fig. 4).

Case study 2: Incorporating an environmental driver: the effect of fire on the demography of *Eryngium cuneifolium*

Background and methods

Eryngium is a fire-adapted perennial herb with a persistent seedbank (Menges & Kimmich 1996; Menges & Quintana-Ascencio 2004) found in Florida rosemary scrub, in recently burned or other disturbed areas (Menges & Kimmich 1996). Fire kills the majority of rosettes and the population recovers through the seedbank (Menges & Kohfeldt 1995). We used demographic data from a single population that forms part of a well-studied meta-population at the Archbold Biological Station, Florida (Appendix A2; Menges & Quintana-Ascencio 2004).

Altering the frequency of fires is one possible management strategy for this endangered species. The recommended fire return interval (FRI) for this species of <15 years (Menges & Quintana-Ascencio 2004) differs from the 15-30 year recommendations for its Florida scrubland habitat (Menges 2007). Alternative management strategies may therefore be required for *Eryngium*. We use perturbation analyses to determine how altering FRIs and the effect of fire on the vital rates affects population growth.

The *Eryngium* IPM (Fig. 5a; Appendix A2) was structured by the natural logarithm of rosette diameter (Menges & Quintana-Ascencio 2004). We assume density independent dynamics to investigate the persistence of the population (Menges & Quintana-Ascencio 2004, see Appendix A5 for model with density dependent recruitment). The intercepts of four vital rates were assumed to be temporally variable (Fig. 5b): survival, growth, flowering probability, and fecundity (the number of flowering stems; Appendix A2). As the demography of *Eryngium* is strongly affected by fire, we modelled the mean of the latent parameter (Q) as a linear function of time since fire (TSF; Figs 5b & S4). Flowering and fecundity were highly correlated, so the flowering (ε^f) and fecundity (ε^{fe}) year effects were sampled from a bivariate normal distribution. Sampling these parameters from univariate distributions results in the latent variable failing to fully account for the covariation among the vital rates (Fig. S5). Posterior samples were again drawn using MCMC sampling in JAGS, using runjags (Denwood in review). Weakly informative priors were used (Appendix A2; see Appendix A3 for a comparison with more informative priors). The vital rates were negatively related with TSF, with survival particularly strongly affected (Figs 5b & S6).

The posterior means were used to parameterise an IPM. At each iteration the latent parameter (Q) was randomly sampled from a normal distribution with mean $\beta_{tsf} \times TSF$ and standard deviation of one. Sub-model specific year effects were drawn from normal

distributions (bivariate normal for flowering and fecundity), with means of zero and the estimated (co)variances. Estimates of germination probability range from 0 to 0.1 and 0.005 to 0.04 for first (g_f) and second year germination (g_{sb}) respectively (Quintana-Ascencio & Menges 2000; Menges & Quintana-Ascencio 2004). To select a fertility scenario for the perturbation analyses predicted dynamics using a range of these estimates and of seed mortality probabilities (0.5, 0.7, 0.9) were compared to those observed in the field (Appendix A2). A model with low first year germination (0.0), high germination from the seedbank (0.04) and low seed mortality (0.5) was selected as it was consistent with observed changes in aboveground population growth (Fig. 6a). That is, aboveground populations were predicted to increase immediately following a fire, but not beyond ten years postfire (Menges & Quintana-Ascencio 2004).

a)
$$S(t+1)=(1-d)(1-g_{sb})S(t)+(1-d)(1-g_f)\int f^t(z)m(z,t)dz,$$
$$n(z',t+1)=s_g^t(z')S(t)+\int_{\Omega}[p^t(z',z)+f^t(z',z)]n(z,t)dz$$
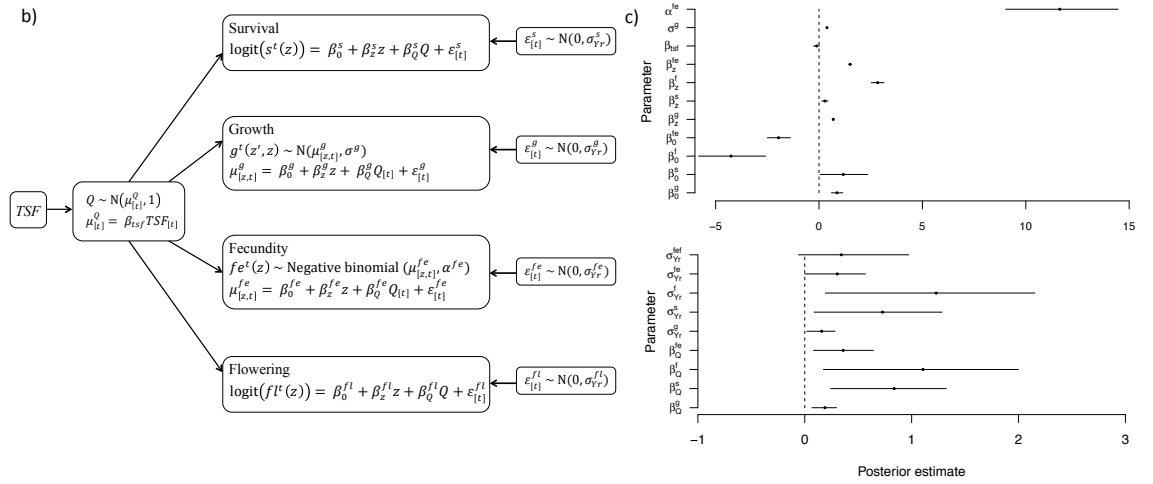
Figure 5: a) *Eryngium* IPM kernel (see Appendix A2). The first term of the seedbank (S) equation is those seeds that remain in the seedbank from t to $t+1$; they do not die, with probability $1-d$, and do not germinate, with probability $1-g_{sb}$. The second term refers to seeds produced that year that enter the seedbank. The size distribution of rosettes at $t+1$ is given by those seeds germinating from the seedbank $s_g^t(z')$, a survival-growth function, $p^t(z',z)$, of rosettes at t and fecundity function, $f^t(z',z)$. b) Structure of *Eryngium* stochastic vital rates model, including equations for each submodel and b) posteriors for this model for (i) fixed effects and (ii) year effects. β_0 parameters are intercepts, β_z and β_Q parameters are slopes with respect to size (z) and the latent parmeter (Q) respectively and ε are submodel specific year effects. σ^g and σ^r are the standard deviation for the growth and recruitment functions respectively and α^{fe} is the dispersion parameter for the fecundity function. σ_{Yr} parameters are the standard deviations of the submodel specific year effects; σ_{Yr}^{fef} is the covariance between the fecundity and flowering year effects. In b) the points show the means and horizontal lines show the 95% credible intervals for each parameter; the vertical dashed line is at 0.

Perturbation analyses

The effects of different fire regimes were explored using a range of constant fire return intervals (FRIs) from two to 30 years. Stochastic population growth rates were estimated by iterating 100 populations for 1,000 years; the first 200 years were excluded as transient dynamics. We found

populations were likely to decline where the time between fires was too short (c.<4 years), because plants do not produce enough seeds to replenish the seedbank, or too long (c.>15 years; Fig. 6b), as they are outcompeted. This is in accordance with a previous study, using a matrix selection approach, which found an optimal FRI of less than 15 years (Menges & Quintana-Ascencio 2004).

To determine how altering the effect of fire on the vital rates affected population growth the β_{tsf} parameter was perturbed. This is a measure of how quickly the environment decays as TSF increases; more negative values of this parameter indicate the quality of the environment decreases more quickly following a fire. Stochastic population growth rates were estimated as before, but the fire regimes were varied randomly throughout the simulations (with the same chance of each FRI occurring), either between 1 and 15 years (optimum for *Eryngium*) or between 15 and 30 years (optimum for Florida scrub habitat). Decreasing β_{tsf} by around 1/3 could make a 15:30 year FRI strategy sustainable for *Eryngium* (Fig. 6c). The effect of altering the temporal decay of the environment is much higher when the FRI is higher, to the extent that decreasing β_{tsf} sufficiently can make longer FRIs preferable for *Eryngium* (Fig. 6c).

Figure 6: (a) Aboveground population growth rate $\left(r = log\left(\frac{N_t}{N_{t-1}}\right) \right)$ estimated from 1000 simulations of 22 years each for *Eryngium*. Red points are the observed growth rates and mean sizes for the study population and three other populations (site numbers 45, 57 and 91) with similar FRIs. (b) Log λ_s under different burning regimes, (c) effect of changing value of β_{tsf} on log λ_s under two different FRIs. In all four plots $g_f = 0.0, g_{sb} = 0.04,$ and $d = 0.5$. Points show the median, thicker bars and thinner bars show interquartile range and 95% quantiles respectively. Dotted vertical line in (c) shows the estimated value of β_{tsf}.

Discussion

Identifying the environmental drivers of variation in demographic performance is challenging. A variety of approaches have been proposed (e.g. Teller *et al.* 2016; Van der Pol *et al.* 2016), but the performance of any method is limited by the degree of temporal replication available. The mean length for a demographic data set is six years in plants and eleven in animals (Salguero-Gomez *et al.* 2015; Salguero-Gomez *et al.* 2016). Yet, simulations suggest 20-25 years of data are needed to identify environmental drivers, determine the temporal window over which they act and reliably estimate the magnitude of their effects (Teller *et al.* 2016; Van der

Pol *et al.* 2016). Efforts to identify drivers in many of these populations will not succeed, forcing population ecologists to assess the likely effects of environmental change using indirect methods. The observation that, in natural populations, different components of demographic performance covary, often positively, (Nur & Sydeman 1999; Jongejans *et al.* 2010; Rotella *et al.* 2012) implies different demographic processes respond (at least in part) to the same drivers. We have demonstrated how a structural equation modelling (SEM) framework can be used to incorporate a temporal axis of environmental variation into a demographic model. The resulting multi-process model—coupled via a latent 'environmental quality' variable—requires fewer parameters than its unstructured (UCM) counterpart. In principle, SEM models may yield more precise estimates of population growth, though this comes at a potential cost of increased bias when the model is insufficiently flexible. In practice, in our simulation study the UCM and SEM approaches yielded comparable estimates of population growth rate. Thus, the main advantage of the SEM approach is that it identifies the main axes of demographic variation, which provide a basis for understanding how populations may respond to environmental change.

When it is not possible to explicitly identify environmental drivers of demographic variation, local perturbation analysis of model parameters can be used to explore the potential response of a population to environmental change (Rees & Ellner 2009). These analyses typically consider each parameter in turn, assessing its effect on metrics such as population growth rate while holding all else constant. However, the existence of (positive) temporal correlations among demographic processes suggests multiple processes respond in a coordinated manner to environmental change. A SEM model allows us to identify the potential axis of change and, by focusing perturbation analyses on this axis, makes population level predictions under different environmental conditions possible. For example, this allowed us to make predictions on how life histories may evolve under putative environmental conditions. We identified how the environmental quality would have to change for *Carduus* to alter its flowering strategy; showing that increases in its average vital rates, in particular survival, will lead to selection for a perennial life history. Whilst we focus here on temporal variation this approach could also be used to predict joint demographic responses to spatial variation (Elderd & Miller 2016).

The key limitation is that this interpretation of the model assumes temporal covariances are largely environmentally driven. This may not be true if individuals substantially adjust their allocation strategy in response to environmental conditions. Negative correlations among the vital rates may exist due to life history trade-offs between vital rates, where for example resources are invested in survival or reproduction to the detriment of growth (Koenig & Knops 1998). Negative correlations appear relatively rare however (Jongejans *et al.* 2010), and where they do exist are sometimes attributable to opposing responses to environmental drivers (e.g. Knops, Koenig & Carmen 2007). This suggests the magnitude of trade-off effects is generally

small compared to that of environmental effects, though life history trade-offs may still attenuate environmental driver(s) of covariation.

Explicitly incorporating environmental drivers allows population responses to management strategies or anticipated environmental change to be predicted (e.g. Gotelli & Ellison 2006; Isaza *et al.* 2016). The SEM approach can simplify the process of incorporating such drivers, as they can be included into a single model of the shared environmental axis. Where explicit environmental drivers (e.g. population density or temperature) can be identified, these are typically considered on a process-specific basis, by constructing separate models for survival, reproduction, growth, and recruitment (e.g. Dahlgren, Ostergard & Ehrlen 2014; Williams *et al.* 2015). This would require the addition of four time-since-fire slope parameters in our *Eryngium* case study, one for each temporally variable vital rate (e.g. Evans, Holsinger & Menges 2010). Instead, we introduced a higher-level model, decomposing the shared axis of environmental variation into explained and residual components of variation. Thus the effects of time since fire on all four vital rates were incorporated with the addition of a single parameter. This allowed us to evaluate the population level effects of two alternative management strategies; that is altering the disturbance regime or ameliorating the environment to decrease the rate of decay in environmental quality following a disturbance. We found that whilst the optimum FRI for *Eryngium* is less than 15 years, decreasing the rate of environmental decay could lead to persistent populations under 15-30 year fire regimes (the recommended FRI for the Florida scrub habitat; Menges 2007).

Similar approaches to our analysis have been used previously (Evans, Holsinger & Menges 2010; Evans & Holsinger 2012; Elderd & Miller 2016). However, in previous models the slope terms for the environmental quality parameter (β_Q) were constrained to a value of +1 or -1 among a set of demographic models. These usually operate on different scales, for example probabilities, such as survival and flowering, are typically estimated on a logit scale, whereas fecundity is generally estimated on a log scale; a unit change on these two scales cannot be meaningfully compared. Moreover, differences in the magnitude of the effect of temporal variation among the vital rates were accounted for by the process specific year effects (ε). Thus the main advantage of the SEM approach is lost, as the latent variable cannot be conceived as a simple measure of overall environmental quality.

Adopting a Bayesian approach has a number of benefits (Elderd & Miller 2016), for example allowing the effects of difference sources of uncertainty to be quantified (Evans, Holsinger & Menges 2010). Uncertainty is likely to be very high for most data sets (Metcalf *et al.* 2015). Parameter uncertainty can have important ecological implications, for example failing to account for it may underestimate the risk of extinction (Ludwig 1996). Using a Bayesian approach also allows for posterior predictive checks (Gelman *et al.* 2004). These are particularly important when fitting very constrained models, for example when assuming the temporal covariation in the vital rates may be explained by a single environmental axis. Sometimes, as in

the *Eryngium* case study, additional axes may be necessary to fully account for the covariation in the vital rates. We recommend starting with a simple model structure and slowly adding in complexity.

Rapid levels of environmental change have increased interest in determining how population processes respond to environmental stochasticity (Stenseth *et al.* 2002; Evans 2012). However, the long-term individual level data needed to accurately quantify such responses are often lacking, especially for rare species. Where positive covariances exist among vital rates these can be exploited under a SEM approach to allow predictions on the joint responses of vital rates to environmental variation. Where insufficient data exist to identify environmental drivers the SEM approach may offer the best alternative for predicting population responses to environmental change.

Acknowledgements

References

Benton, T.G. & Grant, A. (1996) How to keep fit in the real world: Elasticity analyses and selection pressures on life histories ln a variable environment. *American Naturalist,* **147,** 115-139.

Boyce, M.S., Haridas, C.V., Lee, C.T. & Demography, N.S. (2006) Demography in an increasingly variable world. *Trends in Ecology & Evolution,* **21,** 141-148.

Caswell, H. (2001) Matrix population models: Construction, analysis, and interpretation. *Matrix population models: Construction, analysis, and interpretation***,** i-xxii, 1-722.

Childs, D.Z., Metcalf, C.J.E. & Rees, M. (2010) Evolutionary bet-hedging in the real world: empirical evidence and challenges revealed by plants. *Proceedings of the Royal Society B-Biological Sciences,* **277,** 3055-3064.

Childs, D.Z., Rees, M., Rose, K.E., Grubb, P.J. & Ellner, S.P. (2003) Evolution of complex flowering strategies: an age- and size-structured integral projection model. *Proceedings of the Royal Society B-Biological Sciences,* **270,** 1829-1838.

Childs, D.Z., Rees, M., Rose, K.E., Grubb, P.J. & Ellner, S.P. (2004) Evolution of size-dependent flowering in a variable environment: construction and analysis of a stochastic integral projection model. *Proceedings of the Royal Society B-Biological Sciences,* **271,** 425-434.

Clutton-Brock, T.H. & Pemberton, J.M. (2004) *Soay Sheep: Dynamics and Selection in an Island Population*.

Cohen, D. (1966) Optimizing reproduction in a randomly varying environment. *Journal of Theoretical Biology,* **12,** 119-&.

Coulson, T. (2012) Integral projections models, their construction and use in posing hypotheses in ecology. *Oikos,* **121,** 1337-1350.

Crone, E.E., Ellis, M.M., Morris, W.F., Stanley, A., Bell, T., Bierzychudek, P., ... & Menges, E.S. (2013) Ability of Matrix Models to Explain the Past and Predict the Future of Plant Populations. *Conservation Biology,* **27,** 968-978.

Dahlgren, J.P., Ostergard, H. & Ehrlen, J. (2014) Local environment and density-dependent feedbacks determine population growth in a forest herb. *Oecologia,* **176,** 1023-1032.

Darling, E.S. & Cote, I.M. (2008) Quantifying the evidence for ecological synergies. *Ecology Letters,* **11,** 1278-1286.

Denwood, M.J. (in review) runjags: An R package providing interface utilities, parallel computing methods and additional distributions for MCMC models in JAGS. Journal of Statistical Software.

Doak, D.F., Morris, W.F., Pfister, C., Kendall, B.E. & Bruna, E.M. (2005) Correctly estimating how environmental stochasticity influences fitness and population growth. *American Naturalist,* **166,** E14-E21.

Ehrlen, J., Morris, W.F., von Euler, T. & Dahlgren, J.P. (2016) Advancing environmentally explicit structured population models of plants. *Journal of Ecology,* **104,** 292-305.

Elderd, B.D. & Miller, T.E.X. (2016) Quantifying demographic uncertainty: Bayesian methods for integral projection models. *Ecological Monographs,* **86,** 125-144.

Ellner, S.P., Childs, D.Z. & Rees, M. (2016) *Data-driven modelling of structured populations: A practical guide to the Integral Projection Model*. Springer, Switzerland.

Evans, M.E.K. & Holsinger, K.E. (2012) Estimating covariation between vital rates: A simulation study of connected vs. separate generalized linear mixed models (GLMMs). *Theoretical Population Biology,* **82,** 299-306.

Evans, M.E.K., Holsinger, K.E. & Menges, E.S. (2010) Fire, vital rates, and population viability: a hierarchical Bayesian analysis of the endangered Florida scrub mint. *Ecological Monographs,* **80,** 627-649.

Evans, M.R. (2012) Modelling ecological systems in a changing world. *Philosophical Transactions of the Royal Society B-Biological Sciences,* **367,** 181-190.

Fieberg, J. & Ellner, S.P. (2001) Stochastic matrix models for conservation and management: a comparative review of methods. *Ecology Letters,* **4,** 244-266.

Gelman, A., Carlin, J.B., Stern, H.S. & Rubin, D.B. (2004) *Bayesian Data Analysis, Second Edition*. Chapman and Hall/CRC.

Gotelli, N.J. & Ellison, A.M. (2006) Forecasting extinction risk with nonstationary matrix models. *Ecological Applications,* **16,** 51-61.

Grace, J.B., Anderson, T.M., Olff, H. & Scheiner, S.M. (2010) On the specification of structural equation models for ecological systems. *Ecological Monographs,* **80,** 67-87.

Grace, J.B. & Bollen, K.A. (2008) Representing general theoretical concepts in structural equation models: the role of composite variables. *Environmental and Ecological Statistics,* **15,** 191-213.

Inchausti, P. & Weimerskirch, H. (2001) Risks of decline and extinction of the endangered Amsterdam albatross and the projected impact of long-line fisheries. *Biological Conservation,* **100,** 377-386.

Isaza, C., Martorell, C., Cevallos, D., Galeano, G., Valencia, R. & Balslev, H. (2016) Demography of Oenocarpus bataua and implications for sustainable harvest of its fruit in western Amazon. *Population Ecology,* **58,** 463-476.

Jenkins, D., Watson, A. & Miller, G.R. (1963) Population studies on red grouse, Lagopus-lagopus-scoticus (Lath), in northeast Scotland. *Journal of Animal Ecology,* **32,** 317-376.

Jongejans, E. & De Kroon, H. (2005) Space versus time variation in the population dynamics of three co-occurring perennial herbs. *Journal of Ecology,* **93,** 681-692.

Jongejans, E., de Kroon, H., Tuljapurkar, S. & Shea, K. (2010) Plant populations track rather than buffer climate fluctuations. *Ecology Letters,* **13,** 736-743.

Knops, J.M.H., Koenig, W.D. & Carmen, W.J. (2007) Negative correlation does not imply a tradeoff between growth and reproduction in California oaks. *Proceedings of the National Academy of Sciences of the United States of America,* **104,** 16982-16985.

Koenig, W.D. & Knops, J.M.H. (1998) Scale of mast-seeding and tree-ring growth. *Nature,* **396,** 225-226.

Ludwig, D. (1996) Uncertainty and the assessment of extinction probabilities. *Ecological Applications,* **6,** 1067-1076.

Menges, E.S. (2007) Integrating demography and fire management: an example from Florida scrub. *Australian Journal of Botany,* **55,** 261-272.

Menges, E.S. & Kimmich, J. (1996) Microhabitat and time-since-fire: Effects on demography of Eryngium cuneifolium (Apiaceae), a Florida scrub endemic plant. *American Journal of Botany,* **83,** 185-191.

Menges, E.S. & Kohfeldt, N. (1995) Life history strategies of Florida scrub plants in relation to fire. *Bulletin of the Torrey Botanical Club,* **122,** 282-297.

Menges, E.S. & Quintana-Ascencio, P.F. (2004) Population viability with fire in Eryngium cuneifolium: Deciphering a decade of demographic data. *Ecological Monographs,* **74,** 79-99.

Metcalf, C.J.E., Ellner, S.P., Childs, D.Z., Roberto, S.-G., Merow, C., McMahon, S.M., Jongejans, E. & Rees, M. (2015) Statistical modelling of annual variation for inference on stochastic population dynamics using Integral Projection Models. *Methods in Ecology and Evolution,* **6,** 1007-1017.

Morris, W.F. & Doak, D.F. (2002) Quantitative Conservation Biology: Theory and Practice of Population Viability Analysis. *Quantitative Conservation Biology: Theory and Practice of Population Viability Analysis***,** i-xvi, 1-480.

Nur, N. & Sydeman, W.J. (1999) Survival, breeding probability and reproductive success in relation to population dynamics of Brandt's cormorants Phalacrocorax penicillatus. *Bird Study,* **46,** 92-103.

Ohlberger, J., Scheuerell, M.D. & Schindler, D.E. (2016) Population coherence and environmental impacts across spatial scales: a case study of Chinook salmon. *Ecosphere,* **7**.

Ottersen, G., Planque, B., Belgrano, A., Post, E., Reid, P.C. & Stenseth, N.C. (2001) Ecological effects of the North Atlantic Oscillation. *Oecologia,* **128,** 1-14.

Parmesan, C., Burrows, M.T., Duarte, C.M., Poloczanska, E.S., Richardson, A.J., Schoeman, D.S. & Singer, M.C. (2013) Beyond climate change attribution in conservation and ecological research. *Ecology Letters,* **16,** 58-71.

Plummer, M. (2003) JAGS: a program for analysis of Bayesian graphical models using Gibbs sampling. pp. 125. Proceedings of the 3rd international workshop on distributed statistical computing. Technische Universit at Wien, Wien, Austria.

Popay, A.I. & Medd, R.W. (1990) The biology of Australian weeds 21. Carduus-nutans-ssp-nutans. *Plant Protection Quarterly,* **5,** 3-13.

Post, E. & Stenseth, N.C. (1999) Climatic variability, plant phenology, and northern ungulates. *Ecology,* **80,** 1322-1339.

Qiu, W. & Joe, H. (2015) clusterGeneration: Random Cluster Generation (with Specified Degree of Separation). . R package version 1.3.4. http://CRAN.R-project.org/package=clusterGeneration.

Quintana-Ascencio, P.F. & Menges, E.S. (2000) Competitive abilities of three narrowly endemic plant species in experimental neighborhoods along a fire gradient. *American Journal of Botany,* **87,** 690-699.

R Core Team (2016) R: A language and environment for statistical computing. R Foundation for Statistical Computing, Vienna, Austria.

Rees, M., Childs, D.Z., Metcalf, J.C., Rose, K.E., Sheppard, A.W. & Grubb, P.J. (2006) Seed dormancy and delayed flowering in monocarpic plants: Selective interactions in a stochastic environment. *American Naturalist,* **168,** E53-E71.

Rees, M. & Ellner, S.P. (2009) Integral projection models for populations in temporally varying environments. *Ecological Monographs,* **79,** 575-594.

Rotella, J.J., Link, W.A., Chambert, T., Stauffer, G.E. & Garrott, R.A. (2012) Evaluating the demographic buffering hypothesis with vital rates estimated for Weddell seals from 30 years of mark-recapture data. *Journal of Animal Ecology,* **81,** 162-173.

Salguero-Gomez, R., Jones, O.R., Archer, C.R., Bein, C., de Buhr, H., Farack, C., ... & Vaupel, J.W. (2016) COMADRE: a global data base of animal demography. *Journal of Animal Ecology,* **85,** 371-384.

Salguero-Gomez, R., Jones, O.R., Archer, C.R., Buckley, Y.M., Che-Castaldo, J., Caswell, H., ... & Vaupel, J.W. (2015) The COMPADRE Plant Matrix Database: an open online repository for plant demography. *Journal of Ecology,* **103,** 202-218.

Stenseth, N.C. & Mysterud, A. (2005) Weather packages: finding the right scale and composition of climate in ecology. *Journal of Animal Ecology,* **74,** 1195-1198.

Stenseth, N.C., Mysterud, A., Ottersen, G., Hurrell, J.W., Chan, K.S. & Lima, M. (2002) Ecological effects of climate fluctuations. *Science,* **297,** 1292-1296.

Teller, B.J., Adler, P.B., Edwards, C.B., Hooker, G. & Ellner, S.P. (2016) Linking demography with drivers: climate and competition. *Methods in Ecology and Evolution,* **7,** 171-183.

Thorson, J.T., Scheuerell, M.D., Shelton, A.O., See, K.E., Skaug, H.J. & Kristensen, K. (2015) Spatial factor analysis: a new tool for estimating joint species distributions and correlations in species range. *Methods in Ecology and Evolution,* **6,** 627-637.

Tomimatsu, H. & Ohara, M. (2010) Demographic response of plant populations to habitat fragmentation and temporal environmental variability. *Oecologia,* **162,** 903-911.

Tuljapurkar, S. (1990) Delayed reproduction and fitness in variable environments. *Proceedings of the National Academy of Sciences of the United States of America,* **87,** 1139-1143.

Van der Pol, M., Bailey, L.D., McLean, N., Rijsdijk, L., Lawson, C.R. & Brouwer, L. (2016) Identifying the best climatic predictors in ecology and evolution. *Methods in Ecology and Evolution,* **7,** 1246-1257.

Vindenes, Y., Edeline, E., Ohlberger, J., Langangen, O., Winfield, I.J., Stenseth, N.C. & Vollestad, L.A. (2014) Effects of Climate Change on Trait-Based Dynamics of a Top Predator in Freshwater Ecosystems. *American Naturalist,* **183,** 243-256.

Wardle, D.A., Nicholson, K.S. & Rahman, A. (1992) Influence of pasture grass and legume swards on seedling emergence and growth of Carduus-nutans and Cirsium-vulgare. *Weed Research,* **32,** 119-128.

Williams, J.L., Jacquemyn, H., Ochocki, B.M., Brys, R. & Miller, T.E.X. (2015) Lifehistory evolution under climate change and its influence on the population dynamics of a long-lived plant. *Journal of Ecology,* **103,** 798-808.

Zuur, A.F., Fryer, R.J., Jolliffe, I.T., Dekker, R. & Beukema, J.J. (2003) Estimating common trends in multivariate time series using dynamic factor analysis. *Environmetrics,* **14,** 665-685.

Supplementary Figures
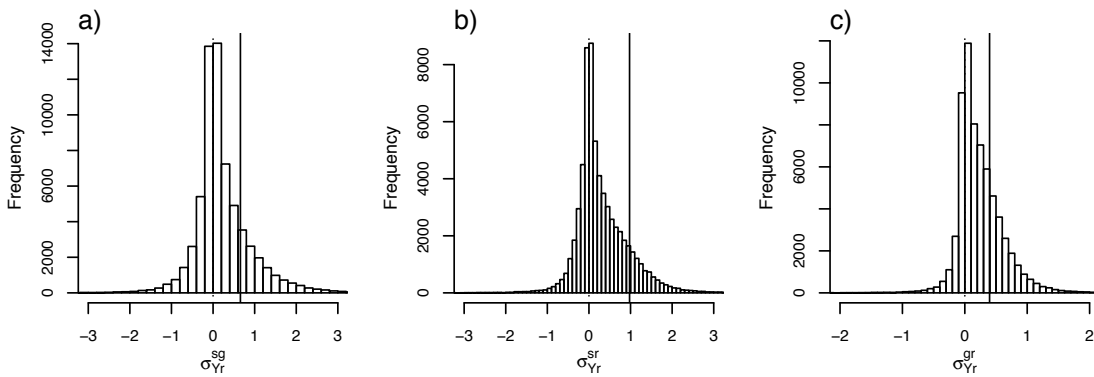
Figure S1: Covariance between the submodel specific year effects in the *Carduus* model for (a) survival and growth, (b) survival and recruit size, (c) growth and recruit size. Dotted line is at zero. Solid line is covariance between random year effects from the corresponding mixed models. The correlations between the random year effects were not significant ($0.13 \leq p \leq 0.37$). If a single latent parameter was insufficient to account for the covariation amongst the vital rates, for example if two vital rates were particularly closely correlated (see Fig. S5), the estimates of the submodel specific year effects for those vital rates would be expected to covary. The modes of the distributions are at zero, suggesting that the latent parameter is able to account for the covariation between the vital rates.
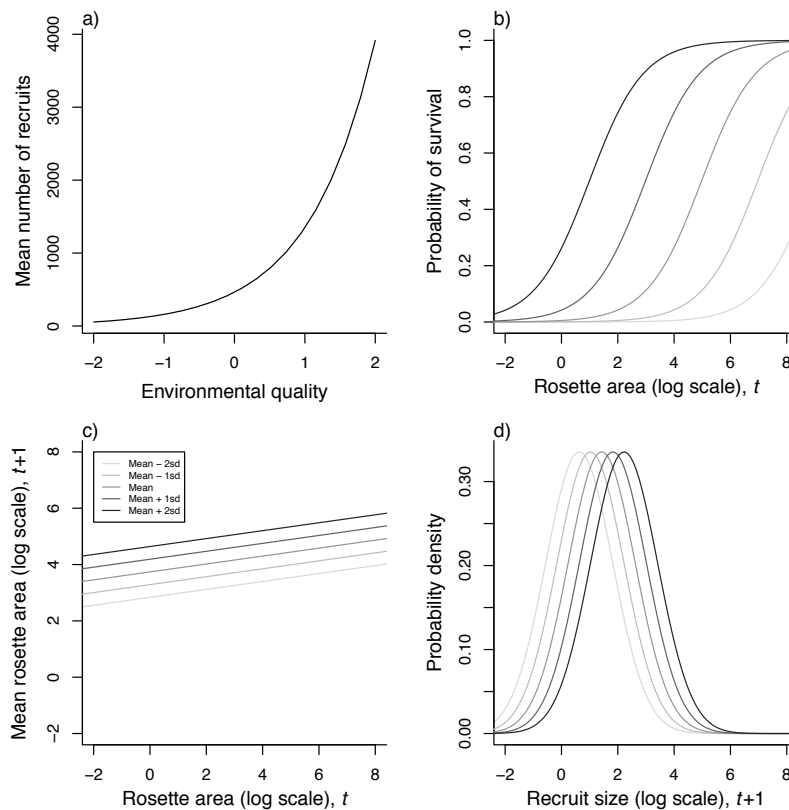
Figure S2: Vital rate functions: (a) recruitment (b) survival (c) growth, and (d) recruit size for the *Carduus* model. The means of the posterior distributions are used as the parameter estimates. The mean function is plotted along with -2, -1, +1 and +2 standard deviations of the latent parameter (Q). The minimum and maximum rosette area seen in the study population are, on a log scale, -1.63 and 7.42 respectively.

17
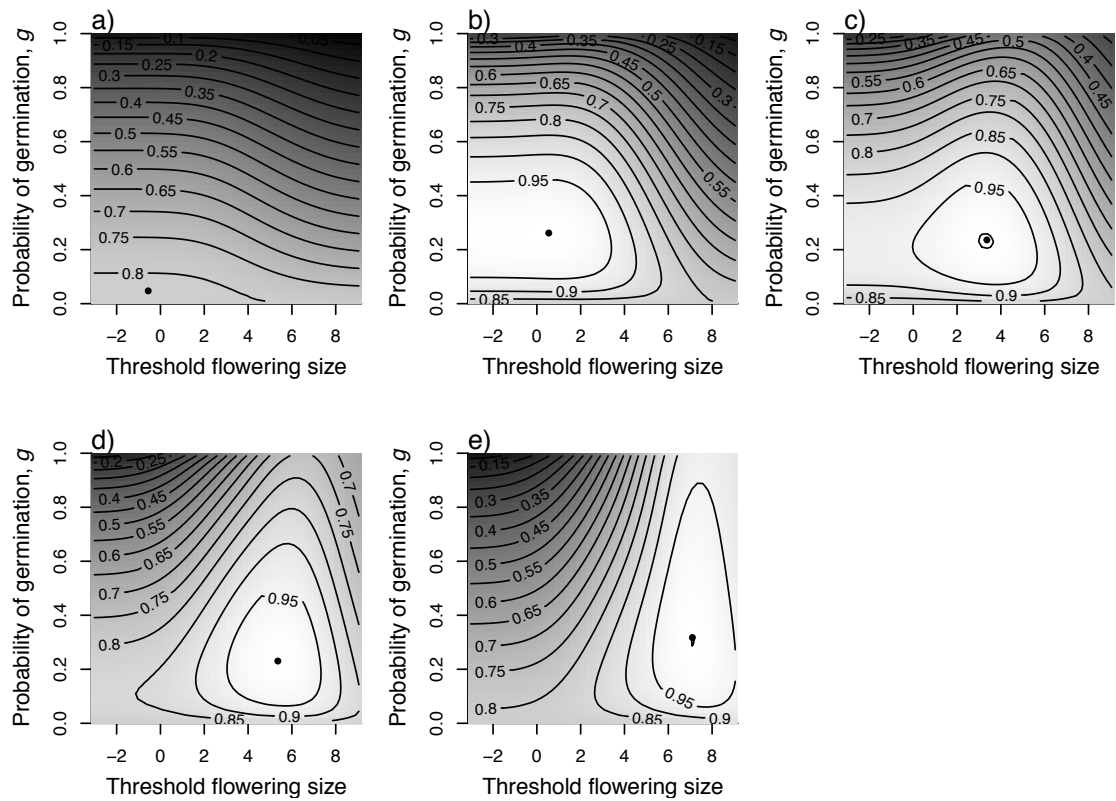
Figure S3: Fitness landscapes for environments with a mean quality of (a) -2, (b) -1, (c) 0, (d) 1 and (e) 2, with a seed mortality (d) of 0.2, assuming that the resident strategy is at the joint flowering intercept and germination probability ESS. The resident strategy is marked by a black point.
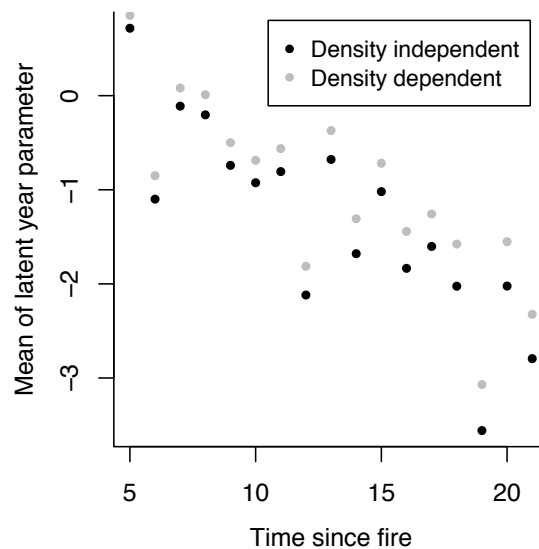
Figure S4: Estimates of the latent year parameter with time since fire. Points are the mean estimate for each year where data were available. The density independent model is described in the main text and Appendix A2; the density dependent model is described in Appendix A5. Including a linear effect of TSF led to better model fit than $log(TSF)$; more complicated models could not be supported due to the lack of replication of TSF (Evans, Holsinger & Menges 2010) and were not evaluated. Previous analyses have shown nonlinear relationships with time since fire, with higher rates of decay in λ when fires were more recent (Menges & Quintana-Ascencio 2004). Data on the period immediately following a fire were not available for this population and a linear decay was consistent within the range of the data used.
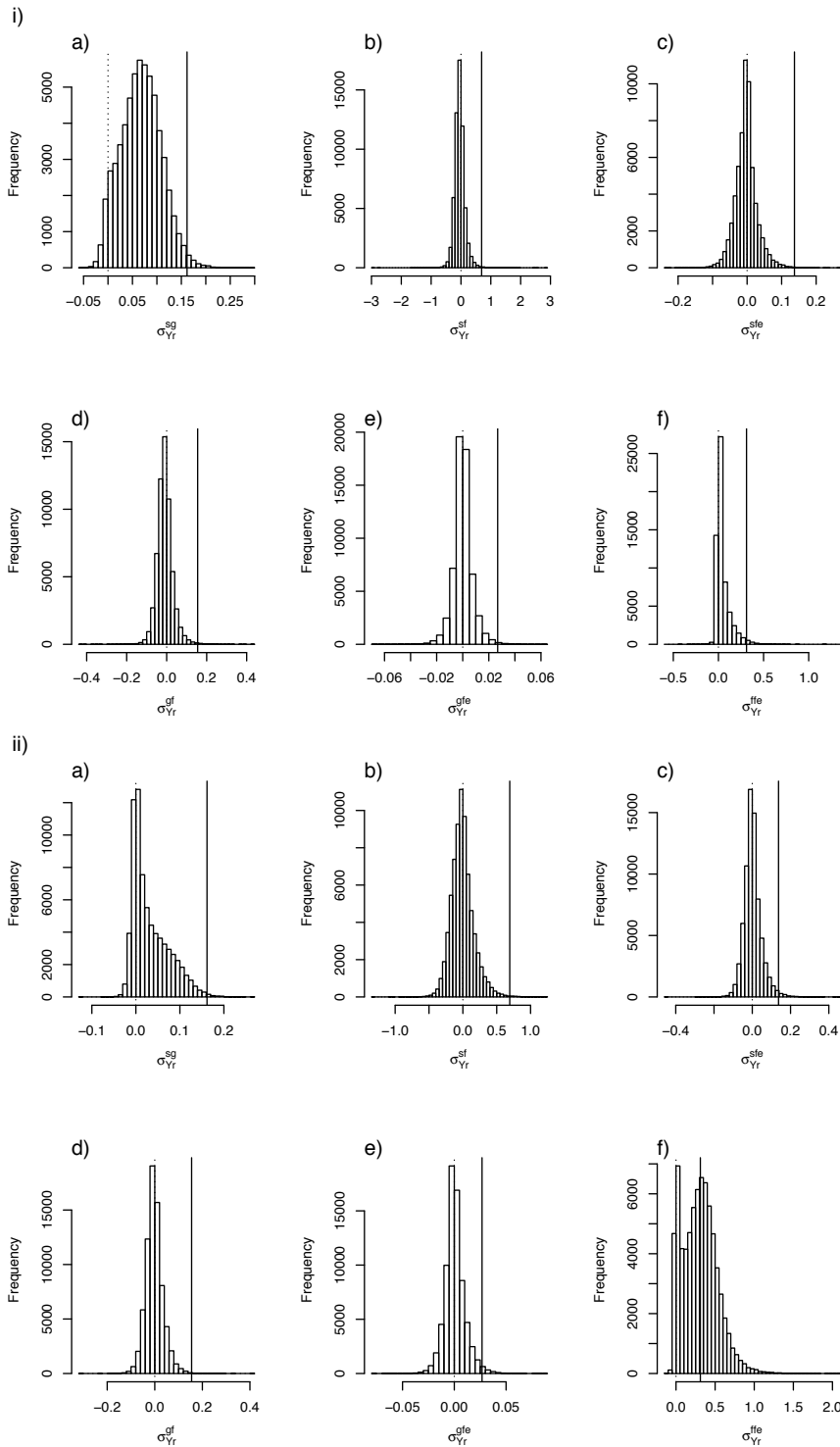
Figure S5: Covariance between submodel specific year effects for the *Eryngium* models excluding i) and including ii) bivariate distribution between flowering and fecundity year effects for a) survival and growth, b) survival and flowering, c) survival and fecundity, d) growth and flowering, e) growth and fecundity, f) fecundity and flowering. Dotted lines are at zero and solid lines show covariance between year effects for mixed models. In i) the mode in plot a) is not at zero, suggesting that the latent parameter is not accounting for the covariation between survival and growth in this model. Allowing the fecundity and flowering year effects to be modelled using a bivariate distribution corrects for this as can be seen in ii).

19
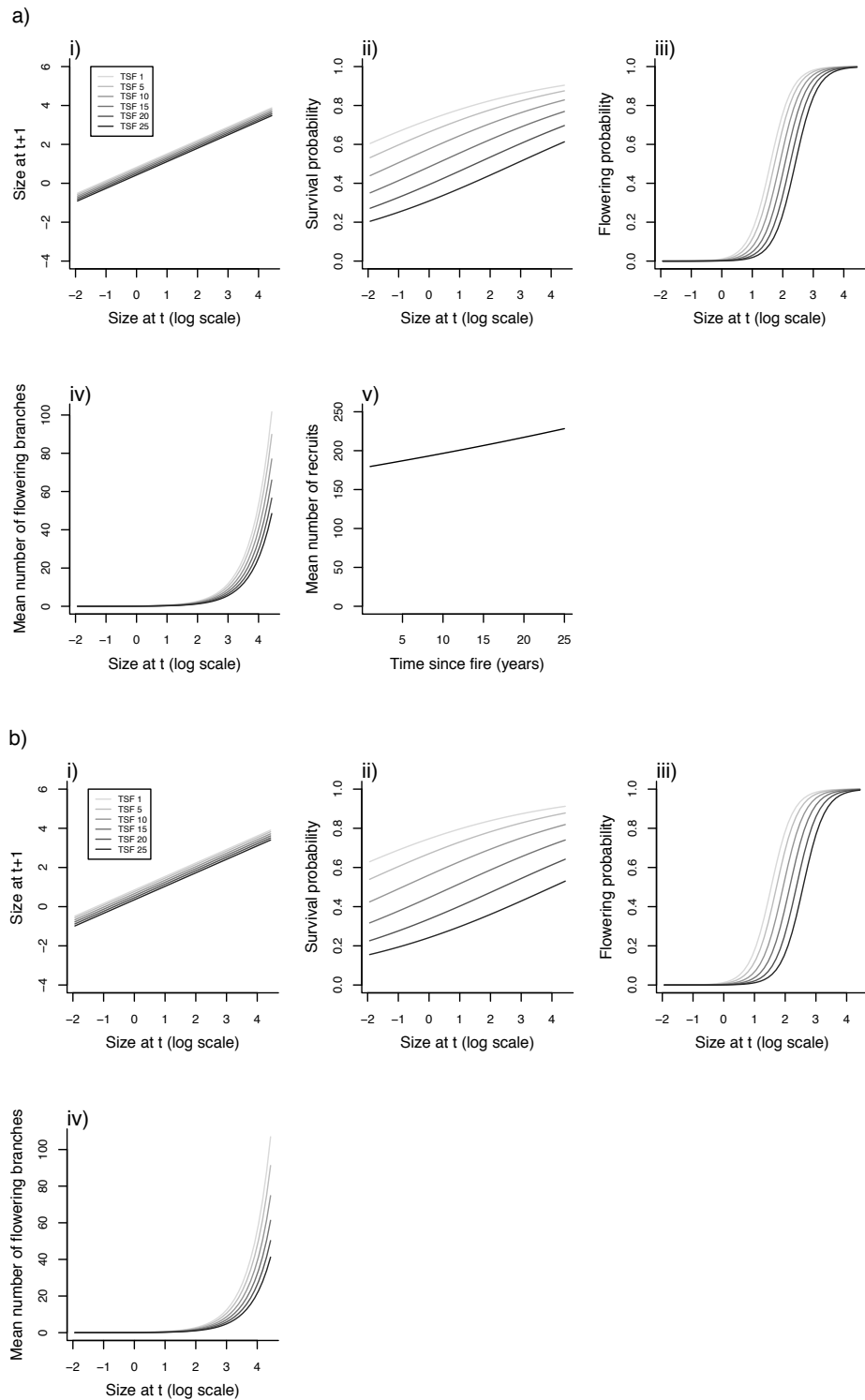
Figure S6: Mean vital rate functions for the *Eryngium* a) density dependent and b) density independent models: i) growth, ii) survival, iii) flowering, iv) fecundity and v) recruitment for one to 25 years since fire (TSF). The plots are created using the means from the posterior distributions as the parameter estimates. See Appendix A5 for details on the density dependent model.

References

Evans, M.E.K., Holsinger, K.E. & Menges, E.S. (2010) Fire, vital rates, and population viability: a hierarchical Bayesian analysis of the endangered Florida scrub mint. *Ecological Monographs,* **80,** 627-649.

Menges, E.S. & Quintana-Ascencio, P.F. (2004) Population viability with fire in Eryngium cuneifolium: Deciphering a decade of demographic data. *Ecological Monographs,* **74,** 79-99.

Appendix A1: Structure and parameterisation of simulation IBMs and IPMs

Simple model (with 4 temporally stochastic parameters):

The IBM is parameterised using data from the Soay sheep population on St Kilda from 1985 to 2013 (Clutton-Brock & Pemberton 2004). For the sake of simplicity the IBM is one sex (female) and each ewe can produce a maximum of one lamb each year (twinning does occur in the study population; Clutton-Brock & Pemberton 2004)).

At every year (t) in the simulation whether each individual survives is decided by sampling randomly from a binomial distribution with a size dependent probability given by $\text{logit}(s^t(z)) = 3.44 + -0.62z + \varepsilon^s_{[t]}$, where $\varepsilon^s_{[t]}$ is a random year effect and z is a measure of size (natural log of the individuals mass). We assume that the effect of size on the vital rates does not vary between years (i.e. only the intercepts vary). The size of surviving individuals in the following time step was sampled randomly from a normal distribution with a mean of $\mu^g_{[z,t]} = 2.38 + 0.24z + \varepsilon^g_{[t]}$ and a standard deviation of 0.14. Surviving individuals reproduce with probability $\text{logit}(r^t(z)) = -7.37 + 2.88z + \varepsilon^r_{[t]}$. The new recruit is female with probability 0.5 (i.e. assuming equal sex ratio) and survives to the next time step with probability $\text{logit}(r_e)) = 1.36$. The size of the new recruits is dependent on maternal size; they are sampled from a normal distribution, with a mean of $\mu^{rs}_{[t+1]} = 1.22 + 0.41z + \varepsilon^{rs}_{[t]}$ and a standard deviation of 0.20.

The year effects ($\varepsilon^s_{[t]}, \varepsilon^g_{[t]}, \varepsilon^r_{[t]}$ and $\varepsilon^{rs}_{[t]}$) were sampled from a covariance matrix at each year in the simulation. The standard deviations (1.05, 0.04, 0.46 and 0.07 for survival, growth, reproduction and recruit size respectively) were parameterised from the data. The correlation matrix was randomly drawn for each simulation from a uniform distribution over the space of positive definite matrices (using rcorrmatrix from the clusterGeneration package in R; Qiu & Joe 2015)

Each of 100 simulations started with a population of 500 recruits and ran for 10,000 years. As the population sizes fluctuated 500 individuals were selected at random, with replacement, after each year and these were used as the starting population for the following year (Metcalf *et al.* 2015). A realistic range of dataset lengths was used (12, 25, and 50 years). One data set of each length was selected at random from the last 8,000 years of each simulation. For each year in the dataset a random number of individuals (between 20 and 150; reflecting the magnitude of numbers of individuals often seen in demographic studies (e.g. Childs *et al.* 2003) and a similar range to that used in (Metcalf *et al.* 2015)) was selected. These were used to parameterise two sets of demographic models; with either an unstructured covariance matrix (UCM approach) or a latent parameter (Q; structural equation modelling (SEM) approach) accounting for the covariance amongst the vital rates (Fig. 1). In the SEM approach the factor loading terms (β_Q) allowed the direction and magnitude of the model wide year effect to differ between vital rates. Each vital rate also contained additional sub-model specific random year

effects, (ε), which accounted for any additional variation among years specific to that vital rate.

The standard deviation of the latent year parameter (Q) in the SEM was constrained to equal one and the factor loading term in the survival submodel was constrained to be positive so that the model was properly identifiable. The signs of the slope terms in the remaining submodels therefore denote whether the remaining vital rates are positively or negatively correlated with survival. Parameters were estimated in JAGS, using runjags (Denwood in review). Prior distributions are show in Table S1. Two chains were run for each model, each with a burn in period of 8×10^5. The chains were thinned, selecting every 500th sample. The IPM was parameterised by sampling from the joint posterior distribution of the parameters. As the sample standard deviation of the latent year parameter differed from one, the β_Q parameters were scaled by the sample standard deviation of the latent year parameters.

The structure of the IPM kernel is shown in Fig. 1. The temporally varying vital rates (survival ($s^t(z)$), growth $g^t(z',z)$, reproduction ($r^t(z)$), and recruit size ($rs^t(z)$)) are parameterised using either the SEM approach or the UCM approach (Fig. 1). Where the UCM approach was used a covariance matrix was estimated from the posterior distributions of the year effects. The probability of a lamb recruiting (r_e) was assumed to be constant among years; this was estimated as the proportion of recruiting individuals across all years. The IPM was iterated for 10,000 years using 100 meshpoints. The stochastic growth rate was estimated, excluding the first 2,000 years of data as $\log \lambda_s = \frac{1}{T-1} \sum_{t=1}^{T-1} \ln(N_{t+1}/N_t)$. This was repeated with 1,000 samples from the posterior for each simulation. The "true" stochastic growth rate was estimated for each simulation by parameterising the IPM using the known parameter values.

Table S1: Prior distributions for the simple simulation study. For normal distributions parameter 1 and 2 are the mean and standard deviation respectively, for uniform distributions they are the minimum and maximum, for multivariate normal distributions (MVN) they are the mean and covariance matrix, for the inverse Wishart distribution they are the scale matrix and degrees of freedom. See Fig. 1 for parameter definitions. A scaled inverse Wishart distribution (Gelman & Hill 2007) is used for the covariance matrix (Σ), where ξ is a vector of scaling parameters, m is a vector of unscaled intercepts and V is the unscaled covariance matrix.

Parameter	Submodel	UCM approach Distribution	Parameter 1	Parameter 2	SEM approach Distribution	Parameter 1	Parameter 2
β_0^s	Survival	-	$\xi^s m^s$	-	Normal	0	100
β_z^s	Survival	Normal	0	100	Normal	0	100
β_Q^s	Survival	-	-	-	Uniform	0	10
ε_{Yr}^s	Survival	MVN	0	$\Sigma = \mathrm{Diag}(\xi)V\mathrm{Diag}(\xi)$	Normal	0	Uniform(0, 10)
β_0^g	Growth	-	$\xi^g m^g$	-	Normal	0	100
β_z^g	Growth	Normal	0	100	Normal	0	100
β_Q^g	Growth	-	-	-	Normal	0	10
ε_{Yr}^g	Growth	MVN	0	$\Sigma = \mathrm{Diag}(\xi)V\mathrm{Diag}(\xi)$	Normal	0	Uniform(0, 10)
σ^g	Growth	Uniform	0	10	Uniform	0	10
β_0^{rs}	Recruit size	-	$\xi^{rs} m^{rs}$		Normal	0	100
β_z^{rs}	Recruit size	Normal	0	100	Normal	0	100
β_Q^{rs}	Recruit size	-	-	-	Normal	0	10
ε_{Yr}^{rs}	Recruit size	MVN	0	$\Sigma = \mathrm{Diag}(\xi)V\mathrm{Diag}(\xi)$	Normal	0	Uniform(0, 10)
σ^{rs}	Recruit size	Uniform	0	10	Uniform	0	10
β_0^r	Reproduction	-	$\xi^r m^r$		Normal	0	100
β_z^r	Reproduction	Normal	0	100	Normal	0	100
β_Q^r	Reproduction	-	-	-	Uniform	0	10
ε_{Yr}^r	Reproduction	MVN	0	$\Sigma = \mathrm{Diag}(\xi)V\mathrm{Diag}(\xi)$	Normal	0	Uniform(0, 10)
Q	All	-	-	-	Normal	0	1
V	All	Inverse Wishart	I(4)	5	-	-	-
m	All	Normal	0	100	-	-	-
ξ	All	Uniform	0	1	-	-	-

Complex model (with seven temporally stochastic parameters):

The IBM is based on data from the Soay sheep population on St Kilda from 1985 to 2013 (Clutton-Brock & Pemberton 2004). As in the simple model above the IBM is one sex (female) and each ewe can produce a maximum of one lamb each year (twinning does occur in the study population; Clutton-Brock & Pemberton 2004)). The IBM contains seven temporally variable vital rates; we assume that the effect of size on the vital rates does not vary between years (i.e. only the intercepts vary), giving a total of seven stochastic parameters. The population is split into two stage classes; juveniles and adults.

At each year (t) in the simulation whether each juvenile in the population survives is decided by sampling randomly from a binomial distribution, with a size (z) dependent probability given by $\text{logit}(s^t(z)) = -15.16 + 6.39z + \varepsilon_{[t]}^s$, where $\varepsilon_{[t]}^s$ is a random year effect and z is a measure of size (natural log of the individuals mass). The size of the surviving juveniles in the following time step was sampled randomly from a normal distribution with a mean of $\mu_{[z,t]}^g = 1.24 + 0.63z + \varepsilon_{[t]}^g$ and a standard deviation of 0.08. Surviving juveniles may mature to adults with probability $\text{logit}(m^t(z)) = -10 + 4z + \varepsilon_{[t]}^m$. Adults at time t survive with probability $\text{logit}(a^t(z)) = -4.38 + 2.12z + \varepsilon_{[t]}^a$. The size of surviving adults at t+1 was sampled randomly from a normal distribution with a mean of $\mu_{[z,t]}^b = 0.69 + 0.78z + \varepsilon_{[t]}^b$ and a standard deviation of 0.06.

Surviving adults and juveniles that have transitioned to the adult stage that year may reproduce with probability $\text{logit}(r^t(z)) = -7.37 + 2.88z + \varepsilon_{[t]}^r$. The new recruit is female with probability 0.5 (i.e. assuming equal sex ratio) and survives to the next time step with probability 0.75 (this is not temporally variable). The size of the new recruits is dependent on maternal size; they are sampled from a normal distribution, with a mean of $\mu_{[t+1]}^c = 1.22 + 0.41z + \varepsilon_{[t]}^c$ and a standard deviation of 0.20.

The year effects ($\varepsilon_{[t]}^s$, $\varepsilon_{[t]}^a$, $\varepsilon_{[t]}^g$, $\varepsilon_{[t]}^b$, $\varepsilon_{[t]}^m$, $\varepsilon_{[t]}^r$, and $\varepsilon_{[t]}^c$) were sampled from a covariance matrix at each year in the simulation. The standard deviations for the year effects were 2.3, 1.14, 0.04, 0.04, 0.5, 0.46 and 0.07 for juvenile survival, adult survival, juvenile growth, adult growth, maturation, reproduction and recruit size respectively. The correlation matrix was randomly drawn for each simulation from a distribution that is uniform over the space of positive definite matrices (using rcorrmatrix from the clusterGeneration package in R; Qiu & Joe 2015)

Each simulation was started with a population of 500 juveniles and was run for 10,000 years. As above 500 individuals were selected at random, with replacement, after each year and these were used as the starting population for the following year (Metcalf *et al.* 2015). The first 2,000 years of the simulation were discarded as transient dynamics.

A realistic range of dataset lengths was used (12, 25, and 50 years). One dataset of each length was selected at random from the last 8,000 years of each simulation. For each year in the dataset a random number of individuals (between 20 and 150; reflecting the magnitude of

numbers of individuals often seen in demographic studies) was selected. These were used to parameterise two sets of demographic models; the first consists of separate mixed effects models (GLMM approach), whilst in the second a latent variable (Q) describes the covariance amongst the vital rates (structural equation modelling (SEM) approach). The factor loading terms (β_Q) allow the direction and magnitude of the model wide year effect to differ between vital rates. The submodels also contain additional year effects, (ε), which account for any additional variation between years.

The standard deviation of the latent year parameter (Q) of the SEM model was constrained to equal one so that the model was properly identified. Additionally, the factor loading term in the juvenile survival submodel (β_Q^s) was constrained to be positive; the signs of the slope terms in the remaining submodels therefore denote whether the remaining vital rates are positively or negatively correlated with survival.

The models were run in JAGS, using *runjags* (Denwood in review). Prior distributions are show in Table S2. Two chains were run for each model. The models were run with a burn in period of 4×10^5 for the SEM models and 5×10^5 for the unstructured approach. Each chain was then run for a further 1.25×10^6 iterations and thinned, selecting every 500th sample, to give a total posterior sample of 5,000 across the two chains. Convergence was assessed using the multivariate psrf score; those models with a psrf>1.05, and a randomly selected 10% of all models were assessed visually. Models that hadn't converged were rerun with a longer burn in and more thinning.

The structure of the IPM is shown in Fig. 1. The temporally variable vital rates are parameterised using either the SEM approach or the GLMM approach described above. The probability of a lamb recruiting (r_e) was assumed to be constant among years; this was estimated as the proportion of recruiting individuals across all years. As the sample standard deviation of the latent year parameter differed from one, the β_Q parameters were scaled by the sample standard deviation of the latent year parameters.

The IPM was iterated for 10,000 years using 100 meshpoints. The stochastic growth rate was estimated, excluding the first 2,000 years of data, as $\log \lambda_s = \frac{1}{T-1} \sum_{t=1}^{T-1} \ln(N_{t+1}/N_t)$. This was repeated with 1,000 samples from the posterior for each simulation. The "true" stochastic growth rate was estimated for each simulation by iterating the IPM using the known parameter values.

Table S2: Prior distributions for the complex simulation study. For normal distributions parameter 1 and 2 are the mean and standard deviation respectively, for uniform distributions they are the minimum and maximum, for multivariate normal distributions (MVN) they are the mean and covariance matrix, for the inverse Wishart distribution they are the scale matrix and degrees of freedom. See Fig. 1 for parameter definitions. A scaled inverse Wishart distribution (Gelman & Hill 2007) is used for the covariance matrix (Σ), where ξ is a vector of scaling parameters, m is a vector of unscaled intercepts and V is the unscaled covariance matrix.

Parameter	Submodel	UCM approach Distribution	Parameter 1	Parameter 2	SEM approach Distribution	Parameter 1	Parameter 2
β_0^s	Juvenile survival	-	$\xi^s m^s$	-	Uniform	-50	50
β_z^s	Juvenile survival	Normal	0	50	Uniform	-50	50
β_Q^s	Juvenile survival	-	-	-	Uniform	0	10
ε_{Yr}^s	Juvenile survival	MVN	0	$\Sigma = \mathrm{Diag}(\xi)V\mathrm{Diag}(\xi)$	Normal	0	Uniform(0, 10)
β_0^a	Adult survival	-	$\xi^a m^a$	-	Uniform	-50	50
β_z^a	Adult survival	Normal	0	50	Uniform	-50	50
β_Q^a	Adult survival	-	-	-	Uniform	-10	10
ε_{Yr}^a	Adult survival	MVN	0	$\Sigma = \mathrm{Diag}(\xi)V\mathrm{Diag}(\xi)$	Normal	0	Uniform(0, 10)
β_0^g	Juvenile growth	-	$\xi^g m^g$	-	Uniform	-50	50
β_z^g	Juvenile growth	Normal	0	50	Uniform	-50	50
β_Q^g	Juvenile growth	-	-	-	Uniform	-10	10
ε_{Yr}^g	Juvenile growth	MVN	0	$\Sigma = \mathrm{Diag}(\xi)V\mathrm{Diag}(\xi)$	Normal	0	Uniform(0, 10)
σ^g	Juvenile growth	Uniform	0	10	Uniform	0	10
β_0^b	Adult growth	-	$\xi^b m^b$	-	Uniform	-50	50
β_z^b	Adult growth	Normal	0	50	Uniform	-50	50
β_Q^b	Adult growth	-	-	-	Uniform	-10	10
ε_{Yr}^b	Adult growth	MVN	0	$\Sigma = \mathrm{Diag}(\xi)V\mathrm{Diag}(\xi)$	Normal	0	Uniform(0, 10)
β_0^m	Maturation	-	$\xi^m m^m$	-	Uniform	-50	50
β_z^m	Maturation	Normal	0	50	Uniform	-50	50
β_Q^m	Maturation	-	-	-	Uniform	-10	10
ε_{Yr}^m	Maturation	MVN	0	$\Sigma = \mathrm{Diag}(\xi)V\mathrm{Diag}(\xi)$	Normal	0	Uniform(0, 10)
β_0^{rs}	Recruit size	-	$\xi^{rs} m^{rs}$	-	Uniform	-50	50
β_z^{rs}	Recruit size	Normal	0	50	Uniform	-50	50
β_Q^{rs}	Recruit size	Uniform	-	-	Uniform	-10	10
ε_{Yr}^{rs}	Recruit size	MVN	0	$\Sigma = \mathrm{Diag}(\xi)V\mathrm{Diag}(\xi)$	Normal	0	Uniform(0, 10)

Parameter	Submodel	UCM approach Distribution	Parameter 1	Parameter 2	SEM approach Distribution	Parameter 1	Parameter 2
σ^{rs}	Recruit size	Uniform	0	10	Uniform	0	10
β_0^r	Reproduction	-	$\xi^r m^r$	-	Uniform	-50	50
β_z^r	Reproduction	Normal	0	50	Uniform	-50	50
β_Q^r	Reproduction	Uniform	-	-	Uniform	-10	10
ε_{Yr}^r	Reproduction	MVN	0	$\Sigma = \text{Diag}(\xi)V\text{Diag}(\xi)$	Normal	0	Uniform(0, 10)
V	All	Inverse Wishart	I(7)	8	-	-	-
m	All	Normal	0	100	-	-	-
ξ	All	Uniform	0	1	-	-	-

Appendix A2: Parameterisation of the case study integral projection models

Carduus IPM:

Carduus nutans is native to Europe, Asia Minor, Siberia and North Africa and has been introduced in Australia, New Zealand, the United States, and Canada. Demographic data were collected on 2,371 *Carduus* rosettes from 1988 to 1996 in Kybeyan, New South Wales, Australia (Rees *et al.* 2006). The majority of individuals in this population (85%) acted as annuals, flowering in their first year (Rees *et al.* 2006).

The *Carduus* IPM is structurally identical to that used by Rees et al (2006), differing only in the way in which temporal variation in the vital rates is modelled (Rees *et al.* 2006 use a kernel selection approach). The structuring variable is the natural logarithm of rosette area (z), a measure of plant size (Rees *et al.* 2006) that predicts individual performance. Rosette area was estimated using the mean of two measurements of the radius and assuming that the plants were circular. The structure of the IPM is shown in Fig. 3a.

The seed production function ($f^t(z)$) is given by $s^t(z)fl(z)f_n(z)$, where, for a plant of size z, $s^t(z)$ is the probability of survival in year t, $fl(z)$ is the flowering probability and $f_n(z)$ is the expected number of seeds produced. The latter two terms are assumed to be constant between years (Rees *et al.* 2006). The probability of flowering was assumed to be size dependent and follow a binomial distribution; the intercept (β_0^f) and slope (β_z^f) were estimated from a generalised linear model as -5.31 and 1.66 respectively. The expected number of seeds, $f_n(z)$ was given by $\exp(A + B\log(\text{size}))$, where $A = 3.28$ and $B = 0.58$ (Rees *et al.* 2006).

The distribution of seedlings recruiting from the seedbank (s_g^t) is given by $g(1 - d)p_e(t)rs^t(z')$, where $p_e(t)$ is the probability of establishment and $rs^t(z')$ is the probability distribution of recruit sizes. Recruit size was assumed to be independent of parental size as data were not available and studies on similar species (e.g. Sletvold 2002) have suggested recruit size is mainly determined by the environment (Rees *et al.* 2006). The survival growth function, $p^t(z',z)$, is given by $s^t(z)(1 - fl(z))g^t(z',z)$, where $g^t(z',z)$ is a probability density function giving the probability of an individual of size z growing to size z'. The flowering probability is included in the survival growth function as flowering is fatal. The fecundity function, $f^t(z',z)$, is given by $gp_e f^t(z)rs^t(z')$.

Recruitment was assumed not to be related to seed production (Rees *et al.* 2006); therefore the probability of seeds establishing in year t, $p_e(t)$, was assumed to be density dependent and was given by

$$p_e(t) = \frac{R(t+1)}{g[(1-d)S(t) + \int_\Omega f^t(z)n(z,t)dz]}. \qquad \text{(eqn A1)}$$

$R(t + 1)$ is the number of recruits in year $t + 1$, whilst the denominator gives the total number of germinating seeds, consisting of those from the seedbank and those produced in year t.

Posterior distributions for the stochastic vital rates model (Fig. 3b) were estimated using Markov Chain Monte Carlo (MCMC) simulations in JAGS, using runjags (Denwood in review).

An initial burnin period of 1.5×10^5 iterations was discarded for each of three chains; which were then run for a further 2×10^6 iterations. The chains were thinned to reduce autocorrelation, with every 100th iteration saved, giving a posterior sample of 60,000. The prior distributions were weakly informative (i.e. within biologically reasonable ranges) to improve mixing (Table S3; see Appendix A3 for comparison with more informative priors). The vital rates were integrated into the IPM using the posterior means as the parameter estimates. As the sample standard deviation of the latent parameter (Q) differed from one, the β_Q factor loading parameters were scaled by the sample standard deviation of the latent parameters.

The IPM was solved using the midpoint rule (Easterling, Ellner & Dixon 2000), using 50 meshpoints. Increasing the number of meshpoints from 50 to 200 did not affect the model output. As the minimum and maximum sizes used were broad and the effect of size at time t on size at time $t + 1$ was relatively small, there was very minimal eviction from the model (Williams, Miller & Ellner 2012). The maximum size used was however much larger than seen in the study population. Most individuals in the study population flowered, and therefore died, in their first year, so there was very limited data available on the growth of larger individuals or maximum size that individuals could reach; ideally this could be supplemented with data from another population or experimental data.

Note that here we used the mean of the posterior distributions as the parameter estimates. By drawing samples randomly from the posterior it would be possible to give a measure of parameter uncertainty and the impacts of this on the results (e.g. Evans, Holsinger & Menges 2010; Diez *et al.* 2014).

Table S3: Prior distributions for the parameters for *Carduus*. For normal distributions parameter 1 and 2 are the mean and standard deviation respectively, for uniform distributions they are the minimum and maximum. The mean values for the β_0 and β_1 prior distributions were based on general linear mixed models (using lme4 in R; Evans, Holsinger & Menges 2010). See Fig. 3 for parameter definitions.

Parameter	Submodel	Distribution	Parameter 1	Parameter 2
β_0^s	Survival	Normal	-5.16	5
β_z^s	Survival	Normal	1.03	5
β_Q^s	Survival	Uniform	0.00	100
ε_{Yr}^s	Survival	Normal	0.00	Uniform(0,5)
β_0^g	Growth	Normal	3.84	5
β_z^g	Growth	Normal	0.12	5
β_Q^g	Growth	Normal	0.00	5
ε_{Yr}^g	Growth	Normal	0.00	Uniform(0,5)
σ^g	Growth	Uniform	0.00	5
β_0^{rs}	Recruit size	Normal	1.45	5
β_Q^{rs}	Recruit size	Normal	0.00	5
ε_{Yr}^{rs}	Recruit size	Normal	0.00	Uniform(0,5)
σ^{rs}	Recruit size	Uniform	0.00	5
β_0^r	Recruitment	Normal	4.62	5
β_Q^r	Recruitment	Normal	0.00	5
σ^r	Recruitment	Uniform	0.00	8
Q	All	Normal	0.00	1

Eryngium IPM:

Demographic data collected from 1990 to 2007 (covering a period of between four and 21 years since fire) on a single population (site number 85) at the Archbold Biological Station (Florida) were used in this study (data from 1988-9 were excluded due to quality concerns Menges & Quintana-Ascencio 2004). The IPM was structured by the natural logarithm of rosette diameter (Menges & Quintana-Ascencio 2004). The structure of the IPM is given by Fig. 5a.

The seed production function, $f^t(z)$, is given by $fl^t(z)fe^t(z) f_n(z)$, where, for a plant of size z, $fl^t(z)$ is the flowering probability, $fe^t(z)$ is the number of flowering stems and $f_n(z)$ is the expected number of seeds produced per flowering stem. The size distribution of plants recruiting from the seedbank ($s_g^t(z')$) is given by $g_{sb}ss^t rs^t(z')$, where ss^t is seedling survival and $rs^t(z')$ is the distribution of recruit sizes. The second term is composed of the survival growth function, and seeds produced that year that germinate immediately. The survival growth function, $p^t(z',z)$ is given by $s^t(z)g^t(z',z)$, where $s^t(z)$ is the survival probability and $g^t(z',z)$ gives the probability of an individual of size z growing to size z'. The fecundity function, $f^t(z',z)$, is $g_f ss^t f^t(z) rs^t(z')$.

Posterior distributions for the stochastic vital rate model were estimated using Markov Chain Monte Carlo (MCMC) simulations in JAGS, using runjags (Denwood in review). An initial burnin period of $3\mathrm{x}10^5$ iterations was discarded for three chains. Each chain was then run for a further $4\mathrm{x}10^6$ iterations. The chains were thinned to reduce autocorrelation, with every 200th iteration saved, resulting in a posterior sample of 60,000. Weakly informative priors were used (Table S4; see Appendix A3 for a comparison with more informative priors). The posterior means were used as the parameter estimates for the vital rates from the vital rates model. As above the β_Q factor loading parameters were scaled by the sample standard deviation of the latent year parameter estimates.

The seedling survival term (ss^t) accounts for the period between emergence in January-May and the annual census in October/November. Yearly data were not available on seedling survival for the duration of the study period, so this was not included in the stochastic vital rates model. Instead four years of data were used, from a total of seven populations (Menges & Quintana-Ascencio 2004). A mixed effect model on seedling survival against time since fire, with year included as a random effect, suggested that seedling survival decreased with time since fire. This was included in the IPM using the following equation, $\mathrm{logit}(ss) = -1.84 + -0.03TSF + \varepsilon_{yr}^{ss}$, where ε_{yr}^{ss} is given by a normal distribution with mean 0 and standard deviation 1.1.

Estimates of germination probability range from 0 to 0.1 and 0.005 to 0.04 for first year germination (g_f) and second year germination (g_{sb}) respectively (Quintana-Ascencio & Menges 2000; Menges & Quintana-Ascencio 2004). The model was run using the lowest (0 and 0.005) and highest (0.1 and 0.04) estimates of each, as well as with a range of seed mortality

probabilities (0.5, 0.7, 0.9, Menges & Quintana-Ascencio 2004) as data were not available on seedbank mortality.

The fecundity term in the SEM was the number of flowering branches. The true fecundity is given by the product of this and the number of stems per flowering stem. The mean number of seeds per stem ($f_n(z)$) across populations (183, Menges & Quintana-Ascencio 2004) was used (Fig. S7a). Neither this nor recruit size were allowed to vary among years due to a lack of data for the study population. Recruit size was assumed to be independent of parental size. As with *Carduus*, the IPM was solved using the midpoint rule (Easterling, Ellner & Dixon 2000), using 50 meshpoints. Increasing the number of meshpoints from 50 to 200 did not affect the model output.

For each scenario 1000 populations were simulated for 22 years (as the study population dataset runs to 21 years since fire), starting with a fire year and with no further fires during that period. At each iteration the latent parameter (Q) was randomly sampled from a normal distribution with mean $\beta_{tsf} \times TSF$ and a standard deviation of one (Fig. S8). This allows the model outputs to be compared to observed population dynamics. Each simulation started with an initial population of 7000 seeds and no aboveground plants (Menges & Quintana-Ascencio 2004).

Fire usually causes the death of all plants, with the population replenishing from the seedbank in the following year (Menges & Quintana-Ascencio 2004), therefore rosette survival is assumed to be zero in years of fire. As reproduction occurs immediately following the census rosettes are allowed to reproduce before the fire occurs, however only seeds entering the seedbank will survive i.e. seedling survival is, like adult survival, assumed to be zero.

All of the fertility scenarios produce population sizes that first increase then decrease with time since fire, which is the trend seen in the observed populations (Fig. S9). Several of the fertility scenarios produce population dynamics similar to those seen in the observed populations (Fig. S10). The mean rosette size generally increases then decreases with increasing time since fire, as seen in the observed populations (Fig. S11). However, in the fertility scenarios with higher germination probabilities the mean size tends to be underestimated, possibly because there is too much recruitment into the population (Appendix A5).

We selected the model with low first year germination (0.0), high germination from the seedbank (0.04) and low seed mortality (0.5) as it was consistent with the change in aboveground population growth observed in the field (Fig. 6a). That is, aboveground populations were predicted to increase immediately following a fire, but not beyond ten years postfire (Menges & Quintana-Ascencio 2004). Additionally the mean rosette size increased then decreased with increasing time since fire, as seen in the observed populations (Fig. S11). The low levels of germination in the first year are in accordance with field observations for this species (Menges & Quintana-Ascencio 2004). The low seedbank mortality is consistent with experiments on a similar species, *Hypericum cumulicola*, (Quintana-Ascencio, Dolan & Menges

1998) and the observed recruitment of *Eryngium* seedlings in a patch after seven years without flowering individuals (Menges & Quintana-Ascencio 2004) would seem unlikely under the highest seed mortality scenario.

Using the selected scenario mean plant size is underestimated in the early years postfire; scenarios with the lowest germination rates produced more realistic mean rosette sizes, however the growth rates were below zero even after a recent fire, which is unrealistic. The study population did not experience a fire during the study period. Previous work suggests the rate of environmental decay may be most rapid immediately postfire (Menges & Quintana-Ascencio 2004), however this was not possible to explore using this population. This may help to explain the inconsistencies between the observed and predicted populations.

Assuming that recruit size was not affected by time since fire may be unrealistic (Fig. S12) and could help to explain why the models tend to underestimate rosette size in the first few years after fire, where the actual recruit sizes may be larger than allowed for in the model (Fig. S11). We only used data from one population in this case study to keep the model simple; it would be preferable to include data from across all of the study populations (Menges & Quintana-Ascencio 2004). This is particularly the case as the study population was not subject to a fire during the study period (Fig. S4).

Population responses to different fire regimes were explored using a range of constant fire return intervals (FRI) from two to 30 years. Note that in reality constant FRIs may be unlikely to occur; fire intervals may be more realistically modelled using for example a Weibull distribution, which allows the probability of fire to increase as TSF increases (e.g. Evans, Holsinger & Menges 2010). Stochastic population growth rates were estimated by iterating populations for 1,000 years and excluding the first 200 years as transient dynamics, for 100 simulations. Populations are likely to decline where the time between fires is too short (c.<4 years), presumably as plants do not produce enough seeds to replenish the seedbank, or too long (c.>15 years; Fig. 6b), as they are outcompeted. This is in accordance with a previous study, using a matrix selection approach, that found an optimal FRI of less than 15 years (Menges & Quintana-Ascencio 2004).

We then perturbed the β_{tsf} parameter, which is a measure of how quickly the environment decays as TSF increases. More negative values of this parameter are found where the quality of the environment decreases more quickly following a fire. Stochastic population growth rates were estimated as before, but the fire regimes were varied randomly throughout the simulations (with the same chance of each FRI occurring), either between 1 and 15 years (optimum for *Eryngium*) or between 15 and 30 years (optimum for Florida scrub habitat). Decreasing β_{tsf} by around 1/3 could make a 15:30 year FRI strategy sustainable for *Eryngium* (Fig. 6c). The effect of altering the temporal decay of the environment is much higher when the FRI is higher, to the extent that decreasing β_{tsf} sufficiently can make longer FRIs preferable for *Eryngium* (Fig. 6c). As TSF increases typically the soil moisture decreases (Weekley *et al.*

2007) and the amount of bare ground decreases as leaf litter builds up and ground lichen cover increases (Menges *et al.* 2008) and Florida rosemary, *Ceratiola ericoides*, which can suppress *Eryngium* germination (Hunter & Menges 2002) dominates. It may be possible to decrease the negative effects of time since fire, for example, through the removal of *C. ericoides* (Menges & Kimmich 1996; Hunter & Menges 2002). *Eryngium* is found in firelanes as well as recently burnt areas (Menges & Kimmich 1996); comparing the rate of environmental decay between populations following mechanical disturbance and fires could help to determine whether mechanical disturbance is a possible alternative to fire as a management tool for this species.

Table S4: Prior distributions for the density independent *Eryngium* model. For normal distributions parameter 1 and 2 are the mean and standard deviation, for uniform distributions they are the minimum and maximum and for multivariate normal distributions they are the vector of the mean and the covariance matrix respectively. The mean values for the β_0 and β_1 prior distributions were taken from general linear mixed models (using lmer in R; Evans, Holsinger & Menges 2010). See Fig. 5 for parameter definitions.

Parameter	Submodel	Distribution	Parameter 1	Parameter 2
β_0^s	Survival	Normal	0.43	1
β_z^s	Survival	Normal	0.26	1
β_Q^s	Survival	Uniform	0	100
ε_{Yr}^s	Survival	Normal	0	Uniform(0,5)
β_0^g	Growth	Normal	0.69	1
β_z^g	Growth	Normal	0.69	1
β_Q^g	Growth	Normal	0	5
ε_{Yr}^g	Growth	Normal	0	Uniform(0,5)
σ^g	Growth	Uniform	0	5
β_0^f	Flowering	Normal	-5.11	1
β_z^f	Flowering	Normal	2.77	1
β_Q^f	Flowering	Normal	0	5
$\varepsilon_{Yr}^f, \varepsilon_{Yr}^{fe}$	Flowering & Fecundity	Multivariate normal	(0,0)	$\begin{pmatrix} (\sigma_{Yr}^f)^2 & (\sigma_{Yr}^f \times \sigma_{Yr}^{fe} \times \rho^f \\ (\sigma_{Yr}^f \times \sigma_{Yr}^{fe} \times \rho^{ffe}) & (\sigma_{Yr}^{fe})^2 \end{pmatrix}$
σ_{Yr}^f	Flowering	Uniform	0	5
σ_{Yr}^{fe}	Fecundity	Uniform	0	5
ρ^{ffe}	Flowering & Fecundity	Uniform	-1	1
β_0^{fe}	Fecundity	Normal	-2.14	1
β_z^{fe}	Fecundity	Normal	1.50	1
β_Q^{fe}	Fecundity	Normal	0	5
$\log(\alpha^{fe})$	Fecundity	Normal	0	0.0001
Q	All	Normal	$\beta_{tsf} \times TSF$	1
β_{tsf}	All	Normal	0	10

Figure S7: Available data on the effect of time since fire on (a) seeds per stem and (b) seedling survival from emergence in January until the annual census in October/November. Each point is a separate population and year combination. Note that Menges and Quintana-Ascencio (2004) found an effect of time since fire on seedling survival, when March precipitation was also included in a regression.
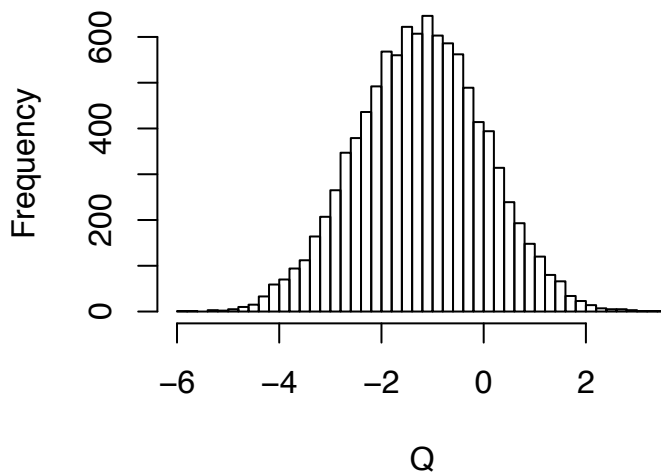
Figure S8: Distribution of the latent parameter (Q) when simulated for 10,000 years with a fire return interval of 22 years. At each time step the latent parameter is sampled from a normal distribution with a mean of $\beta_{tsf} \times TSF$ (where TSF is the number of years since fire) and a standard deviation of one.
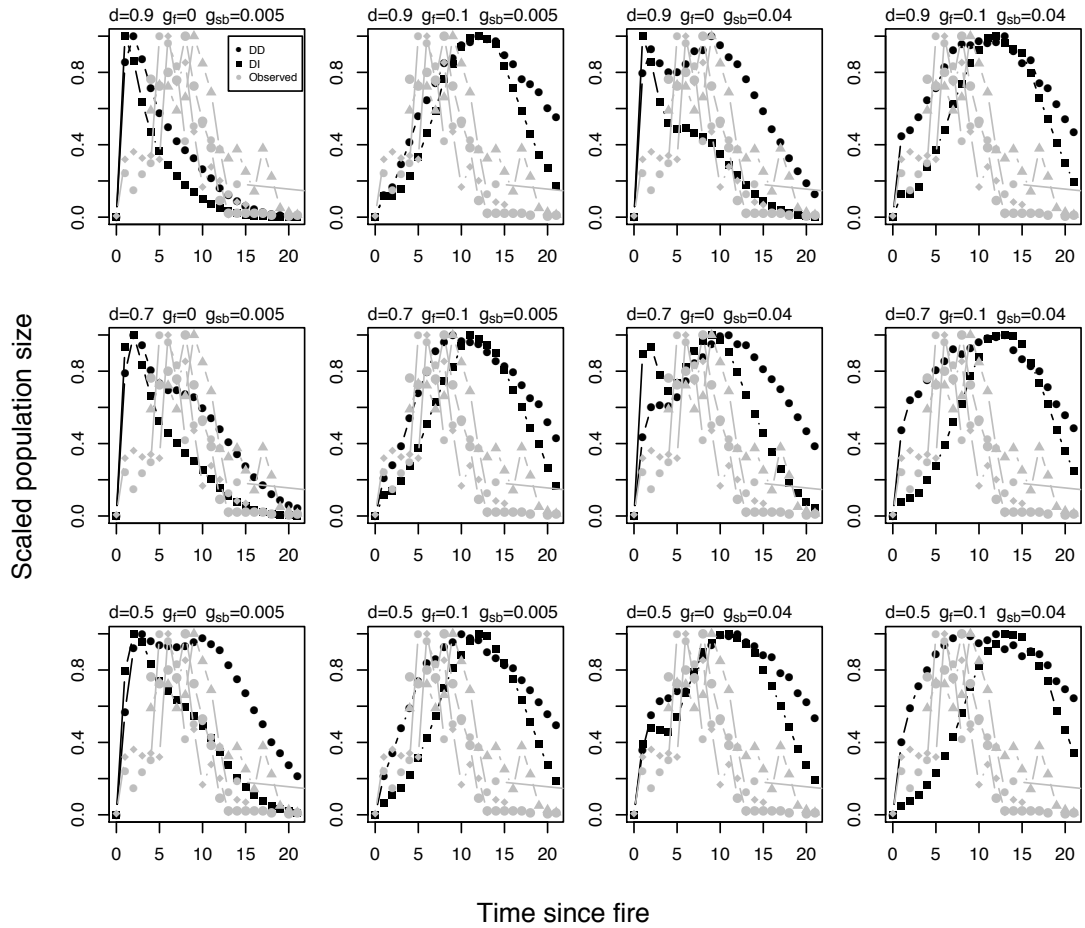
Figure S9: Scaled population size against time since fire for the density dependent (DD) and density independent (DI) models and observed populations for the twelve different fertility scenarios. The fertility scenarios are characterised by seed mortality (d), first year germination (g_f) and germination from the seedbank (g_{sb}). The predicted population sizes are the means for 1000 simulations. The population sizes are scaled by dividing by the maximum population size seen in that population or simulation. See Appendix A5 for details on the density dependent model.
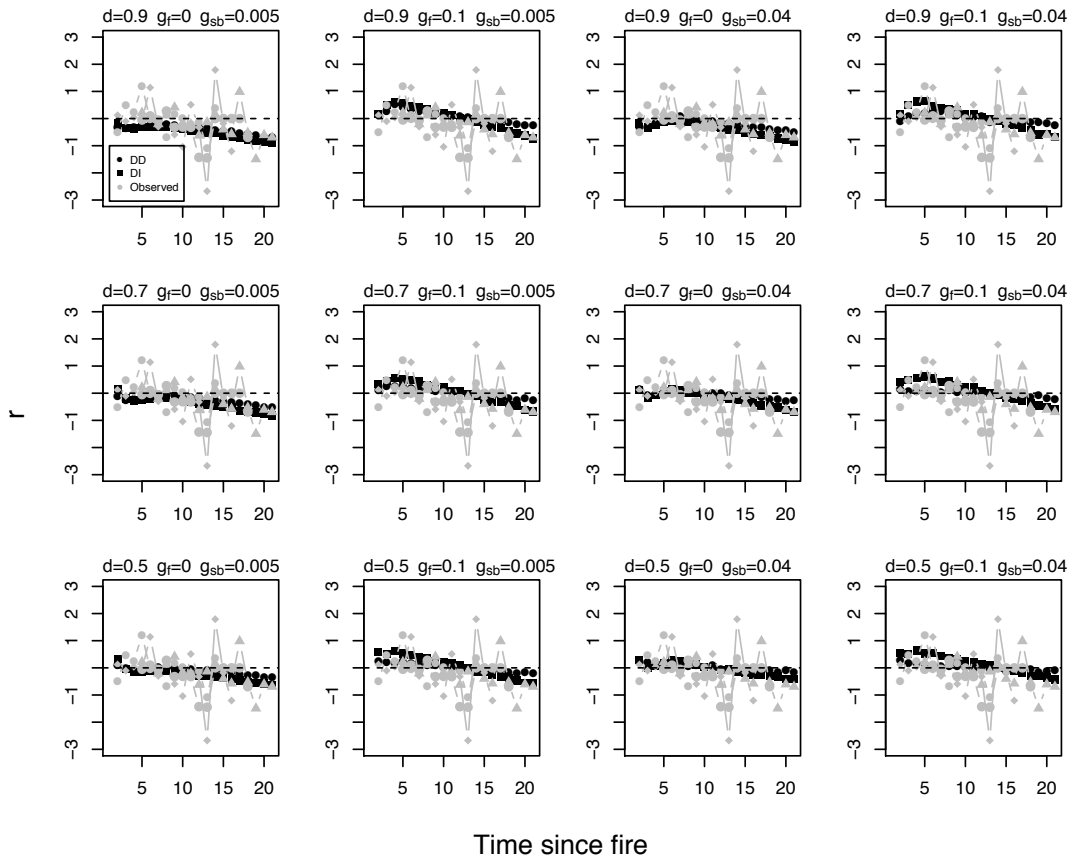
Figure S10: Above ground population growth rate ($log\left(\frac{N_t}{N_{t-1}}\right)$) against time since fire for the density dependent (DD) and density independent (DI) models and observed populations for the twelve different fertility scenarios. The fertility scenarios are characterised by seed mortality (d), first year germination (g_f) and germination from the seedbank (g_{sb}). The predicted growth rates are the means for 1000 simulations. See Appendix A5 for details on the density dependent model.
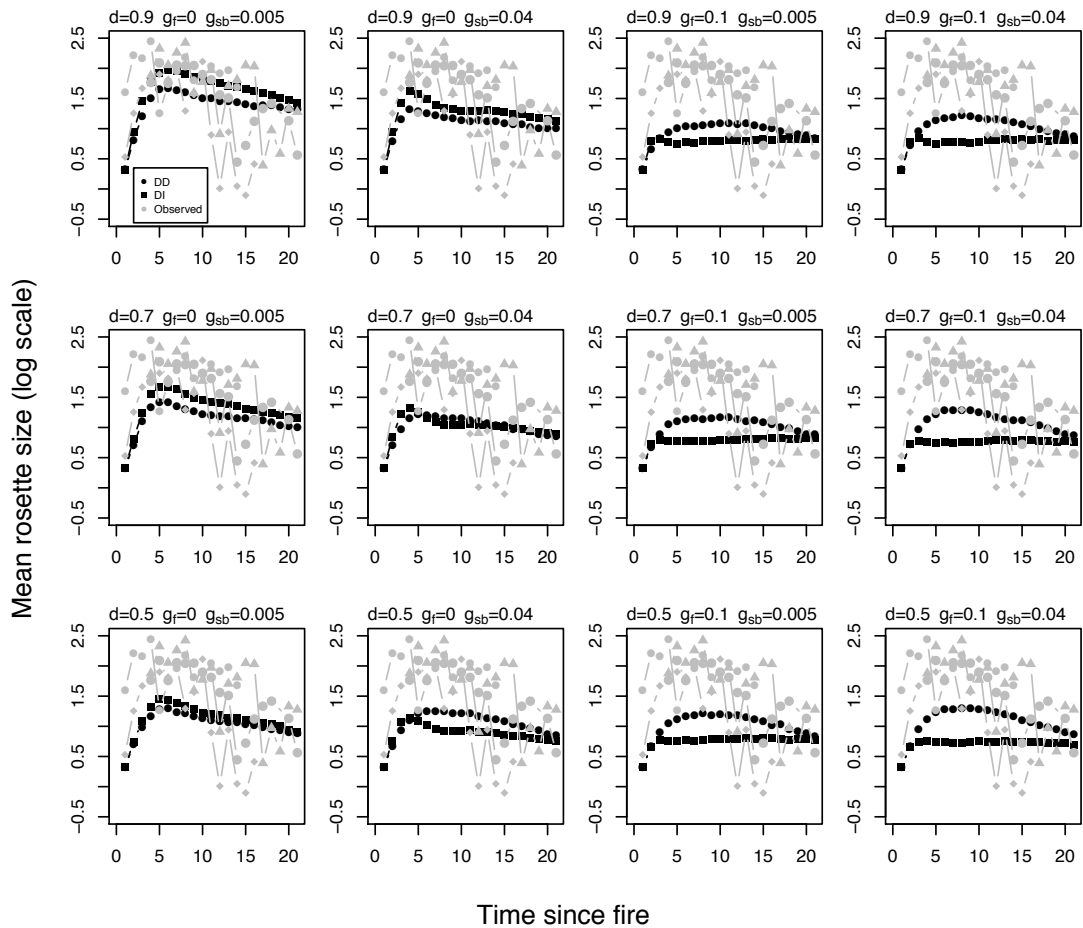
Figure S11: Mean rosette diameter (on a log scale) for the density dependent (DD) and density independent (DI) models and observed populations for the twelve different fertility scenarios. The fertility scenarios are characterised by seed mortality (d), first year germination (g_f) and germination from the seedbank (g_{sb}). The predicted sizes are the means of the mean population size for 1000 simulations. See Appendix A5 for details on the density dependent model.
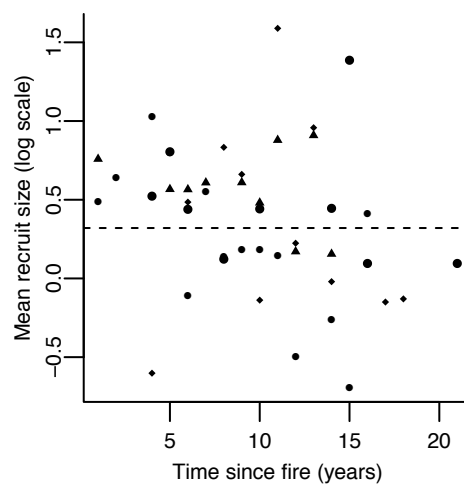
Figure S12: Mean seedling size (log scale) at the annual census over time since fire for four observed populations (each symbol is a different population). Each point is a different time since fire and population combination. Dotted line shows the mean recruit size from the study population, which is used in the IPMs.

Appendix A3: Prior sensitivity

One possible advantage of a Bayesian approach is the ability to include prior information when estimating parameters (e.g. Hobbs *et al.* 2015). This may be useful for example for rare species, where data availability may be low, but expert knowledge or data from different study sites or from closely related species could be included into the priors (e.g. HilleRisLambers, Clark & Lavine 2005).

Where more informative priors are used sensitivity analyses can determine how robust the posterior distributions are to changes in the priors. Here we compare posteriors using our initial fairly broad priors to those using more informative priors where we assume that 50% of the temporal variation in the vital rates can be accounted for by the latent parameter. The magnitude of the standard deviation of the submodel specific year effects is therefore constrained to equal the factor loading terms (β_{Yr}). The use of more informative priors has little effect on most of the fixed effect parameters in the *Carduus* model (Fig. S13a), but decreases the credible intervals and affects the posterior means for the random effects (Fig. S13b). The means of the factor loading parameters for survival (β_{Yr}^{s}) and recruitment (β_{Yr}^{r}) increase, whilst those for recruit size (β_{Yr}^{rs}) and growth (β_{Yr}^{g}) decrease. Including more informative priors leads to slightly higher mean estimates of the β_{Yr} parameters in the survival, flowering and fecundity *Eryngium* submodels (Fig. S14), as well as decreasing the credible intervals.
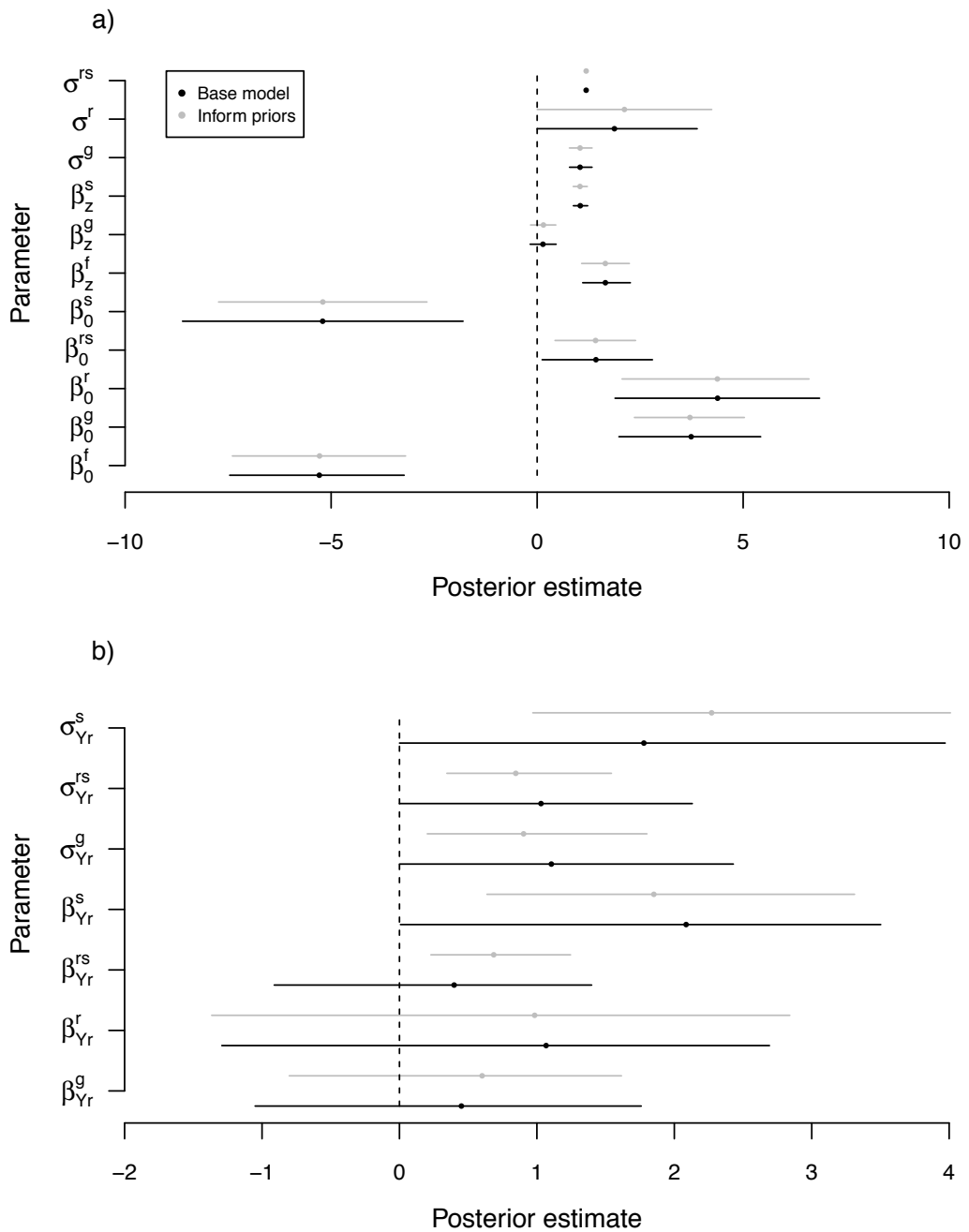
Figure S13: Joint parameter posteriors for the *Carduus* base model and a model with more informative priors; (a) fixed effect parameters (b) year effect parameters. Points show the means and horizontal lines show the 95% credible intervals for each parameter. Vertical dashed line is at 0 in both plots.
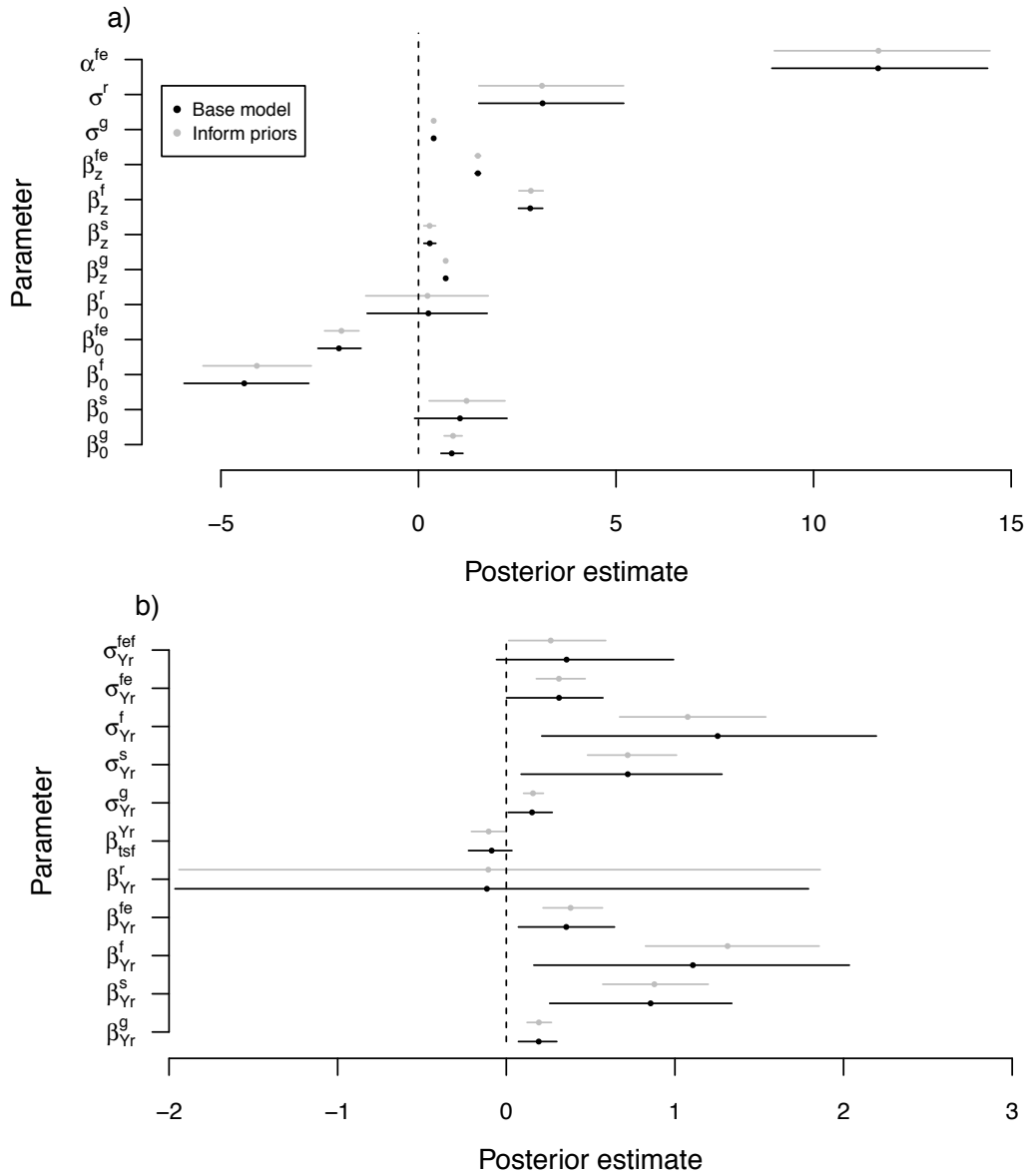
Figure S14: Joint parameter posteriors for the *Eryngium* base model and a model with more informative priors; (a) fixed effect parameters (b) year effect parameters. Both models include the recruitment function (Appendix A5). Points show the means and horizontal lines show the 95% credible intervals for each parameter. Vertical dashed line is at 0 in both plots. See Table 5 for parameter definitions.

Appendix A4: Calculating Evolutionary Stable Strategies

As this population exhibits density dependence, fitness depends on the presence of other life history strategies and was therefore measured using an invasion exponent (Childs *et al.* 2004). The invasion exponent is defined as

$$\vartheta = \lim_{t \to \infty} t^{-1} E[\ln(N_t)], \qquad \text{(eqn A2)}$$

where N_t is the total population size at time t (Tuljapurkar 1990; Metz, Nisbet & Geritz 1992). ϑ is the stochastic growth rate of a rare invader; the maximum likelihood estimator of ϑ is given by

$$\hat{\vartheta} = \frac{\ln(N_t) - \ln(N_1)}{t - 1} \qquad \text{(eqn A3)}$$

The estimated flowering intercept (-5.31) and a germination probability of 0.2 were used to generate a resident time series of 5,000 years. Simulations were started with an initial population of 1000 seeds. The invader inhabits the same 5,000 year time series as the resident; i.e. it uses the same latent year effect and submodel specific year effects at each year of the simulation. As the invader is assumed to be rare, its density does not affect the population growth rate and as such the probability of establishment for the invader is assumed to be equal to that of the resident. The invasion exponent is maximised using a Nelder-Mead algorithm, resulting in new reproductive parameters (flowering intercept and germination probability). These are used to generate a new resident environment; again the invasion exponent is maximised and this process is repeated until the reproductive parameters converge to a specified tolerance (0.001). As the germination probability must lie between 0 and 1 this was modelled using a logistic function. The probability of seed mortality (d) was not known and therefore the model was run multiple times with a wide range of seed mortalities (d=0.01, 0.1, 0.2,...,0.9, 0.99, Rees *et al.* 2006).

The ESS flowering intercept remains roughly constant under changing seed mortalities, and remains within the 95% credible interval of the parameter estimate (Fig. S15a), whilst the ESS germination probability increases linearly with an increasing probability of seed mortality (Fig. S15b). With a flowering intercept of around -5 most plants will flower in their first year. The ESS are generally well characterised, as a relatively small range of strategies have a fitness of over 0.99 (Fig. S15).
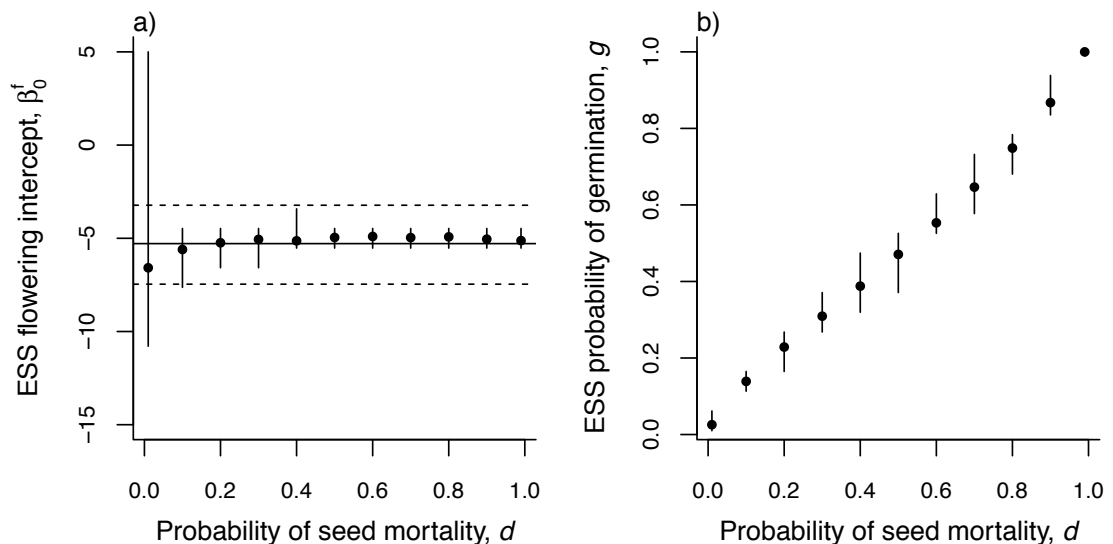

Figure S15: Joint ESS flowering (a) and germination strategies (b) under differing seed mortalities, d. Vertical lines show strategies with fitness over 0.99. In (a) the solid horizontal line shows the estimated flowering intercept and dashed horizontal lines show the 95% credible interval.

Appendix A5: *Eryngium* IPM with density dependent recruitment

To check whether the assumption of density independence affected the model output we also built an IPM with density dependent recruitment. The density independent seedling survival term (ss^t; Appendix A2) was replaced by a density dependent probability of recruitment, $p_e(t)$. This was calculated as in the *Carduus* model (Appendix A2) by dividing the number of recruits each year by the total number of germinating seeds.

      Recruitment was included in the stochastic vital rates model using a poisson lognormal distribution as follows:

$$R(t+1) \sim \text{Poisson}(\lambda^r) \qquad\qquad\qquad\qquad (\text{eqn A4})$$
$$\lambda^r \sim \text{Lognormal}(\mu^r, \sigma^r)$$
$$\mu^r = \beta_0^r + \beta_{Yr}^r Yr_{[t]},$$

where $R(t)$ is the number of recruits in year t. Using a Poisson lognormal distribution to estimate recruit numbers is necessary to allow for overdispersion, however using this distribution results in some unrealistically high recruit numbers. As such the number of recruits is restricted to be less than 300 in the IPM. The mean number of recruits seen in the study population is 12 and the maximum is 94; the largest number of rosettes in one year is 219.

      There appears to be a relatively small effect of TSF on recruitment in this population (Figs S6 & S13); this is contradictory to previous studies that found that seedling survival was negatively affected by time since fire (Menges & Quintana-Ascencio 2004). This is possibly because the population is not subject to a fire during the study period; if the effect is strongest immediately following a fire this will not be apparent from our dataset.

      The addition of the recruitment function had little effect on the distributions of the remaining parameters (Fig. S16). As such there is little difference in the remaining vital rate functions between the density dependent and independent models (Fig. S6).

      The density dependent models produce similar patterns of population size with time since fire as the density independent models; all of the models show population sizes first increasing then decreasing as time since fire increases (Fig. S11). The density dependent models do not underestimate mean size to the same extent as the density independent models (Fig. S13). This suggests that the underestimation may be caused by too much recruitment into the population as recruitment is limited in the density dependent, but not the density independent model.
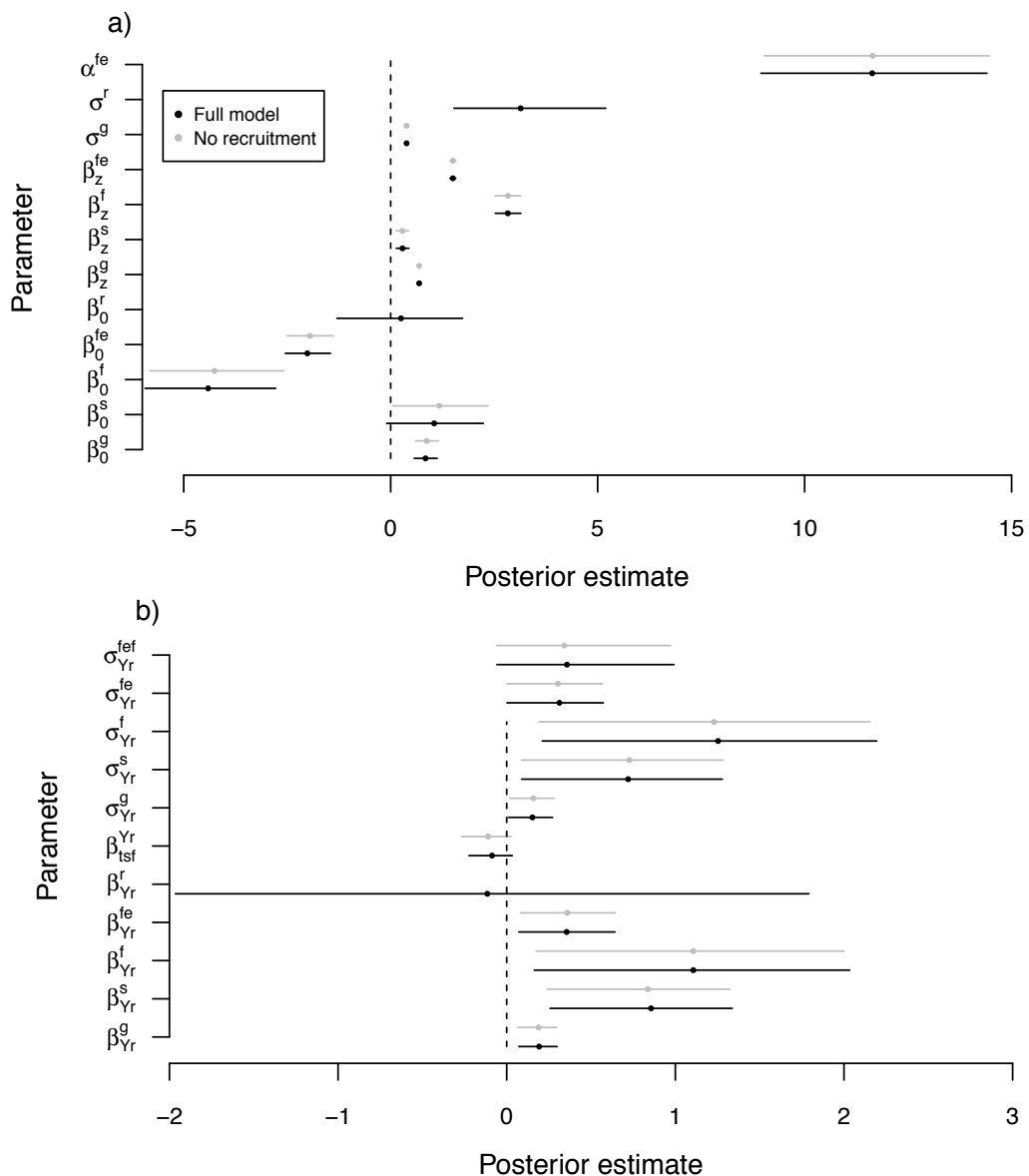
Figure S16: Joint parameter posteriors for *Eryngium* for (a) fixed effects and (b) year effects for models including (for density dependent model) and excluding (for density independent model) recruitment. Points show the means and horizontal lines show the 95% credible intervals for each parameter. Vertical dashed line is at 0 in both plots.

References

Childs, D.Z., Rees, M., Rose, K.E., Grubb, P.J. & Ellner, S.P. (2003) Evolution of complex flowering strategies: an age- and size-structured integral projection model. *Proceedings of the Royal Society B-Biological Sciences,* **270,** 1829-1838.

Childs, D.Z., Rees, M., Rose, K.E., Grubb, P.J. & Ellner, S.P. (2004) Evolution of size-dependent flowering in a variable environment: construction and analysis of a stochastic integral projection model. *Proceedings of the Royal Society B-Biological Sciences,* **271,** 425-434.

Clutton-Brock, T.H. & Pemberton, J.M. (2004) *Soay Sheep: Dynamics and Selection in an Island Population.*

Denwood, M.J. (in review) runjags: An R package providing interface utilities, parallel computing methods and additional distributions for MCMC models in JAGS. Journal of Statistical Software.

Diez, J.M., Giladi, I., Warren, R. & Pulliam, H.R. (2014) Probabilistic and spatially variable niches inferred from demography. *Journal of Ecology,* **102,** 544-554.

Easterling, M.R., Ellner, S.P. & Dixon, P.M. (2000) Size-specific sensitivity: Applying a new structured population model. *Ecology,* **81,** 694-708.

Evans, M.E.K., Holsinger, K.E. & Menges, E.S. (2010) Fire, vital rates, and population viability: a hierarchical Bayesian analysis of the endangered Florida scrub mint. *Ecological Monographs,* **80,** 627-649.

Gelman, A. & Hill, J. (2007) *Data analysis using regression and multilevel/hierarchical models*. Cambridge University Press.

HilleRisLambers, J., Clark, J.S. & Lavine, M. (2005) Implications of seed banking for recruitment of southern Appalachian woody species. *Ecology,* **86,** 85-95.

Hobbs, N.T., Geremia, C., Treanor, J., Wallen, R., White, P.J., Hooten, M.B. & Rhyan, J.C. (2015) State-space modeling to support management of brucellosis in the Yellowstone bison population. *Ecological Monographs,* **85,** 525-556.

Hunter, M.E. & Menges, E.S. (2002) Allelopathic effects and root distribution of Ceratiola ericoides (Empetraceae) on seven rosemary scrub species. *American Journal of Botany,* **89,** 1113-1118.

Menges, E.S., Craddock, A., Salo, J., Zinthefer, R. & Weekley, C.W. (2008) Gap ecology in Florida scrub: Species occurrence, diversity and gap properties. *Journal of Vegetation Science,* **19,** 503-514.

Menges, E.S. & Kimmich, J. (1996) Microhabitat and time-since-fire: Effects on demography of Eryngium cuneifolium (Apiaceae), a Florida scrub endemic plant. *American Journal of Botany,* **83,** 185-191.

Menges, E.S. & Quintana-Ascencio, P.F. (2004) Population viability with fire in Eryngium cuneifolium: Deciphering a decade of demographic data. *Ecological Monographs,* **74,** 79-99.

Metcalf, C.J.E., Ellner, S.P., Childs, D.Z., Roberto, S.-G., Merow, C., McMahon, S.M., Jongejans, E. & Rees, M. (2015) Statistical modelling of annual variation for inference on stochastic population dynamics using Integral Projection Models. *Methods in Ecology and Evolution,* **6,** 1007-1017.

Metz, J.A.J., Nisbet, R.M. & Geritz, S.A.H. (1992) HOW SHOULD WE DEFINE FITNESS FOR GENERAL ECOLOGICAL SCENARIOS. *Trends in Ecology & Evolution,* **7,** 198-202.

Qiu, W. & Joe, H. (2015) clusterGeneration: Random Cluster Generation (with Specified Degree of Separation). . R package version 1.3.4. http://CRAN.R-project.org/package=clusterGeneration.

Quintana-Ascencio, P.F., Dolan, R.W. & Menges, E.S. (1998) Hypericum cumulicola demography in unoccupied and occupied Florida scrub patches with different time-since-fire. *Journal of Ecology,* **86,** 640-651.

Quintana-Ascencio, P.F. & Menges, E.S. (2000) Competitive abilities of three narrowly endemic plant species in experimental neighborhoods along a fire gradient. *American Journal of Botany,* **87,** 690-699.

Rees, M., Childs, D.Z., Metcalf, J.C., Rose, K.E., Sheppard, A.W. & Grubb, P.J. (2006) Seed dormancy and delayed flowering in monocarpic plants: Selective interactions in a stochastic environment. *American Naturalist,* **168,** E53-E71.

Sletvold, N. (2002) Effects of plant size on reproductive output and offspring performance in the facultative biennial Digitalis purpurea. *Journal of Ecology,* **90,** 958-966.

Tuljapurkar, S. (1990) Population dynamics in variable environments. *Lecture Notes in Biomathematics,* **85,** 1-154.

Weekley, C.W., Gagnon, D., Menges, E.S. & Quintana-Ascencio, P.F. (2007) Variation in soil moisture in relation to rainfall, vegetation, gaps, and time-since-fire in Florida scrub. *Ecoscience,* **14,** 377-386.

Williams, J.L., Miller, T.E.X. & Ellner, S.P. (2012) Avoiding unintentional eviction from integral projection models. *Ecology,* **93,** 2008-2014.

Chapter 3: Managing disturbance dependent populations under a changing climate

Bethan J. Hindle[1], Pedro F. Quintana-Ascencio[2], Eric S. Menges[3] & Dylan Z. Childs[1]

[1] Department of Animal and Plant Sciences, Alfred Denny Building, University of Sheffield, Western Bank, Sheffield, S10 2TN, UK

[2] Department of Biology, University of Central Florida, 4000 Central Boulevard, Orlando, FL 32816, USA

[3] Archbold Biological Station, Venus, FL, USA

Abstract

1. The frequency of ecological disturbances, such as fires, is changing due to shifting habitat use and climatic conditions. Disturbance regimes may be manipulated to promote the persistence of disturbance-adapted species. Population viability analyses are often used to predict the range of disturbance regimes under which species may persist. However, longer-term nonlinear effects of time since the disturbance are rarely considered. Additionally, the effects of changes in other abiotic factors, such as climate, are usually disregarded.

2. The effects of some environmental drivers, such as climate, may vary at finer time scales than demographic data are collected. Many studies choose single temporal windows for these drivers *a priori*.

3. We compare population persistence using different fire return intervals (FRIs) under past and predicted future climatic conditions for the rare fire dependent herb *Eryngium cuneifolium*. Nonlinear effects of individual size and time since fire were identified using generalised additive models (GAMs). Functional linear models (FLMs) were used to estimate the cumulative effect of climatic variables across the annual cycle, allowing the strength and direction of the climatic effects to differ over the year. Extinction probabilities and minimum population sizes were estimated under past and forecasted future climatic conditions and a range of FRIs, using an integral projection model.

4. The fastest rate of decay in the vital rates occurs in the first ten years post fire. Under forecasted climate change *E.cuneifolium* is predicted to persist under a much broader range of FRIs, as increasing temperatures increase individual growth. Climatic effects on survival and fecundity do not result in temporal trends in these vital rates due to antagonistic within year effects, for example higher winter temperatures increase fecundity whilst higher summer temperatures are associated with reduced fecundity.

5. Climate is a widespread driver of ecological change. Including responses to predicted climate change can affect predictions of future population viability and therefore management decisions. Antagonistic within year climatic effects highlight the risk of picking temporal windows of influence for climatic drivers *a priori*. Instead FLMs may be used to allow the strength and direction of estimated climatic effects to vary over the annual cycle.

Keywords: *Eryngium cuneifolium*; extinction probability; fire; functional linear model; generalised additive model; integral projection model; nonlinear; non-stationary

Introduction

Disturbances, such as fires or floods, can alter biodiversity and community structure, and may drive patterns of local population extinctions (Turner 2010; Velle *et al.* 2014; Thom & Seidl 2016). The frequency of such events has been altered over recent time scales, due to anthropogenic effects including land use modifications and climate change (Bayley 1995; Restrepo *et al.* 2009; Knorr *et al.* 2014). Many species are adapted to live in frequently disturbed habitats, for example fire-adapted plants may have persistent seed banks, with extreme heat required for germination (e.g. Davies *et al.* 2013). Such species are often outcompeted when disturbance regimes are suboptimal and have therefore often declined as these regimes have changed (O'Connor *et al.* 2017). Management strategies that restore natural disturbance regimes may be used to aid the persistence of these species (Swetnam, Allen & Betancourt 1999; Allen *et al.* 2002; Menges 2007). However, disturbance frequency is not the only environmental factor that will influence population viability. Weather, habitat quality, and biotic interactions are all likely to have important roles (Tschope & Tielborger 2010; Bucharova, Brabec & Munzbergova 2012; Sletvold *et al.* 2013; Bernardo, Albrecht & Knight 2016). Anticipated directional changes in such variables, for example due to climate change (IPCC 2014), may alter population persistence under different disturbance regimes (Harris *et al.* 2006; Flatley & Fule 2016). Population responses to environmental change should therefore be taken into account when planning future management strategies (Hannah, Midgley & Millar 2002; Bernardo, Albrecht & Knight 2016).

Population viability analyses (PVAs) use population models to simulate future dynamics and calculate metrics of performance such as population size, growth rate, and extinction risk (Menges 2000). PVAs have been widely adopted to determine the conservation status of populations and identify appropriate management strategies (e.g. Ryan, Root & Mayer 1993; Lindenmayer & Possingham 1996; Thompson *et al.* 2000; Jaffre & Le Galliard 2016). One quarter of environmentally explicit demographic models in plants have considered the role of disturbance (Ehrlen *et al.* 2016), often with the goal of determining how disturbance regimes can be optimised to maximise the probability of future persistence (e.g. Sanchez-Velasquez *et al.* 2002; Brys *et al.* 2004) or to eradicate invasive species (e.g. Emery & Gross 2005). Most of these studies have assumed that, with the exception of disturbance frequency, populations will continue to experience the same environmental conditions present during the period of observation (though see e.g. Bucharova, Brabec & Munzbergova 2012; Bernardo, Albrecht & Knight 2016). Changing environmental conditions may drastically alter demographic rates; ignoring such effects can therefore produce inaccurate future population predictions (Coulson *et al.* 2001; Crone *et al.* 2013). Climate change has already been implicated in local population extinctions (Wiens 2016) and is predicted to become a large driver of future extinction dynamics (van Vuuren, Sala & Pereira 2006). However, studies of climatic impacts on plant demography are relatively rare (Selwood, McGeoch & Nally 2015; Ehrlen *et al.* 2016).

Incorporating the effects of climate change may provide more accurate predictions of future dynamics (Fieberg & Ellner 2001; Crone *et al.* 2013), allowing the development of management strategies that are appropriate for future environmental conditions (Bucharova, Brabec & Munzbergova 2012; Bernardo, Albrecht & Knight 2016).

Demographic responses to disturbance are often estimated as a function of discrete categories of disturbance events, such as whether or not a fire has recently occurred (e.g. Canales *et al.* 1994; Stevens & Latimer 2015). However, the effect of a disturbance is unlikely to be restricted to the year it occurs and is likely to decrease as time since the disturbance increases (Fieberg & Ellner 2001). For example, community composition may change slowly in the years following a fire as species re-establish at different rates (Menges & Hawkes 1998). Under these circumstances time since disturbance should be included as a predictor of the vital rates (e.g. Evans, Holsinger & Menges 2010; Merow *et al.* 2014), though the response to environmental perturbations may not change linearly with time (Doak & Morris 2010). Generalised additive models (GAMs) are a flexible form of model that allow nonlinear effects to be captured (Wood 2017) and as such may be used to capture nonlinear demographic responses to environmental covariates among years (e.g. Scanga 2014)

Most environmental drivers, such as climatic variables, vary at much finer time scales than the annual time steps at which demographic data are typically collected. The impact of such drivers on the vital rates may play out over long periods, or during a short critical window, and both the magnitude and direction of their effects may vary over the annual cycle (Foster, Schmalzer & Fox 2014; Kruuk, Osmond & Cockburn 2015). This necessitates methods to quantify environmental effects that differ in timing, magnitude, and direction. Vital rate responses to environmental variables are likely to be more similar at closer time points, for example the effect of high temperatures in July is likely to be relatively similar to the effect of high temperatures in August, but may be considerably different to high temperatures in February (Sims *et al.* 2007). Functional linear models allow the response to a climatic covariate to be estimated as a smooth function, allowing the effects to differ in magnitude and direction over time (Roberts 2008; Teller *et al.* 2016).

Here, we explore how forecasted climate change affects population viability under a range of disturbance regimes in the fire-adapted species, *Eryngium cuneifolium*. We used GAMs to capture nonlinear responses to individual size and time since fire. By using FLMs to estimate the climatic responses we allowed the effects to differ in magnitude and direction over the year. *E.cuneifolium* is a rare perennial herb, endemic to Florida rosemary scrub (Menges & Kimmich 1996; Menges & Quintana-Ascencio 2004). Its vital rates are negatively affected by time since fire, as it is outcompeted by shrubs such as *Ceratoila ericoides* (Menges & Kimmich 1996; Quintana-Ascencio & Menges 2000). Previous studies have suggested that fire return intervals (FRIs) of less than 15 years are necessary for its persistence (Menges & Quintana-Ascencio 2004; Menges 2007). While the response of this endemic to differing FRIs has been

well studied, little is known about the effects of climatic variation on its demography. We consider whether future forecasted climate change will affect population viability in this species under a broad range of FRIs. Extinction probabilities and minimum population sizes were estimated by using the vital rate models to parameterise an integral projection model (IPM). Populations were simulated under a range of FRIs using past and future predicted climatic conditions.

Methods

Study system

We used demographic data from twelve populations found in burned areas, from 1990 to 2014, at the Archbold Biological Station, Florida (Menges & Quintana-Ascencio 2004). This included over 10,000 observations of more than 4,000 individual plants. Individual measurements were recorded annually at the end of October/beginning of November. Across all populations and the whole study period time since fire varied from zero to 42 years. The square root of rosette diameter was used as a measure of plant size. The vital rates were assumed to be density independent as *E.cuneifolium* is a rare species and interspecific interactions are more limiting than intraspecific competition (Menges & Kimmich 1996).

The study site undergoes cold, dry winters and hot, wet summers, with the highest monthly temperatures in August and the majority of the precipitation falling between June and September (Fig. 1). Daily weather data were recorded onsite at the Archbold Biological Station. Four climatic covariates were considered; minimum temperature (°C), maximum temperature (°C), precipitation (mm) and the Keetch-Byram drought index (KBDI), which is a function of mean annual precipitation, daily maximum temperature and daily precipitation (Appendix A1; Keetch & Byram 1968). The means of each of the daily climatic variables was calculated every fortnight from the beginning of November in year t until the end October in year $t + 1$, i.e. for the twelve months between each annual census.

Predicted climatic data were available from the Meteorological Research Institute atmospheric general circulation model, version 3.2 (MRI-AGCM3.2), with a 60 km grid size (Mizuta *et al.* 2012). Climatic data were simulated from 1979-2099 (Kusunoki & Mizuta 2013) assuming the moderate emissions scenario, A1B (IPCC 2007). Predicted climatic data from general circulation models (GCMs) often differs from that recorded at local weather stations due to model biases or differences in spatial scale between the predicted and observed data, with forecasted climatic data usually at a broader spatial scale than that required for ecological studies (Ekstrom, Grose & Whetton 2015; Baker *et al.* 2017). A cumulative distribution function transform (CDF-t) approach was therefore used to downscale predictions from the GCM (Appendix A1; Michelangeli, Vrac & Loukos 2009; Lavaysse *et al.* 2012). Temperatures were generally predicted to increase, with particularly strong effects over spring and summer (Fig. 1c and e). Whilst precipitation does not appear to undergo a directional change over the

forecast period (Fig. 1g) the increase in maximum temperatures causes an increase in the KBDI (Fig. 1a). There are no clear trends in the among year variability of the climatic predictors over this period (Fig. 1).
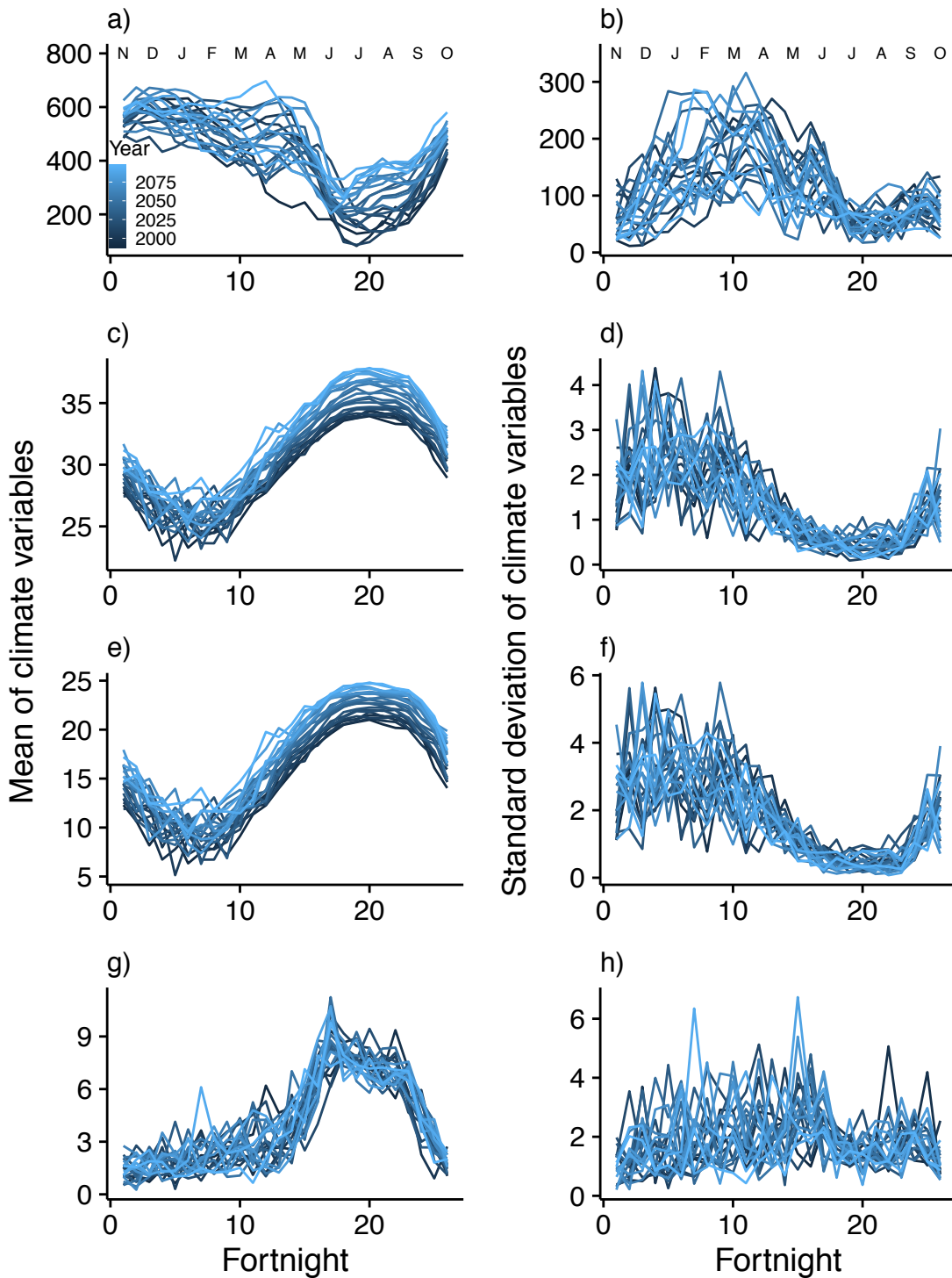

Figure 1: Intra-annual change in the mean (a, c, e, and g) and standard deviation (b, d, f, and h) of the KBDI (a and b), maximum temperature (c and d), minimum temperature (e and f), and precipitation (g and h). Data shown over the 25-year study period (1990-2014) and 85 year forecast period (2015-2099). Each line is the mean (left column) or standard deviation (right column) over a five year period. The letters at the top of the plot indicate the month of the year; the annual census takes place at the end of October or beginning of November. KBDI is on a scale from zero (soil fully saturated) to 800 (maximum possible drought).

Structure of the IPM

As *E.cuneifolium* has a persistent seed bank (Navarra *et al.* 2011) we constructed a two stage stochastic IPM to simulate population dynamics:

$$B(t+1) = (1-d)(1-g_b)B(t) + (1-d)\left(1-g_f\right)\int_\Omega f_\bullet(z)n(z,t)dz,$$

$$n(z',t+1) = k_\bullet(z')B(t) + \int_\Omega [p_\bullet(z',z) + f_\bullet(z',z)\,]n(z,t)dz\,, \qquad \text{(eqn 1)}$$

where $B(t)$ is the number of seeds in the seed bank at time t and $n(z,t)dz$ is the number of individuals in the size range $(z, z+dz)$. The • subscripts indicate functions that vary temporally and spatially, i.e. that are a function of time since fire, climatic variables, and random year and population effects. The first term in the seed bank equation refers to seeds that remain in the seed bank from t to $t+1$; these are seeds that survive, with probability $1-d$, and do not germinate, with probability $1-g_b$. The second term refers to seeds produced during year t that enter the seed bank. The probability of seeds germinating immediately $\left(g_f\right)$ differs to that of those germinating from the seed bank in later years (g_b) (Quintana-Ascencio & Menges 2000; Menges & Quintana-Ascencio 2004). The seed production function, $f_\bullet(z)$, is given by $h_\bullet(z)\,m$, where, for a plant of size z, $h_\bullet(z)$ is the number of flowering stems and m is the number of seeds per flowering stem.

In the rosette equation the size distribution of plants recruiting from the seed bank $(k_\bullet(z'))$ is given by $g_b e_\bullet r_\bullet(z')$, where $e_\bullet$ is the probability of a seedling surviving from emergence (January-March) until the annual census and $r_\bullet(z')$ is the distribution of recruit sizes at the annual census. The survival growth function, $p_\bullet(z',z)$, is given by $s_\bullet(z)g_\bullet(z',z)$, where $s_\bullet(z)$ is the survival probability and $g_\bullet(z',z)$ gives the probability of an individual of size z growing to size z'. The size distribution of recruits from seeds produced that year, $f_\bullet(z',z)$, is given by $g_f e_\bullet h_\bullet(z)\,m r_\bullet(z')$. The IPM was implemented using the quadrature midpoint rule with 100 meshpoints; doubling the number of meshpoints did not affect the results.

Parameterisation of the IPM

A model with no climatic drivers was fitted first for each vital rate; these acted as baselines to evaluate the predictive performance of the climatic models. For example, the probability of survival ($s_\bullet(z)$) for individual i in year t was estimated as a function of size (z) and time since fire (l) as follows:

$$logit(s_\bullet(z_{it})) = \beta^0 + f_z(z_{it}) + f_l(l_{tp}) + \varepsilon_p^p + \varepsilon_{tp}^t. \qquad \text{(eqn 2)}$$

β^0 is an intercept and f_z and f_l are smooth functions of size (z), where z_{it} is the size of individual i in year t, and time since fire (l), where l_{tp} is the number of years since a fire occurred in year t for population p. $\varepsilon_p^p \sim N(0, \sigma^p)$ and $\varepsilon_{tp}^t \sim N(0, \sigma^t)$ are random effects for population and year respectively. The random year effects (ε^t) were estimated separately for each year-population combination (tp), but these were drawn from the same distribution, i.e. the

standard deviation of the random year effects (σ^t) did not differ among populations. The smooth functions (f_z and f_l) are parameterised by spline basis expansion, for example $f_z(z) = \sum_{k=1}^{K} \beta_k^z b_k^z(z)$, where β_k^z are coefficients, $b_k^z(z)$ are basis functions and K is the dimension of the spline basis (Wood 2017).

Four climatic models were fitted for each vital rate, each containing a single climatic variable. The cumulative effect of the climatic variables over the twelve-month period prior to the annual census was estimated using FLMs. The FLMs incorporated the mean of the climatic variable every fortnight (w) from the beginning of November (w=1) to the end of October (w=26) as covariates. For example, the probability of survival was given by

$$logit(s.(z_{it})) = \beta^0 + f_z(z_{it}) + f_d(d_{tp}) + \sum_{w=1}^{W} f_c(w)C_{tw} + \varepsilon_p^p + \varepsilon_{tp}^t, \quad \text{(eqn 3)}$$

where C_{tw} is climatic variable C in year t and fortnight w and $f_c(w)$ is a smooth function over time. The remaining parameters are defined above (equation 2). The smooth function $f_c(w)$ is parameterised using spline basis expansion, as above.

The growth and fecundity models are structurally analogous to the survival models (equations 2 & 3), differing only in the assumed distribution and link function (Gaussian for the growth model and negative binomial with a log link for the fecundity model). A Gaussian distribution was assumed for the recruit size model, which also did not include the size spline. Models were fitted in R (R Core Team 2016) using the *gam* function from the *mgcv* package and a cubic regression spline basis (Wood 2017). Six knots were used for the size and time since fire splines and eight for the climatic splines. Quadratic smoothing penalties, $\sum_j \lambda_j \beta^T \boldsymbol{S}_j \beta$, control the degree of smoothing in the splines, where $\boldsymbol{S}_j$ are known smoothing penalty matrices and λ_j are smoothing parameters (Wood 2017). The smoothing parameters (λ) were estimated using restricted maximum likelihood (REML), as this is less prone to overfitting than generalised cross validation (GCV; Appendix A2; Reiss & Ogden 2009; Wood 2011).

Cluster cross validation was used to assess the predictive performance of each climatic model relative to the base model. The models were refitted excluding each year of data in turn and used to predict the vital rates for all excluded individuals. The individual's observed size at $t - 1$, the observed time since fire, and the estimated population random effects for the individual's population were used for the predictions. The random year effects were marginalized out using a Monte Carlo approach, and the RMSE was calculated for that year as follows

$$RMSE_t = \sqrt{\frac{1}{N_t Y} \sum_{n=1}^{N_t} \sum_{y=1}^{Y} (o_{nt} - p_{nyt})^2}, \quad \text{(eqn 4)}$$

where for year t, N_t is the number of individuals observed and o_{nt} and p_{nyt} are the observed and predicted vital rate respectively for individual n and sample y from the distribution of the random year effect. 500 random samples from the random year effect distribution were used. As sample size differed between years the overall score for each year was given by summing the yearly RMSE scores, weighted by the number of individuals observed in that year, that is

overall $RMSE = \sum_{t=1}^{T} RMSE_t N_t$. Where, for a single vital rate, two climatic models had a better predictive performance than the base model, the cross validation procedure was repeated with a model including both climatic covariates.

As the data available to parameterise the remaining IPM functions were more limited (Menges & Quintana-Ascencio 2004) these were assumed not to be driven by climatic variation. Early seedling survival (e) was estimated using a logistic mixed effects model with a fixed effect of time since fire and a random year effect. The number of seeds per flowering stem (m) was set to the mean observed number (183; Menges & Quintana-Ascencio 2004). Estimates of germination range from 0 to 0.1 in the first year (g_f) and 0.005 to 0.04 from the seed bank (g_b) (Quintana-Ascencio & Menges 2000; Menges & Quintana-Ascencio 2004), whilst seed mortality (d) was unknown. Populations were simulated using a range of the germination estimates and a wide range of seed mortality estimates (0.1, 0.3,…,0.9) and compared to observed aboveground population dynamics (Appendix A3, Menges & Quintana-Ascencio 2004). The selected fertility scenario had low germination ($g_f = 0, g_b = 0.005$) and low seed bank mortality ($d = 0.3$; see Appendix A3 for effects of uncertainty in the seed bank parameters on extinction probabilities).

Population viability in a changing climate

We explored how climate change may affect population viability under a range of FRIs, by simulating populations under the observed climatic conditions during the study period (1990-2014; 'past climate') and forecasted future climate (2015-2099; 'future climate'). The downscaled GCM climatic data were used for both the past and future climate simulations. Populations were simulated for 85 years, starting with a fire year. Temporal variation due to time since fire, climatic effects, and random year effects were incorporated independently of one another. The forecasted climate projections from 2015-2099 were used (in sequence) for the future climate simulations. For the past climate simulations, one year of climatic covariates was randomly selected from the 25 observed years at each iteration. FRIs were simulated using a Weibull cumulative distribution function (e.g. Evans, Holsinger & Menges 2010) with a range of medians (3, 6, 9…, 30; Fig. S1). The FRIs were therefore stochastic, with the probability of fire increasing as time since the last fire increased. Fire was assumed to kill all rosettes (Menges & Kohfeldt 1995). The random year and population effects were incorporated using a kernel selection approach to preserve correlations (Rees & Ellner 2009; Metcalf *et al.* 2015). A population was selected for each simulation from each of eleven populations and all of the vital rates were estimated conditional on the population random effects throughout the simulation (one population with no recruits during the study period was excluded, as a random effect could not be estimated for recruit size). At each iteration a year-population combination was selected at random and used for the random year effects across all of the vital rates.

Three sets of simulations were run, to explore the effects of initial population size, variability in the FRI, and differences among the populations. Unless otherwise stated 1,000 simulations were run for each parameter combination. First, a range of initial population sizes were used (1,000, 7,000, 15,000, or 30,000 seeds). Here, the shape parameter (a) of the Weibull distribution for the FRIs was set to 64, resulting in little variation around the median FRI (Fig. S1). Second, we explored how differences in the variability of fire occurrence affected extinction risk. Here, using an initial population size of 7,000 seeds, four values of a (2, 8, 32, and 64; Fig. S1) were used to simulate the FRIs. Third, to determine how extinction probabilities differed among populations, 500 simulations were run for each of the eleven populations, with a set to 64 and an initial population size of 7,000. Quasi-extinction probabilities were given by the proportion of simulations falling below one individual (including seeds). Minimum population sizes were calculated as the mean of the minimum number of individuals in each simulation.
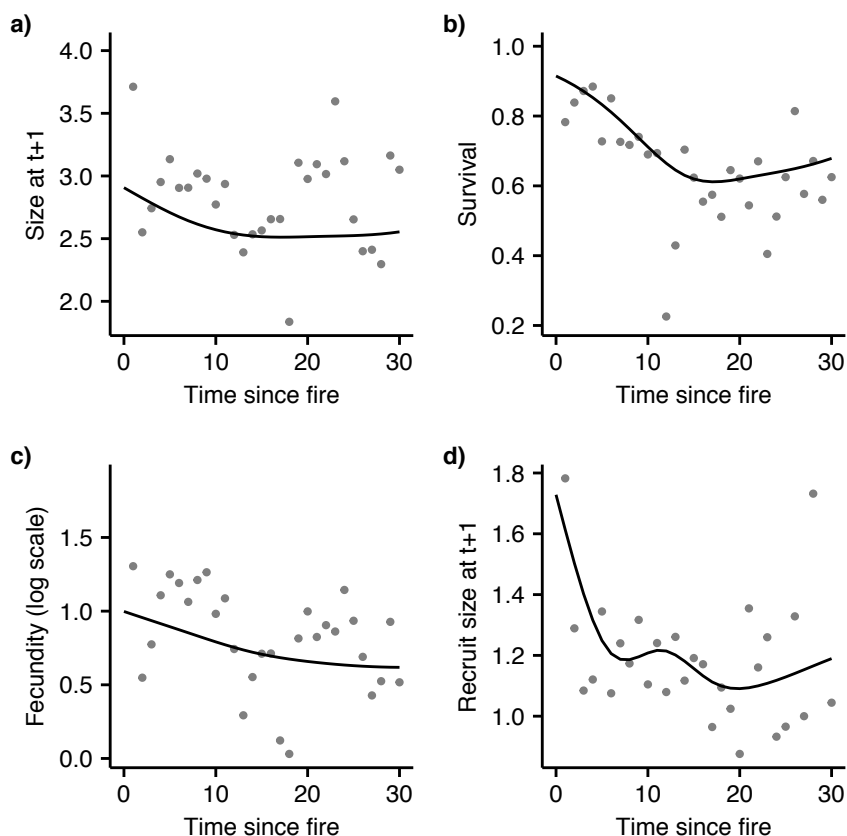
Figure 2: Time since fire models for a) growth, b) survival, c) fecundity, and d) recruit size. Lines show predictions for a median sized individual on a square root scale (2.45) in an average population and year. Points show average for each vital rate across all individuals.

Results

Response of vital rates to time since fire and climatic conditions

The vital rates responded nonlinearly to individual plant size (Fig. S2) and time since fire (Fig. 2). The rates were generally negatively affected by increasing time since fire, with the fastest

decreases in the first ten years post fire. Survival, growth and recruit size appeared to increase slightly after 20 years since fire. However, sample sizes decreased with time since fire (Fig. S3), dropping to an average of 13 individuals per population 25 years postfire. There was also weak evidence of senescence in survival, which decreases in very large (i.e. older) individuals (Fig. S2).

The vital rates responded more to variability in temperature than precipitation. Higher temperatures, particularly over winter and spring, increased growth (Fig. 3a; Table 1). Maximum temperatures were a better predictor of growth than minimum temperatures; including both covariates did not improve the predictive performance beyond that of the maximum temperature model (Table 1). Higher temperatures during summer, when temperatures were at their peak, had a small positive effect on growth compared to the rest of the year (Fig. 3a). Including KBDI as a covariate improved the predictive performance of the survival model. Reduced moisture over winter and spring and increased moisture over summer and autumn were associated with increased survival (Fig. 3c; Table 1). Higher minimum temperatures over winter and spring increased fecundity, whilst higher temperatures during summer decreased fecundity (Fig. 3e, Table 1). Recruits emerge between January and March (Menges & Quintana-Ascencio 2004). Higher maximum temperatures shortly after this period increased recruit size (Fig. 3g; Table 1).

The forecasted temperature increases over the next 85 years (Fig. 1) appear likely to increase growth (Fig. 3b) and recruit size (Fig. 3h). Despite climatic effects being identified in the survival and fecundity models (Fig. 3c and e) these vital rates are not predicted to undergo temporal trends (Fig. 3d and f). Over the annual cycle the climatic effects on these two vital rates are antagonistic, with positive effects over some seasons and negative over others, effectively cancelling each other out (Fig. 3c and e).
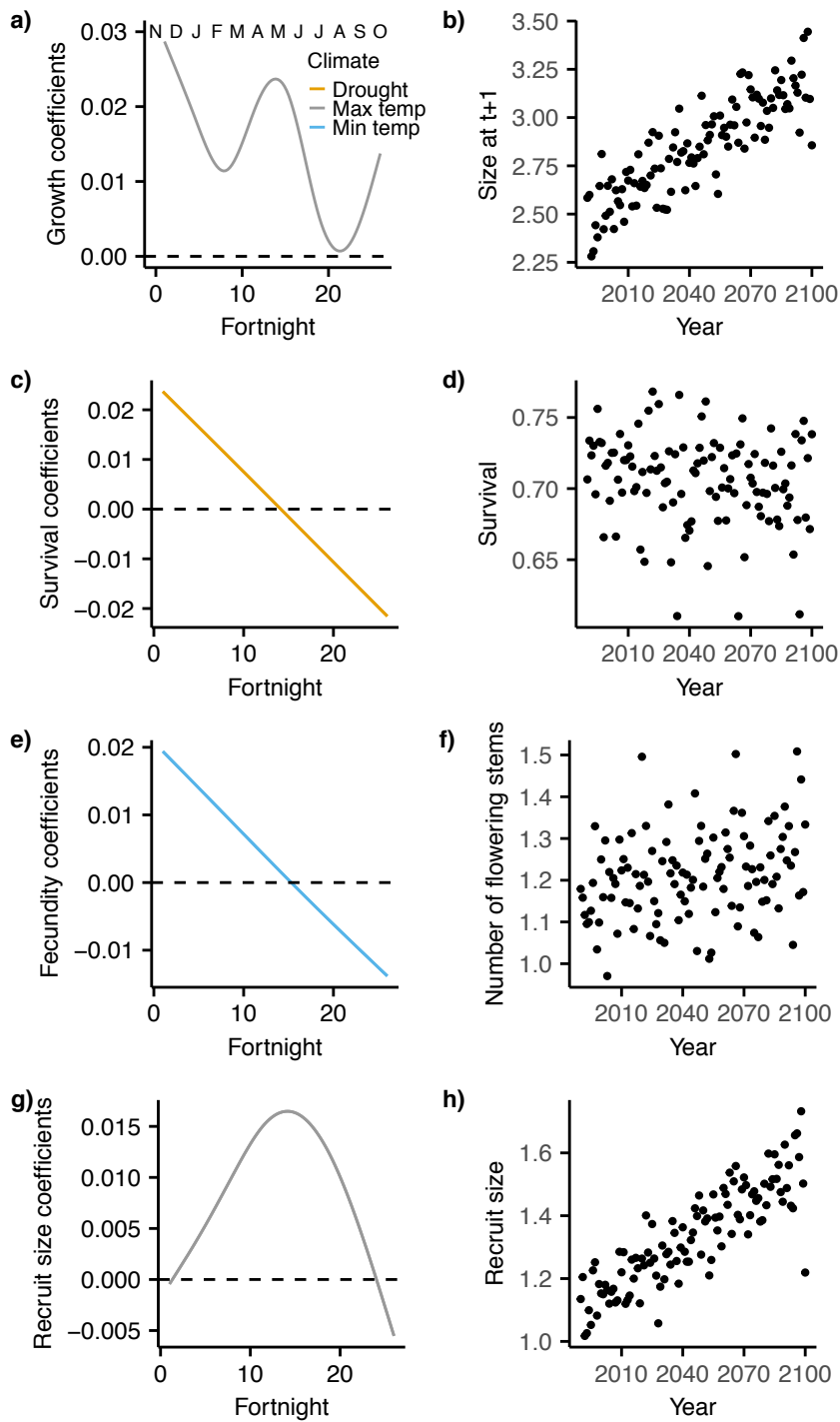
Figure 3: Climatic coefficients over the year preceding the census (left column) and the average annual vital rates estimated using the downscaled climate predictions from 1990 to 2099 (right column). Only the climatic variables with the highest predictive performance are plotted and included in the IPM (Table 1). The coefficients are scaled by the standard deviation of the respective climatic covariate for plotting. Letters at the top of the plot indicate the month of the year. In the right column each point is the prediction for a median sized individual on a square root scale (2.45) ten years post fire and in an average population and year. Increasing the number of knots did not change the pattern in any of the FLMs.

Table 1: Cross validation results comparing the predictive performance of the models. Lower values indicate better predictive performance. Climatic models with a better predictive performance than the base model (with no climatic effects) are highlighted in bold. * denotes the model with the best predictive performance for each vital rate; these are used to parameterise the IPM.

Climate Model	Growth	Survival	Fecundity	Recruit size
Base	3956.3	5039.7	29919.2	988.4
Min temperature	**3905.6**	5055.2	**29888.2***	1003.9
Max temperature	**3854.8***	5071.0	29981.1	**964.4***
Drought	3961.1	**5023.2***	30156.4	997.6
Precipitation	3967.5	5048.7	30102.5	1001.5
Min + max temperature	**3854.9**	-	-	-

Optimal FRIs under a changing climate

In all scenarios the predicted extinction probabilities were lower and minimum population sizes higher under future climatic conditions than past. Under past climatic conditions optimal median FRIs were between nine and fifteen years, with extinction probabilities less than 5% for all initial population conditions over 1,000 individuals, and below 20% with an initial population size of 1,000 seeds (Fig. 4a). Outside of this optimal range mean minimum population sizes were less than 600 individuals, even with an initial population size of 30,000 individuals (Fig. 4b). In the future climate simulations extinction probabilities were below 5% for all median FRIs above three years (Fig. 4b). The largest minimum population sizes were still seen with FRIs between nine and fifteen years. Mean minimum population sizes under these FRIs were between five and eight times as large as those predicted for the same FRIs under past climate (Fig. 4b).

High variability in the FRI ($a = 2$) decreased the extinction probability when the median FRI was very small (<9) or very high (>25) and increased it outside of this range (Fig. 4c and d). There was little difference in the metrics of population performance among the remaining values of a (8, 32, and 64). Extinction risk among populations was very variable. Under past climates the probability of extinction with a median FRI of 30 years varied from 25% to nearly 100% (Fig. 4e). With a median FRI of 15 years the mean minimum population size varied from 10 to over 850 and from 1,500 to over 3,000 among populations under past and future climates respectively (Fig. 4f). Altering the fertility scenario estimates (g_f, g_b, and d) affected the absolute predictions of extinction risk and minimum population size, but not the pattern with respect to FRI or climate (Appendix A3). The probability of extinction remained less than 5% under future climate when the FRI median was over six years (Appendix A3).
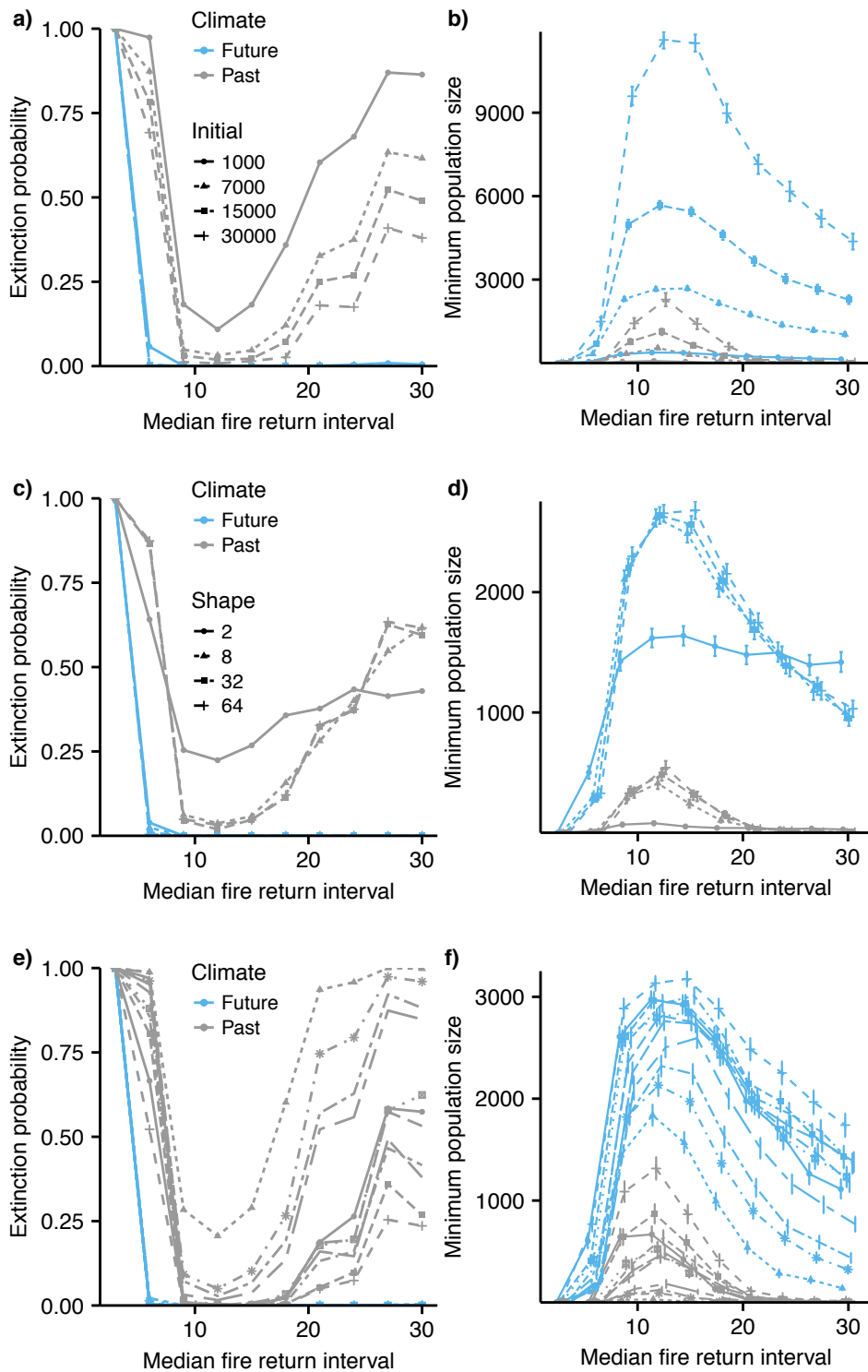
Figure 4: Quasi-extinction probabilities (left column) and minimum population sizes (right column) across a range of FRIs and under past and future climatic conditions. a) and b) show different initial population sizes (number of seeds in seed bank). c) and d) show the effect of changing the level of variability in the FRI, where increasing the shape parameter (a) decreases the variability. In e) and f) each line is a different population. Points show mean of 1,000 simulations (500 in e and f). Error bars in the right column show bootstrapped 95% confidence intervals for the mean. Points were jittered to minimise overplotting.

13

Discussion

Climate change is likely to substantially alter population viability across a broad range of taxonomic groups and geographical locations (Thomas *et al.* 2004; Maclean & Wilson 2011), with implications for the design of appropriate conservation strategies (Bucharova, Brabec & Munzbergova 2012). We found that the range of FRIs under which *E.cuneifolium* is able to persist is likely to increase under forecasted climate change. Optimal disturbance regimes will differ among species within a community, necessitating compromises when determining optimal regimes for the community as a whole (Menges 2007). Under past climatic conditions the probability of persistence for *E.cuneifolium* was low at the upper end of the recommended FRI for Florida rosemary scrub (15-30 years; Menges & Quintana-Ascencio 2004; Menges 2007). Our model predicts that temperature increases towards the end of the 21st century are likely to allow *E.cuneifolium* to persist even with FRIs of 30 years, largely as a result of increasing individual growth. To determine whether the optimal regime for the whole community should be altered due to future environmental change will necessitate predictions of population viability for a range of different species. Under past environmental conditions the performance of *E.cuneifolium* has been limited by the presence of shrubs such as *C. ericoides* (Menges & Kimmich 1996; Menges & Quintana-Ascencio 2004). Thus future optimal FRIs for *E.cuneifolium* are likely to depend on how *C.ericoides* responds to the changing abiotic environment. The climatic effects uncovered in this study may be direct physiological effects or indirect effects, mediated through changes to the competitive ability of *C.ericoides*. Further studies on the influence of climatic conditions on *C.ericoides* and its competitive effects on *E.cuneifolium* are needed to determine the direct and indirect climatic effects operating (e.g. Adler, Dalgleish & Ellner 2012).

Demographic data are often collected annually, yet the vital rates may respond to environmental variation at finer temporal scales (Foster, Schmalzer & Fox 2014; Kruuk, Osmond & Cockburn 2015). Where this occurs, failure to capture effects over the entire annual cycle may lead to inaccurate future predictions at the population level. Demographic studies typically make *a priori* assumptions about the temporal windows over which climatic covariates influence the vital rates, usually selecting a single window (Ehrlen *et al.* 2016; Van der Pol *et al.* 2016). This choice will impact on population predictions. For example, in the case of *E.cuneifolium,* fecundity would be predicted to increase under future temperatures if a winter period was selected, but decrease if a summer period were selected. By capturing the effect of climatic variables over the whole year we found that these effects cancel one another out, resulting in very little net change in predicted future performance. Whilst this method captures nonlinear climatic effects within years, the effects are assumed to be linear among years (Fig. 4). Simultaneously estimating nonlinear effects both within and among years is challenging and likely to require a large degree of temporal replication, with simulations suggesting 20-25 years

14

of demographic data are necessary even to accurately identify effects that are linear across years (Teller *et al.* 2016).

Relationships between environmental drivers and the vital rates are often nonlinear, with, for example, physiological performance reduced when temperatures are too low or too high (Angert, Sheth & Paul 2011). Where the vital rates are recorded on the same temporal scale at which putative environmental drivers vary, such as years since disturbance, nonlinear relationships may be estimated using GAMs (Scanga 2014). The effects of time since fire on the vital rates in *E.cuneifolium* are clearly nonlinear, with the fastest decay in the vital rates seen in the first ten years postfire (Menges & Quintana-Ascencio 2004). Estimating nonlinear relationships usually requires estimates of the vital rates across a broad range of environmental conditions (e.g. Doak & Morris 2010; Diez *et al.* 2014). With a smaller range of observed time since fires, linear relationships would have fitted well. However, this would have led to the vital rate estimates continuing the initial rapid decrease with time since fire and therefore higher predicted extinction probabilities if extrapolated to longer FRIs. Many studies are forced to quantify responses using relatively short time periods following disturbances (Yates & Ladd 2010; Gornish 2013), which may produce inaccurate predictions of future dynamics.

The ability of PVAs to accurately forecast population dynamics has been extensively debated, with many authors cautioning against the literal interpretation of their results (Taylor 1995; Beissinger & Westphal 1998; Brook *et al.* 2000; Menges 2000; Coulson *et al.* 2001; Fieberg & Ellner 2001; Ellner *et al.* 2002). Accurately quantifying future extinction risk is only possible where sufficient data are available to reliably estimate the vital rates and their responses to environmental drivers (Coulson *et al.* 2001; Fieberg & Ellner 2001). Whilst including the effects of environmental drivers may increase the accuracy of future population projections (Bakker *et al.* 2009), uncertainty in the future state of the environment must be acknowledged. In the case of climatic variables this arises from forecast error of the GCM and the downscaling approach. Repeating the analysis using a range of different GCMs, emissions scenarios, and methods for downscaling the GCM data would allow the uncertainty in population viability due to that in the future climate forecasts to be quantified (Baker *et al.* 2017).

Parameter uncertainty in the vital rates may differ across the life cycle. Though this study system is data rich relative to many others (Menges 2000; Crone *et al.* 2011) data describing the seed bank dynamics are relatively limited. Seed banks are often the least well characterised part of the life cycle (Menges 2000; Paniw *et al.* 2017). We found that extinction probabilities under forecasted climate change remained low under two possible scenarios of seed bank dynamics (Appendix A3). However, we did not consider how the seed bank dynamics themselves may be affected by environmental change. Seed banks serve to buffer populations against adverse environmental conditions (Kalisz & McPeek 1992; Venable 2007), yet studies on population level effects of environmental change mediated through seed bank

dynamics are rare. Germination and seed mortality may respond to environmental conditions (e.g. Hawkes 2004; Plue *et al.* 2013; Mackenzie *et al.* 2016), with consequences for future seed bank persistence (Ooi, Auld & Denham 2012) and therefore population responses to future environmental change. Further studies quantifying the effect of drivers of such underground dynamics under a broad range of environmental conditions are necessary to fully understand population responses to future change (Menges 2000).

Due to the intensive effort required to collect demographic data many studies are based on single populations (Menges 2000; Crone *et al.* 2011); where multiple populations are studied the distances between them are often small (Coutts *et al.* 2016). This often leads to local population data being extrapolated to larger spatial scales (Menges 2000). Differences among populations may lead to erroneous predictions of viability for some populations (Johnson *et al.* 2010; Hernandez-Camacho *et al.* 2015). To accurately predict population dynamics for novel populations the causal drivers of differences among populations would have to be identified, their effects quantified, and their levels measured at the new site. This level of data collection is often impractical, especially for rare species of conservation concern, where few populations may exist. However, by studying multiple populations, it is possible to quantify the degree of uncertainty in viability due to population differences and take account of such uncertainty when making management decisions (Ellner & Fieberg 2003). We found large differences in predicted population dynamics among populations, despite relatively small distances among populations, with all populations located at a single site.

We have shown how forecasted climate change may broaden the range of management strategies under which a rare endemic is able to persist, decreasing the intensity of management needed. Climate change is expected to drive widespread population change (Parmesan & Yohe 2003; Maclean & Wilson 2011). Failure to account for these effects may lead to suboptimal conservation planning (Hannah, Midgley & Millar 2002; Hulme 2005; Ibanez *et al.* 2013), yet many population level studies continue to determine optimal management assuming stationary environments (though see Bucharova, Brabec & Munzbergova 2012; Sletvold *et al.* 2013; Bernardo, Albrecht & Knight 2016). Where climatic effects are included in demographic models single temporal periods of influence are often chosen *a priori* (Van der Pol *et al.* 2016), which may lead to inaccurate predictions of future population responses. Statistical tools such as FLMs now provide more biologically realistic frameworks for identifying and quantifying the effects of environmental drivers on the vital rates (Teller *et al.* 2016). The widespread use of such methods is necessary to understand population responses to future change and determine appropriate management strategies for conserving species under future environmental conditions.

References

Adler, P.B., Dalgleish, H.J. & Ellner, S.P. (2012) Forecasting plant community impacts of climate variability and change: when do competitive interactions matter? *Journal of Ecology,* **100,** 478-487.

Allen, C.D., Savage, M., Falk, D.A., Suckling, K.F., Swetnam, T.W., Schulke, T., Stacey, P.B., Morgan, P., Hoffman, M. & Klingel, J.T. (2002) Ecological restoration of Southwestern ponderosa pine ecosystems: A broad perspective. *Ecological Applications,* **12,** 1418-1433.

Angert, A.L., Sheth, S.N. & Paul, J.R. (2011) Incorporating Population-Level Variation in Thermal Performance into Predictions of Geographic Range Shifts. *Integrative and Comparative Biology,* **51,** 733-750.

Baker, D.J., Hartley, A.J., Pearce-Higgins, J.W., Jones, R.G. & Willis, S.G. (2017) Neglected issues in using weather and climate information in ecology and biogeography. *Diversity and Distributions,* **23,** 329-340.

Bakker, V.J., Doak, D.F., Roemer, G.W., Garcelon, D.K., Coonan, T.J., Morrison, S.A., Lynch, C., Ralls, K. & Shaw, R. (2009) Incorporating ecological drivers and uncertainty into a demographic population viability analysis for the island fox. *Ecological Monographs,* **79,** 77-108.

Bayley, P.B. (1995) Understanding large river floodplain ecosystems. *Bioscience,* **45,** 153-158.

Beissinger, S.R. & Westphal, M.I. (1998) On the use of demographic models of population viability in endangered species management. *Journal of Wildlife Management,* **62,** 821-841.

Bernardo, H.L., Albrecht, M.A. & Knight, T.M. (2016) Increased drought frequency alters the optimal management strategy of an endangered plant. *Biological Conservation,* **203,** 243-251.

Brook, B.W., O'Grady, J.J., Chapman, A.P., Burgman, M.A., Akcakaya, H.R. & Frankham, R. (2000) Predictive accuracy of population viability analysis in conservation biology. *Nature,* **404,** 385-387.

Brys, R., Jacquemyn, H., Endels, P., De Blust, G. & Hermy, M. (2004) The effects of grassland management on plant performance and demography in the perennial herb Primula veris. *Journal of Applied Ecology,* **41,** 1080-1091.

Bucharova, A., Brabec, J. & Munzbergova, Z. (2012) Effect of land use and climate change on the future fate of populations of an endemic species in central Europe. *Biological Conservation,* **145,** 39-47.

Canales, J., Trevisan, M.C., Silva, J.F. & Caswell, H. (1994) A demographic-study of an annual grass (Andropogon-brevifolius schwarz) in burnt and unburnt savanna. *Acta Oecologica-International Journal of Ecology,* **15,** 261-273.

Coulson, T., Mace, G.M., Hudson, E. & Possingham, H.P. (2001) The use and abuse of population viability analysis. *Trends in Ecology & Evolution,* **16,** 219-221.

Coutts, S.R., Salguero-Gomez, R., Csergo, A.M. & Buckley, Y.M. (2016) Extrapolating demography with climate, proximity and phylogeny: approach with caution. *Ecology Letters,* **19,** 1429-1438.

Crone, E.E., Ellis, M.M., Morris, W.F., Stanley, A., Bell, T., Bierzychudek, P., ... & Menges, E.S. (2013) Ability of Matrix Models to Explain the Past and Predict the Future of Plant Populations. *Conservation Biology,* **27,** 968-978.

Crone, E.E., Menges, E.S., Ellis, M.M., Bell, T., Bierzychudek, P., Ehrlen, J., Kaye, T.N., Knight, T.M., Lesica, P., Morris, W.F., Oostermeijer, G., Quintana-Ascencio, P.F., Stanley, A., Ticktin, T., Valverde, T. & Williams, J.L. (2011) How do plant ecologists use matrix population models? *Ecology Letters,* **14,** 1-8.

Davies, R.J.P., Whalen, M.A., Mackay, D.A., Taylor, D. & Pisanu, P. (2013) Does soil seed bank diversity limit post-fire regeneration in small, fragmented, long-unburnt remnants of fire adapted vegetation? *Biological Conservation,* **158,** 287-295.

Diez, J.M., Giladi, I., Warren, R. & Pulliam, H.R. (2014) Probabilistic and spatially variable niches inferred from demography. *Journal of Ecology,* **102,** 544-554.

Doak, D.F. & Morris, W.F. (2010) Demographic compensation and tipping points in climate-induced range shifts. *Nature,* **467,** 959-962.

Ehrlen, J., Morris, W.F., von Euler, T. & Dahlgren, J.P. (2016) Advancing environmentally explicit structured population models of plants. *Journal of Ecology,* **104,** 292-305.

Ekstrom, M., Grose, M.R. & Whetton, P.H. (2015) An appraisal of downscaling methods used in climate change research. *Wiley Interdisciplinary Reviews-Climate Change,* **6,** 301-319.

Ellner, S.P. & Fieberg, J. (2003) Using PVA for management despite uncertainty: Effects of habitat, hatcheries, and harvest on salmon. *Ecology,* **84,** 1359-1369.

Ellner, S.P., Fieberg, J., Ludwig, D. & Wilcox, C. (2002) Precision of population viability analysis. *Conservation Biology,* **16,** 258-261.

Emery, S.M. & Gross, K.L. (2005) Effects of timing of prescribed fire on the demography of an invasive plant, spotted knapweed Centaurea maculosa. *Journal of Applied Ecology,* **42,** 60-69.

Evans, M.E.K., Holsinger, K.E. & Menges, E.S. (2010) Fire, vital rates, and population viability: a hierarchical Bayesian analysis of the endangered Florida scrub mint. *Ecological Monographs,* **80,** 627-649.

Fieberg, J. & Ellner, S.P. (2001) Stochastic matrix models for conservation and management: a comparative review of methods. *Ecology Letters,* **4,** 244-266.

Flatley, W.T. & Fule, P.Z. (2016) Are historical fire regimes compatible with future climate? Implications for forest restoration. *Ecosphere,* **7,** 21.

Foster, T.E., Schmalzer, P.A. & Fox, G.A. (2014) Timing matters: the seasonal effect of drought on tree growth. *Journal of the Torrey Botanical Society,* **141,** 225-241.

Gornish, E.S. (2013) Effects of density and fire on the vital rates and population growth of a perennial goldenaster. *Aob Plants,* **5,** 11.

Hannah, L., Midgley, G.F. & Millar, D. (2002) Climate change-integrated conservation strategies. *Global Ecology and Biogeography,* **11,** 485-495.

Harris, J.A., Hobbs, R.J., Higgs, E. & Aronson, J. (2006) Ecological restoration and global climate change. *Restoration Ecology,* **14,** 170-176.

Hawkes, C.V. (2004) Effects of biological soil crusts on seed germination of four endangered herbs in a xeric Florida shrubland during drought. *Plant Ecology,* **170,** 121-134.

Hernandez-Camacho, C.J., Bakker, V.J., Aurioles-Gamboa, D., Laake, J. & Gerber, L.R. (2015) The Use of Surrogate Data in Demographic Population Viability Analysis: A Case Study of California Sea Lions. *Plos One,* **10.**

Hulme, P.E. (2005) Adapting to climate change: is there scope for ecological management in the face of a global threat? *Journal of Applied Ecology,* **42,** 784-794.

Ibanez, I., Gornish, E.S., Buckley, L., Debinski, D.M., Hellmann, J., Helmuth, B., HilleRisLambers, J., Latimer, A.M., Miller-Rushing, A.J. & Uriarte, M. (2013) Moving forward in global-change ecology: capitalizing on natural variability. *Ecology and Evolution,* **3,** 170-181.

IPCC (2007) Climate Change 2007: Synthesis Report. Contribution of Working Groups I, II and III to the Fourth Assessment Report of the Intergovernmental Panel on Climate Change [Core Writing Team, Pachauri, R.K. and Reisinger, A. (eds.)]. IPCC, Geneva, Switzerland, 104pp.

IPCC (2014) Climate change 2014: Synthesis report. Contribution of working groups I, II, III to the Fifth Assessment Report of the Intergovernmental Panel on Climate Change [Core writing team, R.K. Pachauri and L.A. Meyers (eds.)]. IPCC Geneva, Switzerland, 151pp.

Jaffre, M. & Le Galliard, J.F. (2016) Population viability analysis of plant and animal populations with stochastic integral projection models. *Oecologia,* **182,** 1031-1043.

Johnson, H.E., Mills, L.S., Stephenson, T.R. & Wehausen, J.D. (2010) Population-specific vital rate contributions influence management of an endangered ungulate. *Ecological Applications,* **20,** 1753-1765.

Kalisz, S. & McPeek, M.A. (1992) Demography of an age-structured annual - resampled projection matrices, elasticity analyses and seed bank effects. *Ecology,* **73,** 1082-1093.

Keetch, J.J. & Byram, G. (1968) A drought index for forest fire control. Res. Paper SE-38. Asheville, NC: U.S. Department of Agriculture, Forest Service, USDA Forest Service Southern Research Station.

Knorr, W., Kaminski, T., Arneth, A. & Weber, U. (2014) Impact of human population density on fire frequency at the global scale. *Biogeosciences,* **11,** 1085-1102.

Kruuk, L.E.B., Osmond, H.L. & Cockburn, A. (2015) Contrasting effects of climate on juvenile body size in a Southern Hemisphere passerine bird. *Global Change Biology,* **21,** 2929-2941.

Kusunoki, S. & Mizuta, R. (2013) Changes in precipitation intensity over East Asia during the 20th and 21st centuries simulated by a global atmospheric model with a 60 km grid size. *Journal of Geophysical Research-Atmospheres,* **118,** 11007-11016.

Lavaysse, C., Vrac, M., Drobinski, P., Lengaigne, M. & Vischel, T. (2012) Statistical downscaling of the French Mediterranean climate: assessment for present and projection in an anthropogenic scenario. *Natural Hazards and Earth System Sciences,* **12,** 651-670.

Lindenmayer, D.B. & Possingham, H.P. (1996) Ranking conservation and timber management options for leadbeater's possum in southeastern Australia using population viability analysis. *Conservation Biology,* **10,** 235-251.

Mackenzie, B.D.E., Auld, T.D., Keith, D.A., Hui, F.K.C. & Ooi, M.K.J. (2016) The Effect of Seasonal Ambient Temperatures on Fire-Stimulated Germination of Species with Physiological Dormancy: A Case Study Using Boronia (Rutaceae). *Plos One,* **11**.

Maclean, I.M.D. & Wilson, R.J. (2011) Recent ecological responses to climate change support predictions of high extinction risk. *Proceedings of the National Academy of Sciences of the United States of America,* **108,** 12337-12342.

Menges, E.S. (2000) Population viability analyses in plants: challenges and opportunities. *Trends in Ecology & Evolution,* **15,** 51-56.

Menges, E.S. (2007) Integrating demography and fire management: an example from Florida scrub. *Australian Journal of Botany,* **55,** 261-272.

Menges, E.S. & Hawkes, C.V. (1998) Interactive effects of fire and microhabitat on plants of Florida scrub. *Ecological Applications,* **8,** 935-946.

Menges, E.S. & Kimmich, J. (1996) Microhabitat and time-since-fire: Effects on demography of Eryngium cuneifolium (Apiaceae), a Florida scrub endemic plant. *American Journal of Botany,* **83,** 185-191.

Menges, E.S. & Kohfeldt, N. (1995) Life history strategies of Florida scrub plants in relation to fire. *Bulletin of the Torrey Botanical Club,* **122,** 282-297.

Menges, E.S. & Quintana-Ascencio, P.F. (2004) Population viability with fire in Eryngium cuneifolium: Deciphering a decade of demographic data. *Ecological Monographs,* **74,** 79-99.

Merow, C., Latimer, A.M., Wilson, A.M., McMahon, S.M., Rebelo, A.G. & Silander, J.A., Jr. (2014) On using integral projection models to generate demographically driven predictions of species' distributions: development and validation using sparse data. *Ecography,* **37,** 1167-1183.

Metcalf, C.J.E., Ellner, S.P., Childs, D.Z., Roberto, S.-G., Merow, C., McMahon, S.M., Jongejans, E. & Rees, M. (2015) Statistical modelling of annual variation for inference on stochastic population dynamics using Integral Projection Models. *Methods in Ecology and Evolution,* **6,** 1007-1017.

Michelangeli, P.A., Vrac, M. & Loukos, H. (2009) Probabilistic downscaling approaches: Application to wind cumulative distribution functions. *Geophysical Research Letters,* **36**.

Mizuta, R., Yoshimura, H., Murakami, H., Matsueda, M., Endo, H., Ose, T., Kamiguchi, K., Hosaka, M., Sugi, M., Yukimoto, S., Kusunoki, S. & Kitoh, A. (2012) Climate Simulations Using MRI-AGCM3.2 with 20-km Grid. *Journal of the Meteorological Society of Japan,* **90A,** 233-258.

Navarra, J.J., Kohfeldt, N., Menges, E.S. & Quintana-Ascencio, P.F. (2011) Seed bank changes with time since fire in Florida rosemary scrub. *Fire Ecology,* **7,** 17-31.

O'Connor, C.D., Falk, D.A., Lynch, A.M., Swetnam, T.W. & Wilcox, C.P. (2017) Disturbance and productivity interactions mediate stability of forest composition and structure. *Ecological Applications,* **27,** 900-915.

Ooi, M.K.J., Auld, T.D. & Denham, A.J. (2012) Projected soil temperature increase and seed dormancy response along an altitudinal gradient: implications for seed bank persistence under climate change. *Plant and Soil,* **353,** 289-303.

Paniw, M., Quintana-Ascencio, P.F., Ojeda, F. & Salguero-Gomez, R. (2017) Accounting for uncertainty in dormant life stages in stochastic demographic models. *Oikos,* **126,** 900-909.

Parmesan, C. & Yohe, G. (2003) A globally coherent fingerprint of climate change impacts across natural systems. *Nature,* **421,** 37-42.

Plue, J., De Frenne, P., Acharya, K., Brunet, J., Chabrerie, O., Decocq, G., Diekmann, M., Graae, B.J., Heinken, T., Hermy, M., Kolb, A., Lemke, I., Liira, J., Naaf, T., Shevtsova, A., Verheyen, K., Wulf, M. & Cousins, S.A.O. (2013) Climatic control of forest herb seed banks along a latitudinal gradient. *Global Ecology and Biogeography,* **22,** 1106-1117.

Quintana-Ascencio, P.F. & Menges, E.S. (2000) Competitive abilities of three narrowly endemic plant species in experimental neighborhoods along a fire gradient. *American Journal of Botany,* **87,** 690-699.

R Core Team (2016) R: A language and environment for statistical computing. R Foundation for Statistical Computing, Vienna, Austria.

Rees, M. & Ellner, S.P. (2009) Integral projection models for populations in temporally varying environments. *Ecological Monographs,* **79,** 575-594.

Reiss, P.T. & Ogden, R.T. (2009) Smoothing parameter selection for a class of semiparametric linear models. *Journal of the Royal Statistical Society Series B-Statistical Methodology,* **71,** 505-523.

Restrepo, C., Walker, L.R., Shiels, A.B., Bussmann, R., Claessens, L., Fisch, S., Lozano, P., Negi, G., Paolini, L., Poveda, G., Ramos-Scharron, C., Richter, M. & Velazquez, E. (2009) Landsliding and Its Multiscale Influence on Mountainscapes. *Bioscience,* **59,** 685-698.

Roberts, A.M.I. (2008) Exploring relationships between phenological and weather data using smoothing. *International Journal of Biometeorology,* **52,** 463-470.

Ryan, M.R., Root, B.G. & Mayer, P.M. (1993) Status of piping plovers in the great plains of North America - a demographic simulation model. *Conservation Biology,* **7,** 581-585.

Sanchez-Velasquez, L.R., Ezcurra, E., Martinez-Ramos, M., Alvarez-Buylla, E. & Lorente, R. (2002) Population dynamics of Zea diploperennis, an endangered perennial herb: effect of slash and burn practice. *Journal of Ecology,* **90,** 684-692.

Scanga, S.E. (2014) Population dynamics in canopy gaps: nonlinear response to variable light regimes by an understory plant. *Plant Ecology,* **215,** 927-935.

Selwood, K.E., McGeoch, M.A. & Nally, R. (2015) The effects of climate change and land-use change on demographic rates and population viability. *Biological Reviews,* **90,** 837-853.

Sims, M., Elston, D.A., Larkham, A., Nussey, D.H. & Albon, S.D. (2007) Identifying when weather influences life-history traits of grazing herbivores. *Journal of Animal Ecology,* **76,** 761-770.

Sletvold, N., Dahlgren, J.P., Oien, D.-I., Moen, A. & Ehrlen, J. (2013) Climate warming alters effects of management on population viability of threatened species: results from a 30-year experimental study on a rare orchid. *Global Change Biology,* **19,** 2729-2738.

Stevens, J.T. & Latimer, A.M. (2015) Snowpack, fire, and forest disturbance: interactions affect montane invasions by non-native shrubs. *Global Change Biology,* **21,** 2379-2393.

Swetnam, T.W., Allen, C.D. & Betancourt, J.L. (1999) Applied historical ecology: Using the past to manage for the future. *Ecological Applications,* **9,** 1189-1206.

Taylor, B.L. (1995) The reliability of using population viability analysis for risk classification of species. *Conservation Biology,* **9,** 551-558.

Teller, B.J., Adler, P.B., Edwards, C.B., Hooker, G. & Ellner, S.P. (2016) Linking demography with drivers: climate and competition. *Methods in Ecology and Evolution,* **7,** 171-183.

Thom, D. & Seidl, R. (2016) Natural disturbance impacts on ecosystem services and biodiversity in temperate and boreal forests. *Biological Reviews,* **91,** 760-781.

Thomas, C.D., Cameron, A., Green, R.E., Bakkenes, M., Beaumont, L.J., Collingham, Y.C., Erasmus, B.F.N., de Siqueira, M.F., Grainger, A., Hannah, L., Hughes, L., Huntley, B., van Jaarsveld, A.S., Midgley, G.F., Miles, L., Ortega-Huerta, M.A., Peterson, A.T., Phillips, O.L. & Williams, S.E. (2004) Extinction risk from climate change. *Nature,* **427,** 145-148.

Thompson, P.M., Wilson, B., Grellier, K. & Hammond, P.S. (2000) Combining power analysis and population viability analysis to compare traditional and precautionary approaches to conservation of coastal cetaceans. *Conservation Biology,* **14,** 1253-1263.

Tschope, O. & Tielborger, K. (2010) The role of successional stage and small-scale disturbance for establishment of pioneer grass Corynephorus canescens. *Applied Vegetation Science,* **13,** 326-335.

Turner, M.G. (2010) Disturbance and landscape dynamics in a changing world. *Ecology,* **91,** 2833-2849.

Van der Pol, M., Bailey, L.D., McLean, N., Rijsdijk, L., Lawson, C.R. & Brouwer, L. (2016) Identifying the best climatic predictors in ecology and evolution. *Methods in Ecology and Evolution,* **7,** 1246-1257.

van Vuuren, D.P., Sala, O.E. & Pereira, H.M. (2006) The future of vascular plant diversity under four global scenarios. *Ecology and Society,* **11**.

Velle, L.G., Nilsen, L.S., Norderhaug, A. & Vandvik, V. (2014) Does prescribed burning result in biotic homogenization of coastal heathlands? *Global Change Biology,* **20,** 1429-1440.

Venable, D.L. (2007) Bet hedging in a guild of desert annuals. *Ecology,* **88,** 1086-1090.

Wiens, J.J. (2016) Climate-Related Local Extinctions Are Already Widespread among Plant and Animal Species. *Plos Biology,* **14**.

Wood, S.N. (2011) Fast stable restricted maximum likelihood and marginal likelihood estimation of semiparametric generalized linear models. *Journal of the Royal Statistical Society Series B-Statistical Methodology,* **73,** 3-36.

Wood, S.N. (2017) Generalized Additive Models: An Introduction with R. Chapman and Hall/CRC.

Yates, C.J. & Ladd, P.G. (2010) Using population viability analysis to predict the effect of fire on the extinction risk of an endangered shrub Verticordia fimbrilepis subsp fimbrilepis in a fragmented landscape. *Plant Ecology,* **211,** 305-319.
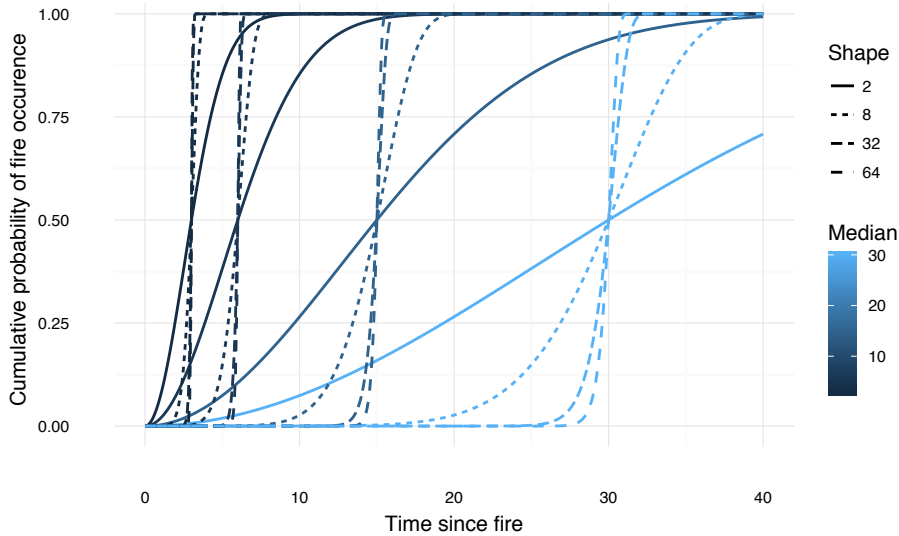
Figure S1: Cumulative probability of a fire occurring under the Weibull distribution with different medians (3, 6, 15, or 30) and shape parameters (2, 8, 32, or 64).
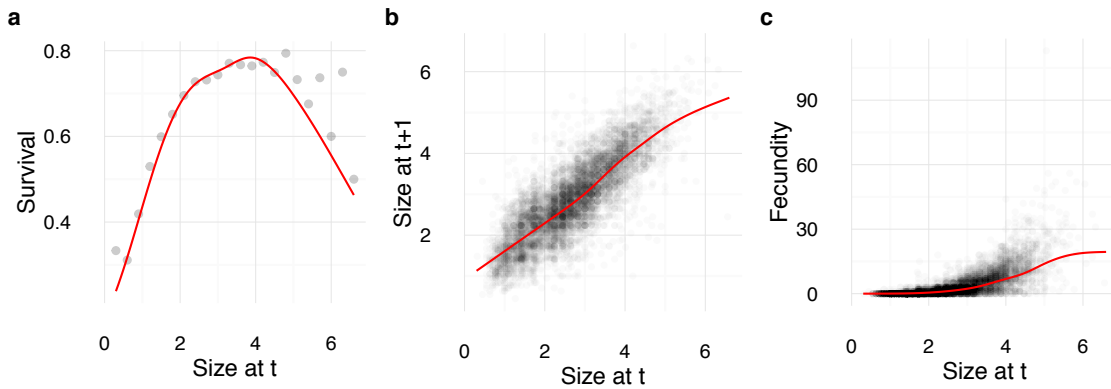

Figure S2: Effect of size on a) survival, b) growth, and c) fecundity. Red lines show the fitted splines, points show raw data, which are split into size bins for the survival data. Predictions were made assuming a time since fire of 15 years and with the random year and population effects set to zero. The square root of rosette diameter was used as the measure of plant size. Raw data is from all twelve populations. Survival decreases at large sizes, presumably due to senescence. Plants either do not flower or produce very few flowering stems until they are sufficiently large.
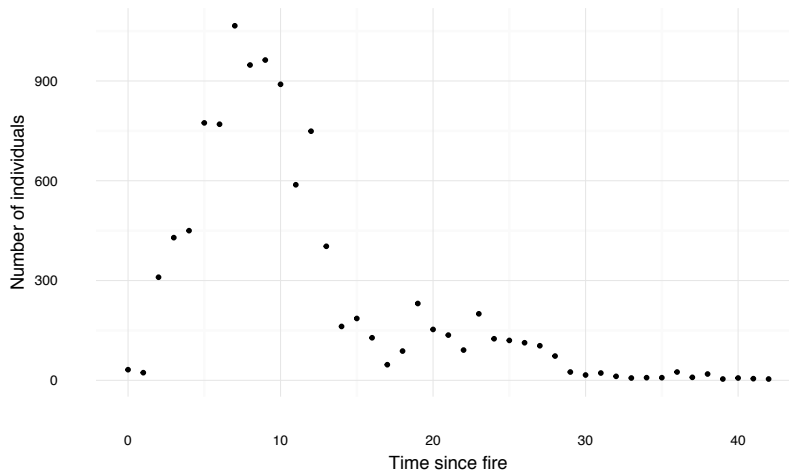
Figure S3: Total number of individuals with survival data, across all twelve populations, against the number of years since fire.

Appendices

Appendix A1: Downscaling of the predicted climate covariates

Predicted climate data from general circulation models (GCMs) may differ from that recorded at local weather stations due to model biases or differences in spatial scale between the predicted and observed data, with forecasted climate data often on a broader spatial scale than that required for ecological studies (Ekstrom, Grose & Whetton 2015; Baker *et al.* 2017). This has necessitated the development of methods to downscale GCM data to a suitable scale for ecological predictions to be made. The MRI-AGCM3.2 (Mizuta *et al.* 2012; Kusunoki & Mizuta 2013) simulations for the study period (1990-2014) predicted higher minimum and lower maximum temperatures than those observed at the study site during this time period (Fig. A1).

GCM predictions for the study site were calculated by averaging across predictions of the four closest grid points to the GPS coordinates of the study site. We used a cumulative distribution function – transform method (CDF-t) to downscale the climate predictions from MRI-AGCM3.2 (Michelangeli, Vrac & Loukos 2009). The transformations were carried out using the CDFt package (Michelangeli, Vrac & Loukos 2009) in R (R Core Team 2016). The CDF of a climate variable (x) at the local scale during the study period (i.e. 1990-2014) is given by F_{Lh} and the CDF during the same period from the GCM is given by F_{Gh}. A transformation T exists whereby $T(F_{Gh}(x)) = F_{Lh}(x)$. T can be found as follows, where u belongs to $[0,1]$, $T(u) = F_{Lh}(F_{Gh}^{-1}(u))$. By assuming that T is stationary the CDF of the local climate variable over a future period ($F_{Lf}(x)$) can be estimated from the predicted GCM data over the future period (F_{Gf}) as $F_{Lf}(x) = T\left(F_{Gf}(x)\right) = F_{Lh}(F_{Gh}^{-1}(F_{Gf}(x)))$.

Cross validation was used to validate the CDF-t approach, by splitting the observed data into a calibration (1990-2004) and evaluation period (2005-2014). T was fitted for each climatic variable using the data from the calibration period. Kolmogorov-Smirnov scores were calculated to compare the fortnightly CDFs of the GCM output and the downscaled data to the fortnightly CDFs of the observed data for the evaluation period (Michelangeli, Vrac & Loukos 2009; Lavaysse *et al.* 2012). The CDF-t was applied directly to the temperature data. To model the strictly positive precipitation data the GCM data was used only above a threshold (θ) that was set so that the number of days with rain>0 was the same in the GCM as in the observed data, that is $F_{Gh}(\theta) = F_{Lh}(0)$ (Lavaysse *et al.* 2012). The downscaling approach improves the fit of all three climatic variables, with the best models for both minimum and maximum temperature given by the CDF-t of minimum temperature from the GCM (Fig. A2).

The Keetch-Byram drought index (KBDI) is calculated from the downscaled temperature and precipitation data. The daily difference between moisture deficiencies is calculated as

$$dQ = \frac{(800-Q)(0.968\exp(0.0486T)-8.3)i}{1+10.88\exp(-0.001736R)},$$
(eqn A1)

where Q is yesterday's KBDI reduced by the daily net precipitation, T is the daily maximum temperature, R is the mean annual precipitation, and i is the time increment (Keetch & Byram 1968; Alexander 1990).

To check whether differences between the observed and predicted climatic variables affected the population dynamics populations were simulated using the observed climate data and the downscaled data over the same time period (1990-2014). Simulations were run for 85 years over a range of median FRIs as in the main text, with an initial population size of 7,000 and a shape parameter of 64 for the FRI distribution. The downscaled climate data slightly overpredicted the risk of extinction relative to the observed data. However, a similar pattern with increasing FRI is seen using both data types and the differences in magnitude are small relative to those between the past and future climatic data (Fig. A3).
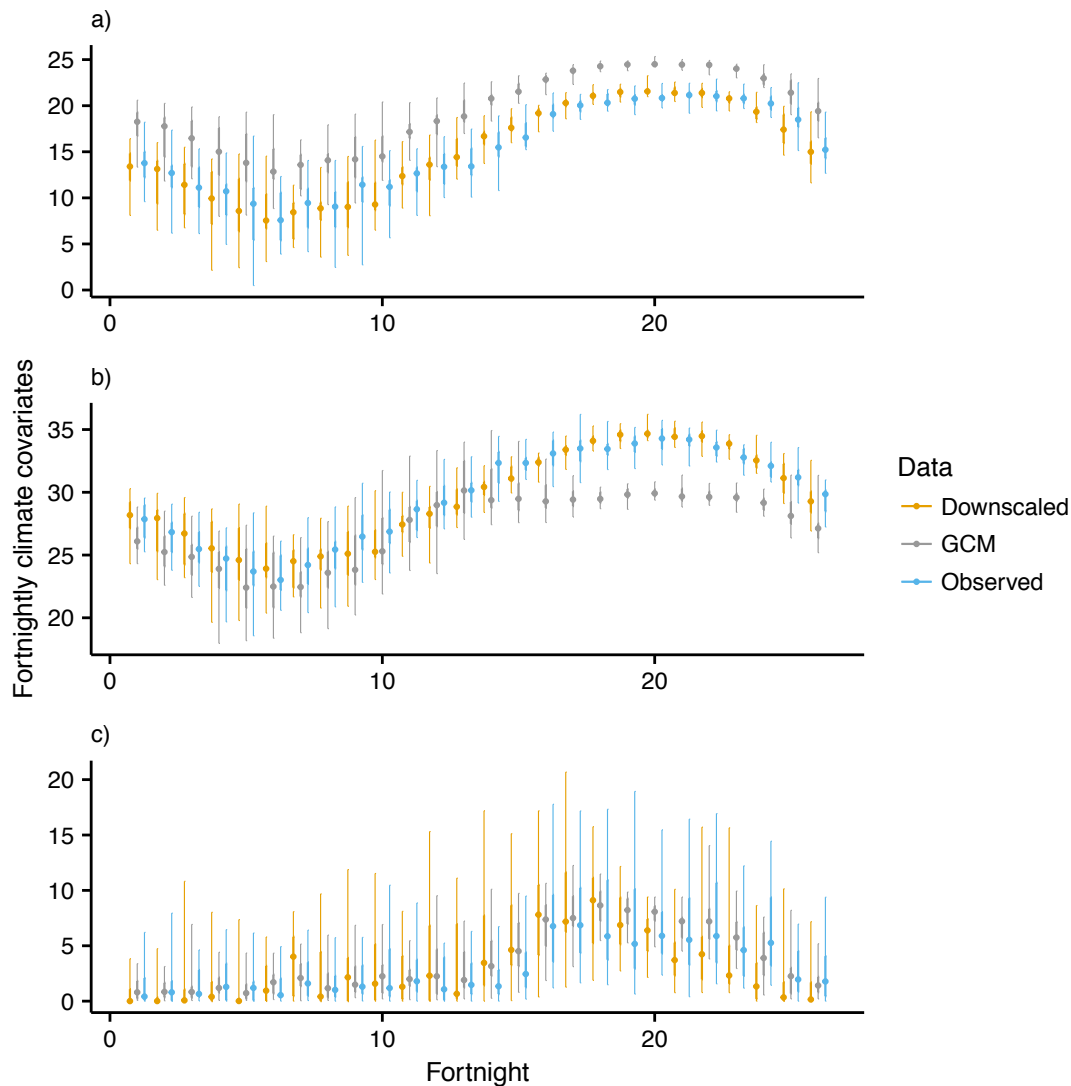
Figure A1: Fortnightly data over the year for a) minimum temperature, b) maximum temperature, and c) precipitation from beginning of November to end of October. Points show medians, thicker lines the interquartile range and thinner lines the 95% quantiles. Both the minimum and maximum temperature downscaled data were corrected by transforming the predicted minimum temperature from the GCM (see Fig. A2).
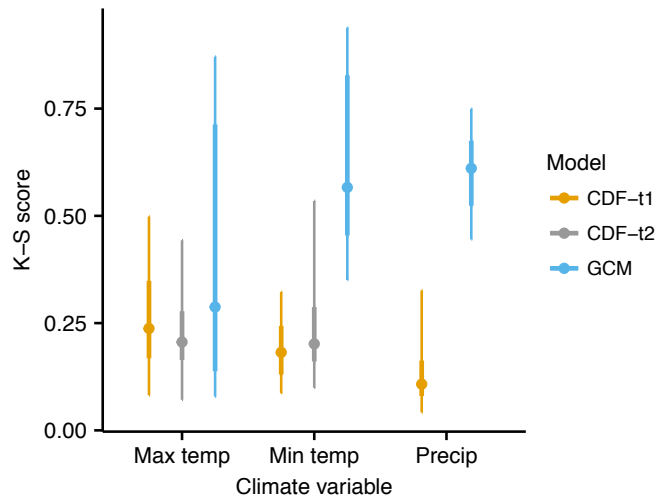
Figure A2: Kolmogorov-Smirnov (KS) scores comparing the CDF of the observed data at Archbold and the GCM, the GCM downscaled using the predicted climatic variable (CDF-t_1) and the GCM downscaled using an alternative climatic variable (CDF-t_2; i.e. using maximum temperature to predict minimum temperature and minimum temperature to predict maximum temperature). Lower KS scores indicate less difference between the CDF of the observed and predicted data. Points show medians, thick lines interquartile range and thin lines 95% quantiles of the KS scores calculated for each fortnight.
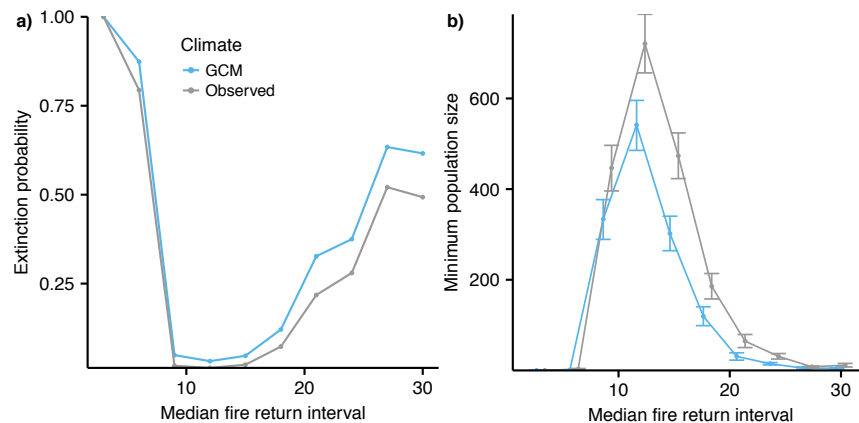
Figure A3: Extinction probabilities (left column) and minimum population sizes (right column) across a range of FRIs and under the observed climatic conditions and those predicted from the downscaled GCM data over the same stud period.

Appendix A2: Simulation study comparing spline bases and methods of estimating smoothing parameters

A simulation study was used to compare the effectiveness of restricted maximum likelihood (REML) and generalised cross validation (GCV) for estimating the smoothing parameter in the GAM, in the context of detecting climatic effects. Fortnightly precipitation data, over a period of 41 fortnights for each year of demographic data, from the UK meteorological office run Stornoway airport station were used (data available from badc.nerc.ac.uk). Survival data were simulated as a function of the precipitation data and GAMs were used to try to recover the known climatic signals.

Survival data were simulated for a range of study lengths (15, 30, or 60 years) and including differing amounts of temporal stochasticity in the survival data (random year effect

24

with mean of 0 and standard deviation of 0, 0.1, 0.5, 1, or 1.5). Ten replicates were used for each combination of study length and temporal stochasticity. Survival data were simulated for a random number, between 30 and 250, of individuals each year. Survival in year t (S^t) was simulated as a function of precipitation and a random year effect as follows

$$\text{logit}(S^t) = \beta_0 + \sum_{j=1}^{K} \beta_j^p P_{tj} + \varepsilon_t, \quad\quad\quad\quad\quad\text{(eqn A2)}$$

where β_0 is the intercept, P_{tj} is the mean precipitation in year t and fortnight j, β^p are known coefficients (given either by a linear or a sine function; see Fig. A3) and the random year effect ($\varepsilon_{[t]}$) is sampled randomly from a normal distribution with a mean of zero and a standard deviation σ_r. The climatic data were centered. β_0 was set to 0.5, giving a mean survival of 0.6.

Using the *mgcv* package in R (Wood 2017) GAMs were fitted, using spline basis expansion (see main text), to the simulated data to determine whether it was possible to recover the known climate signals. For each replicate a GAM was fitted using both REML and GCV. In the case of GCV the degrees of freedom were inflated by 40% to decrease overfitting (Kim & Gu 2004). In both cases a "cs" spline basis was used with eight knots (Teller *et al.* 2016). The "cs" spline basis is a shrinkage version of a cubic regression spline basis that favours setting the coefficients to zero where there is no effect (Wood 2017).

As previously shown the GCV approach was more prone to overfitting than REML (Fig. A4; Reiss & Ogden 2009; Wood 2011). With 15 years of data the GCV approach occasionally produced complicated and spurious effects even with relatively little stochasticity present (Fig. A4). However, using REML particularly, there was evidence of the models failing to pick up the "true" climatic effects. The chance of this happening appeared to increase as the degree of temporal stochasticity increased. The study was therefore repeated using a non-shrinkage version of the cubic regression spline ("cr" spline basis). This approach seemed to perform better with REML and was able to pick out the true climatic effects even with high degrees of stochasticity (Fig. A5). There was some occasional evidence of overfitting, particularly where the true effect was linear (Fig. A5b). In the main study the "cr" spline basis was used with REML and cross validation was used to prevent overfitting by only selecting climate variables that increased the predictive ability of the model on out of sample data.
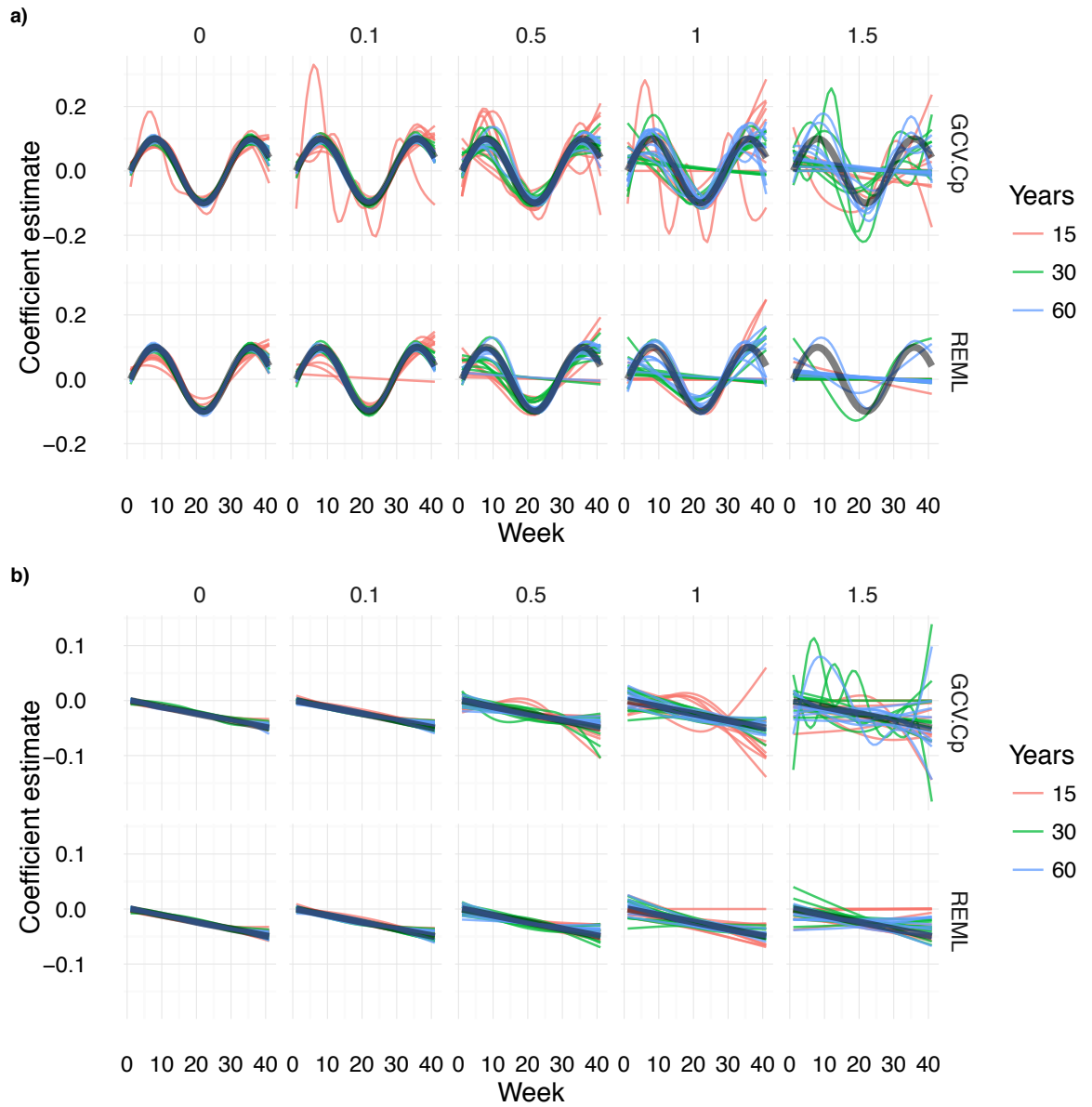
Figure A4: The true (thick black line) and estimated (thin coloured lines) functions for precipitation using a) a sine function and b) a linear function estimated using a "cs" spline basis. The standard deviation of the random year effect is given above each plot and increases from left to right. The colour indicates the number of years of survival data used to estimate the climate coefficients. Each line is the estimated coefficients over time for a single simulation.
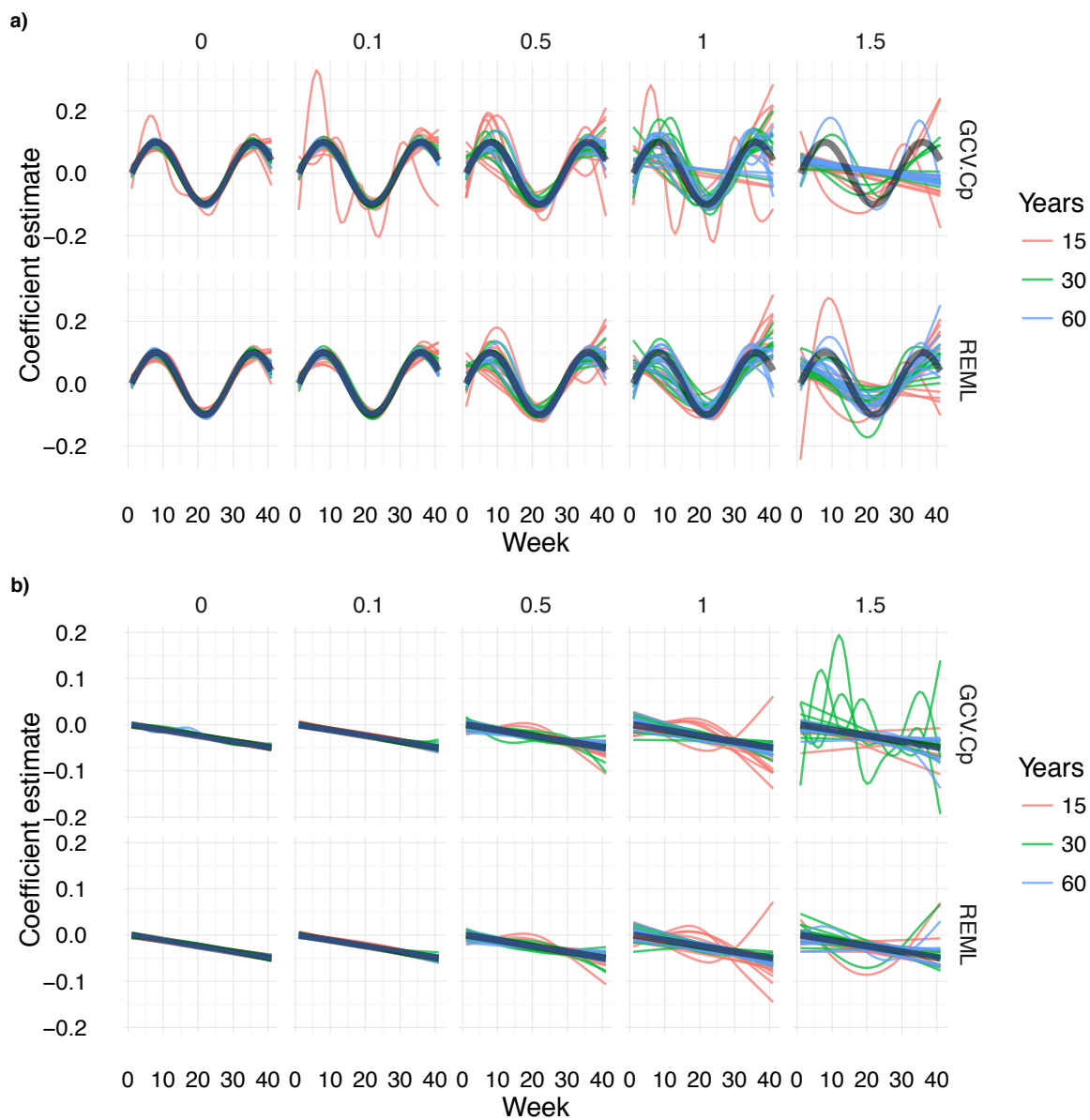
Figure A5: The true (thick black line) and estimated (thin coloured lines) functions for precipitation using a) a sine function and b) a linear function estimated using a "cr" spline basis. The standard deviation of the random year effect is given above each plot and increases from left to right. The colour indicates the number of years of survival data used to estimate the climate coefficients. Each line is the estimated coefficients over time for a single simulation.

Appendix A3: Selecting seed bank parameters

Estimates of germination in the first year (g_f) range from 0 to 0.1, whilst estimates from the seed bank (g_b) range from 0.005 to 0.04 (Quintana-Ascencio & Menges 2000; Menges & Quintana-Ascencio 2004). Data were not available on the probability of mortality in the seed bank (d). Twenty possible fertility scenarios were developed, with every combination of lowest (0 and 0.005) and highest (0.1 and 0.04) estimates of the two germination parameters (g_f and g_b respectively) and a broad range of seed mortality probabilities (0.1, 0.3 0.5, 0.7, 0.9). The simulated dynamics for each fertility scenario were compared to those observed in the field using the above ground population growth rate and mean rosette size against time since fire. 500 simulations were conducted for each scenario, each started with a fire year and a seed bank of

7,000 seeds (Menges & Quintana-Ascencio 2004) and was iterated forward for 30 years without a further fire. Temporal variation in these vital rates was incorporated using a kernel selection approach (Metcalf *et al.* 2015). A population was selected at random for each simulation and all of the vital rates were estimated using the respective population random effect throughout the simulation. At each step a single year worth of climatic data was sampled randomly from the 25 years of the study (i.e. 1990-2014) and the year effects were sampled randomly from every year-population combination across all of the vital rates.

The two fertility scenarios which produced dynamics best fitting to the observed population dynamics were low first year germination ($g_f = 0$), low germination from the seed bank ($g_b = 0.005$), and low seed mortality ($d = 0.3$) and low first year germination ($g_f = 0$), high germination from the seed bank ($g_b = 0.04$), and relatively high seed mortality ($d = 0.7$; Fig. A6). Both scenarios fitted the observed above ground population growth rates well, with generally positive growth rates seen in the first ten years postfire and negative growth rates after this (Fig. A6a). The mean rosette size from the simulations is within the observed range (Fig. A6b). There is more variation in mean rosette size in the observed data than captured in the simulations, possibly as a result of the lack of demographic stochasticity in the model. Additionally as kernel selection was used to preserve the covariance amongst the vital rates only those year and population combinations for which data were available for all of the vital rates were included. The seed bank parameters (g_f, g_b, and d) may also differ among populations or years, according to the environmental conditions. The degree of temporal stochasticity included in the model may therefore be less than that observed. The lack of germination in the first year in these scenarios is consistent with field studies, although first year germination has been seen in laboratory trials (Quintana-Ascencio & Menges 2000; Menges & Quintana-Ascencio 2004).

Estimates of seed mortality in *Hypericum cumulicola* (Quintana-Ascencio, Dolan & Menges 1998), which has a similar life history to *E.cuneifolium*, along with the presence of *Eryngium* seeds in patches that have not been burned for nearly 70 years (Navarra *et al.* 2011), suggest the fertility scenario with lower seed mortality may be more likely. This scenario is therefore used in the main text. Here, to determine the effects of uncertainty in the seed bank dynamics on future population dynamics, we compare extinction probabilities and minimum population sizes using the two selected fertility scenarios shown in Fig. A6. 1,000 simulations were run for the two fertility scenarios under the past and future climatic conditions as in the main text, using an initial population size of 7,000 seeds and a shape parameter for the Weibull distribution of fire occurrence of 64. The second fertility scenario ($g_f = 0, g_b = 0.04, d = 0.7$) produced higher predicted extinction probabilities than the scenario used in the main text (Fig. A7). The optimal FRI remains between ten and fifteen years (Fig. A7). The probability of populations going to extinction under the future climatic conditions remained very small in all but the shortest FRIs (<9 years; Fig. A7). Uncertainty in the seed bank parameter affects

absolute predictions of extinction risk in this population, but not the relative risk between FRIs and climatic conditions.
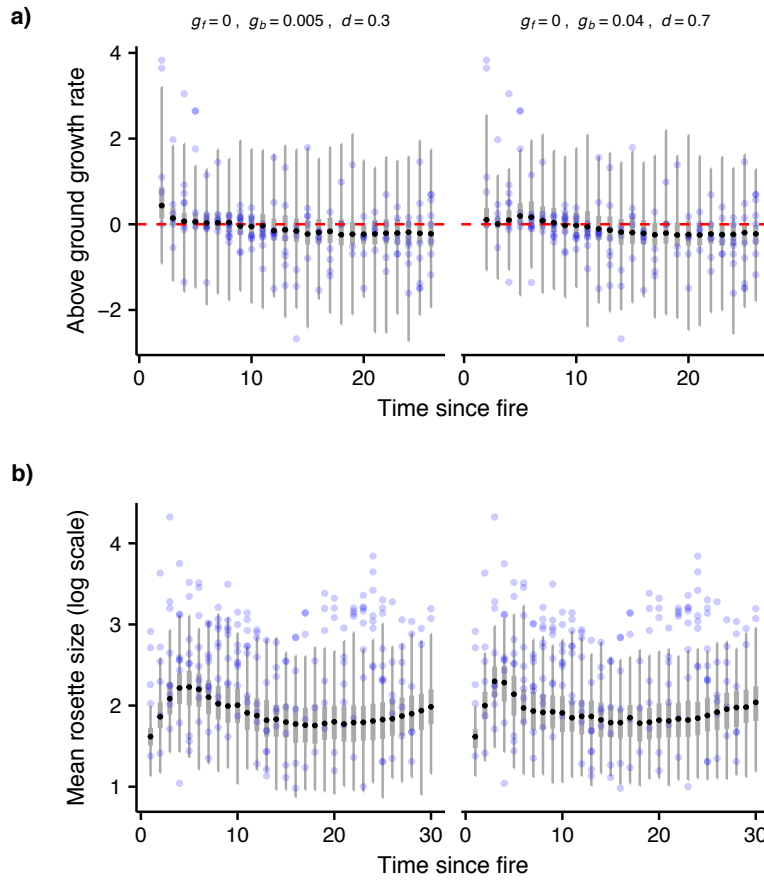

Figure A6: Comparing observed to predicted population dynamics under the two selected fertility scenarios: a) above ground one-step population growth rate and b) mean rosette size. Black points show median, thick grey lines interquartile range and thin grey lines the range across 500 simulations, observed data are shown in blue with each point a different population-year combination.
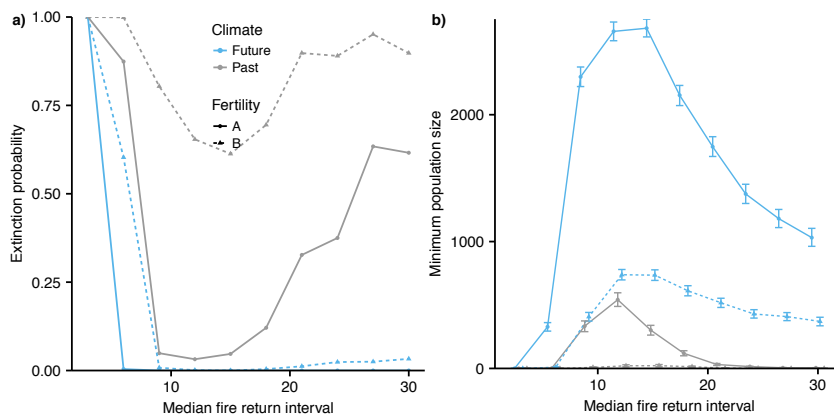

Figure A7: a) Extinction probabilities and b) minimum population sizes across a range of FRIs under two fertility scenarios. Fertility scenarios A and B correspond to $d = 0.3, g_f = 0, g_b = 0.005$ and $d = 0.7, g_f = 0, g_b = 0.04$ respectively, where scenario A is that used in the main text. Points show mean of 1000 simulations and error bars on b) show bootstrapped 95% confidence intervals for the mean.

References

Alexander, M.E. (1990) Computer calculation of the Keetch-Byram Drought Index - programmers beware! Fire Management Notes.

Baker, D.J., Hartley, A.J., Butchart, S.H.M. & Willis, S.G. (2016) Choice of baseline climate data impacts projected species' responses to climate change. *Global Change Biology,* **22,** 2392-2404.

Baker, D.J., Hartley, A.J., Pearce-Higgins, J.W., Jones, R.G. & Willis, S.G. (2017) Neglected issues in using weather and climate information in ecology and biogeography. *Diversity and Distributions,* **23,** 329-340.

Ekstrom, M., Grose, M.R. & Whetton, P.H. (2015) An appraisal of downscaling methods used in climate change research. *Wiley Interdisciplinary Reviews-Climate Change,* **6,** 301-319.

IPCC (2014) Climate change 2014: Synthesis report. Contribution of working groups I, II, III to the Fifth Assessment Report of the Intergovernmental Panel on Climate Change [Core writing team, R.K. Pachauri and L.A. Meyers (eds.)]. IPCC Geneva, Switzerland, 151pp.

Keetch, J.J. & Byram, G. (1968) A drought index for forest fire control. Res. Paper SE-38. Asheville, NC: U.S. Department of Agriculture, Forest Service, USDA Forest Service Southern Research Station.

Kim, Y.J. & Gu, C. (2004) Smoothing spline Gaussian regression: more scalable computation via efficient approximation. *Journal of the Royal Statistical Society Series B-Statistical Methodology,* **66,** 337-356.

Kujala, H., Moilanen, A., Araujo, M.B. & Cabeza, M. (2013) Conservation Planning with Uncertain Climate Change Projections. *Plos One,* **8,** 12.

Kusunoki, S. & Mizuta, R. (2013) Changes in precipitation intensity over East Asia during the 20th and 21st centuries simulated by a global atmospheric model with a 60 km grid size. *Journal of Geophysical Research-Atmospheres,* **118,** 11007-11016.

Lavaysse, C., Vrac, M., Drobinski, P., Lengaigne, M. & Vischel, T. (2012) Statistical downscaling of the French Mediterranean climate: assessment for present and projection in an anthropogenic scenario. *Natural Hazards and Earth System Sciences,* **12,** 651-670.

Menges, E.S. & Quintana-Ascencio, P.F. (2004) Population viability with fire in Eryngium cuneifolium: Deciphering a decade of demographic data. *Ecological Monographs,* **74,** 79-99.

Metcalf, C.J.E., Ellner, S.P., Childs, D.Z., Roberto, S.-G., Merow, C., McMahon, S.M., Jongejans, E. & Rees, M. (2015) Statistical modelling of annual variation for inference on stochastic population dynamics using Integral Projection Models. *Methods in Ecology and Evolution,* **6,** 1007-1017.

Michelangeli, P.A., Vrac, M. & Loukos, H. (2009) Probabilistic downscaling approaches: Application to wind cumulative distribution functions. *Geophysical Research Letters,* **36**.

Mizuta, R., Yoshimura, H., Murakami, H., Matsueda, M., Endo, H., Ose, T., Kamiguchi, K., Hosaka, M., Sugi, M., Yukimoto, S., Kusunoki, S. & Kitoh, A. (2012) Climate Simulations Using MRI-AGCM3.2 with 20-km Grid. *Journal of the Meteorological Society of Japan,* **90A,** 233-258.

Navarra, J.J., Kohfeldt, N., Menges, E.S. & Quintana-Ascencio, P.F. (2011) Seed bank changes with time since fire in Florida rosemary scrub. *Fire Ecology,* **7,** 17-31.

Quintana-Ascencio, P.F., Dolan, R.W. & Menges, E.S. (1998) Hypericum cumulicola demography in unoccupied and occupied Florida scrub patches with different time-since-fire. *Journal of Ecology,* **86,** 640-651.

Quintana-Ascencio, P.F. & Menges, E.S. (2000) Competitive abilities of three narrowly endemic plant species in experimental neighborhoods along a fire gradient. *American Journal of Botany,* **87,** 690-699.

R Core Team (2016) R: A language and environment for statistical computing. R Foundation for Statistical Computing, Vienna, Austria.

Reiss, P.T. & Ogden, R.T. (2009) Smoothing parameter selection for a class of semiparametric linear models. *Journal of the Royal Statistical Society Series B-Statistical Methodology,* **71,** 505-523.

Teller, B.J., Adler, P.B., Edwards, C.B., Hooker, G. & Ellner, S.P. (2016) Linking demography with drivers: climate and competition. *Methods in Ecology and Evolution,* **7,** 171-183.

Wood, S.N. (2011) Fast stable restricted maximum likelihood and marginal likelihood estimation of semiparametric generalized linear models. *Journal of the Royal Statistical Society Series B-Statistical Methodology,* **73,** 3-36.

Wood, S.N. (2017) Generalized Additive Models: An Introduction with R. Chapman and Hall/CRC.

Chapter 4: Winter is coming: uncovering cumulative weather effects in a well-studied population of Soay sheep

Bethan J. Hindle[1*], Jill G.Pilkington[2], Josephine M.Pemberton[2] & Dylan Z. Childs[1]

[1] Department of Animal and Plant Sciences, Alfred Denny Building, University of Sheffield, Sheffield, UK

[2] Institute of Evolutionary Biology, School of Biological Sciences, University of Edinburgh, Edinburgh, UK

Abstract

Identifying the drivers of variation in vital rates is necessary to predict population responses to future climate change. Environmental drivers are usually identified for separate vital rates and age-sex classes. However, vital rates often exhibit positive temporal covariance, suggesting they respond to common axes of variation. Moreover, environmentally explicit models often use average weather conditions during a single time window, chosen *a priori*. Mismatches between these windows and the periods when vital rates are sensitive to the driver decrease predictive performance. Using a demographic structural equation model we show a single axis drives the majority of (co)variation in survival and fecundity across six age-sex classes in a Soay sheep population. This axis provides a simpler target for identifying environmental drivers than treating each process independently. We demonstrate that using functional linear models to determine temporal windows of influence can uncover previously unseen climatic effects, thus increasing the model's predictive performance.

Introduction

Rapid climate change has led to increased interest in the responses of species and ecosystems to environmental variation (Sutherland 2006). Identifying the underlying environmental drivers of vital rates is crucial for predicting how species abundances and distributions will be affected by future climate change (Grosbois *et al.* 2008; Ehrlen & Morris 2015). Environmentally explicit demographic models are widely used to forecast population responses to such change (Altwegg & Anderson 2009; Jenouvrier *et al.* 2012). Identifying the relevant drivers is challenging, because there may be a large number of possibilities (Grosbois *et al.* 2008) and any given variable may have both direct and indirect effects, due to interactions among species (Boggs & Inouye 2012). Moreover, time lags between environmental events and demographic responses can occur (Forchhammer *et al.* 1998), with the effect of a single driver potentially varying in magnitude and direction over time (Kruuk, Osmond & Cockburn 2015). Given the short temporal and spatial extent of most demographic data sets (Salguero-Gomez *et al.* 2016) the number of possible effects can easily exceed the degree of temporal or spatial replication (Ehrlen *et al.* 2016). Methods that make efficient use of available data are necessary to identify causal drivers and the temporal windows over which they act, and to accurately estimate the magnitude of their effects (Dahlgren 2010; Teller *et al.* 2016).

The challenges associated with identifying causal climatic drivers mean that large-scale climatic phenomena, such as the North Atlantic Oscillation (NAO), have often been used as a proxy for, and have frequently outperformed, local weather variables (Post & Stenseth 1999; Hallett *et al.* 2004). However, the relationship between these large-scale indices and local weather may be temporally and/or spatially variable (Stenseth *et al.* 2003; Anders & Post 2006). Thus large-scale indices may provide inaccurate future predictions of population dynamics, whilst using such indices to compare the sensitivity of populations to climatic conditions across large spatial scales may simply recover patterns in the strength of the relationship between the index and local weather variables (Anders & Post 2006; van de Pol *et al.* 2013). The relatively poor predictive performance of local weather variables may partly be caused by a lack of knowledge of when vital rates are sensitive to such variables (Stenseth & Mysterud 2005). Whilst demographic data are typically collected annually the effect of a single climatic variable may differ in magnitude and direction over the year (Kruuk, Osmond & Cockburn 2015). Additionally, time lags between environmental events and demographic responses are common (Terraube *et al.* 2015; Wells *et al.* 2016). They may be caused by indirect effects, mediated through interactions with other species (Brown 2011), or carry-over effects (Norris 2005), where the environment affects individual condition, resulting in delayed consequences for demographic rates such as survival. Indirect effects, through plant productivity, may have a larger effect on herbivore vital rates than the direct effects of changing climatic conditions (Davis, Stephens & Kjellander 2016).

Most studies consider a small number of putative climatic drivers, each acting at a

single time period (e.g. monthly means), chosen *a priori* based on expert knowledge of the focal species or closely related taxa (Fig. 1a; Van der Pol *et al.* 2016). Mismatches between these time periods and the critical windows during which the vital rates are sensitive to variation in the weather will lead to poorly performing models. Sliding window approaches, where an appropriate window is chosen by comparing the fit of models with different intervals, provide a partial resolution to this problem (Fig. 1a; Van der Pol *et al.* 2016). However, a single window is usually selected (Husby *et al.* 2010; Stopher *et al.* 2014; though see Kruuk, Osmond & Cockburn 2015), which does not allow the effect of a single variable to differ over time despite evidence of this occurring in natural populations (Kruuk, Osmond & Cockburn 2015). Ecological responses to environmental factors are likely to be more similar at adjacent time points (Sims *et al.* 2007). For example, the effect of high precipitation in February is likely to be more similar to that of high precipitation in March than August. Functional linear models (FLMs) allow the effect of environmental variables to be estimated as smooth, additive functions over time (Fig. 1b; Roberts 2008; Teller *et al.* 2016). This provides a biologically realistic framework for estimating climatic effects, allowing them to differ in magnitude and direction over the year.

The influence of climatic effects also varies according to individual state variables, such as age and sex (Gaillard *et al.* 2000). Consequently, structured population models are widely used to predict population responses to future change (e.g. Jenouvrier *et al.* 2012). Stochastic structured models consider the means and variances of vital rates (Rees & Ellner 2009). These rates often exhibit positive temporal correlations, with higher reproductive rates in years with high survival and/or growth (Nur & Sydeman 1999; Jongejans *et al.* 2010). Positive correlations among the vital rates of different age-sex classes are also common. For example, years of high juvenile survival occur simultaneously with high adult survival and years that favour female survival also favour males (Saether & Bakke 2000; Rotella *et al.* 2012). These positive covariances suggest the influence of common environmental drivers, yet these processes are typically considered independently (e.g. Coulson *et al.* 2001; Pokallus & Pauli 2015). Multilevel demographic structural equation models (SEMs) allow the joint response of disparate vital rates and/or different age-sex classes to environmental variation to be captured using a biologically meaningful model (Hindle *et al.* 2017). Demographic SEMs introduce latent variable(s) to capture the covariation amongst the vital rates. These can be conceived as axes of common environmental variation, each of which may be driven by a combination of biotic and abiotic variables. The variation in each axis may thus be decomposed into the effects of different drivers, providing a simpler target for the challenging task of determining the underlying drivers of temporal variation than treating each demographic process independently. SEMs have been widely adopted in ecology, for example to model the joint responses of multiple species to environmental change (e.g. Warton *et al.* 2015; Ovaskainen *et al.* 2016). Their use is rare in single species demographic studies (though see Evans, Holsinger & Menges

2010; Hindle *et al.* 2017).

Variation in the vital rates is likely to be driven by a combination of abiotic and biotic variables (Coulson *et al.* 2001; Dahlgren, Ostergard & Ehrlen 2014). Accurately quantifying both sources of variation is necessary to predict long-term population dynamics (Coulson, Rohani & Pascual 2004). For example, the effect of density is unlikely to be independent of the abiotic environment (Wang *et al.* 2009); the negative influence of a high population density may be greater in years with harsh abiotic conditions, as individuals compete over more limited resources (Barbraud & Weimerskirch 2003). In a SEM framework modelling an environmental axis as a function of density and climatic variables allows the effect of density on the vital rates to be modified by the abiotic environment.
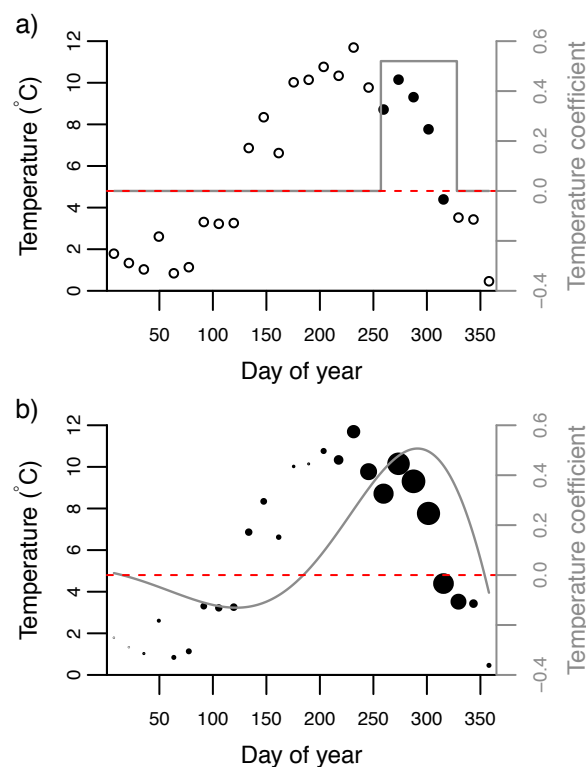
Figure 1: Schematic of a) window based approaches and b) FLM approach to identifying climatic effects. Points show means of raw temperature data calculated every fortnight over a single year. Grey lines show an example of the climatic coefficients that could be generated under either type of approach. The red dashed line is at zero i.e. where temperature has no effect; the effect of temperature is positive above this line and negative below it. Within each subplot the size of the points demonstrates their weight. Open points in a) indicate where temperature is assumed to have no effect. In a) the magnitude or direction of the temperature coefficients cannot differ within the chosen window (although multiple windows could be included), whereas in b) both the magnitude and direction of the temperature coefficients can vary over the year. If the climatic window is chosen *a priori* the position of the vertical grey lines in a) is fixed, whereas under a sliding window approach the start and end of the window are estimated. The FLM can be estimated using spline basis expansion (see equation 6).

In this paper, we investigated the dimensionality of the environment and decomposed the environmental variation into the effects of underlying drivers in a population of Soay sheep, *Ovis aries* (Clutton-Brock & Pemberton 2004). This population exhibits pronounced density

dependent fluctuations, with high survival and fecundity at low densities and population crashes often occurring at high densities (Clutton-Brock *et al.* 1991; Clutton-Brock *et al.* 1992). However, high densities do not always result in crashes, suggesting the population responds to an interaction between density and the abiotic environment (Coulson *et al.* 2001; Clutton-Brock & Pemberton 2004). Previous studies have found that harsh winter weather conditions, such as wet and windy weather, decrease survival and fecundity (Grenfell *et al.* 1998; Milner, Elston & Albon 1999; Catchpole *et al.* 2000; Coulson *et al.* 2001; Stenseth *et al.* 2004; Berryman & Lima 2006; Coulson *et al.* 2008). These studies have typically either used a large-scale index (winter NAO; e.g. Stenseth *et al.* 2004; Berryman & Lima 2006) or have chosen the temporal windows of putative local drivers *a priori* (Catchpole *et al.* 2000; Coulson *et al.* 2001), focusing on the winter period, when the vast majority of mortality occurs (Hallett *et al.* 2004). Longer-term effects, for example through changes in plant productivity or the condition of individuals entering winter have generally not been considered. Moreover, there are strong temporal correlations among the different vital rates, across sex and age classes, with years of high lamb, yearling, and adult survival occurring simultaneously with years of high reproduction (Fig. 2; Coulson *et al.* 1999). Despite this previous studies have identified the drivers of survival and fecundity separately for each age-sex class (e.g. Coulson *et al.* 2001; Coulson *et al.* 2008). We used a demographic SEM to show that just two axes of environmental variation are required to explain the temporal variation in survival, reproduction, and twinning across six age-sex classes. We then decomposed the first axis of environmental variation into the effects of density, a temporal trend, and climatic covariates, using FLMs to determine the critical window over which three local weather variables and NAO acted. We compared the predictive performance of the FLMs to using a large-scale climate index and to selecting the critical window for a local weather variable *a priori*.

Study System

We used thirty years of demographic data (1985-2014) on a population of Soay sheep in the Village Bay area of Hirta, in the St Kilda archipelago off the North-West of Scotland (Clutton-Brock & Pemberton 2004). Nearly 100% of newborn lambs are tagged within days of birth. Population censuses are carried out three times a year (spring, summer, and autumn) and mortality searches ensure the fate of most individuals is known. The lack of large herbivorous competitors and predators of the adults mean the population dynamics are largely driven by intra-specific competition for food (Clutton-Brock & Pemberton 2004).
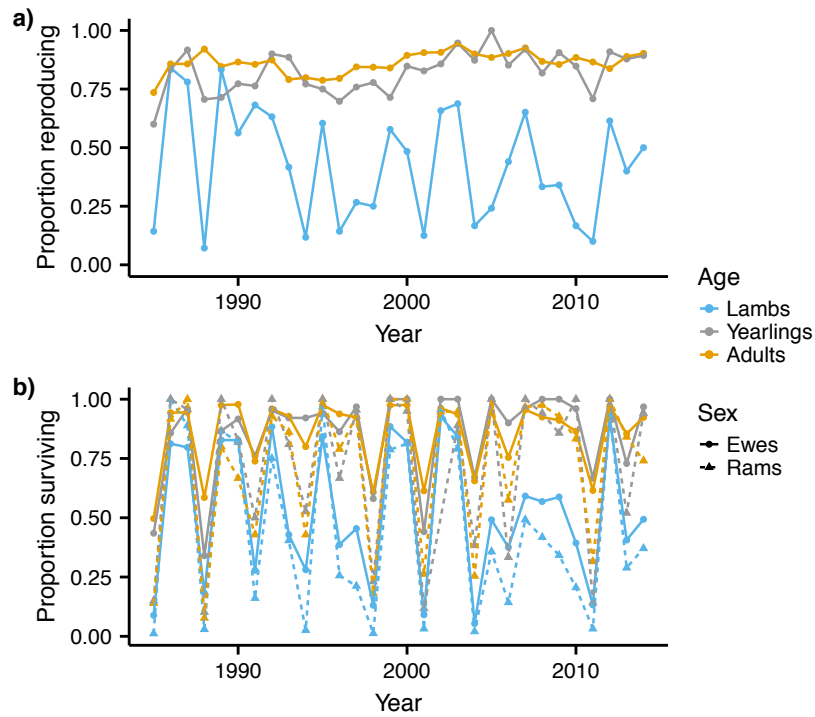
Figure 2: Observed proportion of individuals of individuals a) reproducing (ewes only) and b) surviving over the study period, separated by age-sex class.

For the FLMs we considered NAO and three local weather variables; minimum temperature, precipitation, and maximum wind speed. Cold, wet, and windy conditions may increase heat loss (Webster & Park 1967; Webb & King 1984; McArthur & Ousey 1996) and reduce grazing due to increased time spent sheltering (Stevenson 1994). Cold, wet weather may also have indirect effects through spring-summer vegetation growth and subsequent food availability. The predictive performance of the FLMs was compared to two reference models; using a large-scale climate index (December-March NAO, referred to herein as winter NAO; Coulson *et al.* 2001; Stenseth *et al.* 2004) and a local weather variable with the critical window selected *a priori* (March precipitation; Catchpole *et al.* 2000; Coulson *et al.* 2001). High winter NAO values are associated with warm, wet, and windy weather in northern Europe (Hurrell & VanLoon 1997), thus capturing harsh environmental conditions during the mortality period. Between January and March the body weight of the sheep can decline by as much as 30% (Clutton-Brock *et al.* 1997); high precipitation at the end of this period, before the onset of rapid new vegetation growth, thus appears likely to decrease survival. The winter NAO model differs from the NAO FLM, where monthly NAO values were included over a 19-month period.

NAO data were obtained from the National Center for Atmospheric Research (https://climatedataguide.ucar.edu/climate-data; Hurrell 1995). Daily local weather data were acquired from Stornoway meteorological office, the closest weather station open for the entire study period (approximately 140km from St Kilda; data available from badc.nerc.ac.uk). These data were closely correlated with those from St Kilda from 1999 onwards (when weather stations were set up on site; temperature, $r=0.97$, precipitation, $r=0.85$, wind speed, $r=0.93$; Fig. S1). Missing data (<1% of temperature and precipitation and 6% of wind data) were

interpolated using the *forecast* package (Hyndman & Khandakar 2008) in R (R Core Team 2016).

Structural equation model

Demographic SEMs excluding climatic drivers were constructed to explore the number of axes required to account for the temporal covariation among the vital rates and provide a baseline to evaluate the predictive performance of the climatic models. The population was split into three age classes: lambs (0-1 year), yearlings (1-2 years), and adults (>2 years). Female reproduction is not limited by male availability. A small proportion of yearling and adult ewes produce twins each year (Clutton-Brock & Pemberton 2004). The demographic SEMs therefore included 11 sub-models: August (t) to August (t+1) survival of each age-sex class (6 sub-models, s superscript), spring reproduction of ewes in each age class (3 sub-models, r superscript), and twinning of yearling and adult ewes (2 sub-models, t superscript).

We initially fitted a highly constrained model that assumes temporal variation in the vital rates is driven by a single time-varying environmental axis (e) common to all 11 sub-models (the single-axis model). At low densities differences in the abiotic environment have little effect on survival, as resource availability remains high (Fig. 3a; Grenfell *et al.* 1998). The probability of survival (S) for each age-sex class (except ram lambs - see below) was therefore estimated using threshold models (Fig. 3a), assuming a binomial distribution:

$$logit(S_{\bullet,t}) = \begin{cases} \beta_{\bullet}^{0,s} + \beta_{\bullet}^{t,s}t & \text{if } e(t) < \theta_{\bullet} \\ \beta_{\bullet}^{0,s} + \beta_{\bullet}^{t,s}t - \beta_{\bullet}^{e,s}(e(t) - \theta_{\bullet}) & \text{if } e(t) \geq \theta_{\bullet}, \end{cases} \qquad \text{(eqn 1)}$$

where β^0 are intercepts, β^t and β^e are slope terms for a temporal trend and the first environmental axis (e) respectively, and θ are thresholds. The $\bullet$ subscript indicates parameters estimated separately for each age-sex class. There was no evidence of a threshold in the fecundity (reproduction or twinning) or ram lamb survival sub-models (Fig. S2). The probability of reproduction (R) was estimated using a simple logistic regression:

$$logit(R_{\bullet,t}) = \beta_{\bullet}^{0,r} + \beta_{\bullet}^{t,r}t - \beta_{\bullet}^{e,r}e(t), \qquad \text{(eqn 2)}$$

with the parameters defined as above (equation 1). The twinning and ram lamb survival sub-models were structurally analogous to equation 2.

As the vital rates are highly density dependent and population sizes have generally increased over the study period (Fig. S3; Coulson *et al.* 2008) the environmental axis (e) was modelled as a function of density (D_t; the log10 number of sheep in the population in August of year t) and the study year (t):

$$e(t) = D_t - \alpha^t t - \varepsilon_t^e, \qquad \text{(eqn 3)}$$

where α^t is a slope term for the temporal trend. The random year effects (ε_t^e) account for residual covariation among the vital rates and were sampled from a normal distribution with mean zero and standard deviation σ^e. Including a temporal trend ($\alpha^t t$) here allows for an interaction between density and time across the vital rates, whilst the vital rate specific temporal

trends (given by $\beta^t t$ in equations 1-2) allow for temporal trends in the mean vital rates (Fig. S4).

We used a Bayesian framework for inference. Parameter estimates were obtained using Markov Chain Monte Carlo (MCMC) simulation in JAGS (Plummer 2003), using the R package *runjags* (Denwood in review). Weakly informative priors were used to aid convergence (Table S1). The models were run using two chains, each with a discarded burn-in period of 1×10^5 iterations. The chains were run for a further 6×10^6 iterations, and thinned, keeping every $2,000^{\text{th}}$ sample to produce a total posterior sample of 6,000 across both chains. Posterior predictive checks were used to determine whether the temporal variation in the vital rates was well explained by the initial model (Gelman *et al.* 2004).
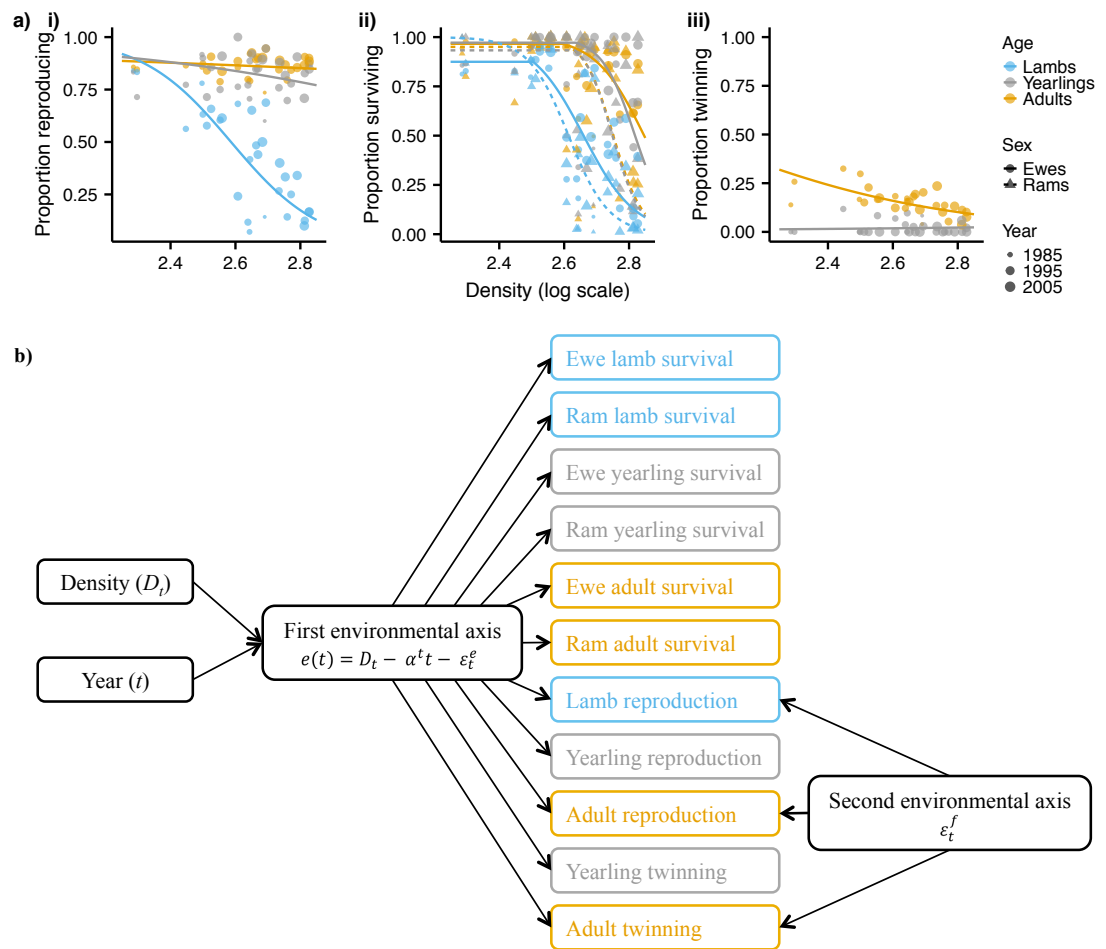
Figure 3: a) Proportion of individuals i) reproducing, ii) surviving, and iii) twinning against population density, separated by age-sex class. Points show observed data. Lines show fitted baseline sub-models (equation 3) for the two-axis model for the midyear of the study, with the random year effect at zero, using the posterior medians. b) Path diagram for the two-axis model. Colours denote the age class and match those used in a). The vital rates are given by equations 1-4. Note that the structure of the single-axis model is the same, excluding the second environmental axis.

Model development

Survival across the six age-sex classes was well predicted by the single-axis model (Fig. 4a). However, posterior predictive checks revealed evidence of unexplained variation in the fecundity sub-models (Fig. 4a; Appendix A1). Independent, sub-model specific random year effects were introduced into the fecundity sub-models to explore this unexplained variation (Appendix A1). The posterior distributions of the corresponding variance terms were concentrated at zero for the yearling reproduction and twinning sub-models. However, the variances of the remaining fecundity components were non-zero, and the associated year effects were positively correlated (Appendix A1). Consequently, we constructed a two-axis model (Fig. 3b), by introducing a second latent variable affecting lamb reproduction, adult reproduction, and adult twinning only. The probability of lamb or adult reproduction was then given by:

$$logit(R_{\bullet,t}) = \beta_\bullet^{0,r} + \beta_\bullet^{t,r}t - \beta_\bullet^{e,r}e(t) + \beta_\bullet^{f,r}\varepsilon_t^f, \qquad \text{(eqn 4)}$$

where β^f is the slope for the second environmental axis, ε_t^f. The adult twinning sub-model is structurally analogous to equation 4. ε_t^f and ε_t^e (equation 3) were sampled from a multivariate normal distribution with means of zero and covariance matrix Σ.
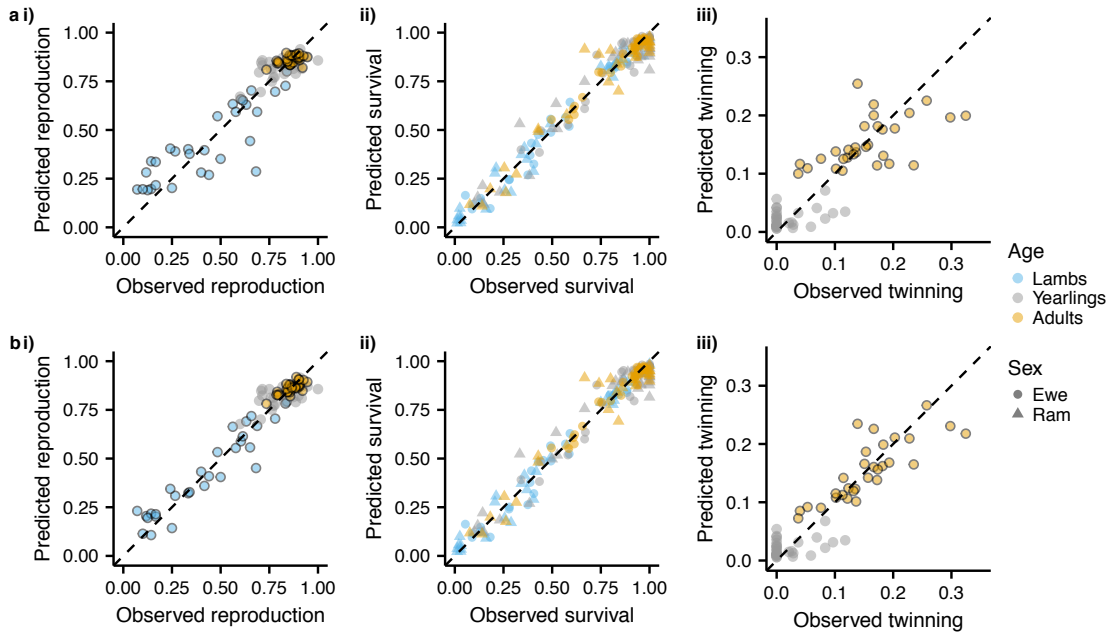
Figure 4: Observed and predicted vital rates using a) the single-axis and b) two-axis model. Black borders around the points indicate those processes partially driven by the second axis (Fig. 3b). The addition of the second axis increases the correlation between observed and predicted vital rates from 0.47 to 0.74 for adult reproduction, 0.58 to 0.81 for adult twinning, and 0.84 to 0.94 for lamb reproduction. Vital rates were predicted using the posterior medians as the parameter estimates, the observed density from $t-1$ and including the estimated random effect for each year. Dashed lines shows a 1:1 correlation.

The vital rates were well predicted using the two-axis model (Fig. 4b). Adding the second environmental axis improved the fit of the lamb reproduction, adult reproduction, and adult twinning sub-models (Fig. 4). However, it was the first axis that captured most of the

variation in the vital rates across the lifecycle. The 95% credible intervals of the β^e slope terms overlap zero in only two of eleven sub-models (adult reproduction and yearling twinning; Appendix A1), indicating the first axis drove variation in survival and fecundity in nearly all age-sex classes. Variation in survival across the age-sex classes and the majority of variation in the most variable fecundity rate (lamb reproduction) was captured by the first axis (Fig. 4). Variation in yearling twinning was not captured by either axis, however this remains low throughout the study period (the maximum number of yearlings twinning in one year was three and no yearlings twinned in 19 out of the 30 years). There was no evidence of correlations between the yearly estimates of the second environmental axis (ε_t^f) and density (D_t) or year (t; Appendix A1), indicating these effects were captured by the first axis. There was also no evidence of a correlation with the sex ratio (Appendix A1), suggesting female fecundity was not limited by male availability.

Identifying climatic drivers

We used the two-axis model for further analysis of environmental effects. Here we consider the first environmental axis (e), which drives the majority of the covariation in the vital rates (Fig. 4). We found no evidence of weather conditions driving variation in the second axis (Appendix A2). In the reference models, the first environmental axis was given by:

$$e(t) = D_t - \beta^m M_t - \alpha^t t - \varepsilon_t^e, \qquad \text{(eqn 5)}$$

where M_t is the climatic variable (winter NAO or mean March precipitation) in year t and β^m is a slope term. For the local weather FLMs the means of the daily variables every fortnight (w) from the beginning of January in t-1 ($w=1$) until the end of July in t ($w=42$), were used as covariates (Fig. S5). Monthly NAO data over the same time period were used for the NAO FLM ($w = 1, 2\ldots, 19$). Seasonality was removed from the weather data by centering (Fig. S5). Each covariate was included in a separate model, with the first environmental axis (e) given by:

$$e(t) = D_t - \sum_{w=1}^{W} f_c(w) C_{tw} - \alpha^t t - \varepsilon_t^e, \qquad \text{(eqn 6)}$$

where C_{tw} is climate variable C in year t and time interval w (fortnight for the local variables and month for NAO) and $f_c(w)$ is a smooth function that allows the effect of the climate covariates to vary smoothly over the 19 month period. The smooth function is parameterised using spline basis expansion, as $f_c(w) = \sum_{k=1}^{K} \beta_k^c b_k(w)$, where β^c are coefficients, $b_k(w)$ are basis functions, and K is the dimension of the spline basis. The FLM was estimated using eight knots and a cubic regression ("cr") spline basis. The degree of smoothing is controlled by a quadratic smoothing penalty, $\Sigma_j \lambda_j \beta^T S_j \beta$, where S_j are known smoothing penalty matrices and λ_j are smoothing parameters (Wood 2016; Wood 2017). In a Bayesian framework the FLM coefficients (β^c) can be estimated using a multivariate normal distribution prior, with precision matrix $\Sigma_j \lambda_j S_j$ (Wood 2016; Wood 2017). The smoothing parameters, λ_j, were estimated as parameters in the model using vague log-uniform priors (Table S1). The *jagam* function in the

mgcv package (Wood 2016) was used to generate the smoothing penalty matrices (**S**) and the spline bases (b_k).

The out of sample predictive performance and the proportion of variance (R^2) in *e* explained for each of the FLMs (equation 6) was compared to the base model (equation 3), and the reference models (equation 5). Leave one out cluster cross validation was used to assess predictive performance. The models were refitted thirty times, leaving out each year of data in turn. The predictive performance of each model was estimated using the expected logwise predictive density ($\widehat{elpd}$) (Vehtari, Gelman & Gabry 2016). Since ignoring the random year effects (ε^e and ε^f) may lead to overly optimistic estimates of a model's predictive performance (Skrondal & Rabe-Hesketh 2009; Pavlou *et al.* 2015), a Monte-Carlo approach was used to calculate the marginal predictive density. The $\widehat{elpd}$ was then

$$\widehat{elpd} = \sum_{i=1}^{n} \log\left(\frac{1}{SM}\sum_{s=1}^{S}\sum_{m=1}^{M} p(y_i|\theta^{s,m})\right), \tag{eqn 7}$$

where *S* is the number of draws from the posterior, *M* is the number of samples from the random year effect distributions and *n* is the number of years of data (Vehtari, Gelman & Gabry 2016). The likelihood $p(y_i|\theta^{s,m})$ is calculated as the product of the likelihoods for each of the eleven sub-models; y_i is the observed data in year *i* and $\theta^{s,m}$ is draw *s* from the posterior of the model that excluded the data from year *i*, with sample *m* from the random effects. Posterior samples were obtained using MCMC sampling in JAGS as above and the $\widehat{elpd}$ was estimated using the whole posterior sample of 6,000 for each year. ε^e and ε^f were sampled from a multivariate normal distribution 1,000 times for each posterior sample. The difference in the predictive ability of two models (A and B) on the deviance scale was given by $-2(\widehat{elpd}^A - \widehat{elpd}^B)$ (Vehtari, Gelman & Gabry 2016).

Climatic model results

The strongest weather effects were over winter, when the vast majority of the mortality occurs, but there was also evidence of longer-term effects, especially during autumn (Fig. 5). The vital rates were driven by the cumulative effect of precipitation from summer *t*-1 until winter in year *t*. Over this time period increased precipitation decreased survival and fecundity, with the strongest effects in autumn and winter (Fig. 5a). High wind speeds had a positive effect in winter and spring *t*-1 and a negative effect over autumn and winter in *t* (Fig. 5b). Higher NAO values from spring in *t*-1 were associated with decreased survival and fecundity, with particularly strong effects over winter in year *t* (Fig. 5d).

Cross validation was not carried out on the temperature FLM, as there was no evidence of an effect on the vital rates (Fig. 5c). The remaining climatic models had a better predictive performance than the baseline model (Table 1), however the gain was marginal in the case of March precipitation. Wind speed was the best performing of the FLMs; wind speed and precipitation both outperformed the monthly NAO FLM (Table 1). However, the winter NAO

model had a better predictive performance than any of the FLMs, with higher winter NAO values associated with decreased survival and fecundity (Table 1). Using an additive framework to include both precipitation and wind speed in a single model did not improve the predictive performance beyond the wind speed FLM (Appendix A2). Models including the precipitation or wind speed FLM as well as winter NAO had marginally better predictive performance than the winter NAO model (Appendix A2).
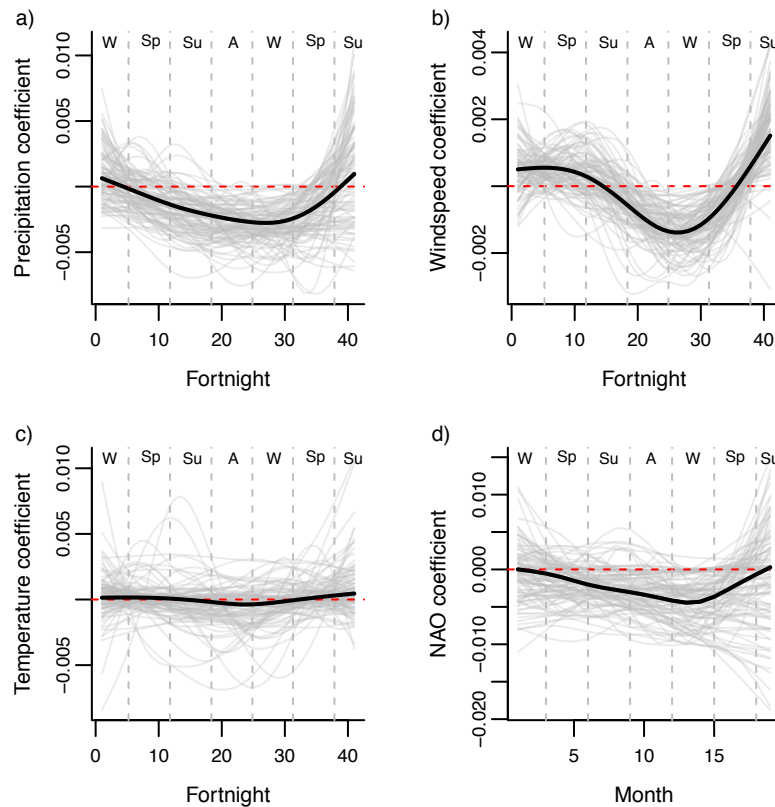

Figure 5: FLMs for a) temperature, b) precipitation, c) wind speed and d) NAO. Thick black lines show the posterior medians, thinner grey lines show 100 simulations from the posterior. The horizontal dashed red line is at 0. Dashed vertical lines and letters at the top of the plot indicate the seasons. Coefficients above the line indicate that higher values of the weather variable during that time period were associated with an increase in survival and fecundity. The rut occurs during autumn and mortality occurs during winter and early spring.

Table 1: Performance of the climatic models. Relative predictive performance is the difference in out of sample predictive performance (equation 7) between the baseline model (with no climate effects; equation 3) and each climate model, on the deviance scale. More negative values indicate models with a better predictive performance. R^2 is the proportion of variation in the first environmental axis (*e*) explained by the fixed effects (i.e. density, the temporal trend, and the relevant climatic variables). Values are the median and 95% quantiles, calculated by sampling from the posterior distribution. R^2 for the base model is 0.68 (0.57-0.74).

Model	Relative predictive performance	R^2
March precipitation	-0.67	0.68 (0.58-0.74)
Monthly NAO FLM	-1.96	0.77 (0.63-0.84)
Fortnightly precipitation FLM	-3.82	0.77 (0.65-0.84)
Fortnightly wind speed FLM	-5.73	0.81 (0.69-0.87)
Winter NAO	-13.57	0.86 (0.79-0.90)

Discussion

The environment may comprise considerably fewer dimensions than the number of vital rate-age-sex combinations to be estimated. Using a demographic SEM to estimate the vital rates simultaneously can thus provide a simpler target for the challenging task of decomposing the variation in the vital rates into the effects of different intrinsic (e.g. density) and extrinsic (e.g. climatic) covariates. In the Soay population a simple demographic SEM with a single axis captured most of the variation in survival, reproduction, and twinning across six age-sex classes, with all vital rates well predicted by two environmental axes. Age and sex differences in mean vital rates and their variability (Gaillard, Festa-Bianchet & Yoccoz 1998; Gaillard *et al.* 2000), have led to vital rates for different age-sex classes being treated independently (e.g. Coulson *et al.* 2001). Positive covariances amongst the vital rates across age-sex classes suggest that, despite differences in the magnitude of environmental effects, common axes of environmental variation drive the variation in vital rates across age-sex classes. Such positive covariances are widespread in natural populations, including in plants (Jongejans *et al.* 2010), birds (Nur & Sydeman 1999), and mammals (Rotella *et al.* 2012), suggesting the SEM approach is widely applicable.

The demographic SEM approach can also provide insights into interactions among the vital rates. Positive correlations among the vital rates may be caused by common environmental drivers acting on disparate vital rates (Nur & Sydeman 1999) or by interactions among the vital rates, such as the selective mortality of reproductive individuals in harsh environmental conditions (Rotella, Clark & Afron 2003). In the Soay population, the first environmental axis affects survival and fecundity, with evidence of strong weather effects over winter, after the rut has occurred. This axis probably reflects over-winter mortality and the selective mortality of reproductive individuals. Much of the mortality in this population occurs late in winter (Hallett *et al.* 2004), with starvation the main cause (Gulland 1991; Gulland 1992). The last two months of pregnancy, which are energetically costly as foetal weight increases quickly, occur before the onset of rapid spring vegetation growth (Robbins 1983). Temporal variation in fecundity in this population occurs predominantly through lamb reproduction (Fig. 3). The effects of a harsh environment are likely to be more extreme in pregnant lambs, undergoing relatively high reproductive costs, leading to increased mortality in this group. As the second environmental axis only drives variation in fecundity sub-models this may act through the probability of individuals conceiving. We do not decompose variation in the second axis, as it accounts for little variation in the vital rates, however there was no evidence of density dependence in this axis or of it being driven by male availability. This is unsurprising as a single male may fertilise multiple females each year (Coltman *et al.* 1999), suggesting males are unlikely to limit female reproduction. Instead it could be driven by body condition entering the rut, as heavier ewes are more likely to conceive (Clutton-Brock *et al.* 1996).

Despite this population being well studied, with multiple previous studies attempting to determine underlying drivers (e.g. Clutton-Brock *et al.* 1991; Clutton-Brock *et al.* 1992; Grenfell *et al.* 1998; Milner, Elston & Albon 1999; Catchpole *et al.* 2000; Coulson *et al.* 2001; Stenseth *et al.* 2004), previously unseen weather effects were identified using the FLMs, with the vital rates affected by cumulative effects from up to twelve months prior to the mortality period. The choice of possible environmental drivers, and the periods over which they are assumed to act, are important modeling decisions yet many studies provide little justification for their chosen variables (Ehrlen *et al.* 2016; Van der Pol *et al.* 2016). Previous results, that increased wind speeds and precipitation over winter increase mortality (Milner, Elston & Albon 1999; Coulson *et al.* 2001) were supported by the FLMs. However, high precipitation and wind speeds during the autumn rut appear nearly as costly as during winter. Rutting is energetically costly, with decreased foraging time and increased energy expenditure (Stevenson & Bancroft 1995); environmental conditions during this period may therefore have substantial effects on body condition and subsequent survival (Barboza *et al.* 2004).

Indirect effects can cause lags between the critical window over which a climatic variable acts and the demographic response (Terraube *et al.* 2015). The magnitude of indirect climatic effects on population dynamics, mediated through interactions with other species, can be larger than direct effects (Cahill *et al.* 2013; Davis, Stephens & Kjellander 2016). In the Soays higher maximum wind speeds in winter and spring *t*-1 appear to increase survival in year *t*, independently of any density effects. The weight of individuals in summer is not affected by density during the previous winter (Clutton-Brock *et al.* 1991), indicating that by summer individuals are able to regain their condition following harsh winters. Possibly these lagged weather effects may occur indirectly by influencing vegetation growth. Although wind speed seems unlikely to directly influence plant productivity it may be correlated with other environmental variables that do; as climatic covariates often covary it can be difficult to isolate causal drivers (Grosbois *et al.* 2008; Ehrlen *et al.* 2016).

Large-scale climate phenomena are often better predictors of vital rates than local weather variables (Post & Stenseth 1999; Hallett *et al.* 2004). However, such indices cannot improve the mechanistic understanding of how populations respond to environmental variation (Stenseth *et al.* 2003), without also considering the associations between such indices and local weather conditions (e.g. Almaraz & Amat 2004; Anders & Post 2006). The relationship between large-scale drivers and local weather conditions may not be temporally (Stenseth *et al.* 2003) or spatially (van de Pol *et al.* 2013) stationary, decreasing the ability of large-scale drivers to accurately predict population dynamics into the future or to extrapolate results beyond the population level. We show that the use of sophisticated statistical tools to determine the temporal windows over which local variables act can improve their predictive performance. Thus a lack of knowledge of such windows is one reason for the disparity in predictive performance between local and large-scale climatic variables (Stenseth & Mysterud 2005).

However, the local variables were still outperformed by a large-scale climatic index (winter NAO). A likely reason for the relatively high predictive performance of such large-scale indices is that they incorporate the effects of multiple local variables. Although in reality interactions between local variables are likely to be important (Stenseth & Mysterud 2005; Ehrlen *et al.* 2016), including multiple variables is not simple due to correlations among them (Grosbois *et al.* 2008). More mechanistic approaches to combining the effects of multiple interacting local covariates may therefore improve the predictive performance of local models and be more useful for predicting the effects of future change than a reliance on large-scale indices (Stenseth & Mysterud 2005).

Rapid climate change has increased interest in predicting ecological responses to environmental variation, with structured population models widely used to predict population responses to future change (e.g. Hunter *et al.* 2010; Salguero-Gomez *et al.* 2012). For accurate predictions relevant drivers and their temporal windows of influence must be identified and their effects must be accurately quantified. We have demonstrated that the dimensionality of the environment can be remarkably low, suggesting the influence of common environmental drivers across the vital rates and life cycle, and thus providing a simpler target for identifying such drivers. By incorporating climatic drivers over extended temporal periods FLMs can increase the predictive performance of local variables. Including interactions among climatic variables may further increase the predictive performance of local models, beyond that of large-scale indices (Stenseth & Mysterud 2005).

References

Almaraz, P. & Amat, J.A. (2004) Complex structural effects of two hemispheric climatic oscillators on the regional spatio-temporal expansion of a threatened bird. *Ecology Letters,* **7,** 547-556.

Altwegg, R. & Anderson, M.D. (2009) Rainfall in arid zones: possible effects of climate change on the population ecology of blue cranes. *Functional Ecology,* **23,** 1014-1021.

Anders, A.D. & Post, E. (2006) Distribution-wide effects of climate on population densities of a declining migratory landbird. *Journal of Animal Ecology,* **75,** 221-227.

Barboza, P.S., Hartbauer, D.W., Hauer, W.E. & Blake, J.E. (2004) Polygynous mating impairs body condition and homeostasis in male reindeer (Rangifer tarandus tarandus). *Journal of Comparative Physiology B-Biochemical Systemic and Environmental Physiology,* **174,** 309-317.

Barbraud, C. & Weimerskirch, H. (2003) Climate and density shape population dynamics of a marine top predator. *Proceedings of the Royal Society B-Biological Sciences,* **270,** 2111-2116.

Berryman, A. & Lima, M. (2006) Deciphering the effects of climate on animal populations: Diagnostic analysis provides new interpretation of soay sheep dynamics. *American Naturalist,* **168,** 784-795.

Boggs, C.L. & Inouye, D.W. (2012) A single climate driver has direct and indirect effects on insect population dynamics. *Ecology Letters,* **15,** 502-508.

Brown, G.S. (2011) Patterns and causes of demographic variation in a harvested moose population: evidence for the effects of climate and density-dependent drivers. *Journal of Animal Ecology,* **80,** 1288-1298.

Cahill, A.E., Aiello-Lammens, M.E., Fisher-Reid, M.C., Hua, X., Karanewsky, C.J., Ryu, H.Y., Sbeglia, G.C., Spagnolo, F., Waldron, J.B., Warsi, O. & Wiens, J.J. (2013) How does climate change cause extinction? *Proceedings of the Royal Society B-Biological Sciences,* **280**.

Catchpole, E.A., Morgan, B.J.T., Coulson, T.N., Freeman, S.N. & Albon, S.D. (2000) Factors influencing Soay sheep survival. *Journal of the Royal Statistical Society Series C-Applied Statistics,* **49,** 453-472.

Clutton-Brock, T.H., Illius, A.W., Wilson, K., Grenfell, B.T., MacColl, A.D.C. & Albon, S.D. (1997) Stability and instability in ungulate populations: An empirical analysis. *American Naturalist,* **149,** 195-219.

Clutton-Brock, T.H. & Pemberton, J.M. (2004) *Soay Sheep: Dynamics and Selection in an Island Population*.

Clutton-Brock, T.H., Price, O.F., Albon, S.D. & Jewell, P.A. (1991) Persistent instability and population regulation in soay sheep. *Journal of Animal Ecology,* **60,** 593-608.

Clutton-Brock, T.H., Price, O.F., Albon, S.D. & Jewell, P.A. (1992) Early development and population fluctuations in soay sheep. *Journal of Animal Ecology,* **61,** 381-396.

Clutton-Brock, T.H., Stevenson, I.R., Marrow, P., MacColl, A.D., Houston, A.I. & McNamara, J.M. (1996) Population fluctuations, reproductive costs and life-history tactics in female Soay sheep. *Journal of Animal Ecology,* **65,** 675-689.

Coltman, D.W., Bancroft, D.R., Robertson, A., Smith, J.A., Clutton-Brock, T.H. & Pemberton, J.M. (1999) Male reproductive success in a promiscuous mammal: behavioural estimates compared with genetic paternity. *Molecular Ecology,* **8,** 1199-1209.

Coulson, T., Albon, S., Pilkington, J. & Clutton-Brock, T. (1999) Small-scale spatial dynamics in a fluctuating ungulate population. *Journal of Animal Ecology,* **68,** 658-671.

Coulson, T., Catchpole, E.A., Albon, S.D., Morgan, B.J.T., Pemberton, J.M., Clutton-Brock, T.H., Crawley, M.J. & Grenfell, B.T. (2001) Age, sex, density, winter weather, and population crashes in Soay sheep. *Science,* **292,** 1528-1531.

Coulson, T., Ezard, T.H.G., Pelletier, F., Tavecchia, G., Stenseth, N.C., Childs, D.Z., Pilkington, J.G., Pemberton, J.M., Kruuk, L.E.B., Clutton-Brock, T.H. & Crawley, M.J. (2008) Estimating the functional form for the density dependence from life history data. *Ecology,* **89,** 1661-1674.

Coulson, T., Rohani, P. & Pascual, M. (2004) Skeletons, noise and population growth: the end of an old debate? *Trends in Ecology & Evolution,* **19,** 359-364.

Dahlgren, J.P. (2010) Alternative regression methods are not considered in Murtaugh (2009) or by ecologists in general. *Ecology Letters,* **13,** E7-E9.

Dahlgren, J.P., Ostergard, H. & Ehrlen, J. (2014) Local environment and density-dependent feedbacks determine population growth in a forest herb. *Oecologia,* **176,** 1023-1032.

Davis, M.L., Stephens, P.A. & Kjellander, P. (2016) Beyond Climate Envelope Projections: Roe Deer Survival and Environmental Change. *Journal of Wildlife Management,* **80,** 452-464.

Denwood, M.J. (in review) runjags: An R package providing interface utilities, parallel computing methods and additional distributions for MCMC models in JAGS. Journal of Statistical Software.

Ehrlen, J. & Morris, W.F. (2015) Predicting changes in the distribution and abundance of species under environmental change. *Ecology Letters,* **18,** 303-314.

Ehrlen, J., Morris, W.F., von Euler, T. & Dahlgren, J.P. (2016) Advancing environmentally explicit structured population models of plants. *Journal of Ecology,* **104,** 292-305.

Evans, M.E.K., Holsinger, K.E. & Menges, E.S. (2010) Fire, vital rates, and population viability: a hierarchical Bayesian analysis of the endangered Florida scrub mint. *Ecological Monographs,* **80,** 627-649.

Forchhammer, M.C., Stenseth, N.C., Post, E. & Langvatn, R. (1998) Population dynamics of Norwegian red deer: density-dependence and climatic variation. *Proceedings of the Royal Society B-Biological Sciences,* **265,** 341-350.

Gaillard, J.M., Festa-Bianchet, M. & Yoccoz, N.G. (1998) Population dynamics of large herbivores: variable recruitment with constant adult survival. *Trends in Ecology & Evolution,* **13,** 58-63.

Gaillard, J.M., Festa-Bianchet, M., Yoccoz, N.G., Loison, A. & Toigo, C. (2000) Temporal variation in fitness components and population dynamics of large herbivores. *Annual Review of Ecology and Systematics,* **31,** 367-393.

Gelman, A., Carlin, J.B., Stern, H.S. & Rubin, D.B. (2004) *Bayesian Data Analysis, Second Edition.* Chapman and Hall/CRC.

Grenfell, B.T., Wilson, K., Finkenstadt, B.F., Coulson, T.N., Murray, S., Albon, S.D., Pemberton, J.M., Clutton-Brock, T.H. & Crawley, M.J. (1998) Noise and determinism in synchronized sheep dynamics. *Nature,* **394,** 674-677.

Grosbois, V., Gimenez, O., Gaillard, J.M., Pradel, R., Barbraud, C., Clobert, J., Moller, A.P. & Weimerskirch, H. (2008) Assessing the impact of climate variation on survival in vertebrate populations. *Biological Reviews,* **83,** 357-399.

Gulland, F.M.D. (1991) The role of parasites in the population dynamics of Soay sheep on St. Kilda. PhD Thesis, University of Cambridge.

Gulland, F.M.D. (1992) The role of nematode parasites in soay sheep (Ovis-aries L) mortality during a population crash. *Parasitology,* **105,** 493-503.

Hallett, T.B., Coulson, T., Pilkington, J.G., Clutton-Brock, T.H., Pemberton, J.M. & Grenfell, B.T. (2004) Why large-scale climate indices seem to predict ecological processes better than local weather. *Nature,* **430,** 71-75.

Hindle, B.J., Rees, M., Sheppard, A.W., Quintana-Ascencio, P.F., Menges, E.S. & Childs, D.Z. (2017) Exploring population responses to environmental change when there's never enough data; a factor analytic approach. *BioRxiv.*

Hunter, C.M., Caswell, H., Runge, M.C., Regehr, E.V., Amstrup, S.C. & Stirling, I. (2010) Climate change threatens polar bear populations: a stochastic demographic analysis. *Ecology,* **91,** 2883-2897.

Hurrell, J.W. (1995) Decadal trends in the North-Atlantic Oscillation - regional temperatures and precipitation. *Science,* **269,** 676-679.

Hurrell, J.W. & VanLoon, H. (1997) Decadal variations in climate associated with the north Atlantic oscillation. *Climatic Change,* **36,** 301-326.

Husby, A., Nussey, D.H., Visser, M.E., Wilson, A.J., Sheldon, B.C. & Kruuk, L.E.B. (2010) Contrasting patterns of phenotypic plasticity in reproductive traits in two great tit (Parus major) populations. *Evolution,* **64,** 2221-2237.

Hyndman, R.J. & Khandakar, Y. (2008) Automatic time series forecasting: The forecast package for R. *Journal of Statistical Software,* **27,** 1-22.

Jenouvrier, S., Holland, M., Stroeve, J., Barbraud, C., Weimerskirch, H., Serreze, M. & Caswell, H. (2012) Effects of climate change on an emperor penguin population: analysis of coupled demographic and climate models. *Global Change Biology,* **18,** 2756-2770.

Jongejans, E., de Kroon, H., Tuljapurkar, S. & Shea, K. (2010) Plant populations track rather than buffer climate fluctuations. *Ecology Letters,* **13,** 736-743.

Kruuk, L.E.B., Osmond, H.L. & Cockburn, A. (2015) Contrasting effects of climate on juvenile body size in a Southern Hemisphere passerine bird. *Global Change Biology,* **21,** 2929-2941.

McArthur, A.J. & Ousey, J.C. (1996) The effect of moisture on the thermal insulation provided by the coat of a thoroughbred foal. *Journal of Thermal Biology,* **21,** 43-48.

Milner, J.M., Elston, D.A. & Albon, S.D. (1999) Estimating the contributions of population density and climatic fluctuations to interannual variation in survival of Soay sheep. *Journal of Animal Ecology,* **68,** 1235-1247.

Norris, D.R. (2005) Carry-over effects and habitat quality in migratory populations. *Oikos,* **109,** 178-186.

Nur, N. & Sydeman, W.J. (1999) Survival, breeding probability and reproductive success in relation to population dynamics of Brandt's cormorants Phalacrocorax penicillatus. *Bird Study,* **46,** 92-103.

Ovaskainen, O., Abrego, N., Halme, P. & Dunson, D. (2016) Using latent variable models to identify large networks of species-to-species associations at different spatial scales. *Methods in Ecology and Evolution,* **7,** 549-555.

Pavlou, M., Ambler, G., Seaman, S. & Omar, R.Z. (2015) A note on obtaining correct marginal predictions from a random intercepts model for binary outcomes. *Bmc Medical Research Methodology,* **15**.

Plummer, M. (2003) JAGS: a program for analysis of Bayesian graphical models using Gibbs sampling. pp. 125. Proceedings of the 3rd international workshop on distributed statistical computing. Technische Universit at Wien, Wien, Austria.

Pokallus, J.W. & Pauli, J.N. (2015) Population dynamics of a northern-adapted mammal: disentangling the influence of predation and climate change. *Ecological Applications, 25,* 1546-1556.

Post, E. & Stenseth, N.C. (1999) Climatic variability, plant phenology, and northern ungulates. *Ecology, 80,* 1322-1339.

R Core Team (2016) R: A language and environment for statistical computing. R Foundation for Statistical Computing, Vienna, Austria.

Rees, M. & Ellner, S.P. (2009) Integral projection models for populations in temporally varying environments. *Ecological Monographs, 79,* 575-594.

Robbins, C.T. (1983) *Wildlife feeding and nutrition*.

Roberts, A.M.I. (2008) Exploring relationships between phenological and weather data using smoothing. *International Journal of Biometeorology, 52,* 463-470.

Rotella, J.J., Clark, R.G. & Afron, A.D. (2003) Survival of female Lesser Scaup: Effects of body size, age, and reproductive effort. *Condor, 105,* 336-347.

Rotella, J.J., Link, W.A., Chambert, T., Stauffer, G.E. & Garrott, R.A. (2012) Evaluating the demographic buffering hypothesis with vital rates estimated for Weddell seals from 30 years of mark-recapture data. *Journal of Animal Ecology, 81,* 162-173.

Saether, B.E. & Bakke, O. (2000) Avian life history variation and contribution of demographic traits to the population growth rate. *Ecology, 81,* 642-653.

Salguero-Gomez, R., Jones, O.R., Archer, C.R., Bein, C., de Buhr, H., Farack, C., ... & Vaupel, J.W. (2016) COMADRE: a global data base of animal demography. *Journal of Animal Ecology, 85,* 371-384.

Salguero-Gomez, R., Siewert, W., Casper, B.B. & Tielborger, K. (2012) A demographic approach to study effects of climate change in desert plants. *Philosophical Transactions of the Royal Society B-Biological Sciences, 367,* 3100-3114.

Sims, M., Elston, D.A., Larkham, A., Nussey, D.H. & Albon, S.D. (2007) Identifying when weather influences life-history traits of grazing herbivores. *Journal of Animal Ecology, 76,* 761-770.

Skrondal, A. & Rabe-Hesketh, S. (2009) Prediction in multilevel generalized linear models. *Journal of the Royal Statistical Society Series a-Statistics in Society, 172,* 659-687.

Stenseth, N.C., Chan, K.S., Tavecchia, G., Coulson, T., Mysterud, A., Clutton-Brock, T. & Grenfell, B. (2004) Modelling non-additive and nonlinear signals from climatic noise in ecological time series: Soay sheep as an example. *Proceedings of the Royal Society B-Biological Sciences, 271,* 1985-1993.

Stenseth, N.C. & Mysterud, A. (2005) Weather packages: finding the right scale and composition of climate in ecology. *Journal of Animal Ecology, 74,* 1195-1198.

Stenseth, N.C., Ottersen, G., Hurrell, J.W., Mysterud, A., Lima, M., Chan, K.S., Yoccoz, N.G. & Adlandsvik, B. (2003) Studying climate effects on ecology through the use of climate indices: the North Atlantic Oscillation, El Nino Southern Oscillation and beyond. *Proceedings of the Royal Society B-Biological Sciences, 270,* 2087-2096.

Stevenson, I. (1994) Male-biased mortality in Soay sheep. PhD Thesis, University of Cambridge.

Stevenson, I.R. & Bancroft, D.R. (1995) Fluctuating trade-offs favour precocial maturity in male Soay sheep. *Proceedings of the Royal Society B-Biological Sciences, 262,* 267-275.

Stopher, K.V., Bento, A.I., Clutton-Brock, T.H., Pemberton, J.M. & Kruuk, L.E.B. (2014) Multiple pathways mediate the effects of climate change on maternal reproductive traits in a red deer population. *Ecology, 95,* 3124-3138.

Sutherland, W.J. (2006) Predicting the ecological consequences of environmental change: a review of the methods. *Journal of Applied Ecology, 43,* 599-616.

Teller, B.J., Adler, P.B., Edwards, C.B., Hooker, G. & Ellner, S.P. (2016) Linking demography with drivers: climate and competition. *Methods in Ecology and Evolution, 7,* 171-183.

Terraube, J., Villers, A., Ruffino, L., Iso-Iivari, L., Henttonen, H., Oksanen, T. & Korpimaki, E. (2015) Coping with fast climate change in northern ecosystems: mechanisms underlying the population-level response of a specialist avian predator. *Ecography, 38,* 690-699.

van de Pol, M., Brouwer, L., Brooker, L.C., Brooker, M.G., Colombelli-Negrel, D., Hall, M.L., Langmore, N.E., Peters, A., Pruett-Jones, S., Russell, E.M., Webster, M.S. & Cockburn, A. (2013) Problems with using large-scale oceanic climate indices to compare climatic sensitivities across populations and species. *Ecography, 36,* 249-255.

Van der Pol, M., Bailey, L.D., McLean, N., Rijsdijk, L., Lawson, C.R. & Brouwer, L. (2016) Identifying the best climatic predictors in ecology and evolution. *Methods in Ecology and Evolution, 7,* 1246-1257.

Vehtari, A., Gelman, A. & Gabry, J. (2016) Practical Bayesian model evaluation using leave-one-out cross-validation and WAIC. arXiv:1507.04544v5.

Wang, G.M., Hobbs, N., Twombly, S., Boone, R., Illius, A., Gordon, I. & Gross, J. (2009) Density dependence in northern ungulates: interactions with predation and resources. *Population Ecology, 51,* 123-132.

Warton, D.I., Blanchet, F.G., O'Hara, R.B., Ovaskainen, O., Taskinen, S., Walker, S.C. & Hui, F.K.C. (2015) So Many Variables: Joint Modeling in Community Ecology. *Trends in Ecology & Evolution,* **30,** 766-779.

Webb, D.R. & King, J.R. (1984) Effects of wetting on insulation of bird and mammal coats. *Journal of Thermal Biology,* **9,** 189-191.

Webster, A.J.F. & Park, C. (1967) The effect of jute coats on the heat losses of two breeds of sheep exposed to different environments. pp. 483-490. Animal Production.

Wells, K., O'Hara, R.B., Cooke, B.D., Mutze, G.J., Prowse, T.A.A. & Fordham, D.A. (2016) Environmental effects and individual body condition drive seasonal fecundity of rabbits: identifying acute and lagged processes. *Oecologia,* **181,** 853-864.

Wood, S.N. (2016) Just Another Gibbs Additive Modeller: Interfacing JAGS and mgcv. arXiv:1602.02539

Wood, S.N. (2017) Generalized Additive Models: An Introduction with R. Chapman and Hall/CRC.

Supplementary Figures
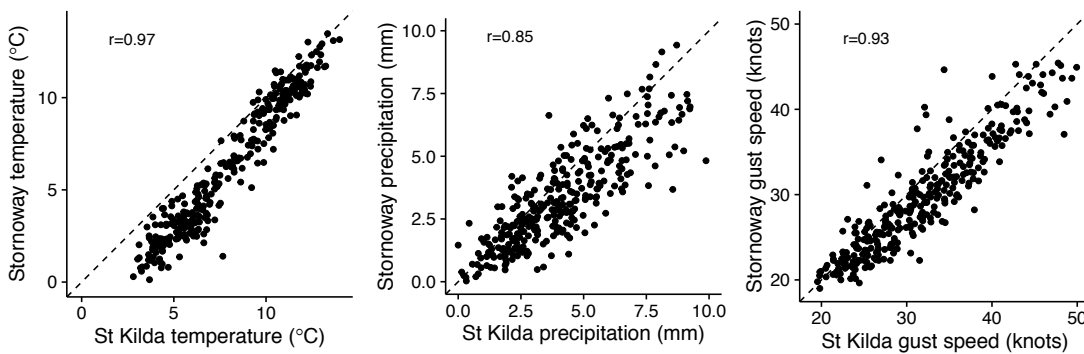
Figure S1: Correlation between minimum temperature, mean precipitation, and maximum windspeed on St Kilda and from the meteorological office station at Stornoway airport (150km away). Dashed lines show 1:1 lines.
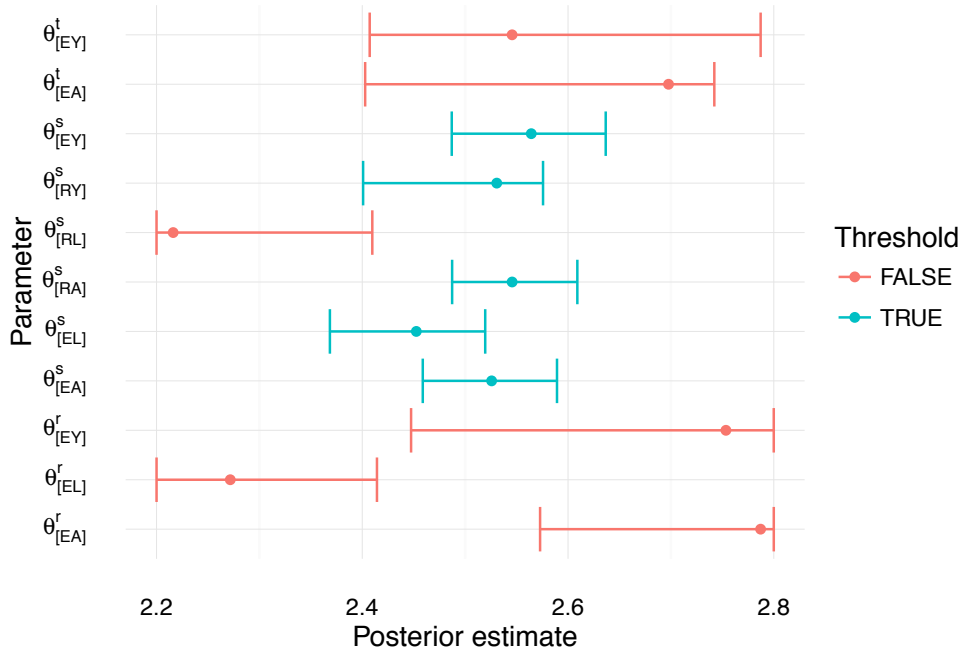
Figure S2: Posterior distributions (mode and 95% credible intervals) for model using threshold models for all of the vital rate sub-models (see equation 1 in main text). Subscripts show the sex and stage class (i.e. EA is ewe adult) and superscripts show the vital rate (survival, reproduction or twinning). Colours denote whether or not the threshold parameter is retained in that sub-model. The posteriors of the threshold parameters for the survival sub-models (with the exception of ram lamb survival) are well defined, whilst those of the fecundity models and ram lamb survival are broader and often focused at either end of the prior (see Qian 2014).
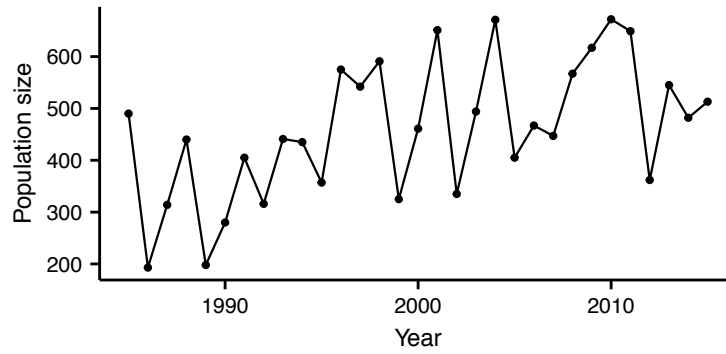
Figure S3: Total population size in the Village Bay area of Hirta over the study period. Whilst highly variable the number of individuals has generally increased over time.
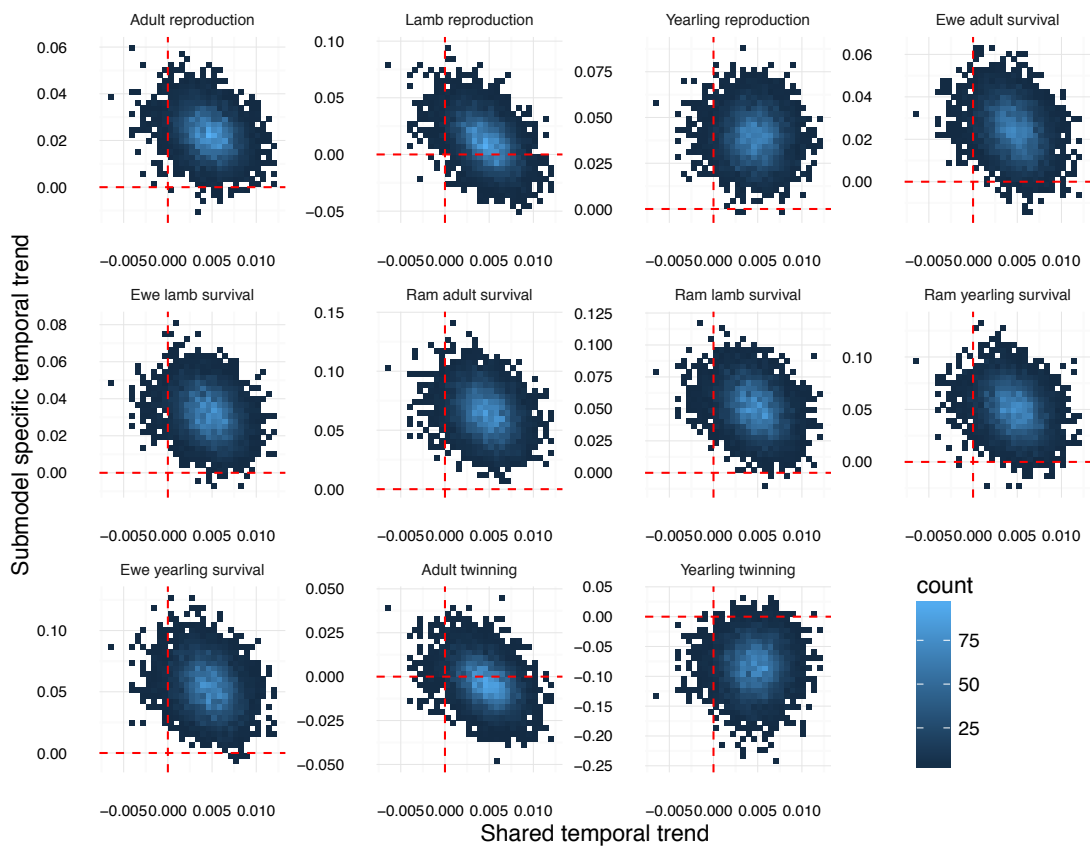

Figure S4: Bivariate plot of the posterior distributions for the two types of temporal trend included in the structural equation model (SEM). Including the shared temporal trend ($\alpha^t t$; see equation 3) in the first environmental axis (e) allows for an interaction between density and time across the vital rates, whilst the submodel specific temporal trends (given by $\beta^t t$; see equations 1-2 & 4) allow for temporal trends in the vital rate means. Both trends were retained as the parameters were not strongly correlated.
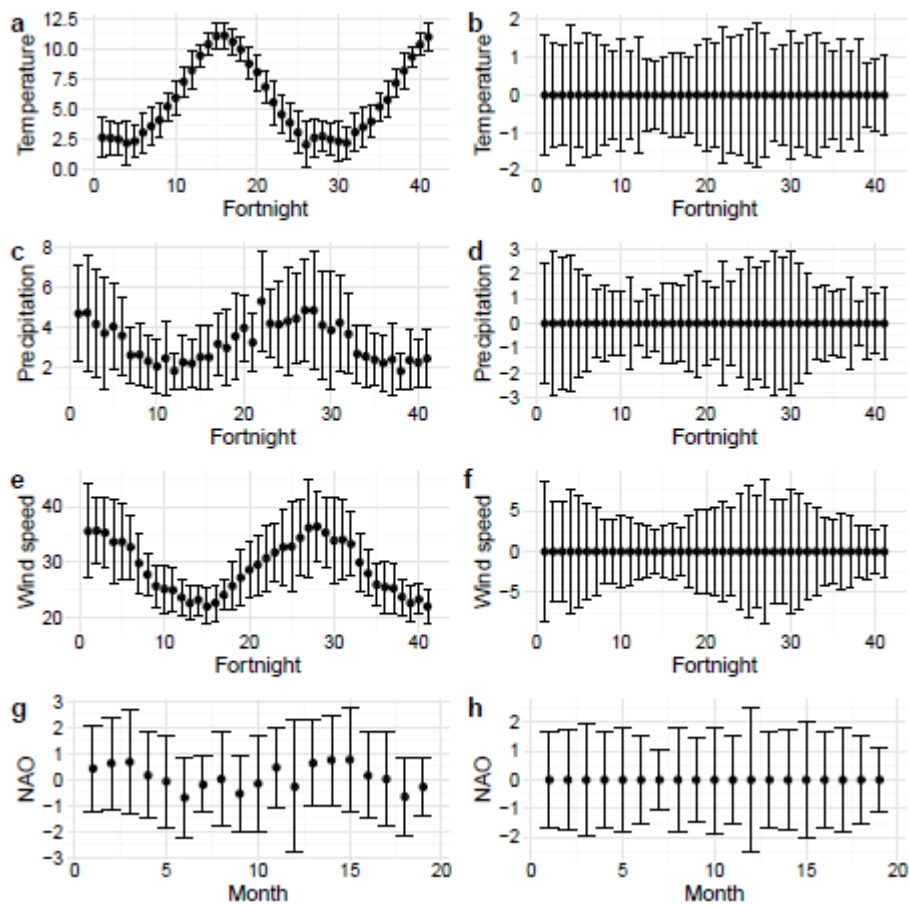
Figure S5: Mean (points) and standard deviation (error bars) of a) temperature (°C), c) precipitation (mm), e) wind speed (knots) and g) NAO. b), d), f) and h) show the mean and standard deviation of the centered climate covariates. The covariates were centered to remove seasonality from the data.

References

Qian, S.S. (2014) Ecological threshold and environmental management: A note on statistical methods for detecting thresholds. *Ecological Indicators,* **38,** 192-197.

Supplementary Tables

Table S1: Priors for the structural equation models. For the uniform distributions (U) and log-uniform distribution (LU) the first and second parameters refer to the minimum and maximum, for the normal distribution (N) they are the mean and standard deviation. For parameter definitions see equations 1-4 for parameters in all models and equations 5-6 for additional parameters in climate models. Note that • is used when referring to parameters for each of the demographic classes, otherwise subscripts indicate which classes are referred to with E for ewes, R for rams, L for lambs, Y for yearlings, and A for adults. Weakly informative priors are used to aid convergence of the threshold models, for example by restricting the threshold parameters to the range of observed densities.

Parameter	Model	Submodel(s)	Prior
$\beta_\bullet^{0,r}$	All	Reproduction	N(0, 100)
$\beta_\bullet^{t,r}$	All	Reproduction	N(0, 1)
$\beta_\bullet^{e,r}$	All	Reproduction	N(0, 100)
$\beta_\bullet^{f,r}$	All	Lamb and adult reproduction	U(0, 100)
$\beta_\bullet^{0,t}$	All	Twinning	N(0, 100)
$\beta_\bullet^{t,t}$	All	Twinning	N(0, 1)
$\beta_\bullet^{e,t}$	All	Twinning	N(0, 100)
$\beta_\bullet^{f,t}$	All	Adult twinning	U(0, 100)
$\beta_{[E]}^{0,s}$	All	Ewe survival	U(-5, 5)
$\beta_{[R]}^{0,s}$	All	Ram yearling and adult survival	U(-10, 10)
$\beta_{[RL]}^{0,s}$	All	Ram lamb survival	N(0, 100)
$\beta_\bullet^{t,s}$	All	Survival (except ram lambs)	U(-1, 1)
$\beta_{[RL]}^{t,s}$	All	Ram lamb survival	N(0, 1)
$\beta_\bullet^{e,s}$	All	Survival (except ram lambs)	U(0, 50)
$\beta_{[RL]}^{e,s}$	All	Ram lamb survival	N(0,100)
$\theta_{[EL]}$	All	Ewe lamb survival	U(2.2, 2.8)
$\theta_\bullet$	All	Survival (except lambs)	U(2.4, 2.8)
σ_e	All	All	U(0, 0.2)
σ_f	All	All	1
ρ_{ef}	All	Adult and lamb reproduction and adult twinning	U(-1, 1)
α^t	All	All	U(-0.05, 0.05)
β^n	Climate	All	U(-0.5, 0.5)
λ	Climate	All	LU(-10, 20)

Appendices

Appendix A1: Exploring the dimensionality of the environment

Posterior predictive checks from the model with a single axis of environmental variation (see main text, equations 1-3) showed that the variation in survival across the six age-sex classes was well explained using a single axis of environmental variation (Fig. 4a). There was some unexplained variation in the fecundity (reproduction and twinning) sub-models (Fig. 4a). Vital rate specific temporal error terms ($\varepsilon_{\bullet,t}^f$) were included into the fecundity models with the probability of reproduction now given by

$$logit(R_{\bullet,t}) = \beta_\bullet^{0,r} + \beta_\bullet^{t,r}t - \beta_\bullet^{e,r}e(t) + \varepsilon_{\bullet,t}^{f,r}. \qquad \text{(eqn A1)}$$

See main text (equations 1-4) for parameter definitions. The twinning models are not shown but were structurally analogous to the reproduction models. The posterior distributions of the $\varepsilon_{\bullet,t}^{f}$ terms suggest that there was residual variation in the lamb reproduction, adult reproduction, and adult twinning sub-models (Fig. A1). The posterior distributions for the standard deviations of the error terms in yearling reproduction and twinning are concentrated at zero and these terms were therefore excluded. As the estimates of the vital rate specific error terms were positively correlated the sub-model specific temporal error terms were replaced by a second environmental axis. This accounted for any covariance among lamb reproduction, adult reproduction, and adult twinning not accounted for by the first axis (e). The probability of lamb or adult reproduction therefore becomes

$$logit\big(R_{\bullet,t}\big) = \beta_{\bullet}^{0,r} + \beta_{\bullet}^{t,r}t - \beta_{\bullet}^{e,r}e(t) + \beta_{\bullet}^{f,r}\varepsilon_{t}^{f}, \qquad \text{(eqn A2)}$$

where β^f is the slope for the second latent environmental axis (ε^f) and ε^f and ε^e are sampled from a multivariate normal distribution with means of zero and a covariance matrix $\Sigma = \begin{matrix} \sigma_e\sigma_e & \sigma_e\sigma_f\rho_{ef} \\ \sigma_e\sigma_f\rho_{ef} & \sigma_f\sigma_f \end{matrix}$. σ_f was constrained to equal one for make the model identifiable. The structure of the adult twinning model is analogous to the lamb and adult reproduction models. Including the second environmental axis increased the agreement between the observed and predicted fecundity vital rates (Fig. 4b). The first axis of environmental variation affects nine of the vital rates, with the posteriors of the β^e terms only overlapping zero for yearling reproduction and yearling twinning (Fig. A2). There was no evidence of correlation between the yearly estimates of the second environmental axis and density or the year of study (Fig. A3), suggesting the effects of these variables were accounted for by the first environmental axis (e). There was also no evidence of a correlation with the sex ratio, suggesting the availability of males did not limit female reproduction. This is unsurprising as a single male can fertilise multiple females in any given year (Pemberton *et al.* 1996; Coltman *et al.* 1999).
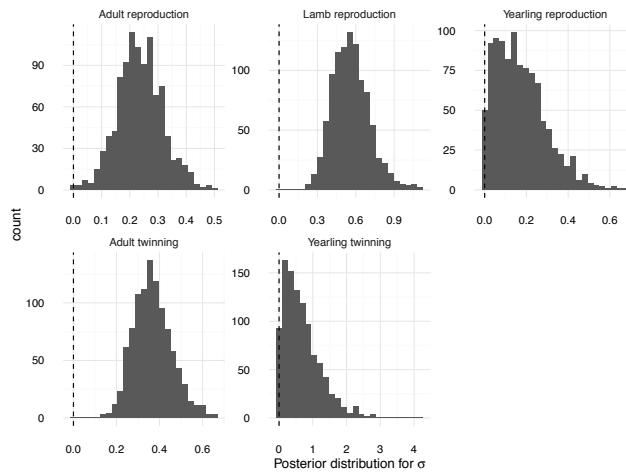

Figure A1: Posterior distributions of the standard deviations of the additional error terms ε^f in the fecundity models (see equation A1).
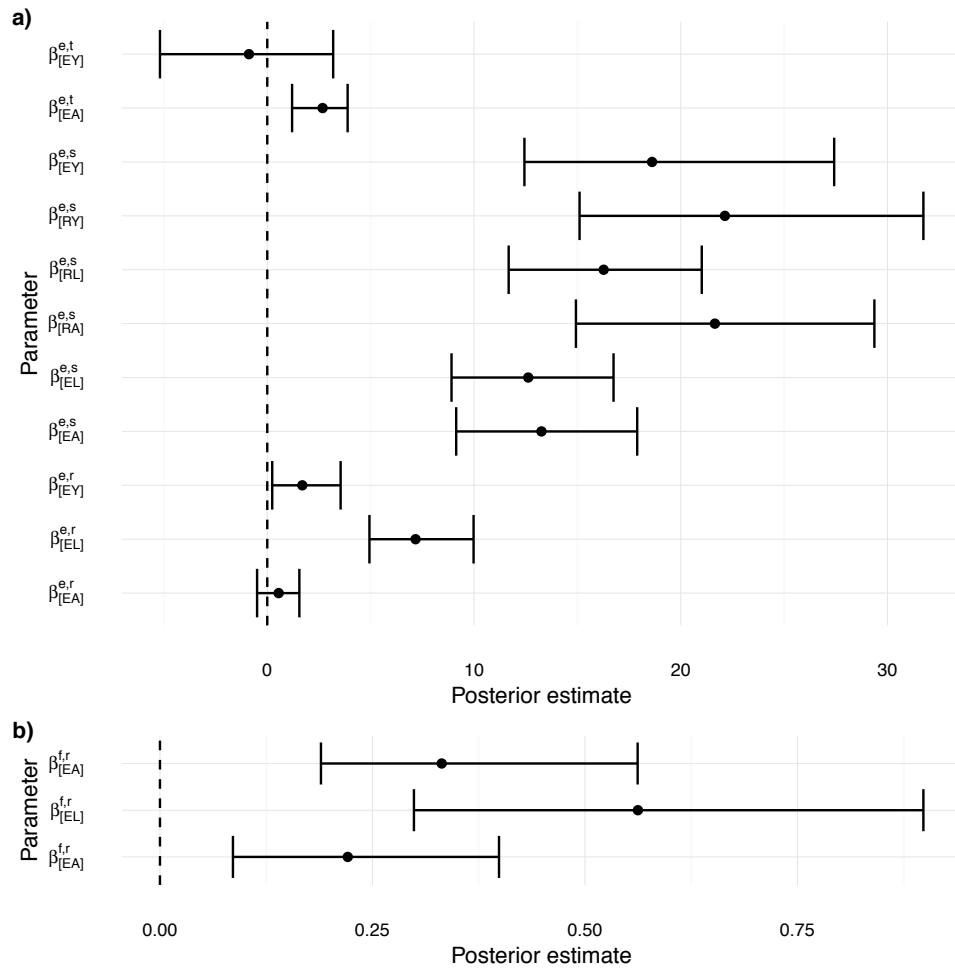
Figure A2: Posterior estimates (modes and 95% credible intervals) for the slope terms for a) the first and b) the second axes of environmental variation. The superscripts s, r, and t refer to whether the parameter is in a survival, reproduction or twinning sub-model. The subscripts give the demographic class, with the first letter referring to the sex (i.e. E for ewe and R for ram) and the second letter the stage class (i.e Lamb, Yearling or Adult).
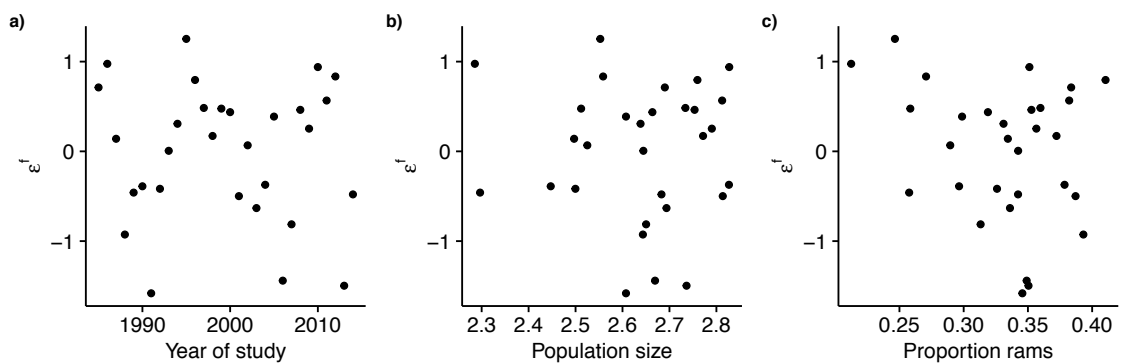

Figure A3: Correlation between a) the year of the study, b) population size (log 10 number of individuals in August of year t), and c) the proportion of rams in the population and the reproductive latent effect (ε^f).

Appendix A2: The effects of multiple climatic covariates

Incorporating multiple local climatic covariates in the first axis of environmental variation

The predictive performance of both the wind speed and precipitation FLMs was better than the baseline model (Table 1). As such we modelled the first temporal axis of variation (e) as a function of both wind speed (G) and precipitation (P) as follows

$$e(t) = D_t - \sum_{w=1}^{W} f_g(w)G_{tw} - \sum_{w=1}^{W} f_p(w)P_{tw} - \alpha^t t - \varepsilon_t^e. \qquad \text{(eqn A3)}$$

where D_t is the density in year t, α^t is a temporal trend, G_{tw} and P_{tw} are the mean wind speed and precipitation respectively in fortnight w and year t, and $f_g(w)$ and $f_p(w)$ are smooth functions for how the effects of wind speed and precipitation vary over the year. These smooth functions are estimated by spline basis expansion, as in the main text (equation 6). ε_t^e accounts for any residual temporal covariation in the vital rates. Cluster cross validation was performed as in the main text (equation 7) and the predictive performance of this model was compared to the single climatic covariate wind speed and precipitation models.
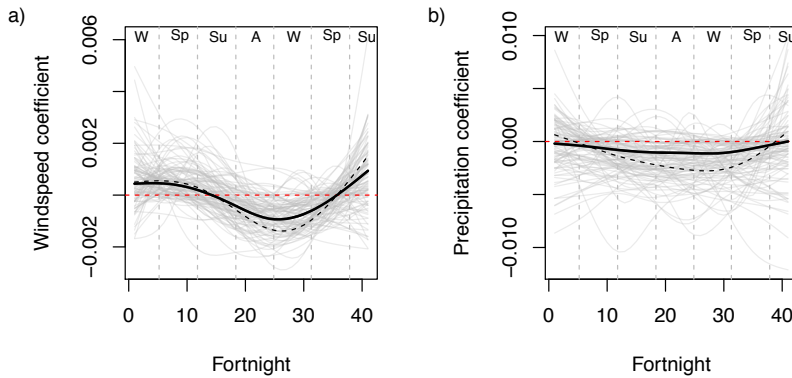

Figure A4: FLM with two climatic covariates; a) wind speed and b) precipitation (see equation A3). Thick black lines show the posterior medians, thinner grey lines show 100 simulations from the posterior. Thin dashed black lines show the medians from the respective single climatic variable FLMs. The horizontal dashed red line is at 0. Dashed vertical lines and letters at the top of the plot indicate the seasons. Coefficients above the line indicate that higher values of the climatic covariate during that time period were associated with an increase in fecundity.

Table A1: Difference in the predictive performance of the FLM with the highest predictive performance (wind speed) and the other models on a deviance scale. Lower values indicate models with a higher predictive performance.

Model	Relative predictive ability	R^2
Precipitation	1.91	0.77 (0.65-0.84)
Precipitation and wind speed	1.56	0.81 (0.70-0.88)
Wind speed	0.00	0.81 (0.69-0.87)

Similar effects are seen for each climatic covariate when wind speed and precipitation are included in the same model as when these are modelled separately (Fig. A4). Higher precipitation generally has a negative effect on the vital rates whilst higher wind speeds have a positive effect in Spring year $t-1$ and negative over autumn and winter in year t. However, the

effect sizes are decreased for both climatic covariates in the joint model, relative to including each climatic covariate in a separate model (Fig. A4). This is unsurprising as the wind speed and precipitation are correlated (r=0.71, p<0.01). Climatic covariates are often correlated with each other (Grosbois *et al.* 2008), sometimes making it difficult to determine variables are drivers and which are simply correlated with drivers (Ehrlen *et al.* 2016). Including both variables does not improve the predictive ability of the model beyond that of the wind speed only model (Table A1). Here an additive relationship between the climatic covariates was assumed. In reality it is often an interaction between climatic covariates that affects the vital rates (Stenseth & Mysterud 2005), for example here wet and windy weather may be a lot worse thermodynamically than the additive effect would suggest.

Incorporating broadscale and local climatic covariates

Including winter NAO and the local weather variables in a single model can determine whether the FLMs are able to identify effects beyond those seen in the winter NAO model. Here the first axis of environmental variation is given by

$$e(t) = D_t - \beta^N NAO_t - \sum_{w=1}^{W} f_c(w)C_{tw} - \alpha^t t - \varepsilon_t^e, \qquad \text{(eqn A4)}$$

where NAO_t is winter NAO in year t, β^N is a slope term and the remaining parameters are defined in equation 6 and details on fitting the model are the same as those provided in the main text. This was repeated using both precipitation and wind speed as the local variable (C).

Including the winter NAO term decreases the magnitude of the coefficients for both precipitation and wind speed (Fig. A5). The largest decreases are during winter, as would be expected given that high winter NAO values are associated with wet and windy winters. However, it is not only the magnitude of the coefficients during winter that is altered, possibly because weather may be correlated within years and changes in the winter NAO term may also therefore be correlated with changes in the weather outside of winter. Including the local weather variables does not change the magnitude of the β^N slope term in either model (Fig. A5). The models including the local covariates in addition to the winter NAO term have a better predictive performance than the model with just the winter NAO term, however this is marginal, especially in the case of the precipitation model (Table A2).

Table A2: Difference in the predictive performance of model with the highest predictive performance (wind speed and winter NAO) and the other models on a deviance scale. Lower values indicate models with a better predictive performance. R^2 is the proportion of variation in the first environmental axis (e) explained by the fixed effects (i.e. density, the temporal trend, and the relevant climatic variables). Values are the median and 95% quantiles, calculated by sampling from the posterior distribution. R^2 for the base model is 0.68 (0.57-0.74).

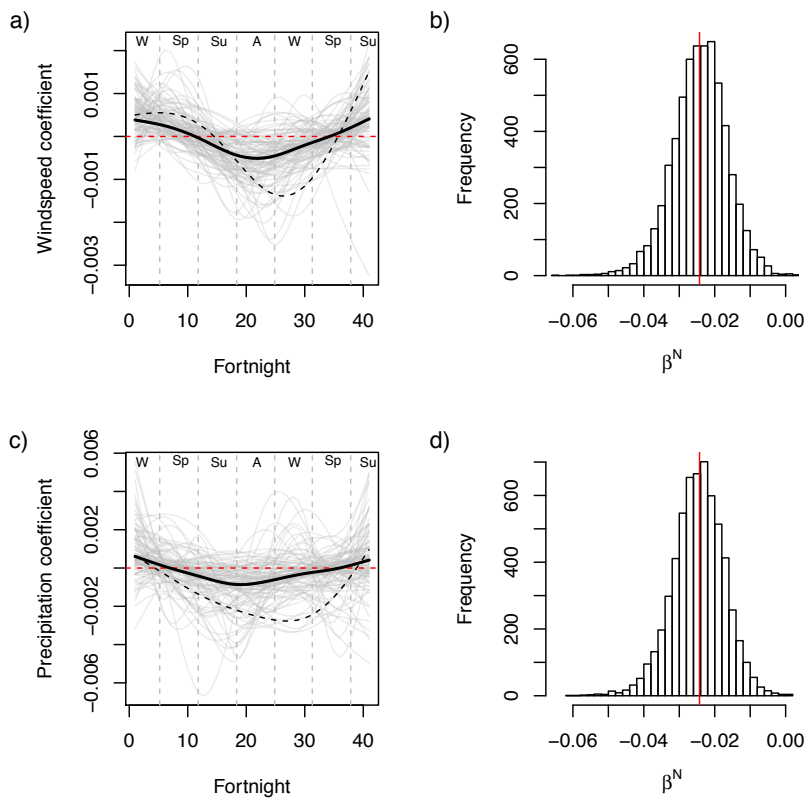| Model	Relative predictive ability	R^2
Precipitation	11.00	0.77 (0.65-0.84)
Wind speed	9.09	0.81 (0.69-0.87)
Winter NAO	1.24	0.86 (0.79-0.90)
Precipitation + Winter NAO	1.17	0.86 (0.79-0.91)
Wind speed + Winter NAO	0.00	0.87 (0.80-0.91)

Figure A5: Estimates of climatic coefficients for the wind speed and winter NAO model (top row) and the precipitation and winter NAO model (bottom row). a) and c) show the FLMs for windspeed and precipitation respectively. Thick black lines show the posterior medians, thinner grey lines show 100 simulations from the posterior. Thin dashed black lines show the medians from the respective single weather variable FLMs. The horizontal dashed red line is at 0. Dashed vertical lines and letters at the top of the plot indicate the seasons. Coefficients above the line indicate that higher values of the weather variable during that time period were associated with an increase in survival and fecundity. b) and d) show the posterior distribution for β^N. The vertical red line shows the equivalent parameter from the model with winter NAO only (i.e. without a local covariate).

Climatic effects in the reproductive latent effect

As the first axis of environmental variation affected both survival and fecundity (Fig. A2) we assumed that this accounted for temporal variation in reproduction due to the selective mortality

of reproductive individuals. That is we assume that for example a lamb that is pregnant has a higher mortality risk in a 'bad' winter than a lamb that is not pregnant and therefore the proportion of lambs reproducing is lower in 'bad' winters as a higher proportion of pregnant lambs have died. As the second environmental axis only affects reproduction (Fig. A3) we assume that this affects the probability of individuals conceiving, for example by affecting the condition of the sheep entering the rutting period. Climatic covariates were therefore included from January $t - 1$ until November in year t, when the rut occurs. The same local variables were included as in the first environmental axis (minimum temperature, precipitation, and maximum wind speed).

The probability of lamb reproduction or adult reproduction is now given by

$$logit(R_{\bullet,t}) = \beta_{\bullet}^{0,r} + \beta_{\bullet}^{t,r}t - \beta_{\bullet}^{e,r}e(t) + \beta_{\bullet}^{f,r}a(t), \tag{eqn A5}$$

where $a(t) = \sum_{w=1}^{W} f_c(w)C_{tw} + \varepsilon_t^f$ and $\beta_{\bullet}^{f,r}$ is a slope parameter. The remaining parameters are defined in equation 6 and details on fitting the model are the same as those provided in the main text. The adult twinning model is structurally the same as equation A5 so is not shown. Six knots were used for the spline. Weather variables were not included in the first axis of environmental variation (i.e. e is given by equation 3 in the main text).

Precipitation, wind speed, and monthly NAO did not appear to act on the second axis of environmental variation (Fig. A6). There was some evidence that increased temperatures over the spring and summer preceding the rut may increase fecundity (Fig. A6a). Higher temperatures over this period may increase vegetation growth, therefore increasing resource availability and the condition in which the ewes enter the rut. However cross validation (see equation 7) showed that including the temperature FLM did not improve the predictive performance of the base model ($\widehat{elpd} = -864.4$ for temperature model and $\widehat{elpd} = -863.9$ for base model).
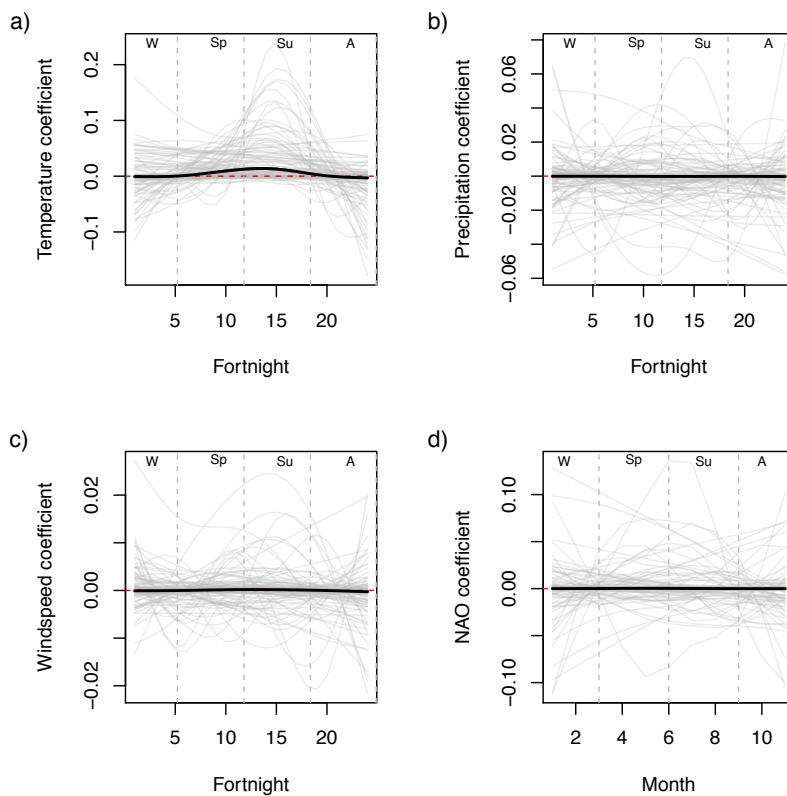
Figure A6: Functional linear models for the second axis of environmental variation with a) temperature, b) precipitation, c) wind speed, and d) NAO. Thick black lines show the posterior medians, thinner grey lines show 100 simulations from the posterior. The horizontal dashed red line is at 0. Dashed vertical lines and letters at the top of the plot indicate the seasons. Coefficients above the line indicate that higher values of the climatic covariate during that time period were associated with an increase in fecundity.

References

Coltman, D.W., Bancroft, D.R., Robertson, A., Smith, J.A., Clutton-Brock, T.H. & Pemberton, J.M. (1999) Male reproductive success in a promiscuous mammal: behavioural estimates compared with genetic paternity. *Molecular Ecology,* **8,** 1199-1209.

Ehrlen, J., Morris, W.F., von Euler, T. & Dahlgren, J.P. (2016) Advancing environmentally explicit structured population models of plants. *Journal of Ecology,* **104,** 292-305.

Grosbois, V., Gimenez, O., Gaillard, J.M., Pradel, R., Barbraud, C., Clobert, J., Moller, A.P. & Weimerskirch, H. (2008) Assessing the impact of climate variation on survival in vertebrate populations. *Biological Reviews,* **83,** 357-399.

Pemberton, J.M., Smith, J.A., Coulson, T.N., Marshall, T.C., Slate, J., Paterson, S., Albon, S.D. & CluttonBrock, T.H. (1996) The maintenance of genetic polymorphism in small island populations: Large mammals in the Hebrides. *Philosophical Transactions of the Royal Society of London Series B-Biological Sciences,* **351,** 745-752.

Stenseth, N.C. & Mysterud, A. (2005) Weather packages: finding the right scale and composition of climate in ecology. *Journal of Animal Ecology,* **74,** 1195-1198.

Chapter 5: Exploring temporal shifts in population dynamics in an age and sex structured population

Bethan J. Hindle[1*], Jill G.Pilkington[2], Josephine M.Pemberton[2] & Dylan Z. Childs[1]

[1] Department of Animal and Plant Sciences, Alfred Denny Building, University of Sheffield, Sheffield, UK

[2] Institute of Evolutionary Biology, School of Biological Sciences, University of Edinburgh, Edinburgh, UK

Abstract

1. Temporal shifts in population dynamics, such as the loss of population cycling, occur frequently. As the dynamical behaviour of a system can have important consequences for processes such as extinction, understanding the causes of such shifts is important for species management. This is challenging in natural populations, where the dynamics may be driven by complex interactions between intrinsic and extrinsic factors.

2. As vital rates typically vary according to individual state variables (e.g. age) structured population models are frequently used to explore population dynamics. Demographic rates are often temporally correlated, which may have significant impacts on population dynamics. By introducing latent variables to account for the covariation among the vital rates a demographic structural equation modelling (SEM) approach allows the joint responses of drivers on disparate vital rates to be explored.

3. The dynamics in a well-studied population of Soay sheep appear to have undergone a temporal shift, from unstable overcompensatory dynamics, with regular population crashes, to relatively stable population sizes. We explored possible causes of this shift using an age and sex structured matrix population model (MPM), parameterised using a demographic SEM.

4. A single axis of environmental variation explained the variation in population sizes in this population, providing a simple target for perturbation analyses. The MPM accurately predicted one-step ahead population sizes. However, despite incorporating a range of possible factors including density dependence, population structure, non-linearities in the demographic rates, environmental and demographic stochasticity, and temporal trends in the vital rates the MPM did not capture the observed dynamical behaviour. Simulated populations did not exhibit the period three cycling observed at the start of the study period, nor the observed shift in stability.

5. Population models are rarely validated based on their dynamical behaviour. Here, we have shown the importance of such validation, as a model with good one-step ahead predictive performance was unable to capture the dynamics of the system. Putative drivers not explored here that warrant further consideration include the role of parasites and asymmetric competition.

Introduction

The mechanisms driving population cycles have interested ecologists for decades (Kendall *et al.* 1999; Barraquand *et al.* 2017). Many putative drivers have been explored, such as host-enemy interactions (e.g. predators and parasites; Cattadori, Haydon & Hudson 2005; Vik *et al.* 2008) and overcompensatory intraspecific density dependence (Grenfell *et al.* 1992; Barraquand *et al.* 2014). Strict, consistent cycling is rare. Instead, temporal shifts in a population's dynamics are frequently observed. For example, many previously cycling populations in northern Europe, including mammals (Lindstrom & Hornfeldt 1994), birds (Ludwig *et al.* 2006), and insects (Esper *et al.* 2007), have collapsed to steady states in recent years (Ims, Henden & Killengreen 2008; Cornulier *et al.* 2013). Understanding the causes of temporal shifts in population dynamics is important for species and ecosystem management (Cornulier *et al.* 2013; Barraquand *et al.* 2017). The loss and gain of cyclical dynamics may have important consequences for population persistence, with smaller and more variable populations generally at higher risk of extinction (Inchausti & Halley 2003). Moreover, shifts in the dynamics of one species may have knock-on effects for interacting species and ecosystem processes (Ims & Fuglei 2005; Rydgren *et al.* 2007; Ecke *et al.* 2017). Identifying the drivers of dynamics in natural populations is challenging, as there may be complex interactions between intrinsic (e.g. density dependence and population structure) and extrinsic (e.g. climatic conditions, predator densities, and presence of parasites) factors (Bjornstad & Grenfell 2001; Coulson, Rohani & Pascual 2004; Radchuk, Ims & Andreassen 2016; Barraquand *et al.* 2017; Gamelon *et al.* 2017).

The mechanisms driving population dynamics have traditionally been identified using time series analyses, commonly using autoregressive models on logged population sizes (Grenfell *et al.* 1998; Coulson, Milner-Gulland & Clutton-Brock 2000; Bjornstad & Grenfell 2001). However, populations that differ in structure will exhibit different dynamics (Benton, Plaistow & Coulson 2006; Pelletier *et al.* 2012), even if the populations are the same initial size and subject to the same environmental conditions (Coulson *et al.* 2001; Benton & Beckerman 2005). At a local scale variation in population size is driven by temporal variation in vital rates, such as survival and reproduction. Population structure has important consequences for the dynamics, because the mean and variability of such rates typically differ according to individual state variables, such as age, sex, and size (Gaillard, Festa-Bianchet & Yoccoz 1998; Gaillard *et al.* 2000; Coulson *et al.* 2001). For example, the survival of prime aged individuals is generally higher and less temporally variable than that of juveniles or senescent individuals (Gaillard, Festa-Bianchet & Yoccoz 1998; Gaillard *et al.* 2000). Moreover, correlations between density and the proportion of individuals in different age classes can lead to spurious density effects being identified, if population structure is not taken into account (Festa-Bianchet, Gaillard & Cote 2003).

A recognition of the importance of population structure for dynamics has led to the widespread use of structured population models, such as matrix population models (MPMs;

Caswell 2001) and integral projection models (IPMs; Easterling, Ellner & Dixon 2000; Ellner, Childs & Rees 2016). Such models are constructed from longitudinal, individual-based data (Coulson 2012) and are typically structured by variables such as age (Pardo *et al.* 2017), stage (Menges & Quintana-Ascencio 2004), or size (Dahlgren, Bengtsson & Ehrlen 2016). Structured population models are frequently parameterised solely based on female demographic rates (though see e.g. Jenouvrier *et al.* 2010; Gerber & White 2014; Tsai *et al.* 2015), despite the widespread observation that the mean and variability of demographic rates frequently differ between the sexes (Owen-Smith 1993; Tavecchia *et al.* 2001; Clutton-Brock *et al.* 2002; Gaskin, Futerman & Chapman 2002; Toigo & Gaillard 2003). Single sex models may thus produce biased predictions of population dynamics, if the demographic rates are density dependent and differ between the sexes, or if male availability limits female reproduction (Mysterud, Coulson & Stenseth 2002; Rankin & Kokko 2007).

Whilst demographic rates frequently differ according to such individual state variables, such as age, size, and sex, it does not necessarily follow that they will respond independently to environmental change. Covariances among demographic processes are frequently observed in natural populations and may be driven by common environmental drivers across vital rates (Jongejans *et al.* 2010; Rotella *et al.* 2012) or due to tradeoffs between different vital rates (Koenig & Knops 1998). These covariances may have important implications for the stability and dynamics of the population (Coulson, Gaillard & Festa-Bianchet 2005). For example, positive or negative covariances typically increase or decrease the variability in population growth rate respectively. One of two approaches for parameterising stochastic structured population models, matrix selection, where stochasticity is introduced by resampling annual matrices or kernels (Rees & Ellner 2009), automatically preserves covariances. In an element selection approach, temporally variable parameters are sampled at each iteration from their estimated joint probability distributions (Rees & Ellner 2009; Vindenes *et al.* 2014). However, it is difficult to predict population responses to changes in the temporal co(variances) using matrix or traditional element selection methods.

An alternative approach is to parameterise a demographic structural equation model (SEM; Chapters 2 and 4). Here, one or more latent variable(s) are introduced to account for the covariation among the rates. Where demographic processes positively covary, as is often the case in natural populations (Nur & Sydeman 1999; Jongejans *et al.* 2010; Rotella *et al.* 2012), the latent variable can be conceived as a measure of environmental quality (Chapter 2). Variation in the latent variable may be decomposed into the effects of known drivers and residual variation (Chapters 2 and 4). Perturbing such drivers and the amount of residual variation allows the effect of such drivers and environmental stochasticity respectively on the population dynamics to be explored, whilst accounting for covariations among the demographic processes.
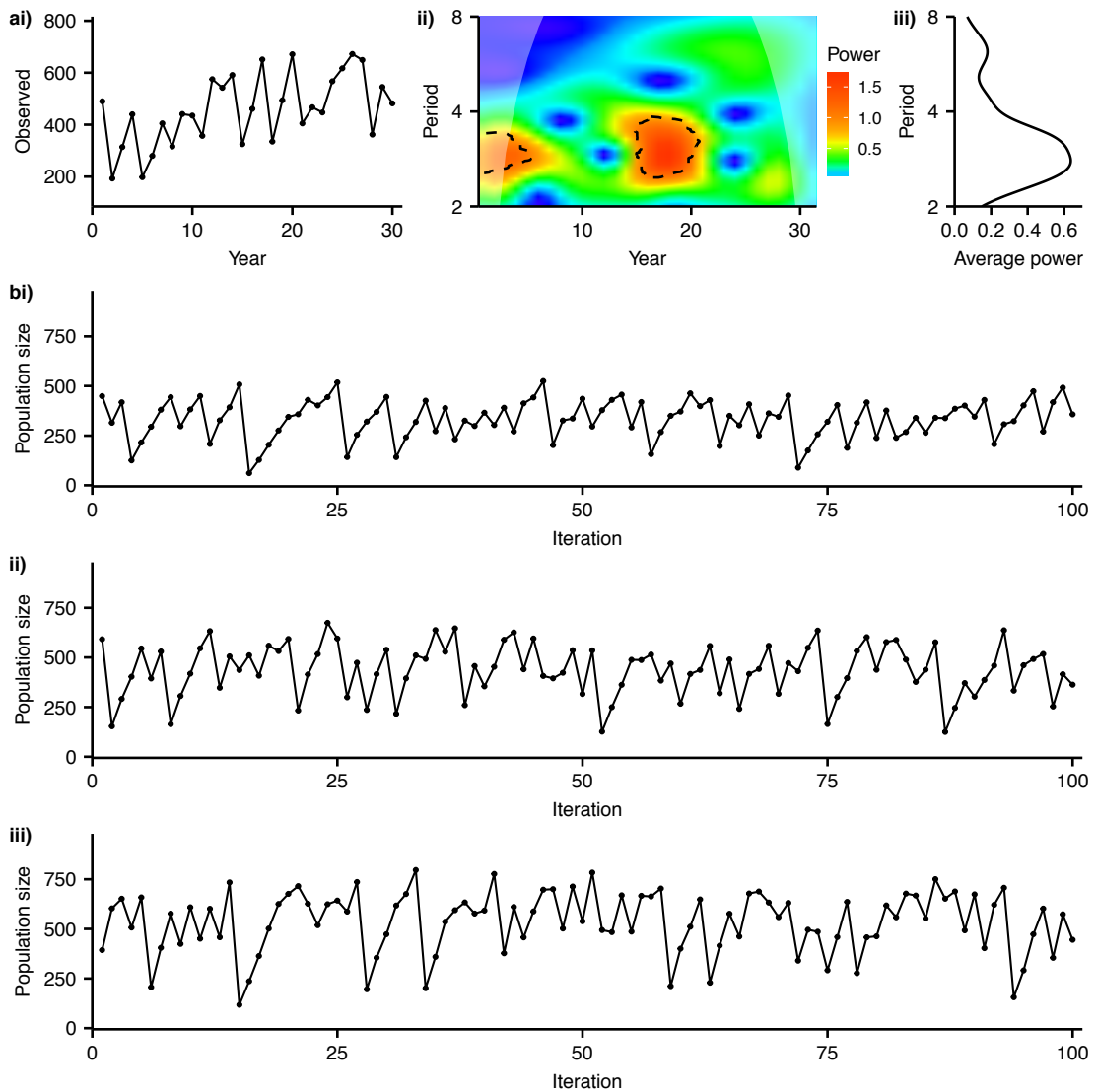
Figure 1: ai) Observed population sizes over the study period. ii) Wavelet power spectrum and iii) average wavelet power over the time series for the observed population sizes. In ii) dashed black lines denote significant periodicity (at the p<0.05 level, assessed using white noise simulation algorithms) and faded areas show the cone of influence, where edge effects may affect the reliability of the results. In ii) and iii) the y-axis is on a log scale. b) Simulated dynamics under the stochastic model for years at the i) start (t=1), ii) middle (t=15), and iii) end (t=30) of the study period.

The Soay sheep, *Ovis aries*, population on Hirta has been the subject of a detailed demographic study since 1985 (Clutton-Brock & Pemberton 2004). The first twenty years of the study period were characterised by unstable, overcompensatory population dynamics. The most frequent pattern during this period was two years of increasing population sizes followed by a crash, where population sizes decreased by up to 60% (Fig. 1; Clutton-Brock *et al.* 1991; Grenfell *et al.* 1992; Clutton-Brock *et al.* 1997; Coulson *et al.* 2008). Towards the end of the study period population sizes have appeared relatively stable however, with only one crash in the latter ten years (Fig. 1). Here, we consider the possible causes of this apparent shift in stability. We use a MPM, parameterised by a demographic SEM, to explore the population dynamics. As the Soay population has no large herbivorous competitors or adult predators the

demographic rates are largely driven by intraspecific density dependence and winter weather conditions (Chapter 4; Coulson *et al.* 2001). Population size has increased over the course of the study period (Coulson *et al.* 2008), due to a positive temporal trend in the survival of smaller sheep (Ozgul *et al.* 2009). Thus, we consider first whether the shift can be explained by temporal trends in the vital rates, using the deterministic backbone of the MPM to explore changes to the dynamics over the study period. We then explore the effects of variation on the dynamics by introducing both environmental and demographic stochasticity. As the vital rates differ between the sexes (Chapter 4; Coulson *et al.* 2001), resulting in fluctuations in the sex ratio (Stevenson & Bancroft 1995), we also consider whether males significantly impact population dynamics by comparing projected dynamics under single and two-sex models.
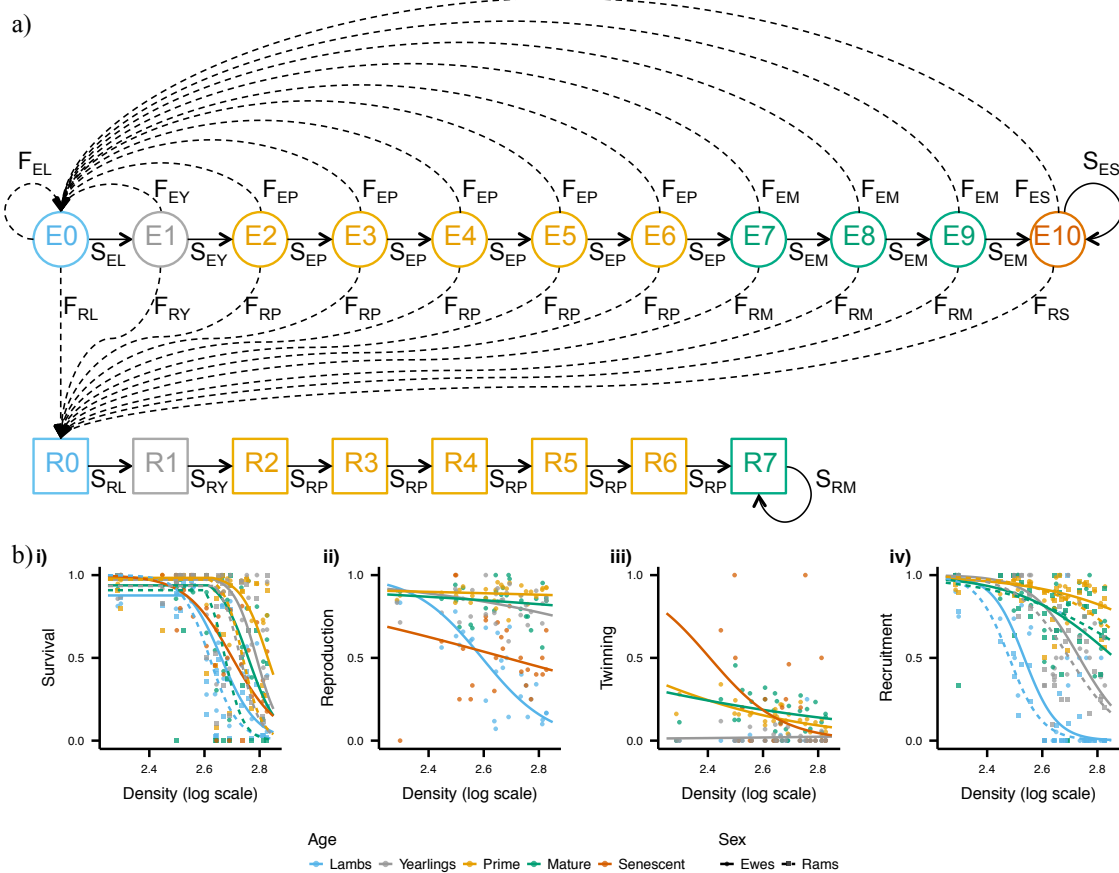

Figure 2: a) Structure of the two-sex age structured matrix population model (MPM). Squares represent rams (R) and circles are ewes (E). S_{sa} and F_{sa} are survival (solid lines) and fecundity (dashed lines) respectively for sex *s* and age *a*. Note that in the case of fecundity sex (*s*) refers to that of the newborn lamb, whilst age (*a*) is that of the mother. The fecundity functions are given by $F_{sa} = S_{Ea}R_{Ea}L_{sa}(0.5(1 - T_{Ea}) + T_{Ea}L_{sa} + T_{Ea}(1 - L_{sa}))$, where R_{Ea} and T_{Ea} are the probability of a ewe of age class *a* reproducing and twinning respectively. L_{sa} is the probability of a newborn lamb of sex *s*, and with a mother in age class *a*, surviving from its birth in spring until the summer census. The sex ratio at birth is assumed to be 1:1. All of the functions are temporally variable. Colour denotes age class and are given by the legend in Fig. 1b. b) Fitted sub-models for i) survival, ii) reproduction, iii) twinning, and iv) recruitment. Points show observed data. Lines show fitted models for the midyear of the study (*t*=15) and the random year effects at zero using the posterior medians.

5

Methods

Structure of the matrix population model

The study population is located in the Village Bay area of Hirta, in the St Kilda archipelago off the North-West coast of Scotland (Clutton-Brock & Pemberton 2004). Thirty years of demographic data (1985-2014) were used. During this period close to 100% of newborn lambs were tagged within days of birth. Population censuses were carried out three times a year (spring, summer, and autumn) and mortality searches ensured the fate of most individuals is known.

A matrix population model (MPM; Fig. 2a), structured by sex and age, was constructed to explore the population dynamics. The ewes were split into five age classes: lambs (0-1 years), yearlings (1-2 years), and prime (2-6 years), mature (7-9 years), and senescent adults (9< years). The same classes were used for rams, except all individuals over six years were grouped into a single (mature) class, as few rams survive above six. Male availability is unlikely to limit female reproduction, as males can sire multiple lambs in a single year (Pemberton *et al.* 1996; Coltman *et al.* 1999) and female reproduction in yearlings and adults is unrelated to relative male density. As such male reproduction was not included. Females of one year or older may produce twins (Clutton-Brock & Pemberton 2004). The vital rates were estimated using a demographic SEM (Chapters 2 and 4) with 26 sub-models: August (*t*) to August (*t+1*) survival of each age-sex class (9 sub-models, *s* superscript), spring reproduction of ewes in each age class (5 sub-models, *r* superscript), twinning of ewes aged at least one year old (4 sub-models, *t* superscript), and the spring-August recruitment of newborn lambs of each sex with mother in each age-class (8 sub-models, *l* superscript, as few lambs are born to older ewes mature and senescent ewes are categorised together here).

The demographic SEM had three environmental axes that drove the variation in the demographic rates (Fig. 3). The first axis (*e*) was included in all 26 sub-models and represents the decline in condition over winter, which in harsh years results in high overwinter mortality, reduced fecundity due to the higher mortality of reproducing individuals (Chapter 4), and lower recruitment due to the poor condition of surviving ewes in spring (Clutton-Brock *et al.* 1992). As the demographic rates in this population are strongly density dependent this primary axis was assumed to be a function of density (D_t; log total number of individuals in August of year *t*). To allow the effect of density to be modified by the environmental conditions the first axis was thus given by

$$e(t) = D_t - \alpha^t t - \varepsilon_t^e, \qquad\qquad (\text{eqn 1})$$

where $\alpha^t t$ is a temporal trend, accounting for the general increase in demographic rates seen over the study period (Coulson *et al.* 2008; Ozgul *et al.* 2009), and ε^e is a random year effect, accounting for any remaining covariation among the vital rates. A second axis (ε^f) accounts for remaining covariation amongst the fecundity models only (excluding yearling reproduction and twinning; see Chapter 4). A third axis (ε^l) was incorporated to account for the remaining

variation in recruitment; this axis is likely to be driven by variation in the abiotic environment during the spring lambing period.

Survival was estimated using threshold models (with the exception of ram lambs and senescent ewes, see below), as at low densities food is plentiful and the environmental conditions thus have little effect on survival (Fig. 2b; Chapter 4; Grenfell *et al.* 1998). The probability of survival was therefore given by

$$logit(S_{\bullet,t}) = \begin{cases} \beta_{\bullet}^{0,s} + \beta_{\bullet}^{t,s}t & \text{if } e(t) < \theta_{\bullet} \\ \beta_{\bullet}^{0,s} + \beta_{\bullet}^{t,s}t - \beta_{\bullet}^{e,s}(e(t) - \theta_{\bullet}) & \text{if } e(t) \geq \theta_{\bullet}, \end{cases} \qquad \text{(eqn 2)}$$

where $\beta_{\bullet}^{0,s}$ are intercepts, $\beta_{\bullet}^{t,s}$ and $\beta_{\bullet}^{e,s}$ are slopes for a temporal trend and the first environmental axis (e) respectively and $\theta_{\bullet}$ are threshold parameters. The $\bullet$ subscript indicates parameters that differ as a function of age-sex class. The temporal trends here ($\beta_{\bullet}^{t}t$) allow for trends in the mean of each demographic rate, whilst that in the first environmental axis ($\alpha^{t}t$) allows for an interaction between density and time across the rates (Chapter 4).

The reproduction, twinning, ram lamb survival, and senescent ewe survival models were estimated using simple logistic regressions as there was no evidence of thresholds in these models (Fig. 2b; Chapter 4). The probability of reproduction was given by

$$logit(R_{\bullet,t}) = \beta_{\bullet}^{0,r} + \beta_{\bullet}^{t,r}t - \beta_{\bullet}^{e,r}e(t) + \beta_{\bullet}^{f,r}\varepsilon_t^f, \qquad \text{(eqn 3)}$$

where ε_t^f is the second environmental axis and $\beta_{\bullet}^{f,r}$ is the slope term for this axis. The remaining parameters are defined as in the survival sub-models above (equation 2). The twinning and ram lamb and senescent ewe survival sub-models are not shown as they are structurally analogous to the reproduction sub-models (excluding the second environmental axis in the case of the survival sub-models). Note that the second environmental axis (ε_t^f) is not included in the yearling reproduction or yearling twinning models, as there was no evidence of unexplained variation in these processes (Chapter 4).

The probability of recruitment was estimated using a simple logistic regression (Fig. 2b) as follows:

$$logit(L_{\bullet,t}) = \beta_{\bullet}^{0,l} - \beta_{\bullet}^{e,l}e(t) + \beta_{\bullet}^{l,l}\varepsilon_t^l, \qquad \text{(eqn 4)}$$

where ε^l is the third environmental axis, sampled from a normal distribution, with mean zero and standard deviation σ^l, and $\beta_{\bullet}^{l,l}$ is the slope term for this axis. The remaining parameters are defined as above (equation two). Note that here the parameters differ according to the sex of the lamb and age class of the mother.

Markov Chain Monte Carlo (MCMC) simulation in JAGS (Plummer 2003), using the R (R Core Team 2016) package *runjags* (Denwood in review), was used to obtain parameter estimates. Weakly informative priors were used (Table S1). Three chains were burned in for 4×10^5 iterations, run for 2×10^6 iterations and thinned, keeping every 1,000[th] sample to give a total posterior sample of 6,000 iterations across the three chains. The posterior medians were used as parameter estimates in the following analyses.

We validated the model by comparing one-step ahead predictions of a) the vital rates for each age-sex class and b) the number of individuals in each age-sex class to the observed values. In both cases the demographic rates were estimated for each year using the observed density in year t, the observed year t, and the estimated values of the random year effects for each axis. The number of individuals (N) at $t + 1$ was then predicted as follows:

$$N_{t+1} = \mathbf{A}_t(N_t)\, N_t, \qquad\qquad\qquad\qquad \text{(eqn 5)}$$

where N_t is the observed vector of population sizes in year t and $\mathbf{A_t}$ is the matrix of transitions shown by Fig. 2a.
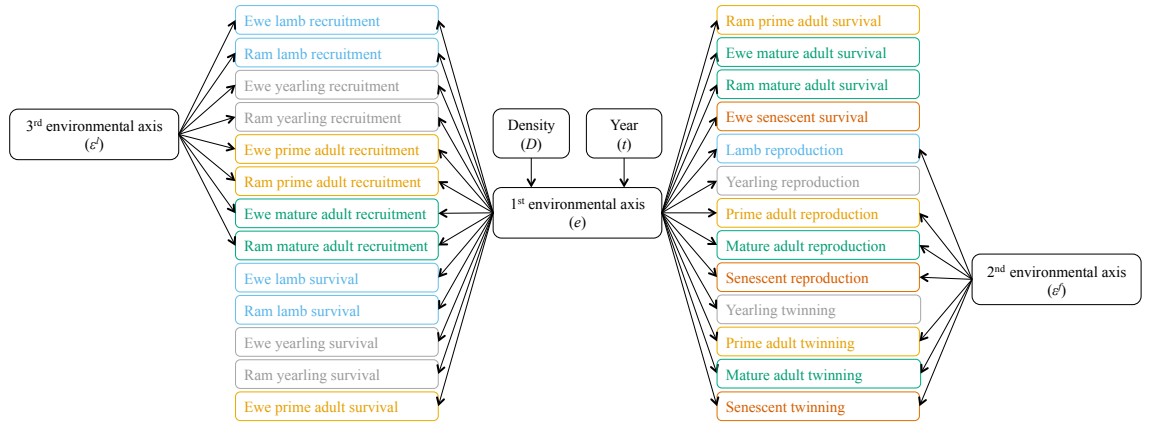

Figure 3: Path diagram for the two-axis model. Colours denote the age class and match those used in Fig. 2. The demographic rates are given by equations 1-4. The single-sex model is structurally analogous, excluding the ram age classes. In the case of recruitment the sex refers to that of the newborn lamb, whilst age is that of its mother.

Simulating model dynamics

First, we considered whether the deterministic model produces intrinsic population cycles and whether those dynamics change over the study period, according to the temporal trend (t). If improving conditions, represented in the model by the temporal trends ($\beta^t t$ and $\alpha^t t$), are responsible for the temporal shift in stability this would be captured by the deterministic model. Thus, we simulated populations (using equation 5) assuming no environmental stochasticity (i.e. by setting the latent variables, ε^e, ε^f, and ε^l, to zero) until the simulated population reached a steady state. This was repeated for each year of the study (i.e. $t = 1, 2, 3, \dots, 30$) and the steady states were compared across the study period. To compare the dynamical behaviour of the stochastic model to that observed, populations were simulated for 100 years, following a 500-year run-in period. At each year of the simulation the latent variables were sampled from their estimated distributions. This was repeated three times, fixing the temporal trend variable to t=1, t=15, and t=30, and the simulated population sizes were compared to those observed.

Next, we explored how increasing environmental variability affected population stability. 1,000 populations were simulated for 500 years, starting at the equilibrium population size. At each iteration the random year effect (ε^e) for the first environmental axis was sampled from a normal distribution with mean of zero and a standard deviation that increased linearly

across the 500-year simulation from zero to double that estimated in the model ($\sigma^e = 2\overline{\sigma^e}$, where $\overline{\sigma^e}$ is the value estimated from the observed data). Here, we only considered variation in the first environmental axis (e), as this explains the majority of the variation in the vital rates; the second (ε^f) and third environmental axes (ε^l) were set to zero (see Appendix A1 for the effects of perturbing the other axes). Additionally, we only considered the effects of environmental stochasticity (see Appendix A2 for effects of demographic stochasticity). This was carried out for a year at the beginning and end of the study period ($t = 1$ and 30 respectively). Two measures of persistence were calculated; the mean population size and the coefficient of variation (CV). To explore how the different demographic processes were affected by increasing levels of environmental variation each rate was predicted at each of the 500 time steps, setting D (equation 1) to the mean total density estimated during the above simulations for that time step, and sampling the random year effect for the first environmental axis (ε^e) 1,000 times, from the distribution used for each time step above (i.e. increasing σ^e linearly across the 500 time steps).

Sex-differences

We then constructed a one-sex MPM that was structurally analogous to the two-sex model, without the ram classes (Fig. 2a). It was parameterised using a demographic SEM with three environmental axes (equations 1-4; Fig. 3). The log of the total number of ewes was used as the measure of density (D; equation 1). The above analyses were repeated using the single sex model and the estimates of population size were compared to those produced by the two sex model.

Wavelet analyses

We used wavelet analyses (Torrence & Compo 1998; Cazelles *et al.* 2008) to determine whether there was evidence of population cycles in the dynamics simulated using the MPM, whether these corresponded to the periodicity of those observed, and whether either the temporal trends or the degree of environmental variation affected the presence or period of the cycles. We conducted wavelet analyses with the Morlet wavelet (Grenfell, Bjornstad & Kappey 2001; Kausrud *et al.* 2008), using the R package *WaveletComp* (Roesch & Harald 2014). We applied the wavelet analysis first to the observed time series of total population sizes. The temporal trend in the observed time series was removed using local polynomial regression (Roesch & Harald 2014) and population size was standardised to have zero mean and unit variance (Grenfell, Bjornstad & Kappey 2001).

We then used the MPM to simulate nine populations (using equation 5), with every pairwise combination of a) low ($\sigma^e = 0.5\overline{\sigma^e}$), medium ($\sigma^e = \overline{\sigma^e}$), and high ($\sigma^e = 2\overline{\sigma^e}$) environmental variation and b) setting the temporal trend variable (t) to 1, 15, and 30. Each population was simulated for 100,000 years, following a 1,000 year run in period. At each year

of each simulation the random year effect in the first environmental axis was sampled from a normal distribution with the respective standard deviations given above. The second and third environmental axes were set to zero as these axes had little effect on the population dynamics (Appendix A1). Wavelet analyses were carried out as above for each of the nine simulated time series of total population size.
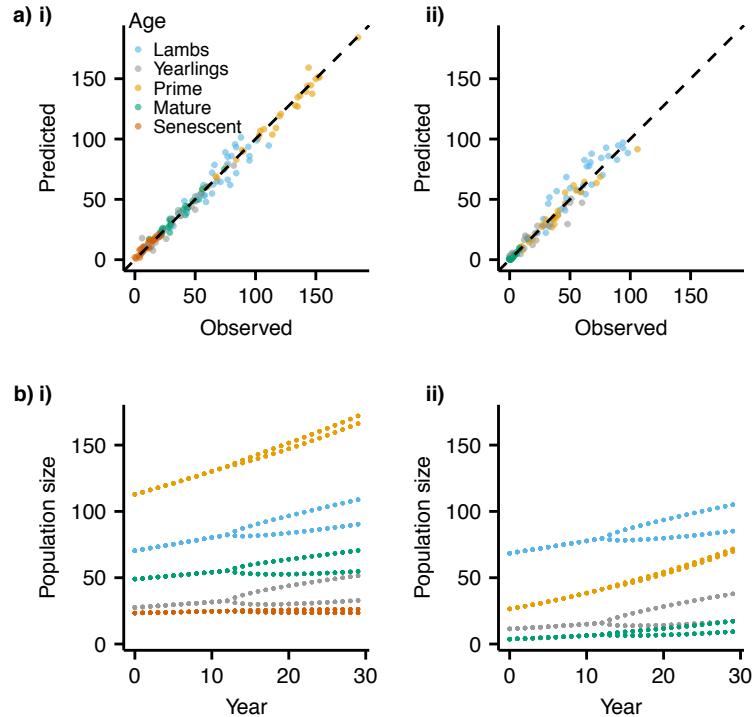

Figure 4: a) Observed and predicted population sizes for each age class for i) ewes and ii) rams. Predictions are made using the observed density at *t* and the estimated random year effects for each year. Dashed line is at 1:1, where predicted values are equal to those observed. The slight overprediction in the number of ram lambs may be explained by yearly deviations in the sex ratio of newborns (assumed to be 1:1 here; see Fig. S3). b) Steady states predicted by simulating using the deterministic MPM. i) and ii) show the number of ewes and rams respectively in each age class.

Results

The observed vital rates (Fig. S1) and population sizes (Fig. 4a) for each age-sex class were well predicted by the model (Fig. 4a), suggesting three axes of environmental variation were sufficient to capture the variation in survival, fecundity, and recruitment across the lifecycle. The first environmental axis drove most of the variation in the vital rates (Fig. S2; Chapter 4), with the 95% confidence intervals of the slope terms only overlapping zero for five of the 26 sub-models.

Equilibrium population sizes were predicted to increase over the study period (Fig. 4b), as observed (Fig. 1ai). However, unlike in the observed population, the degree of instability appeared to increase over the study period, with the deterministic model undergoing a period doubling bifurcation at year thirteen (Fig. 4b). The deterministic model also predicted a change the population structure over time, with the number of prime rams increasing more rapidly than the number of prime ewes (Fig. 4b).

Environmentally stochastic simulations produced population sizes in a similar range to those observed and exhibited large population crashes (Fig. 1b) similar to those seen in the observed dynamics (Fig. 1ai). However, the simulations show more successive years of population increase than are observed in the population. Whilst observed crashes typically occurred after 2 years of population increase (Fig. 1a), the simulated populations undergo 4-5 years of successive population increase (Fig. 1b). The simulated populations showed no evidence of an increase in stability over the study period, with larger crashes observed under higher values of the temporal trend effect, t (Fig. 1b). Incorporating demographic stochasticity into the model had little effect on the simulations of population dynamics (Appendix A2).
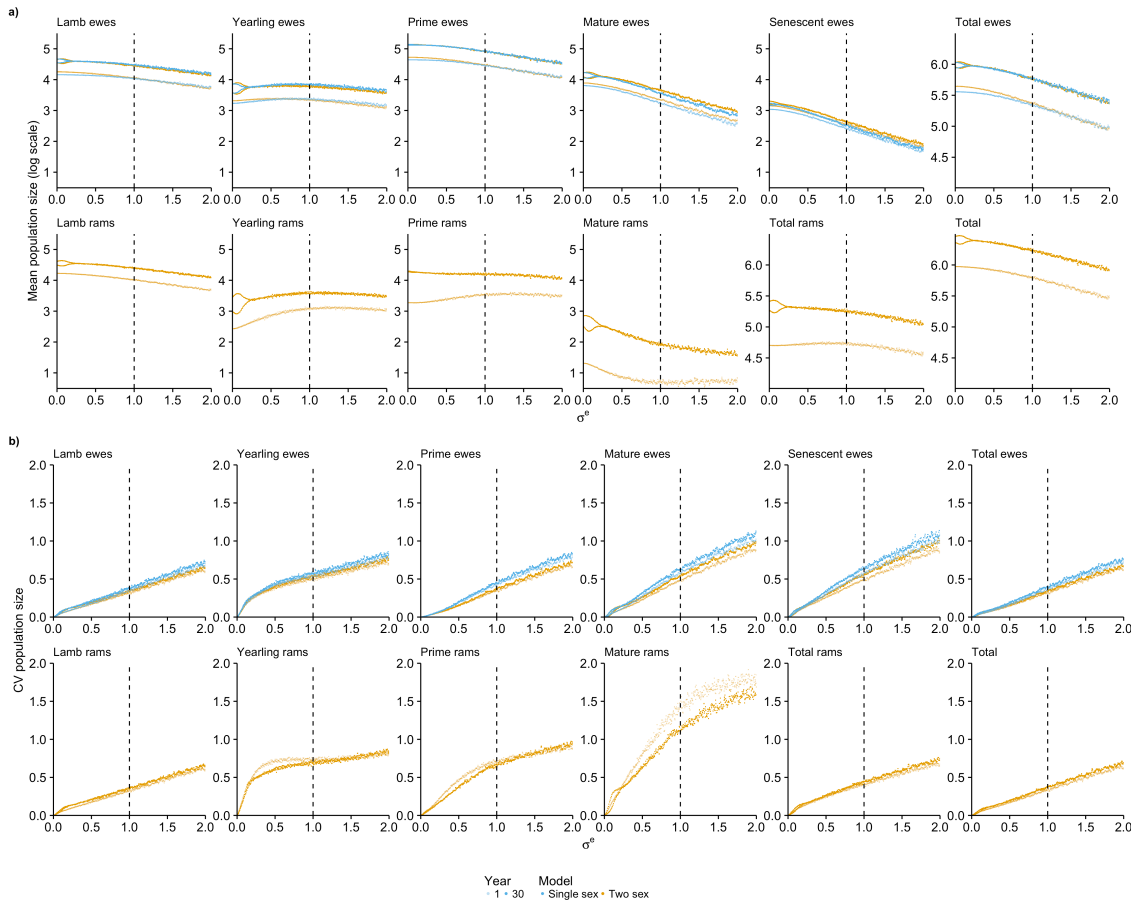

Figure 5: a) Mean and b) coefficient of variation (CV) for the number of individuals in each age-sex class, from 1,000 simulations over 500 years. The degree of variation in the first axis of environmental variation was increased linearly from zero to twice that estimated in the model. Simulations are shown from a year at the start ($t = 1$; transparent points) and the end ($t = 30$; opaque points) of the study period. Note that the y-axis scales in a) differ between the total sub-plots and the separate age-sex class sub-plots. The vertical dashed line indicates where the variability in the first environmental axis is equal to that estimated in the model.

Increasing the level of environmental stochasticity in the model generally decreased population sizes (Fig. 5a). However, the effects differed among age-sex classes, resulting in differences in the projected population structure. Noticeably, at low levels of environmental variation, the number of yearlings of both sexes actually increased with increasing environmental variation (Fig. 5a). Populations are generally larger and slightly more variable

11

towards the end of the study period (Fig. 5). These responses to increasing the degree of environmental variation differ little over the study period (Fig. 5).
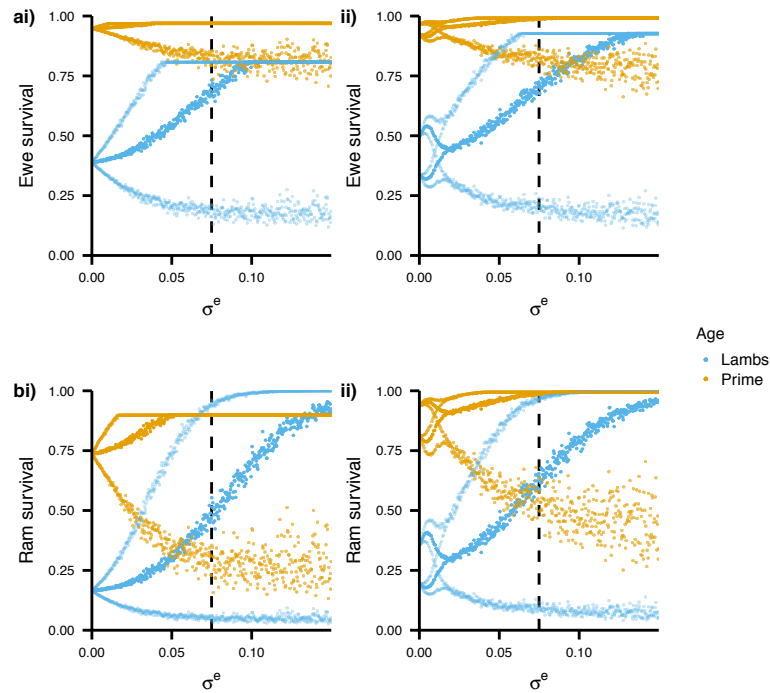

Figure 6: Predicted lamb and prime adult survival under increasing levels of environmental variation for a) ewes and b) rams in the i) first ($t = 1$) and last ($t = 30$) years of the study period. Plots show the median and 95% quantiles (faded points) for each demographic rate. Each demographic rate is estimated 1,000 times using the mean density at that timestep from fig. 5 and sampling the random year effect for the first environmental axis from a normal distribution, where the standard deviation increases linearly from zero to twice that estimates in the model over the 500 time steps. See Fig. S4 for the remaining demographic rates. The vertical dashed line indicates where the variability in the first environmental axis is equal to that estimated in the model.

As the degree of environmental variation increases the average total population sizes decrease (Fig. 5a), resulting in an increase in the average demographic rates (Figs 6 and S4). Nonlinearities in the relationship between the first environmental axis and each demographic process mean that the distribution of, for example, survival probabilities at a specific population density may be skewed (Figs 6 and S4). Survival of lambs is particularly sensitive to the environmental conditions (Figs 2b and 6). For example, at low levels of environmental variation ram lamb survival is positively skewed (Fig. 6bi), thus increasing the degree of environmental variation generally increases survival. This results in the initial increase in the number of yearlings (Fig. 5a). As the average ram lamb survival increases over the time series, due to the decrease in total density, it becomes negatively skewed and increasing the degree of environmental variation causes an overall decrease in survival. Conversely prime adult survival quickly reaches its threshold value and is negatively skewed. Increasing the degree of environmental variation increases the degree of negative skew, causing a general decrease in survival (Fig. 6). As the temporal trend effect (t) increases the demographic rates increase, but

there is little difference in the pattern in how they respond to increasing environmental variation (Fig. 6).

Despite survival differing between the sexes, with for example ram survival generally lower and more temporally variable than ewe survival (Fig. 2b) there was little difference in the simulated population dynamics under the single and two sex models (Fig. 5). Moreover, increasing the level of stochasticity in all three environmental axes simultaneously produces very similar dynamics to only perturbing the first environmental axis (Appendix A1). Thus suggesting that the population dynamics are effectively driven by the reduction in the condition of ewes overwinter.
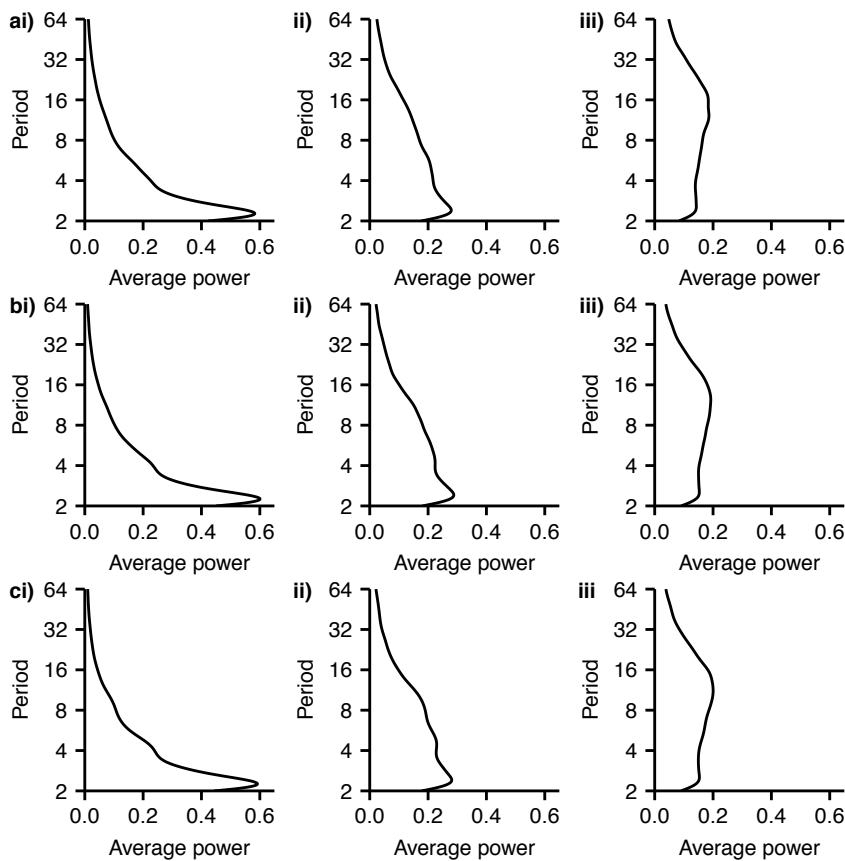

Figure 7: Average wavelet power for simulated population sizes with the year of study increasing from top to bottom (a) $t = 1$, b) $t = 15$, c) $t = 30$) and the amount of variation in the first environmental axis increasing from left to right ($\sigma^e =$ i) $0.5\overline{\sigma^e}$, ii) $\overline{\sigma^e}$, iii) $2\overline{\sigma^e}$). For each plot a population is simulated for 100,000 years and the wavelet power is averaged across the time series. Note that the y-axis is on a log scale. See Fig. 1b for examples of the simulated population dynamics for each year under the observed level of environmental variation (i.e. $\sigma^e = \overline{\sigma^e}$).

The wavelet analysis on the observed time series shows clear evidence of 3-year periodicity (Fig. 1aiii), though the cycles are not constant over time, with cycling regimes observed in the years 1-7 and 15-20. There is little evidence of any cycling in the last ten years of the time series (Fig. 1aii). There was no evidence of periodic regimes of three or more years in any of the model simulations (Figs 1b and 7). With low levels of environmental variation there was evidence of cycling with a periodicity just over two, but this is lost as the degree of

environmental variation increases (Fig. 7). The temporal trend had little effect on the periodicity of population size (Fig. 7).

Discussion

Using a demographic SEM to parameterise an age and sex structured MPM, we have demonstrated that a single axis of environmental variation drives most of the variation in population sizes in a population of Soay sheep. Our model effectively captures the different responses of each sex-age class to increasing environmental variation. However, simulations showed that, while it has very good short term predictive performance, the MPM fails to capture the observed dynamical behaviour of the study system. Neither deterministic nor stochastic simulated populations exhibited the period three cycling observed at the start of the study period, or the apparent shift in stability towards the end of the study period.

The demographic SEM approach demonstrates that the environment may be of considerably lower dimension than is typically assumed. Three axes of environmental variation were sufficient to explain the variation in survival, fecundity, and recruitment across nine age-sex classes. Moreover, the first axis is sufficient to explain short-term variation in population size. In the Soay population, the first environmental axis captures variation in body condition over the winter period, which results in higher mean mortality, selective mortality of reproductive individuals (Chapter 4), and lower recruitment among the offspring of surviving ewes (Clutton-Brock *et al.* 1992). Thus, even demographic processes that occur at different time periods may be governed by the same environmental axis. For example, newborn lamb survival to the summer is negatively correlated with overwinter mortality, presumably as a result of reduced body condition of ewes following high mortality winter periods. A similar effect has been seen in other herbivores. For example, in reindeer the overwinter condition of the females is more important than the abiotic spring conditions for early offspring survival (Veiberg *et al.* 2017).

A combination of intrinsic and extrinsic factors can drive shifts in dynamical behaviour (Barraquand *et al.* 2017). Many previous studies have considered the drivers of demographic variation and population dynamics in the Soay population (Clutton-Brock *et al.* 1991; Clutton-Brock *et al.* 1992; Grenfell *et al.* 1992; Milner, Elston & Albon 1999; Catchpole *et al.* 2000; Coulson *et al.* 2001; Stenseth *et al.* 2004; Berryman & Lima 2006; Hone & Clutton-Brock 2007; Coulson *et al.* 2008). These have demonstrated that the demographic rates exhibit strong intra-specific density dependence, with high densities combined with harsh abiotic conditions resulting in large population crashes (Chapter 4; Coulson, Milner-Gulland & Clutton-Brock 2000; Coulson *et al.* 2001; Coulson *et al.* 2008). The relationship between density and the demographic rates is thought to be nonlinear, with little effect at low densities as food is plentiful (Grenfell *et al.* 1998; Stenseth *et al.* 2004). As the demographic rates vary across age classes in the Soay sheep incorporating age structure increases the amount of variation in population size explained by a population model (Coulson *et al.* 2001; Coulson *et al.* 2008).

Increases in survival over the study period, the cause of which is unknown, have resulted in an increase in population sizes over time (Berryman & Lima 2006). However, these effects (age structure, nonlinear effects of density dependence, a temporal trend in the demographic rates, and interactions between density and the abiotic environmental conditions) were not sufficient to capture the observed dynamical behaviour of this study system.

The MPM had a high one-step ahead predictive performance. However, neither the deterministic nor stochastic simulations could replicate the observed dynamical behaviour. Simulations using a previous age structured model showed similar behaviour to that predicted here (Coulson *et al.* 2001). The performance of population models is often validated using measures such as the proportion of explained variation in population size, population growth rate, and/or size or age distributions (Coulson *et al.* 2008; Dahlgren & Ehrlen 2009; Simmonds & Coulson 2015). Such measures have clear limitations. Coulson et al. (2008) show that a population model with a high r^2 (0.85; Berryman & Lima 2006) uses a functional form for density dependence that is inconsistent with demographic data. Comparisons between the observed dynamical behaviour and that predicted by a population model are used to validate model performance relatively rarely, and often only when the initial aim of parameterising the model is to explain specific dynamical behaviour, such as population cycles (e.g. Williams *et al.* 2004; Radchuk, Ims & Andreassen 2016). The dynamical behaviour of a system has important consequences for processes such as extinction (Inchausti & Halley 2003). Thus we suggest that population models should more widely be validated based on their dynamical behaviour, before for example, being used to predict future population dynamics or extinction risk.

Demographic stochasticity arises from the stochastic nature of birth and death processes in finite populations (Engen, Bakke & Islam 1998). Failing to account for demographic stochasticity can result in an underestimation of extinction risk and population instability, particularly in small populations (Benson *et al.* 2016; White *et al.* 2017). The size of the Soay sheep population has increased by about 60% over the study period, reducing the role of demographic stochasticity in the population. In principle, a combination of improving conditions and the reduced impact of demographic stochasticity might have been responsible for the observed shift in dynamics. However, demographic stochasticity had little effect on the simulated dynamics in this population, suggesting that even at the beginning of the study period population sizes were sufficiently large for demographic stochasticity to have little effect on the dynamics.

Demographic rates are strongly positively correlated in this population, though the mean and variance of these rates differ among age-sex classes (Coulson *et al.* 2001). Thus, shifting environmental conditions lead to changes to population structure. Such changes are common in natural populations. For example in a population of black-browed albatross, *Thalassarche melanophris,* climate change is causing the population to be increasingly dominated by young individuals (Pardo *et al.* 2017). In a population of reindeer, *Rangifer*

tarandus, the sex ratio has become increasing female biased as male survival is more strongly affected by increasing winter precipitation (Peeters *et al.* 2017). Our model suggests that, in the Soay population, improving environmental conditions are leading to a less female-biased sex ratio among adults. Our perturbation analysis indicates that increasing environmental variation has a similar effect. Changes to population structure may have important consequences (Schmickl & Karsai 2010; Hultine *et al.* 2016; Petry *et al.* 2016). For example, increasingly male biased sex ratios might increase male aggression towards females or increase competition for food, leading to decreased female survival (Mysterud, Coulson & Stenseth 2002; Le Galliard *et al.* 2005; Rankin & Kokko 2007).

In the Soay population, including males had little effect on the predicted population dynamics and thus did not help to explain the observed dynamical behaviour. Whether variation in individual vital rates is driven by variation in the total population size or a particular subset of the population depends on whether resource use and spatial distributions differ according to individual state variables such as sex (Mysterud, Coulson & Stenseth 2002). Yet many studies fail to justify their choice of measure of density (Mysterud, Coulson & Stenseth 2002). As the Soays compete over the same food sources and the sexes are not spatially segregated, it seems likely that the total number of individuals in the population is a reasonable proxy for the competitive environment experienced by individuals of every class. However, the strong correlation between the number of rams and ewes ($r^2 = 0.86$) and the ewe biased sex ratio means that ewe vital rates are well explained by the density of ewes alone and projections of total population size follow the trajectory of female population size. The ability of a single male to fertilise multiple females in this population (Pemberton *et al.* 1996; Coltman *et al.* 1999) also contributes to the lack of importance of males in this population, as they do not appear to limit female reproduction.

However, we used a simplistic measure of density (total population size), which assumes the effect each individual has on its conspecifics is the same regardless of whether the individual is a lamb or an adult ram. In reality, the effect that an individual has on its conspecifics is likely to differ according to individual state variables such as age and size (Gamelon *et al.* 2016), as larger individuals are expected to have greater energy requirements and therefore use more resources (Peters 1983). Recently developed methods allow asymmetric interactions to be incorporated into structured population models, allowing the effect an individual has on its conspecifics to vary according to state variables such as size (Bassar *et al.* 2016). The assumption that each individual had the same effect on its conspecifics may be one reason for the failure of the model to capture the observed dynamics.

Interspecific interactions are important drivers of unstable population dynamics (Cattadori, Haydon & Hudson 2005; Vik *et al.* 2008). However, plant-herbivore dynamics are generally thought to be insufficient to drive population cycles, due to a lack of overcompensatory or time-delayed feedback (Reynolds *et al.* 2012). The biomass of grass in

August on Hirta is correlated with current population density and not with density over the previous winter (Clutton-Brock & Pemberton 2004), which suggests the absence of delayed density dependence. However, there is the possibility of more subtle interactions between herbivores and vegetation. For example delayed herbivore induced defences (Hartley & DeGabriel 2016) or transient changes in community composition may be sufficient to destabilise population dynamics (Reynolds *et al.* 2012). We have also not considered the role of parasites, which have been found to be important drivers of population cycles in other herbivores (Townsend *et al.* 2011). Strongyle nematodes are thought to compound the effects of low food availability in the Soay population, contributing to overwinter mortality rates (Gulland 1992; Gulland *et al.* 1993; Milner, Elston & Albon 1999). Thus temporal variation in parasite loads (Hance *et al.* 2007; Molnar, Dobson & Kutz 2013) is another putative driver of the dynamics of the Soay population that warrants further consideration.

By constructing a structured population model, parameterised with a demographic SEM, we were able to demonstrate that most variation in population size is driven by a single environmental axis in the Soay sheep population. Though our model predicted one-step ahead population sizes well, it failed to reproduce the 3-year population cycles observed early in the study, or to provide an explanation for the apparent shift from unstable, overcompensatory dynamics to a relatively stable regime. These results emphasise the need to evaluate the full dynamical behaviour of population models when validating their predictive performance.

Acknowledgements

References
Barraquand, F., Louca, S., Abbott, K.C., Cobbold, C.A., Cordoleani, F., DeAngelis, D.L., Elderd, B.D., Fox, J.W., Greenwood, P., Hilker, F.M., Murray, D.L., Stieha, C.R., Taylor, R.A., Vitense, K., Wolkowicz, G.S.K. & Tyson, R.C. (2017) Moving forward in circles: challenges and opportunities in modelling population cycles. *Ecology Letters,* **20,** 1074-1092.
Barraquand, F., Pinot, A., Yoccoz, N.G. & Bretagnolle, V. (2014) Overcompensation and phase effects in a cyclic common vole population: between first and second-order cycles. *Journal of Animal Ecology,* **83,** 1367-1378.
Bassar, R.D., Childs, D.Z., Rees, M., Tuljapurkar, S., Reznick, D.N. & Coulson, T. (2016) The effects of asymmetric competition on the life history of Trinidadian guppies. *Ecology Letters,* **19,** 268-278.

Benson, J.F., Mahoney, P.J., Sikich, J.A., Serieys, L.E.K., Pollinger, J.P., Ernest, H.B. & Riley, S.P.D. (2016) Interactions between demography, genetics, and landscape connectivity increase extinction probability for a small population of large carnivores in a major metropolitan area. *Proceedings of the Royal Society B-Biological Sciences,* **283,** 10.

Benton, T.G. & Beckerman, A.P. (2005) Population dynamics in a noisy world: Lessons from a mite experimental system. *Advances in Ecological Research, Vol. 37: Population Dynamics and Laboratory Ecology,* **37,** 143-181.

Benton, T.G., Plaistow, S.J. & Coulson, T.N. (2006) Complex population dynamics and complex causation: devils, details and demography. *Proceedings of the Royal Society B-Biological Sciences,* **273,** 1173-1181.

Berryman, A. & Lima, M. (2006) Deciphering the effects of climate on animal populations: Diagnostic analysis provides new interpretation of soay sheep dynamics. *American Naturalist,* **168,** 784-795.

Bjornstad, O.N. & Grenfell, B.T. (2001) Noisy clockwork: Time series analysis of population fluctuations in animals. *Science,* **293,** 638-643.

Caswell, H. (2001) Matrix population models: Construction, analysis, and interpretation. *Matrix population models: Construction, analysis, and interpretation*, i-xxii, 1-722.

Catchpole, E.A., Morgan, B.J.T., Coulson, T.N., Freeman, S.N. & Albon, S.D. (2000) Factors influencing Soay sheep survival. *Journal of the Royal Statistical Society Series C-Applied Statistics,* **49,** 453-472.

Cattadori, I.M., Haydon, D.T. & Hudson, P.J. (2005) Parasites and climate synchronize red grouse populations. *Nature,* **433,** 737-741.

Cazelles, B., Chavez, M., Berteaux, D., Menard, F., Vik, J.O., Jenouvrier, S. & Stenseth, N.C. (2008) Wavelet analysis of ecological time series. *Oecologia,* **156,** 287-304.

Clutton-Brock, T.H., Coulson, T.N., Milner-Gulland, E.J., Thomson, D. & Armstrong, H.M. (2002) Sex differences in emigration and mortality affect optimal management of deer populations. *Nature,* **415,** 633-637.

Clutton-Brock, T.H., Illius, A.W., Wilson, K., Grenfell, B.T., MacColl, A.D.C. & Albon, S.D. (1997) Stability and instability in ungulate populations: An empirical analysis. *American Naturalist,* **149,** 195-219.

Clutton-Brock, T.H. & Pemberton, J.M. (2004) *Soay Sheep: Dynamics and Selection in an Island Population*.

Clutton-Brock, T.H., Price, O.F., Albon, S.D. & Jewell, P.A. (1991) Persistent instability and population regulation in soay sheep. *Journal of Animal Ecology,* **60,** 593-608.

Clutton-Brock, T.H., Price, O.F., Albon, S.D. & Jewell, P.A. (1992) Early development and population fluctuations in soay sheep. *Journal of Animal Ecology,* **61,** 381-396.

Coltman, D.W., Bancroft, D.R., Robertson, A., Smith, J.A., Clutton-Brock, T.H. & Pemberton, J.M. (1999) Male reproductive success in a promiscuous mammal: behavioural estimates compared with genetic paternity. *Molecular Ecology,* **8,** 1199-1209.

Cornulier, T., Yoccoz, N.G., Bretagnolle, V., Brommer, J.E., Butet, A., Ecke, F., Elston, D.A., Framstad, E., Henttonen, H., Hornfeldt, B., Huitu, O., Imholt, C., Ims, R.A., Jacob, J., Jedrzejewska, B., Millon, A., Petty, S.J., Pietiainen, H., Tkadlec, E., Zub, K. & Lambin, X. (2013) Europe-Wide Dampening of Population Cycles in Keystone Herbivores. *Science,* **340,** 63-66.

Coulson, T. (2012) Integral projections models, their construction and use in posing hypotheses in ecology. *Oikos,* **121,** 1337-1350.

Coulson, T., Catchpole, E.A., Albon, S.D., Morgan, B.J.T., Pemberton, J.M., Clutton-Brock, T.H., Crawley, M.J. & Grenfell, B.T. (2001) Age, sex, density, winter weather, and population crashes in Soay sheep. *Science,* **292,** 1528-1531.

Coulson, T., Ezard, T.H.G., Pelletier, F., Tavecchia, G., Stenseth, N.C., Childs, D.Z., Pilkington, J.G., Pemberton, J.M., Kruuk, L.E.B., Clutton-Brock, T.H. & Crawley, M.J. (2008) Estimating the functional form for the density dependence from life history data. *Ecology,* **89,** 1661-1674.

Coulson, T., Gaillard, J.M. & Festa-Bianchet, M. (2005) Decomposing the variation in population growth into contributions from multiple demographic rates. *Journal of Animal Ecology,* **74,** 789-801.

Coulson, T., Milner-Gulland, E.J. & Clutton-Brock, T. (2000) The relative roles of density and climatic variation on population dynamics and fecundity rates in three contrasting ungulate species. *Proceedings of the Royal Society B-Biological Sciences,* **267,** 1771-1779.

Coulson, T., Rohani, P. & Pascual, M. (2004) Skeletons, noise and population growth: the end of an old debate? *Trends in Ecology & Evolution,* **19,** 359-364.

Dahlgren, J.P., Bengtsson, K. & Ehrlen, J. (2016) The demography of climate-driven and density-regulated population dynamics in a perennial plant. *Ecology,* **97,** 899-907.

Dahlgren, J.P. & Ehrlen, J. (2009) Linking environmental variation to population dynamics of a forest herb. *Journal of Ecology,* **97,** 666-674.

Denwood, M.J. (in review) runjags: An R package providing interface utilities, parallel computing methods and additional distributions for MCMC models in JAGS. *Journal of Statistical Software*.

Easterling, M.R., Ellner, S.P. & Dixon, P.M. (2000) Size-specific sensitivity: Applying a new structured population model. *Ecology,* **81,** 694-708.

Ecke, F., Angeler, D.G., Magnusson, M., Khalil, H. & Hornfeldt, B. (2017) Dampening of population cycles in voles affects small mammal community structure, decreases diversity, and increases prevalence of a zoonotic disease. *Ecology and Evolution,* **7,** 5331-5342.

Ellner, S.P., Childs, D.Z. & Rees, M. (2016) *Data-driven modelling of structured populations: A practical guide to the Integral Projection Model*. Springer, Switzerland.

Engen, S., Bakke, O. & Islam, A. (1998) Demographic and environmental stochasticity - Concepts and definitions. *Biometrics,* **54,** 840-846.

Esper, J., Buntgen, U., Frank, D.C., Nievergelt, D. & Liebhold, A. (2007) 1200 years of regular outbreaks in alpine insects. *Proceedings of the Royal Society B-Biological Sciences,* **274,** 671-679.

Festa-Bianchet, M., Gaillard, J.M. & Cote, S.D. (2003) Variable age structure and apparent density dependence in survival of adult ungulates. *Journal of Animal Ecology,* **72,** 640-649.

Gaillard, J.M., Festa-Bianchet, M. & Yoccoz, N.G. (1998) Population dynamics of large herbivores: variable recruitment with constant adult survival. *Trends in Ecology & Evolution,* **13,** 58-63.

Gaillard, J.M., Festa-Bianchet, M., Yoccoz, N.G., Loison, A. & Toigo, C. (2000) Temporal variation in fitness components and population dynamics of large herbivores. *Annual Review of Ecology and Systematics,* **31,** 367-393.

Gamelon, M., Grotan, V., Engen, S., Bjorkvoll, E., Visser, M.E. & Saether, B.E. (2016) Density dependence in an age-structured population of great tits: identifying the critical age classes. *Ecology,* **97,** 2479-2490.

Gamelon, M., Grotan, V., Nilsson, A.L.K., Engen, S., Hurrell, J.W., Jerstad, K., Phillips, A.S., Rostad, O.W., Slagsvold, T., Walseng, B., Stenseth, N.C. & Saether, B.E. (2017) Interactions between demography and environmental effects are important determinants of population dynamics. *Science Advances,* **3**.

Gaskin, T., Futerman, P. & Chapman, T. (2002) Increased density and male-male interactions reduce male longevity in the medfly, Ceratitis capitata. *Animal Behaviour,* **63,** 121-129.

Gerber, L.R. & White, E.R. (2014) Two-sex matrix models in assessing population viability: when do male dynamics matter? *Journal of Applied Ecology,* **51,** 270-278.

Grenfell, B.T., Bjornstad, O.N. & Kappey, J. (2001) Travelling waves and spatial hierarchies in measles epidemics. *Nature,* **414,** 716-723.

Grenfell, B.T., Price, O.F., Albon, S.D. & Clutton-Brock, T.H. (1992) Overcompensation and population-cycles in an ungulate. *Nature,* **355,** 823-826.

Grenfell, B.T., Wilson, K., Finkenstadt, B.F., Coulson, T.N., Murray, S., Albon, S.D., Pemberton, J.M., Clutton-Brock, T.H. & Crawley, M.J. (1998) Noise and determinism in synchronized sheep dynamics. *Nature,* **394,** 674-677.

Gulland, F.M.D. (1992) The role of nematode parasites in soay sheep (Ovis-aries L) mortality during a population crash. *Parasitology,* **105,** 493-503.

Gulland, F.M.D., Albon, S.D., Pemberton, J.M., Moorcroft, P.R. & Clutton-Brock, T.H. (1993) Parasite-associated polymorphism in a cyclic ungulate population. *Proceedings of the Royal Society B-Biological Sciences,* **254,** 7-13.

Hance, T., van Baaren, J., Vernon, P. & Boivin, G. (2007) Impact of extreme temperatures on parasitoids in a climate change perspective. *Annual Review of Entomology*, pp. 107-126. Annual Reviews, Palo Alto.

Hartley, S.E. & DeGabriel, J.L. (2016) The ecology of herbivore-induced silicon defences in grasses. *Functional Ecology,* **30,** 1311-1322.

Hone, J. & Clutton-Brock, T.H. (2007) Climate, food, density and wildlife population growth rate. *Journal of Animal Ecology,* **76,** 361-367.

Hultine, K.R., Grady, K.C., Wood, T.E., Shuster, S.M., Stella, J.C. & Whitham, T.G. (2016) Climate change perils for dioecious plant species. *Nature Plants,* **2,** 8.

Ims, R.A. & Fuglei, E. (2005) Trophic interaction cycles in tundra ecosystems and the impact of climate change. *Bioscience,* **55,** 311-322.

Ims, R.A., Henden, J.A. & Killengreen, S.T. (2008) Collapsing population cycles. *Trends in Ecology & Evolution,* **23,** 79-86.

Inchausti, P. & Halley, J. (2003) On the relation between temporal variability and persistence time in animal populations. *Journal of Animal Ecology,* **72,** 899-908.

Jenouvrier, S., Caswell, H., Barbraud, C. & Weimerskirch, H. (2010) Mating Behavior, Population Growth, and the Operational Sex Ratio: A Periodic Two-Sex Model Approach. *American Naturalist,* **175,** 739-752.

Jongejans, E., de Kroon, H., Tuljapurkar, S. & Shea, K. (2010) Plant populations track rather than buffer climate fluctuations. *Ecology Letters,* **13,** 736-743.

Kausrud, K.L., Mysterud, A., Steen, H., Vik, J.O., Ostbye, E., Cazelles, B., Framstad, E., Eikeset, A.M., Mysterud, I., Solhoy, T. & Stenseth, N.C. (2008) Linking climate change to lemming cycles. *Nature,* **456,** 93-U93.

Kendall, B.E., Briggs, C.J., Murdoch, W.W., Turchin, P., Ellner, S.P., McCauley, E., Nisbet, R.M. & Wood, S.N. (1999) Why do populations cycle? A synthesis of statistical and mechanistic modeling approaches. *Ecology,* **80,** 1789-1805.

Koenig, W.D. & Knops, J.M.H. (1998) Scale of mast-seeding and tree-ring growth. *Nature,* **396,** 225-226.

Le Galliard, J.F., Fitze, P.S., Ferriere, R. & Clobert, J. (2005) Sex ratio bias, male aggression, and population collapse in lizards. *Proceedings of the National Academy of Sciences of the United States of America,* **102,** 18231-18236.

Lindstrom, E.R. & Hornfeldt, B. (1994) Vole cycles, snow depth and fox predation. *Oikos,* **70,** 156-160.

Ludwig, G.X., Alatalo, R.V., Helle, P., Linden, H., Lindstrom, J. & Siitari, H. (2006) Short- and long-term population dynamical consequences of asymmetric climate change in black grouse. *Proceedings of the Royal Society B-Biological Sciences,* **273,** 2009-2016.

Menges, E.S. & Quintana-Ascencio, P.F. (2004) Population viability with fire in Eryngium cuneifolium: Deciphering a decade of demographic data. *Ecological Monographs,* **74,** 79-99.

Milner, J.M., Elston, D.A. & Albon, S.D. (1999) Estimating the contributions of population density and climatic fluctuations to interannual variation in survival of Soay sheep. *Journal of Animal Ecology,* **68,** 1235-1247.

Molnar, P.K., Dobson, A.P. & Kutz, S.J. (2013) Gimme shelter - the relative sensitivity of parasitic nematodes with direct and indirect life cycles to climate change. *Global Change Biology,* **19,** 3291-3305.

Mysterud, A., Coulson, T. & Stenseth, N.C. (2002) The role of males in the dynamics of ungulate populations. *Journal of Animal Ecology,* **71,** 907-915.

Nur, N. & Sydeman, W.J. (1999) Survival, breeding probability and reproductive success in relation to population dynamics of Brandt's cormorants Phalacrocorax penicillatus. *Bird Study,* **46,** 92-103.

Owen-Smith, N. (1993) Comparative mortality rates of male and female kudus - the costs of sexual size dimorphism. *Journal of Animal Ecology,* **62,** 428-440.

Ozgul, A., Tuljapurkar, S., Benton, T.G., Pemberton, J.M., Clutton-Brock, T.H. & Coulson, T. (2009) The Dynamics of Phenotypic Change and the Shrinking Sheep of St. Kilda. *Science,* **325,** 464-467.

Pardo, D., Jenouvrier, S., Weimerskirch, H. & Barbraud, C. (2017) Effect of extreme sea surface temperature events on the demography of an age-structured albatross population. *Philosophical Transactions of the Royal Society B-Biological Sciences,* **372,** 10.

Peeters, B., Veiberg, V., Pedersen, A.O., Stien, A., Irvine, R.J., Aanes, R., S'Ther, B.E., Strand, O. & Hansen, B.B. (2017) Climate and density dependence cause changes in adult sex ratio in a large Arctic herbivore. *Ecosphere,* **8**.

Pelletier, F., Moyes, K., Clutton-Brock, T.H. & Coulson, T. (2012) Decomposing variation in population growth into contributions from environment and phenotypes in an age-structured population. *Proceedings of the Royal Society B-Biological Sciences,* **279,** 394-401.

Pemberton, J.M., Smith, J.A., Coulson, T.N., Marshall, T.C., Slate, J., Paterson, S., Albon, S.D. & CluttonBrock, T.H. (1996) The maintenance of genetic polymorphism in small island populations: Large mammals in the Hebrides. *Philosophical Transactions of the Royal Society of London Series B-Biological Sciences,* **351,** 745-752.

Peters, R.H. (1983) The ecological impacts of body size. Cambridge University Press, Cambridge, UK.

Petry, W.K., Soule, J.D., Iler, A.M., Chicas-Mosier, A., Inouye, D.W., Miller, T.E.X. & Mooney, K.A. (2016) Sex-specific responses to climate change in plants alter population sex ratio and performance. *Science,* **353,** 69-71.

Plummer, M. (2003) JAGS: a program for analysis of Bayesian graphical models using Gibbs sampling. pp. 125. Proceedings of the 3rd international workshop on distributed statistical computing. Technische Universit at Wien, Wien, Austria.

R Core Team (2016) R: A language and environment for statistical computing. R Foundation for Statistical Computing, Vienna, Austria.

Radchuk, V., Ims, R.A. & Andreassen, H.P. (2016) From individuals to population cycles: the role of extrinsic and intrinsic factors in rodent populations. *Ecology,* **97,** 720-732.

Rankin, D.J. & Kokko, H. (2007) Do males matter? The role of males in population dynamics. *Oikos,* **116,** 335-348.

Rees, M. & Ellner, S.P. (2009) Integral projection models for populations in temporally varying environments. *Ecological Monographs,* **79,** 575-594.

Reynolds, J.J.H., Lambin, X., Massey, F.P., Reidinger, S., Sherratt, J.A., Smith, M.J., White, A. & Hartley, S.E. (2012) Delayed induced silica defences in grasses and their potential for destabilising herbivore population dynamics. *Oecologia,* **170,** 445-456.

Roesch, A. & Harald, S. (2014) WaveletComp: Computational Wavelet Analysis. R package version 1.0. https://CRAN.R-project.org/package=WaveletComp

Rotella, J.J., Link, W.A., Chambert, T., Stauffer, G.E. & Garrott, R.A. (2012) Evaluating the demographic buffering hypothesis with vital rates estimated for Weddell seals from 30 years of mark-recapture data. *Journal of Animal Ecology,* **81,** 162-173.

Rydgren, K., Okland, R.H., Pico, F.X. & de Kroon, H. (2007) Moss species benefits from breakdown of cyclic rodent dynamics in boreal forests. *Ecology,* **88,** 2320-2329.

Schmickl, T. & Karsai, I. (2010) The interplay of sex ratio, male success and density-independent mortality affects population dynamics. *Ecological Modelling,* **221,** 1089-1097.

Simmonds, E.G. & Coulson, T. (2015) Analysis of phenotypic change in relation to climatic drivers in a population of Soay sheep Ovis aries. *Oikos,* **124,** 543-552.

Stenseth, N.C., Chan, K.S., Tavecchia, G., Coulson, T., Mysterud, A., Clutton-Brock, T. & Grenfell, B. (2004) Modelling non-additive and nonlinear signals from climatic noise in ecological time series: Soay sheep as an example. *Proceedings of the Royal Society B-Biological Sciences,* **271,** 1985-1993.

Stevenson, I.R. & Bancroft, D.R. (1995) Fluctuating trade-offs favour precocial maturity in male Soay sheep. *Proceedings of the Royal Society B-Biological Sciences,* **262,** 267-275.

Tavecchia, G., Pradel, R., Boy, V., Johnson, A.R. & Cezilly, F. (2001) Sex- and age-related variation in survival and cost of first reproduction in greater flamingos. *Ecology,* **82,** 165-174.

Toigo, C. & Gaillard, J.M. (2003) Causes of sex-biased adult survival in ungulates: sexual size dimorphism, mating tactic or environment harshness? *Oikos,* **101,** 376-384.

Torrence, C. & Compo, G.P. (1998) A practical guide to wavelet analysis. *Bulletin of the American Meteorological Society,* **79,** 61-78.

Townsend, S.E., Newey, S., Thirgood, S.J. & Haydon, D.T. (2011) Dissecting the drivers of population cycles: Interactions between parasites and mountain hare demography. *Ecological Modelling,* **222,** 48-56.

Tsai, W.P., Liu, K.M., Punt, A.E. & Sun, C.L. (2015) Assessing the potential biases of ignoring sexual dimorphism and mating mechanism in using a single-sex demographic model: the shortfin mako shark as a case study. *Ices Journal of Marine Science,* **72,** 793-803.

Veiberg, V., Loe, L.E., Albon, S.D., Irvine, R.J., Tveraa, T., Ropstad, E. & Stien, A. (2017) Maternal winter body mass and not spring phenology determine annual calf production in an Arctic herbivore. *Oikos,* **126,** 980-987.

Vik, J.O., Brinch, C.N., Boutin, S. & Stenseth, N.C. (2008) Interlinking hare and lynx dynamics using a century's worth of annual data. *Population Ecology,* **50,** 267-274.

Vindenes, Y., Edeline, E., Ohlberger, J., Langangen, O., Winfield, I.J., Stenseth, N.C. & Vollestad, L.A. (2014) Effects of Climate Change on Trait-Based Dynamics of a Top Predator in Freshwater Ecosystems. *American Naturalist,* **183,** 243-256.

White, R.S.A., Wintle, B.A., McHugh, P.A., Booker, D.J. & McIntosh, A.R. (2017) The scaling of population persistence with carrying capacity does not asymptote in populations of a fish experiencing extreme climate variability. *Proceedings of the Royal Society B-Biological Sciences,* **284**.

Williams, C.K., Ives, A.R., Applegate, R.D. & Ripa, J. (2004) The collapse of cycles in the dynamics of North American grouse populations. *Ecology Letters,* **7,** 1135-1142.
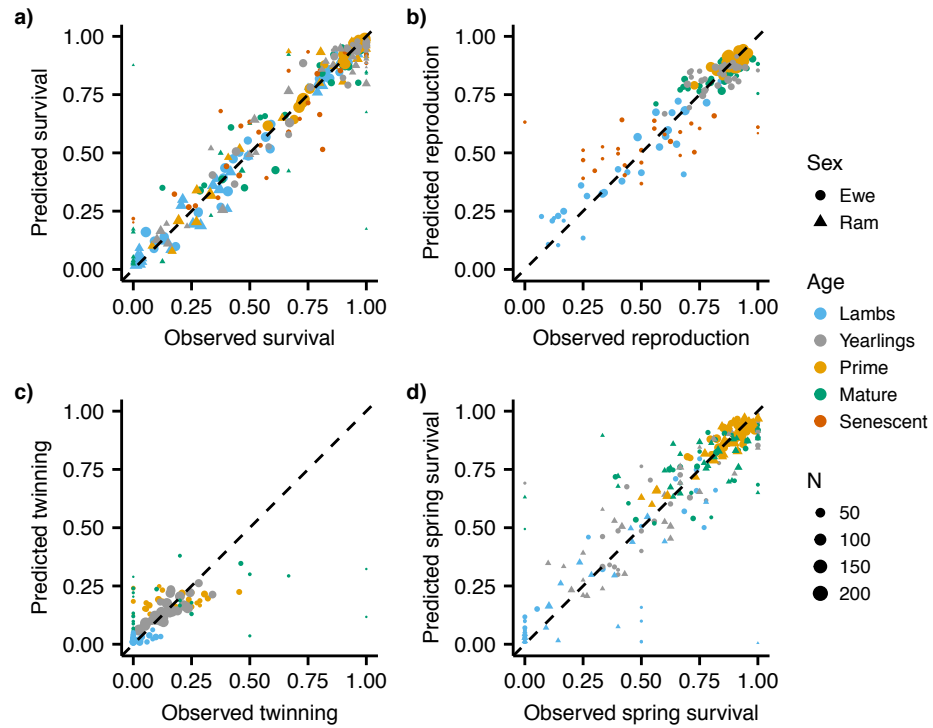
Figure S1: Observed and predicted proportions of individuals a) surviving, b) reproducing, and c) twinning and d) of newborn individuals surviving from spring to summer. Vital rates were predicted using the posterior medians as the parameter estimates, the observed density from $t-1$ and including the estimated random effect for each year. Dashed lines show a 1:1 correlation. Note that in d) age refers to the age of the newborn's mother, whilst sex is that of the newborn itself. In the remaining plots both age and sex are those of the focal individual.
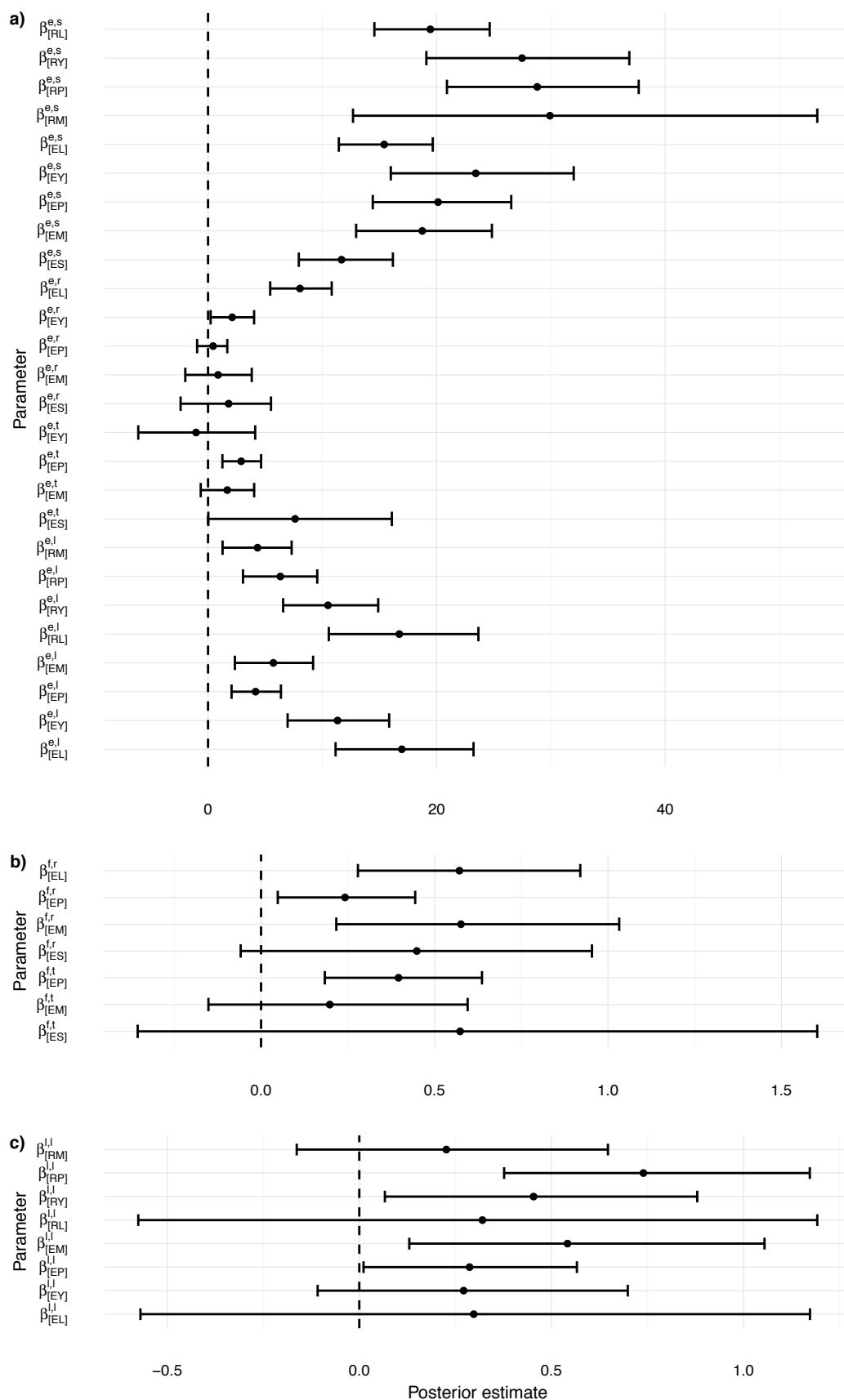
Figure S2: Posteriors of the slope terms for a) first, b) second, c) third environmental axes. Dashed vertical lines are at zero. Points and error bars show median and 95% credible intervals respectively. See equations 1-4 in main text for parameter definitions. Subscripts refer to sex and age (i.e. EL is a ewe lamb). Superscripts refer to environmental axis and vital rate.
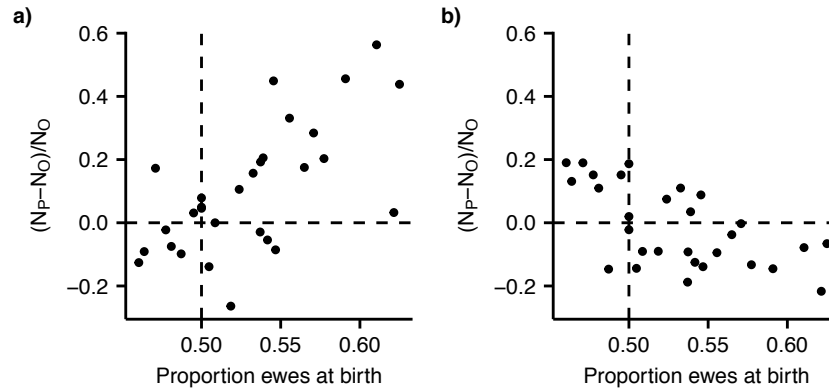
Figure S3: Error in the predicted number of a) ram and b) ewe lambs for each year against the observed sex ratio at birth. N_o and N_p are the observed and predicted number of individuals respectively. A sex ratio of 0.5 is assumed in the model (vertical dashed line). The horizontal dashed line is at zero, where the observed number of lambs equals that observed. The degree by which the number of ram and ewe lambs are overpredicted increases and decreases respectively with the observed proportion of females at birth.
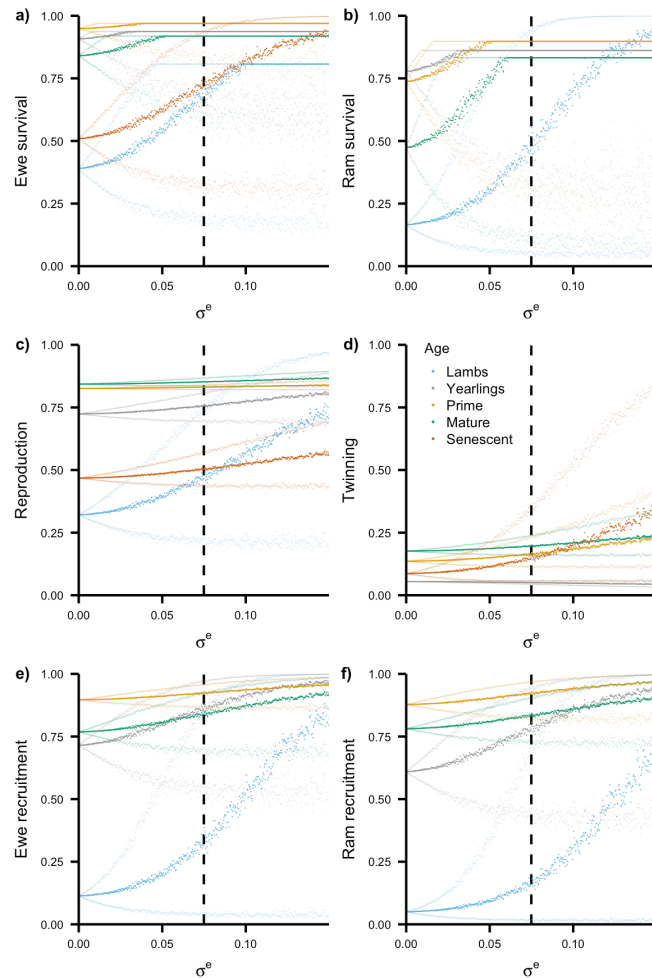
Figure S4: Predicted demographic rates under increasing levels of environmental variation for a) ewe survival, b) ram survival, c) reproduction, d) twinning, e) recruitment of ewes, and f) recruitment of rams. Plots show the median and 95% quantiles (faded points) for each demographic rate. Each demographic rate is estimated 1,000 times using the mean density at that timestep from fig. 4, setting t to 1, and sampling the random year effect for the first environmental axis from a normal distribution, where the standard deviation increases linearly from zero to twice that estimates in the model over the 500 time steps. The dashed line indicates where the variability in the first environmental axis is equal to that estimated in the model.

Table S1: Priors for the structural equation models. For the uniform distributions (U) the first and second parameters refer to the minimum and maximum, for the normal distribution (N) they are the mean and standard deviation. Where distributions are truncated (t) the first and second parameters refer to the lower and upper limits respectively. For parameter definitions see eqn 1-3. Note that • is used when referring to parameters for each of the demographic classes, otherwise subscripts indicate which classes are referred to with E for ewes, R for rams, L for lambs, Y for yearlings, P for prime, M for mature, S for senescent. Weakly informative priors are used to aid convergence of the threshold models, for example by restricting the threshold parameters to the range of observed densities.

Parameter	Submodel(s)	Prior
$\beta_\bullet^{0,r}$	Reproduction	N(0, 100)
$\beta_\bullet^{t,r}$	Reproduction	U(-1, 1)
$\beta_\bullet^{e,r}$	Reproduction	N(0, 100)
$\beta_\bullet^{f,r}$	Reproduction (excluding yearlings)	N(0, 100) t(0,)
$\beta_\bullet^{0,t}$	Twinning	N(0, 100)
$\beta_\bullet^{t,t}$	Twinning	U(-1, 1)
$\beta_\bullet^{e,t}$	Twinning	N(0, 100)
$\beta_\bullet^{f,t}$	Twinning (excluding lambs/yearlings)	N(0, 100)t(0,)
$\beta_\bullet^{0,s}$	Survival (excluding ram lamb & senescent ewe)	U(-10, 10)
$\beta_{[RL]}^{0,s}$	Ram lamb & senescent ewe survival	N(0, 100)
$\beta_\bullet^{t,s}$	Survival	U(-0.3, 0.3)
$\beta_\bullet^{e,s}$	Survival (excluding ram lambs & senescent ewes)	U(0, 50)
$\beta_{[RL]}^{e,s}$	Ram lamb & senescent ewe survival	N(0,100) t(0,)
$\theta_\bullet$	Survival	U(2.3, 2.8)
σ_e	All	U(0, 0.2)
σ_f	Reproduction and twinning	1
σ_l	Newborn spring survival	1
ρ_{ef}	All	U(-1, 1)
α^t	All	U(-0.05, 0.05)

Appendices

Appendix A1: Perturbing different axes of environmental variation

The demographic structural equation model contains three axes of environmental variation; the first drives variation in all of the vital rates, the second in fecundity, and the third in the spring survival of newborn lambs (Fig. 3). As the majority of the variation in the vital rates is well explained using the primary axis however, in the main text we focus on the effects of increasing variation in that axis only. Here, we consider the effects of environmental variation in the second and third axes. As in the main text, we simulate 1,000 populations for 500 iterations, whilst increasing the degree of variability in the environment. In the first group of simulations, we increase the standard deviation of the second temporal axis (σ^f) linearly from zero to two (as this is set to one in the model), whilst setting the standard deviations for the first (σ^e) and third (σ^l) axes to zero. Next we increase (σ^l) linearly from zero to two whilst setting (σ^e) and (σ^l) to zero. Finally we simultaneously increase all three parameters (σ^e, σ^f and σ^l) to double their values estimated in the model. We compare the estimated population sizes across the age-

sex classes from these two sets of simulations to those where (σ^e) was perturbed in the main text.

Increasing the degree of variability in the second and third environmental axes has relatively little effect on predicted population sizes (Figure A1). Predicted population dynamics when all three axes are perturbed are very similar to those when only the first axis is perturbed (Figure A1). As the first environmental axis drives the majority of the variation in the vital rates (Chapter 4) this is unsurprising and suggests that the population dynamics are primarily driven by over winter mortality.
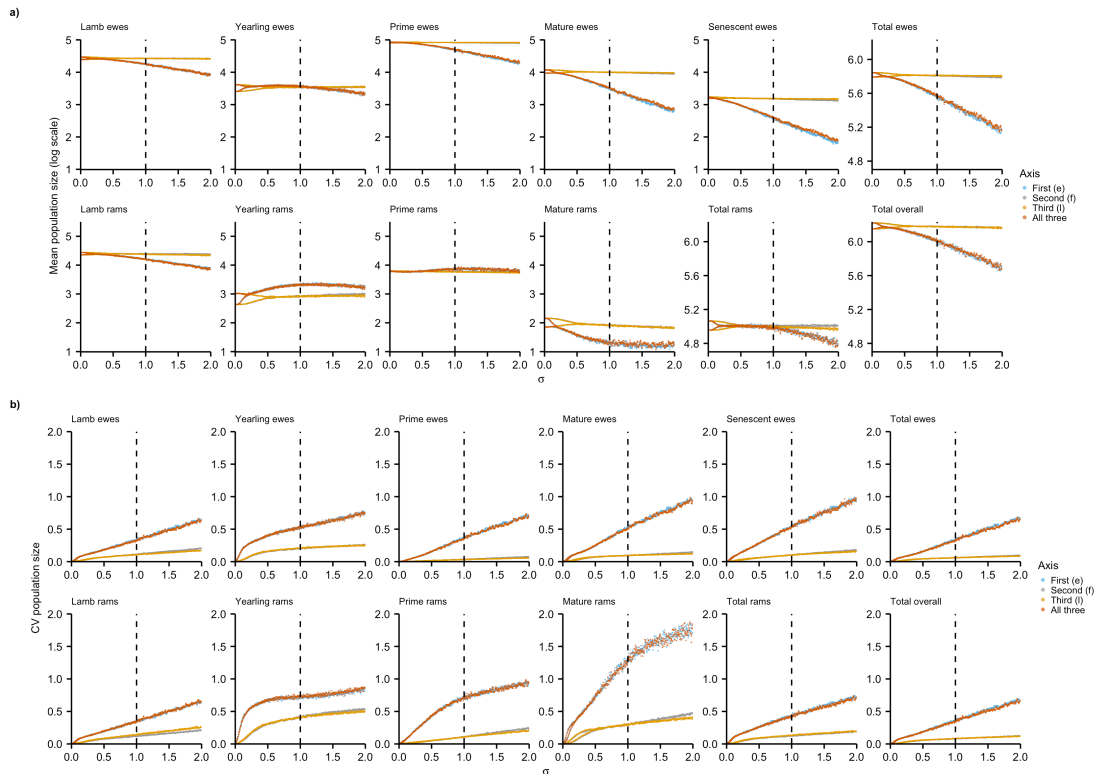
Figure A1: a) Mean and b) coefficient of variation (CV) of number of individuals in each age-sex class 1000 simulations, whilst increasing the degree of variation in each axis of environmental variation. Dashed vertical line indicates where the standard deviation of the perturbed axis (or axes) is equal to that estimated in the model.

Appendix A2: The effects of demographic stochasticity

Here, we consider the effect of demographic stochasticity as well as environmental stochasticity. In the main text we assume that environmental variation drives all of the variation in the vital rates, with all individuals experiencing the same environment each year. Demographic stochasticity refers to the effect of stochastic realisations of the vital rate probabilities with finite populations and as such has larger impacts on the population dynamics of small populations (Caswell 2001).

As population sizes increased over the study period we explore whether the effects of demographic stochasticity decrease over this period. Demographic stochasticity was incorporated into the models by randomly sampling the demographic processes from binomial

distributions. The probabilities of survival, fecundity, and recruitment were estimated for each age-sex class as in the main text (equations 1-4). We compare the dynamics of simulated populations including and excluding demographic stochasticity, first by simulating populations under the observed conditions (i.e. by setting the standard deviations of the latent variables to those estimated in the model). There appears to be little variation in the projected dynamics between the models with and without demographic stochasticity (Fig. A2). Population crashes are seen both with and without demographic stochasticity, the average population sizes are similar, and there are still sequences of 4-5 years of population increases without a decrease (Fig. A2).
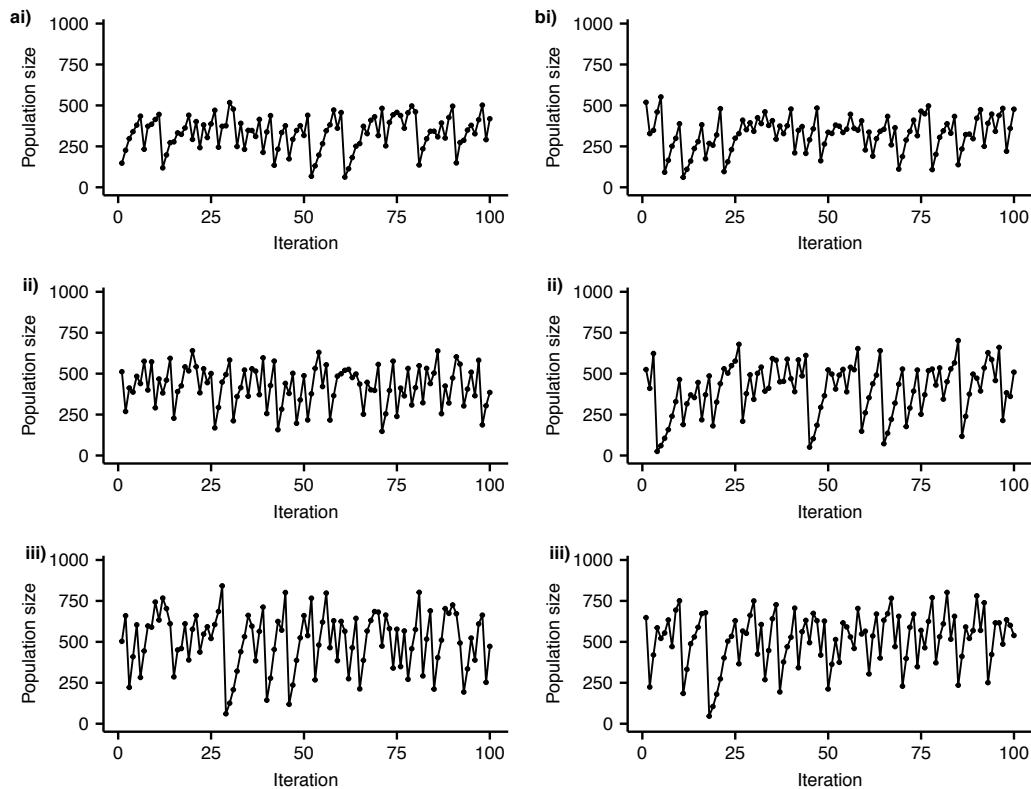
Figure A2: Simulated population dynamics a) excluding and b) including demographic stochasticity for a year at the i) start ($t=1$), ii) middle ($t=15$), and iii) end ($t=30$) of the study period.

Next we consider how the effect of demographic stochasticity varies according to the degree of environmental stochasticity. As in the main text 1,000 populations were simulated for 500 time steps, whilst slowly increasing the standard deviation of the random effect in the first environmental axis from zero to twice that estimated in the model. This was repeated using the models including and excluding demographic stochasticity for years at the start and end of the study period ($t=1$ and $t=30$ respectively).

Under the model incorporating demographic stochasticity population sizes are more variable at very low and very high levels of environmental variability (i.e. when σ^e is very small or large) than in the model with only environmental stochasticity (Figure A3). Where there is little environmental variability (i.e. σ^e is small) the degree of variability in population

27

sizes is higher in the model with demographic stochasticity. However, differences in mean population size appear relatively small and only occur at high levels of environmental variation (Figure A3). Total population sizes decrease as the degree of environmental stochasticity increases, thus the effect of demographic stochasticity increases as its effects are larger in small populations.
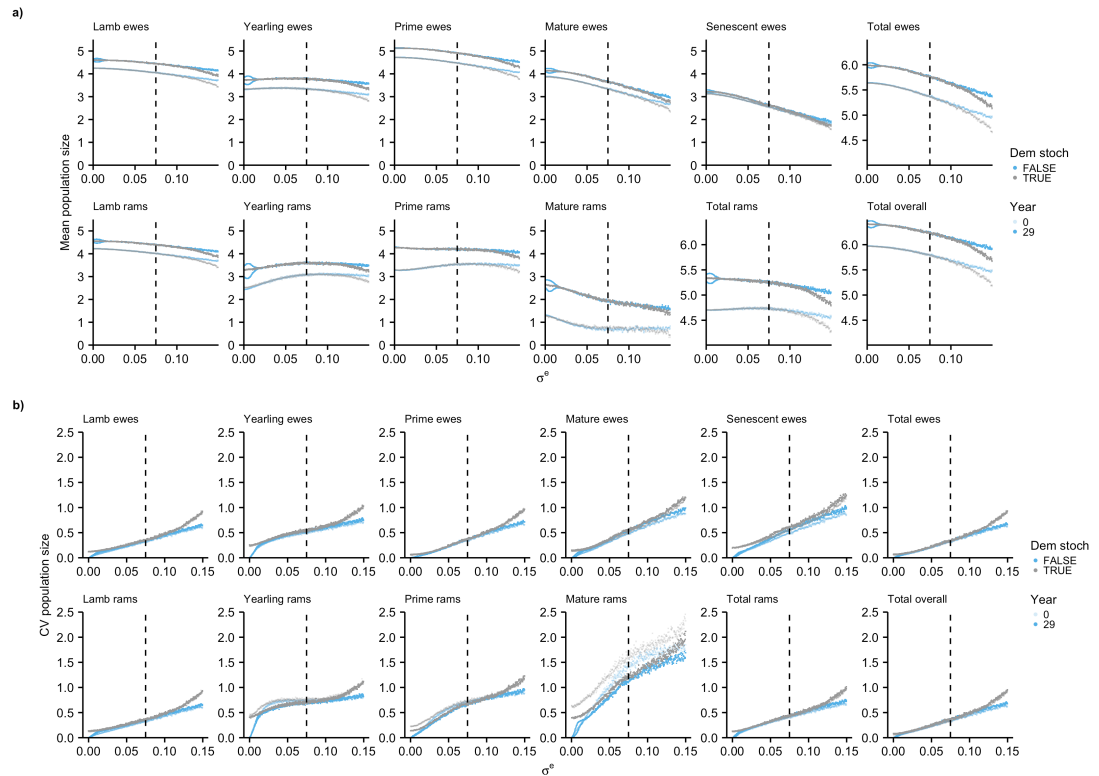
Figure A3: a) Mean and b) CV of number of individuals in each age-sex class 1000 simulations, whilst increasing the degree of variation in the first axis of environmental variation. Dashed vertical line indicates where the standard deviation of the perturbed axis is equal to that estimated in the model. Colours indicate models including (true) and excluding (false) demographic stochasticity, whilst transparency of the points indicates study year.

References

Caswell, H. (2001) Matrix population models: Construction, analysis, and interpretation. *Matrix population models: Construction, analysis, and interpretation*, i-xxii, 1-722.

Chapter 6: General Discussion

Synthesis

Climate change is predicted to cause widespread ecological change, driving variation in species' abundances, spatial distributions, and risk of extinction and community composition (Walther *et al.* 2002; Parmesan & Yohe 2003; Parmesan 2006; Maclean & Wilson 2011). Accounting for population responses to such change is therefore necessary in order to design appropriate management strategies for future environmental conditions (Bernardo, Albrecht & Knight 2016). Structured population models are widely used to explore population responses to environmental variation (Ehrlen *et al.* 2016). Such models are parameterised by using individual longitudinal data to estimate demographic rates, such as survival and reproduction (Coulson 2012). Estimating such rates as a function of environmental drivers thus allows population responses to environmental change to be predicted by perturbing the drivers (Gotelli & Ellison 2006; Hunter *et al.* 2010). Identifying the drivers of variation in the demographic rates is challenging however, as environmental effects are often complex (Grosbois *et al.* 2008; Ehrlen *et al.* 2016) and the degree of temporal replication in many demographic data sets is relatively small (Salguero-Gomez *et al.* 2015; Salguero-Gomez *et al.* 2016). Throughout this thesis I have applied novel statistical techniques to explore population responses to environmental variation.

First, I describe a methodology for capturing temporal covariation among demographic rates, via one or more latent variable(s) (Chapters 2, 4, and 5). This provides a structured method for modelling a temporal covariance matrix, allowing hypotheses about how the environment drives the joint response of disparate demographic processes to be explored. For example, in a population of Soay sheep, variation in demographic rates is largely driven by a single environmental axis, which impacts on survival, fecundity, and recruitment across the lifecycle (Chapters 4 and 5). This demographic structural equation model (SEM) may be applied wherever it is feasible to construct a stochastic, demographic projection model. Where demographic processes are positively correlated the latent variable(s) can be conceived as axes of 'environmental quality', which can provide the basis for further analyses (see below; Chapters 2, 4, and 5). Positive covariances among demographic processes are widespread in natural populations, suggesting this approach should be widely applicable (Nur & Sydeman 1999; Altwegg *et al.* 2006; Jongejans *et al.* 2010; Rotella *et al.* 2012; though see Compagnoni *et al.* 2016). In this thesis I have used relatively simple SEMs, only accounting for temporal variation among demographic processes and using a maximum of three environmental axes. However, this general approach would also be applicable in more complicated situations, such as accounting for spatio-temporal covariation in demographic rates.

Perturbation analyses of the environmental axes introduced under the demographic SEM allow population responses to environmental change to be predicted (Chapters 2 and 5). Ideally, to predict how a population might respond to environmental change, the explicit drivers

of variation in the demographic rates should be identified (e.g. Chapter 3; Gotelli & Ellison 2006). However, there is a substantial mismatch between the temporal extent of many demographic data sets (mean of six and eleven years in plants and animals respectively; Salguero-Gomez et al. 2015; Salguero-Gomez et al. 2016) and the number of years of data required to accurately identify environmental drivers, determine their temporal periods of influence, and quantify their effects (20-25 years; Teller et al. 2016; Van der Pol et al. 2016). Many studies have thus resorted to indirect methods of determining population responses to environmental change. For example, prospective sensitivity analyses may be used to determine how variation in different demographic processes affects the population growth rate (Morris, Shertzer & Rice 2011; Bentzen & Powell 2012; Chiquet et al. 2013). However, as covariations among the vital rates can have significant impacts on population growth, considering each vital rate separately may lead to erroneous conclusions (Aiello-Lammens & Akcakaya 2017). Thus, as perturbing the environmental axes in the demographic SEM approach accounts for the fact that multiple demographic processes typically respond in concert to environmental change, this may represent the best alternative for exploring possible population-level responses to environmental change, where causal drivers cannot be identified (Chapter 2).

Where data are sufficiently replicated the demographic SEM approach can provide a simpler target for identifying underlying environmental drivers (Chapters 2 and 4). As the mean and variability of different vital rates differ across the life cycle (Gaillard, Festa-Bianchet & Yoccoz 1998; Gaillard et al. 2000) drivers are typically identified separately for each process (Coulson et al. 2001; Pokallus & Pauli 2015). However, where demographic processes are positively correlated (Nur & Sydeman 1999; Altwegg et al. 2006; Jongejans et al. 2010; Rotella et al. 2012) variation in these disparate processes is likely to be driven by common underlying variables. Identifying the common axes of environmental variation that drive such covariation can thus provide a much simpler target for the challenging task of identifying the underlying drivers than treating each demographic process independently (Chapter 4). For example, in a population of Soay sheep I decompose the variation in a single environmental axis rather than treating the 11 demographic processes independently (Chapter 4).

One reason that decomposing temporal variation in the demographic rates is challenging is that demographic data are typically collected annually, whereas the effects of such drivers may occur at much finer time scales (Foster, Schmalzer & Fox 2014; Kruuk, Osmond & Cockburn 2015). This necessitates methods that can not only accurately identify causal drivers and quantify their effects, but also determine the temporal windows over which they act (Teller et al. 2016; Van der Pol et al. 2016). These windows are usually chosen *a priori*, typically with little justification provided (Ehrlen et al. 2016; Van der Pol et al. 2016). I have shown how functional linear models (FLMs) may be combined with a demographic SEM to allow the demographic response to a climatic variable to be estimated as a cumulative effect over a year, whilst allowing the effects to differ in magnitude and direction over time (Chapter

4; Roberts 2008; Teller *et al.* 2016). Temporal differences in both the magnitude and direction of the effect of a single climatic variable suggest that the choice of such windows can have significant implications for population predictions (Chapters 3 and 4; Kruuk, Osmond & Cockburn 2015). For example, survival of *E.cuneifolium* can be positively (winter) or negatively (summer) affected by increased levels of drought, depending on the time of year (Chapter 3). Overall these antagonistic effects appear to cancel each other out, leading to the prediction that the increase in drought expected under climate change will have little effect on survival in this species (Chapter 3). However, if a single temporal window was adopted, either positive or negative trends may have appeared likely depending on the period chosen. Using the FLM approach can uncover previously unknown climatic effects, even in well studied populations, and thus can increase the predictive performance of demographic models, relative to selecting windows *a priori* (Chapter 4).

Statistical considerations

One of the main challenges with identifying climatic drivers of demographic variation is that there can be a large number of putative drivers, which increases the risk of overfitting, especially if the data set contains limited temporal replication (Frederiksen *et al.* 2014). In this thesis I used leave-one-out cluster cross validation to select climatic variables that increased out of sample predictive performance (Chapters 3 and 4). Cross validation is rarely used in studies of the environmental drivers of demographic rates (Grosbois *et al.* 2008), probably partly because it can be computer intensive. When identifying environmental drivers the aim is often to predict population responses to a future change in those drivers (e.g. Chapter 3; Gotelli & Ellison 2006); thus out-of-sample predictive performance is important (Wenger & Olden 2012). It is impossible to test the predictive performance of the model over the future temporal period over which predictions are to be made. However, cluster cross validation, where the data are split into training and validation sets according to a grouping variable, such as year of study, has the advantage of at least testing the predictive performance under a year of environmental conditions that was not used to train the model (Wenger & Olden 2012). Many studies instead rely on within sample measures, such as Akaike Information Criteria (AIC), which may be subject to overfitting (Raffalovich *et al.* 2008; Murtaugh 2009; Dahlgren 2010; Van der Pol *et al.* 2016). Moreover, the use of measures such as AIC is not straightforward for hierarchical models, which are typically necessary for dependent demographic data clustered in time or space (Vaida & Blanchard 2005).

In addition to choosing appropriate measures of predictive performance, methods to reduce overfitting by 'regularising' estimated climatic effects should also be more widely adopted in ecology (Dahlgren 2010; Teller *et al.* 2016). The FLM provides one example of such an approach (Roberts 2008; Teller *et al.* 2016). Here, the coefficients for a single variable, such as temperature, can be estimated as a smooth function over time or space (Teller *et al.* 2016).

Alternative methods to reduce overfitting, which I did not explore in this thesis, include the use of shrinkage techniques, such as the elastic net, where penalties are introduced on the size of coefficient estimates (Hoerl & Kennard 1970; Tibshirani 1996; Zou & Hastie 2005). In a Bayesian framework such shrinkage may be applied by altering the priors on the slope coefficients (Park & Casella 2008; Li & Lin 2010).

In addition to methods for testing whether particular covariates drive variation in demographic processes, it is important to validate whether population models adequately capture the observed dynamics at the population level (Chapter 5). Many studies using structured population models provide little or no detail of whether attempts have been made to validate model performance at the population level. In the case of structured population models this may be partly driven by the short temporal periods over which demographic data are collected (Salguero-Gomez *et al.* 2015; Salguero-Gomez *et al.* 2016); it is difficult to validate model predictions against the observed dynamics when these only extend over a few years. Where validation takes place methods typically include comparing observed and predicted population growth rates, size or age distributions, or either average or one-step ahead predictions of population size (Dahlgren & Ehrlen 2009; Simmonds & Coulson 2015). Relatively few studies compare the dynamical behaviour of the model to that of the observed population. However, even where a model appears to have a good one-step ahead predictive performance it may not capture the observed dynamical behaviour (Chapter 5). Poor model performance may suggest important processes have been excluded (Chapter 5), decreasing the reliability of any future predictions. Moreover, processes such as extinction may be influenced by the dynamical behaviour of the system (Inchausti & Halley 2003). Thus, a range of methods, including an evaluation of the dynamical behaviour, is necessary to validate the predictive performance of population models (Chapter 5).

Future directions

Understudied elements of the life cycle

Accurately predicting population responses to environmental change requires quantifying the effects of the environment across the entire life cycle (Radchuk, Turlure & Schtickzelle 2013). Yet, even in relatively well-studied species, with decades of demographic data on marked individuals, there are often gaps in the data, for example on cryptic stages, such as dormant plants and seed banks (Lesica & Steele 1994; Menges 2000; Alahuhta *et al.* 2017; Paniw *et al.* 2017). Where data are scarce or unavailable population dynamics may be compared over a range of different values for the missing demographic rate (e.g. Chapters 2 and 3; Menges & Quintana-Ascencio 2004; Rees *et al.* 2006) or where limited data exist a Bayesian approach may be used to quantify the effect of uncertainty in such estimates at the population level (Paniw *et al.* 2017). Whilst using a range of values provides a measure of the uncertainty in population responses due to missing parameters, it does not allow for environmental effects in

the unknown processes. For example, environmental conditions, such as temperature and soil moisture, are known to influence several elements of seed bank dynamics, including seed mortality and germination (e.g. Mickelson & Grey 2006; Navarra *et al.* 2011; Cochrane 2017; Rezvani & Zaefarian 2017). Thus variation in seed bank dynamics, driven by environmental variation, may have implications for how populations respond to future environmental change. Further studies on the effect of environmental variation in cryptic life stages such as seed banks are thus needed in natural populations (e.g. Paniw *et al.* 2017).

The role of density dependence

Density dependence is prevalent throughout natural populations (e.g. Coulson, Milner-Gulland & Clutton-Brock 2000; Dahlgren, Ostergard & Ehrlen 2014) and has important consequences for species management, including in the success of translocations (Abeli *et al.* 2016), harvesting strategies (Freckleton *et al.* 2003), and biological control measures (Halpern & Underwood 2006). Thus accurate predictions of population responses to future environmental change necessitate the effect of density dependence on demographic rates to be accurately quantified, in addition to those of abiotic variables (Ehrlen & Morris 2015; Ehrlen *et al.* 2016). Density dependent feedbacks may be complicated, with the effect an individual has on a conspecific likely to depend on the abiotic environment (Jacquemyn, Brys & Honnay 2009; Wang *et al.* 2009), the age and states of interacting individuals (Myrvold & Kennedy 2015; Bassar *et al.* 2016; Gamelon *et al.* 2016), and the degree of spatial and temporal overlap between the individuals (Coulson *et al.* 1997).

However, simplistic measures of density are typically used in population models, such as the total number of individuals or the number of individuals in a specific age or sex class, usually with little justification provided (Mysterud, Coulson & Stenseth 2002). In the Soay sheep population, my age and sex structured model failed to capture the observed population cycles or the shift from apparent overcompensatory dynamics to relatively stable population sizes (Chapter 5). This population is food limited, with nearly all mortality occurring over the winter period, mainly caused by starvation (Clutton-Brock *et al.* 1991). Mortality is likely to be a function of the per capita food availability, rather than density *per se*. I used total population size as a measure of density and allowed the effects of density on individuals to differ according to age-sex class and according to the abiotic environment (Chapter 5). However, by using total population size I effectively assumed that the influence an individual had on its conspecifics was identical, regardless of whether it was a 13kg lamb or a 40kg adult ram. This is biologically unrealistic; larger individuals, with larger energy requirements, would typically be expected to have a greater effect, via resource consumption, on other individuals (Peters 1983). Allowing the effect of each individual to differ according to state variables, such as size or age, may be necessary to capture the observed dynamical behaviour.

Interactions among environmental drivers

I focused on the additive effects of environmental variables in this thesis (Chapters 3 and 4). In the Soay sheep population, I found that a model including the additive effects of multiple climatic variables (wind speed and precipitation) exhibited worse predictive performance than a model with a single climatic variable (Chapter 4). However, I did not consider an interaction between the two variables. In reality interactions between drivers are likely to occur (Nicole *et al.* 2011), for example high levels of precipitation may decrease an animal's thermal tolerance, exacerbating the effect of low temperatures or high wind speeds (Webb & King 1984). The better predictive performance of large-scale climatic indices, such as the North Atlantic Oscillation (NAO), relative to local weather variables, is likely to be partly due to our failure to include interactions between local variables (Chapter 4; Hallett *et al.* 2004; Stenseth & Mysterud 2005).

Including the effects of multiple climatic variables and the interactions between them is challenging because such variables are often correlated (Grosbois *et al.* 2008) and the interactions may be lagged. Using functional linear models (FLMs) to determine the temporal periods of influence for environmental drivers can increase the predictive performance of local climate models (Chapter 4), though the approach requires a high degree of temporal replication, and including interactions in such models would further increase the sample size requirements. Simulation studies suggest 20-25 years of demographic data are necessary to accurately identify the temporal periods of influence and quantify the effects of additive climatic drivers (Teller *et al.* 2016). Thus very few demographic data sets are likely to be sufficiently replicated to accurately quantify interactive effects. A possible alternative may be to use FLMs to identify the temporal periods over which climatic variables act and the shapes of the relationships, which could then be used to parameterise parametric models (Yee & Mitchell 1991).

Beyond the population

The predicted effects of future climate change are diverse, including changes to abundance, spatial distributions, phenology, and evolutionary change (Parmesan *et al.* 1999; Walther *et al.* 2002; Parmesan 2006). Such responses will not occur independently from each other, for example, range expansions may be more likely where species have also increased in abundance (Gaston *et al.* 2000). Despite this, environmentally explicit population models have typically been used to predict the effects of environmental change at the population level, using measures such as population growth rate (Hunter *et al.* 2010; Salguero-Gomez *et al.* 2012). Conversely, predictions of the effect of climate change on species distributions have typically been made using species distribution models (SDMs), often on continental or global scales (Guisan & Zimmermann 2000; Guisan & Thuiller 2005; Elith & Leathwick 2009). Here, environmental covariates are linked to species presence data. Future predictions of such environmental covariates may thus be used to predict where species will be able to exist under anticipated

future conditions. Thus such approaches do not typically take into account abundance or population dynamics, instead assuming that species are at equilibrium; that is populations are only present where the environmental conditions are suitable, and they are present in all locations where that is the case (Guisan & Zimmermann 2000; Guisan & Thuiller 2005; Araujo & Guisan 2006).

Extending demographic approaches to predict population dynamics at wider spatial scales (Merow *et al.* 2014; Swab *et al.* 2015; Evans *et al.* 2016) may allow for more biologically realistic and useful future predictions, incorporating effects on abundance and distributions (Ehrlen & Morris 2015). A major constraint however is the lack of longitudinal individual data at broad spatial scales (Menges 2000; Coutts *et al.* 2016). Large differences in population dynamics among geographically nearby populations suggests that extrapolating results based on demographic data from a single, or a few closely located, study population(s) to wider spatial scales is risky (Chapter 3; Johnson *et al.* 2010; Hernandez-Camacho *et al.* 2015; Coutts *et al.* 2016). However, there have been concerted recent efforts to address the limited spatial scale of most demographic data sets. For example, the deposition of matrices from matrix population models (MPM)s for hundreds of plant and animal species into open online repositories has facilitated studies at broader scales than are usually possible (Salguero-Gomez *et al.* 2015; Salguero-Gomez *et al.* 2016). Similarly projects, such as PlantPopNet, are attempting to collect demographic data on a specific species at much wider spatial scales than previous demographic studies have typically focused (Wardle *et al.* 2014). Such efforts will allow responses to environmental change at wider spatial scales to be predicted using a demographic framework.

Conclusions

Rapid rates of environmental change necessitate accurate methods for predicting ecological responses (Stenseth *et al.* 2002; Maclean & Wilson 2011). However, environmental effects on demographic performance can be complex, and the degree of temporal replication in most data sets is limited (Salguero-Gomez *et al.* 2015; Salguero-Gomez *et al.* 2016). Throughout this thesis I have used sophisticated statistical methods to enable such limited data to be used efficiently. I demonstrate how SEM approaches provide a biologically informed way to explore joint demographic responses to environmental change, allowing for predictions even when the explicit underlying drivers cannot be identified, or providing a simpler target for the effects of such drivers to be quantified. Furthermore, I illustrate the importance of considering the temporal windows of influence of environmental predictors. The complexity of population responses to environmental variation has resulted in many studies making necessary simplifying assumptions, for example selecting from a small sample of putative drivers, each acting over single *a priori* chosen temporal windows (Ehrlen *et al.* 2016; Van der Pol *et al.* 2016). My results suggest that the use of such assumptions may negatively affect the reliability of predictions of future population dynamics. Statistical tools that can deal with the challenges of

identifying drivers and their windows of influence, while quantifying their effects are relatively rarely used in this context (Dahlgren 2010; Teller *et al.* 2016). I demonstrate that the use of such methods can provide novel insights into population responses to environmental variation, even in well-studied populations, and improve our ability to predict future population dynamics under environmental change.

References

Abeli, T., Cauzzi, P., Rossi, G., Adorni, M., Vagge, I., Parolo, G. & Orsenigo, S. (2016) Restoring population structure and dynamics in translocated species: learning from wild populations. *Plant Ecology,* **217,** 183-192.

Aiello-Lammens, M.E. & Akcakaya, H.R. (2017) Using global sensitivity analysis of demographic models for ecological impact assessment. *Conservation Biology,* **31,** 116-125.

Alahuhta, K., Crone, E., Ettinger, A., Hens, H., Jakalaniemi, A. & Tuomi, J. (2017) Instant death, slow death and the consequences of assumptions about prolonged dormancy for plant population dynamics. *Journal of Ecology,* **105,** 471-483.

Altwegg, R., Roulin, A., Kestenholz, M. & Jenni, L. (2006) Demographic effects of extreme winter weather in the barn owl. *Oecologia,* **149,** 44-51.

Araujo, M.B. & Guisan, A. (2006) Five (or so) challenges for species distribution modelling. *Journal of Biogeography,* **33,** 1677-1688.

Bassar, R.D., Childs, D.Z., Rees, M., Tuljapurkar, S., Reznick, D.N. & Coulson, T. (2016) The effects of asymmetric competition on the life history of Trinidadian guppies. *Ecology Letters,* **19,** 268-278.

Bentzen, R.L. & Powell, A.N. (2012) Population Dynamics of King Eiders Breeding in Northern Alaska. *Journal of Wildlife Management,* **76,** 1011-1020.

Bernardo, H.L., Albrecht, M.A. & Knight, T.M. (2016) Increased drought frequency alters the optimal management strategy of an endangered plant. *Biological Conservation,* **203,** 243-251.

Chiquet, R.A., Ma, B.L., Ackleh, A.S., Pal, N. & Sidorovskaia, N. (2013) Demographic analysis of sperm whales using matrix population models. *Ecological Modelling,* **248,** 71-79.

Clutton-Brock, T.H., Price, O.F., Albon, S.D. & Jewell, P.A. (1991) Persistent instability and population regulation in soay sheep. *Journal of Animal Ecology,* **60,** 593-608.

Cochrane, A. (2017) Modelling seed germination response to temperature in Eucalyptus L'Her. (Myrtaceae) species in the context of global warming. *Seed Science Research,* **27,** 99-109.

Compagnoni, A., Bibian, A.J., Ochocki, B.M., Rogers, H.S., Schultz, E.L., Sneck, M.E., Elderd, B.D., Iler, A.M., Inouye, D.W., Jacquemyn, H. & Miller, T.E.X. (2016) The effect of demographic correlations on the stochastic population dynamics of perennial plants. *Ecological Monographs,* **86,** 480-494.

Coulson, T. (2012) Integral projections models, their construction and use in posing hypotheses in ecology. *Oikos,* **121,** 1337-1350.

Coulson, T., Albon, S., Guinness, F., Pemberton, J. & CluttonBrock, T. (1997) Population substructure, local density, and calf winter survival in red deer (Cervus elaphus). *Ecology,* **78,** 852-863.

Coulson, T., Catchpole, E.A., Albon, S.D., Morgan, B.J.T., Pemberton, J.M., Clutton-Brock, T.H., Crawley, M.J. & Grenfell, B.T. (2001) Age, sex, density, winter weather, and population crashes in Soay sheep. *Science,* **292,** 1528-1531.

Coulson, T., Milner-Gulland, E.J. & Clutton-Brock, T. (2000) The relative roles of density and climatic variation on population dynamics and fecundity rates in three contrasting ungulate species. *Proceedings of the Royal Society B-Biological Sciences,* **267,** 1771-1779.

Coutts, S.R., Salguero-Gomez, R., Csergo, A.M. & Buckley, Y.M. (2016) Extrapolating demography with climate, proximity and phylogeny: approach with caution. *Ecology Letters,* **19,** 1429-1438.

Dahlgren, J.P. (2010) Alternative regression methods are not considered in Murtaugh (2009) or by ecologists in general. *Ecology Letters,* **13,** E7-E9.

Dahlgren, J.P. & Ehrlen, J. (2009) Linking environmental variation to population dynamics of a forest herb. *Journal of Ecology,* **97,** 666-674.

Dahlgren, J.P., Ostergard, H. & Ehrlen, J. (2014) Local environment and density-dependent feedbacks determine population growth in a forest herb. *Oecologia,* **176,** 1023-1032.

Ehrlen, J. & Morris, W.F. (2015) Predicting changes in the distribution and abundance of species under environmental change. *Ecology Letters,* **18,** 303-314.

Ehrlen, J., Morris, W.F., von Euler, T. & Dahlgren, J.P. (2016) Advancing environmentally explicit structured population models of plants. *Journal of Ecology,* **104,** 292-305.

Elith, J. & Leathwick, J.R. (2009) Species Distribution Models: Ecological Explanation and Prediction Across Space and Time. *Annual Review of Ecology Evolution and Systematics*, pp. 677-697. Annual Reviews, Palo Alto.

Evans, M.E.K., Merow, C., Record, S., McMahon, S.M. & Enquist, B.J. (2016) Towards Process-based Range Modeling of Many Species. *Trends in Ecology & Evolution, 31,* 860-871.

Foster, T.E., Schmalzer, P.A. & Fox, G.A. (2014) Timing matters: the seasonal effect of drought on tree growth. *Journal of the Torrey Botanical Society, 141,* 225-241.

Freckleton, R.P., Matos, D.M.S., Bovi, M.L.A. & Watkinson, A.R. (2003) Predicting the impacts of harvesting using structured population models: the importance of density-dependence and timing of harvest for a tropical palm tree. *Journal of Applied Ecology, 40,* 846-858.

Frederiksen, M., Lebreton, J.D., Pradel, R., Choquet, R. & Gimenez, O. (2014) Identifying links between vital rates and environment: a toolbox for the applied ecologist. *Journal of Applied Ecology, 51,* 71-81.

Gaillard, J.M., Festa-Bianchet, M. & Yoccoz, N.G. (1998) Population dynamics of large herbivores: variable recruitment with constant adult survival. *Trends in Ecology & Evolution, 13,* 58-63.

Gaillard, J.M., Festa-Bianchet, M., Yoccoz, N.G., Loison, A. & Toigo, C. (2000) Temporal variation in fitness components and population dynamics of large herbivores. *Annual Review of Ecology and Systematics, 31,* 367-393.

Gamelon, M., Grotan, V., Engen, S., Bjorkvoll, E., Visser, M.E. & Saether, B.E. (2016) Density dependence in an age-structured population of great tits: identifying the critical age classes. *Ecology, 97,* 2479-2490.

Gaston, K.J., Blackburn, T.M., Greenwood, J.J.D., Gregory, R.D., Quinn, R.M. & Lawton, J.H. (2000) Abundance-occupancy relationships. *Journal of Applied Ecology, 37,* 39-59.

Gotelli, N.J. & Ellison, A.M. (2006) Forecasting extinction risk with nonstationary matrix models. *Ecological Applications, 16,* 51-61.

Grosbois, V., Gimenez, O., Gaillard, J.M., Pradel, R., Barbraud, C., Clobert, J., Moller, A.P. & Weimerskirch, H. (2008) Assessing the impact of climate variation on survival in vertebrate populations. *Biological Reviews, 83,* 357-399.

Guisan, A. & Thuiller, W. (2005) Predicting species distribution: offering more than simple habitat models. *Ecology Letters, 8,* 993-1009.

Guisan, A. & Zimmermann, N.E. (2000) Predictive habitat distribution models in ecology. *Ecological Modelling, 135,* 147-186.

Hallett, T.B., Coulson, T., Pilkington, J.G., Clutton-Brock, T.H., Pemberton, J.M. & Grenfell, B.T. (2004) Why large-scale climate indices seem to predict ecological processes better than local weather. *Nature, 430,* 71-75.

Halpern, S.L. & Underwood, N. (2006) Approaches for testing herbivore effects on plant population dynamics. *Journal of Applied Ecology, 43,* 922-929.

Hernandez-Camacho, C.J., Bakker, V.J., Aurioles-Gamboa, D., Laake, J. & Gerber, L.R. (2015) The Use of Surrogate Data in Demographic Population Viability Analysis: A Case Study of California Sea Lions. *Plos One, 10.*

Hoerl, A.E. & Kennard, R.W. (1970) Ridge regression - biased estimation for nonorthogonal problems. *Technometrics, 12,* 55-&.

Hunter, C.M., Caswell, H., Runge, M.C., Regehr, E.V., Amstrup, S.C. & Stirling, I. (2010) Climate change threatens polar bear populations: a stochastic demographic analysis. *Ecology, 91,* 2883-2897.

Inchausti, P. & Halley, J. (2003) On the relation between temporal variability and persistence time in animal populations. *Journal of Animal Ecology, 72,* 899-908.

Jacquemyn, H., Brys, R. & Honnay, O. (2009) Large population sizes mitigate negative effects of variable weather conditions on fruit set in two spring woodland orchids. *Biology Letters, 5,* 495-498.

Johnson, H.E., Mills, L.S., Stephenson, T.R. & Wehausen, J.D. (2010) Population-specific vital rate contributions influence management of an endangered ungulate. *Ecological Applications, 20,* 1753-1765.

Jongejans, E., de Kroon, H., Tuljapurkar, S. & Shea, K. (2010) Plant populations track rather than buffer climate fluctuations. *Ecology Letters, 13,* 736-743.

Kruuk, L.E.B., Osmond, H.L. & Cockburn, A. (2015) Contrasting effects of climate on juvenile body size in a Southern Hemisphere passerine bird. *Global Change Biology, 21,* 2929-2941.

Lesica, P. & Steele, B.M. (1994) Prolonged dormancy in vascular plants and implications for monitoring studies. *Natural Areas Journal, 14,* 209-212.

Li, Q. & Lin, N. (2010) The Bayesian Elastic Net. *Bayesian Analysis, 5,* 151-170.

Maclean, I.M.D. & Wilson, R.J. (2011) Recent ecological responses to climate change support predictions of high extinction risk. *Proceedings of the National Academy of Sciences of the United States of America, 108,* 12337-12342.

Menges, E.S. (2000) Population viability analyses in plants: challenges and opportunities. *Trends in Ecology & Evolution,* **15,** 51-56.

Menges, E.S. & Quintana-Ascencio, P.F. (2004) Population viability with fire in Eryngium cuneifolium: Deciphering a decade of demographic data. *Ecological Monographs,* **74,** 79-99.

Merow, C., Latimer, A.M., Wilson, A.M., McMahon, S.M., Rebelo, A.G. & Silander, J.A., Jr. (2014) On using integral projection models to generate demographically driven predictions of species' distributions: development and validation using sparse data. *Ecography,* **37,** 1167-1183.

Mickelson, J.A. & Grey, W.E. (2006) Effect of soil water content on wild oat (Avena fatua) seed mortality and seedling emergence. *Weed Science,* **54,** 255-262.

Morris, J.A., Shertzer, K.W. & Rice, J.A. (2011) A stage-based matrix population model of invasive lionfish with implications for control. *Biological Invasions,* **13,** 7-12.

Murtaugh, P.A. (2009) Performance of several variable-selection methods applied to real ecological data. *Ecology Letters,* **12,** 1061-1068.

Myrvold, K.M. & Kennedy, B.P. (2015) Density dependence and its impact on individual growth rates in an age-structured stream salmonid population. *Ecosphere,* **6**.

Mysterud, A., Coulson, T. & Stenseth, N.C. (2002) The role of males in the dynamics of ungulate populations. *Journal of Animal Ecology,* **71,** 907-915.

Navarra, J.J., Kohfeldt, N., Menges, E.S. & Quintana-Ascencio, P.F. (2011) Seed bank changes with time since fire in Florida rosemary scrub. *Fire Ecology,* **7,** 17-31.

Nicole, F., Dahlgren, J.P., Vivat, A., Till-Bottraud, I. & Ehrlen, J. (2011) Interdependent effects of habitat quality and climate on population growth of an endangered plant. *Journal of Ecology,* **99,** 1211-1218.

Nur, N. & Sydeman, W.J. (1999) Survival, breeding probability and reproductive success in relation to population dynamics of Brandt's cormorants Phalacrocorax penicillatus. *Bird Study,* **46,** 92-103.

Paniw, M., Quintana-Ascencio, P.F., Ojeda, F. & Salguero-Gomez, R. (2017) Accounting for uncertainty in dormant life stages in stochastic demographic models. *Oikos,* **126,** 900-909.

Park, T. & Casella, G. (2008) The Bayesian Lasso. *Journal of the American Statistical Association,* **103,** 681-686.

Parmesan, C. (2006) Ecological and evolutionary responses to recent climate change. *Annual Review of Ecology Evolution and Systematics*, pp. 637-669.

Parmesan, C., Ryrholm, N., Stefanescu, C., Hill, J.K., Thomas, C.D., Descimon, H., Huntley, B., Kaila, L., Kullberg, J., Tammaru, T., Tennent, W.J., Thomas, J.A. & Warren, M. (1999) Poleward shifts in geographical ranges of butterfly species associated with regional warming. *Nature,* **399,** 579-583.

Parmesan, C. & Yohe, G. (2003) A globally coherent fingerprint of climate change impacts across natural systems. *Nature,* **421,** 37-42.

Peters, R.H. (1983) The ecological impacts of body size. Cambridge University Press, Cambridge, UK.

Pokallus, J.W. & Pauli, J.N. (2015) Population dynamics of a northern-adapted mammal: disentangling the influence of predation and climate change. *Ecological Applications,* **25,** 1546-1556.

Radchuk, V., Turlure, C. & Schtickzelle, N. (2013) Each life stage matters: the importance of assessing the response to climate change over the complete life cycle in butterflies. *Journal of Animal Ecology,* **82,** 275-285.

Raffalovich, L.E., Deane, G.D., Armstrong, D. & Tsao, H.S. (2008) Model selection procedures in social research: Monte-Carlo simulation results. *Journal of Applied Statistics,* **35,** 1093-1114.

Rees, M., Childs, D.Z., Metcalf, J.C., Rose, K.E., Sheppard, A.W. & Grubb, P.J. (2006) Seed dormancy and delayed flowering in monocarpic plants: Selective interactions in a stochastic environment. *American Naturalist,* **168,** E53-E71.

Rezvani, M. & Zaefarian, F. (2017) Effect of some environmental factors on seed germination of Eryngium caeruleum M. Bieb. populations. *Acta Botanica Brasilica,* **31,** 220-228.

Roberts, A.M.I. (2008) Exploring relationships between phenological and weather data using smoothing. *International Journal of Biometeorology,* **52,** 463-470.

Rotella, J.J., Link, W.A., Chambert, T., Stauffer, G.E. & Garrott, R.A. (2012) Evaluating the demographic buffering hypothesis with vital rates estimated for Weddell seals from 30 years of mark-recapture data. *Journal of Animal Ecology,* **81,** 162-173.

Salguero-Gomez, R., Jones, O.R., Archer, C.R., Bein, C., de Buhr, H., Farack, C., ... & Vaupel, J.W. (2016) COMADRE: a global data base of animal demography. *Journal of Animal Ecology,* **85,** 371-384.

Salguero-Gomez, R., Jones, O.R., Archer, C.R., Buckley, Y.M., Che-Castaldo, J., Caswell, H., ... & Vaupel, J.W. (2015) The COMPADRE Plant Matrix Database: an open online repository for plant demography. *Journal of Ecology,* **103,** 202-218.

Salguero-Gomez, R., Siewert, W., Casper, B.B. & Tielborger, K. (2012) A demographic approach to study effects of climate change in desert plants. *Philosophical Transactions of the Royal Society B-Biological Sciences,* **367,** 3100-3114.

Simmonds, E.G. & Coulson, T. (2015) Analysis of phenotypic change in relation to climatic drivers in a population of Soay sheep Ovis aries. *Oikos,* **124,** 543-552.

Stenseth, N.C. & Mysterud, A. (2005) Weather packages: finding the right scale and composition of climate in ecology. *Journal of Animal Ecology,* **74,** 1195-1198.

Stenseth, N.C., Mysterud, A., Ottersen, G., Hurrell, J.W., Chan, K.S. & Lima, M. (2002) Ecological effects of climate fluctuations. *Science,* **297,** 1292-1296.

Swab, R.M., Regan, H.M., Matthies, D., Becker, U. & Bruun, H.H. (2015) The role of demography, intra-species variation, and species distribution models in species' projections under climate change. *Ecography,* **38,** 221-230.

Teller, B.J., Adler, P.B., Edwards, C.B., Hooker, G. & Ellner, S.P. (2016) Linking demography with drivers: climate and competition. *Methods in Ecology and Evolution,* **7,** 171-183.

Tibshirani, R. (1996) Regression shrinkage and selection via the Lasso. *Journal of the Royal Statistical Society Series B-Methodological,* **58,** 267-288.

Vaida, F. & Blanchard, S. (2005) Conditional Akaike information for mixed-effects models. *Biometrika,* **92,** 351-370.

Van der Pol, M., Bailey, L.D., McLean, N., Rijsdijk, L., Lawson, C.R. & Brouwer, L. (2016) Identifying the best climatic predictors in ecology and evolution. *Methods in Ecology and Evolution,* **7,** 1246-1257.

Walther, G.R., Post, E., Convey, P., Menzel, A., Parmesan, C., Beebee, T.J.C., Fromentin, J.M., Hoegh-Guldberg, O. & Bairlein, F. (2002) Ecological responses to recent climate change. *Nature,* **416,** 389-395.

Wang, G.M., Hobbs, N., Twombly, S., Boone, R., Illius, A., Gordon, I. & Gross, J. (2009) Density dependence in northern ungulates: interactions with predation and resources. *Population Ecology,* **51,** 123-132.

Wardle, G., Buckley, Y., Ehrlen, E., Blomberg, S., Crone, E., Salguero-Gomez, R., Csergo, A.M., Roach, D., Garcia Gonzalez, M.B., Laine, A.-L. & van Groenendael, J. (2014) PlantPopNet: A spatially distributed model system for population ecology. *Ecology Society of Australia Annual Conference*.

Webb, D.R. & King, J.R. (1984) Effects of wetting on insulation of bird and mammal coats. *Journal of Thermal Biology,* **9,** 189-191.

Wenger, S.J. & Olden, J.D. (2012) Assessing transferability of ecological models: an underappreciated aspect of statistical validation. *Methods in Ecology and Evolution,* **3,** 260-267.

Yee, T.W. & Mitchell, N.D. (1991) Generalized additive-models in plant ecology. *Journal of Vegetation Science,* **2,** 587-602.

Zou, H. & Hastie, T. (2005) Regularization and variable selection via the elastic net. *Journal of the Royal Statistical Society Series B-Statistical Methodology,* **67,** 301-320.